

# **VIBRATIONS OF THIN-WALLED COMPOSITE I-BEAMS**

THESIS SUBMITTED TO OSMANIA UNIVERSITY

FOR THE AWARD OF THE DEGREE OF

*DOCTOR OF PHILOSOPHY*

IN

MECHANICAL ENGINEERING

BY

**N.V. SRINIVASULU**



**DEPARTMENT OF MECHANICAL ENGINEERING  
UNIVERSITY COLLEGE OF ENGINEERING  
OSMANIA UNIVERSITY  
HYDERABAD-500007.**

**2009**

## **CERTIFICATE**

This is to certify that the thesis entitled “**Vibrations of Thin-Walled Composite I-Beam**” submitted by **Mr. N.V.Srinivasulu**, for the award of the degree of **Doctor of Philosophy** to **Osmania University**, Hyderabad is a record of bonafide research work carried out by him. The contents of the thesis have not been submitted to any other institute or University for the award of any degree.

Dr.C.KAMESWARA RAO  
SUPERVISOR,  
Principal,  
Tirumala Engineering College  
Hyderabad

Dr.P.RAVINDER REDDY,  
SUPERVISOR  
Professor & Head,  
Department of Mech. Engg.,  
CBIT, Hyderabad.

**Head of Department of Mechanical Engineering.  
College of Engineering  
Osmania University, Hyderabad.**

Date:

## **CERTIFICATE**

This is to certify that the thesis entitled “**Vibrations of Thin-Walled Composite I-Beams**” does not constitute any part of thesis dissertation/monograph submitted by me to this or any other university / institute.

**Date:**

**N.V.SRINIVASULU**  
**Research Scholar**

**Dedicated to  
My Beloved Parents  
&  
My Family**

## ACKNOWLEDGEMENTS

The author wishes to express his deep sense of gratitude to **Dr.C.Kameswara Rao**, Principal, Tirumala Engineering. College, Hyderabad and **Dr. P.Ravinder Reddy**, Professor & Head , Department of Mechanical Engineering, CBIT, Hyderabad, for their esteemed guidance and encouragement in carrying and completing the dissertation work.

The author thanks **Vaastushilpi. Dr.B.N.Reddy**, Chairman, **Mr.D.Kamalakar Reddy**, Secretary and Correspondent, CBIT, Hyderabad, **Prof. I.Ramachandra Reddy**, Director of CBIT., for their constant cooperation and help for pursuing this course. **Dr.B.Chennakeshava Rao**, Principal, **Dr.P.Jayapal Reddy**, Professor , MED, CBIT, Hyderabad and **Dr.G.C.M.Reddy**, Professor for their valuable suggestions.

He is grateful to acknowledge **Dr.A.M.K.Prasad**, Professor & Head, Department of Mechanical .Engineering. University college of Engineering, Hyderabad, for his help and permission to carry out this work. His grateful thanks are also extended to his grateful thanks to **Dr.Sriram Venkatesh**, Chairman, Board of studies and **Dr.M.Komaraiah**, Director, CMR college of Engineering & Technology, Hyderabad for their valuable guidance and remarks throughout the work.

The author also expresses heartfelt thanks to his parents **Sri. N.Giddaiah** and **Smt. N. Suseelamma** , **Mrs. Rama Devi (wife)** , **Ms. Dhana Sree**, **Ms.Vinoothna Sree (daughters)** and **Mr. Anirudh (son)** and brothers **N.V.Ramanaiah**, **N.Madan Mohan** and **Mrs & Mr. R.V.Krishna Murthy** and **Mrs & Mr. K.Bhaskar** for their cooperation. He would also like to convey my appreciation for the unstinted support extended by relatives.

The author would like to record my sincere thanks for the support extended by all persons involved in the manufacture of composites. He would like to acknowledge the

valuable contribution of Mr.Ramana , Tirumala fibre industries, Balanagar, Hyderabad for their guidance to manufacture glass epoxy specimens.

The author thanks Mr K. Ravi Kiran Reddy for helping him in typing thesis. Finally, the author thanks all colleagues, friends and well wishers without whose help this research work would not have been successfully completed.

## ABSTRACT

In an effort to reduce weight while maintaining high strength, many contemporary structural systems are designed with lower margins of safety than predecessors. The criterion for minimum weight design is predominant in the design of aircraft, missile, and spacecraft vehicles. One obvious means of obtaining a high strength, minimum weight design is the use of light, thin-walled structural members of high strength alloys. Thin-walled beams of open sections such as I, Z, Channel and angle sections are frequently used for intricate structures in spacecrafts. Due to low torsional rigidity of thin-walled beams of open sections, the problem of torsional vibrations and stability is of prime interest. For the last three to four decades mechanical vibrations have been recognized as a major factor in the design. Mechanical vibrations produce increased stress, energy loss and noise that should be considered in the design stages if these undesirable effects are to be avoided, or minimised.

The research work carried out particularly deals with dynamic analysis of lengthy uniform thin-walled composite I-beams of open section. Fibre-Reinforced Plastics (FRP) have been increasingly used over the past few decades in a variety of structures that require high ratio of stiffness and strength to weight. The analytical model developed by Lee and Kim [11] is taken and the dynamic behaviour of a thin-walled I-section composite beam is studied in detail. This model accounts for the coupling of flexural and torsional modes for arbitrary laminate stacking sequence configuration, i.e. symmetric as well as unsymmetric, and various boundary conditions are also discussed in detail. A displacement-based one-dimensional finite element model is developed to predict natural frequencies and corresponding vibration modes for a thin-walled composite beam and the equations of motion are derived from Hamilton's principle.

Further experiments are conducted by taking two specimens of glass-epoxy composite rectangular laminated beams of different fibre orientations and natural frequencies are determined for a cantilever beam by impact experiment. These results are compared with the natural frequencies of composite rectangular laminated beams by using ANSYS R10.0 .the numerical results from finite element analysis showed in general a good agreement with experimental values.

The present research work is extended with the assumption that the finite element analysis of laminated composite I-beams will be valid and the effect of fibre angle, modulus ratio, height-to-thickness ratio, and boundary conditions on the vibration frequencies and mode shapes of the composite I-beams is studied. Using ANSYS R10.0, (general purpose FEA software) the modal and harmonic analysis are carried out and the results obtained are presented in graphical form, for uniform and tapered composite I-beams. The modal and harmonic analysis is also carried out for a cantilever composite I-beam for two cases, with its bigger end fixed and smaller end free and again with its smaller end fixed and bigger end free. The study was extended to know the behaviour of the same composite I-beam with circular holes in the web.



## **List of Papers brought out on this research work:**

### **INTERNATIONAL JOURNALS**

1. “Finite Element Analysis of Thin-Walled Composite I-Beam”, International Journal of Current Sciences 10(2): 485-498(2004).
2. “Finite Element Analysis of Thin-Walled Tapered Composite I-Beam”, is accepted for publication in International Journal of Current Sciences, Vol.15, 2009.
3. “Finite Element Analysis of Thin Walled Composite Cantilever I-Beam”, under review in The Open Mechanical Engineering Journal, Bentham Science Publishers Ltd.
4. “Numerical And Experimental Analysis of Glass-Epoxy Rectangular Laminates”, is accepted for publication in International Journal of Applied Engineering Research (IJAER).

### **INTERNATIONAL CONFERENCES**

1. “Galerkin’s Finite Element Analysis of Free Torsional Vibrations Tapered Cantilever I-Beams”, Proceedings of First International conference on Vibration Engineering and Technology of Machinery (VETOMAC-I), Indian Institute of Science, Bangalore, October, 2000.
2. “Dynamic stability of thin – walled Wide flanged I-Beam”, is accepted for International Conference on Nuclear Engineering (ICONE-12), organized jointly by American Society of Mechanical Engineers (ASME) and Japan Society of Mechanical Engineers (JSME) , during 24-25, April, 2004, in USA.
3. “Torsional Vibrations of Thin-Walled Beams Using Dynamic Stiffness Approach”, accepted for International Conference on Nuclear Engineering

(ICONE-12), organised jointly by American Society of Mechanical Engineers (ASME) and Japan Society of Mechanical Engineers (JSME), during 24-25, April, 2004, in USA.

4. “Comparison of performance of conventional beams and composite beams – a case study”, International Conference on Nuclear Engineering (ICONE14), July 2009, Belgium.
5. “Effect Of Modular Ratio And Height To Thickness Ratio On Modal Analysis of a Thin-Walled Composite I-Beam”, VETOMAC-IV, Organised by Osmania University, Hyderabad, .pp 245-282., Dec.14-19, 2004.
6. “Finite Element Analysis of Thin-Walled Tapered Cantilever Composite I-Beam”, International Conference on Computational Methods In Engineering And Sciences (CMES2009), Hyderabad, 8-10, January 2009, pp 801-805.
7. “Theoretical and experimental Vibration Analysis of Glass-Epoxy Thin-Walled Composite Beams”, World Academy of Science Engineering And Technology (WASET) Conference, International conference on Mechanical, Industrial and Manufacture Engineering (ICMIME’10), January, 29-31, 2010, at Cape Town, South Africa.

## **NATIONAL CONFERENCES**

1. “Vibrations of Stepped Beams on Elastic Foundation” , Proceedings of National conference on Emerging Trends in Mechanical Engineering at Roorkee college of Engineering, Roorkee, March,2000.
2. “Vibrations of Cantilever Beams with Distributed Lumped Masses”, MINAC-2002, University college of Engineering. J.N.T.U., Ananthapur. (A.P), 2001.
3. “Torsional Vibrations and Stability of Lengthy Thin Walled Open Section Beams on Elastic Foundation, National Symposium on Rotor Dynamics (NSRD-2003),during Dec 15-14,2003.,organised by IIT, Guwahati in association with The Vibration Institute of India.

## LIST OF FIGURES

<b>Figure No</b>	<b>Description</b>	<b>Page No</b>
1.1	Layered Model Showing Dropped Layer	7
1.2	Sandwich Construction	7
1.3	Layered Shell With Nodes at Mid plane	7
1.4	Layered Shell with Nodes at Bottom Surface	8
3.1	Meshing model of an ISJB-150	49
3.2	Different mode shapes of an ISJB-150	52
3.3	Frequency variation of an ISJB - 150	54
3.4	Meshing model of an ISLB-150	55
3.5	Different mode shapes of an ISLB-150	56
3.6	Frequency variation of an ISLB – 150	59
3.7	Meshing model of an ISJB-150 tapered beam	60
3.8	Different mode shapes of an ISJB-150 tapered beam	61
3.9	Frequency variation of an ISJB – 150 tapered beam	64
3.10	Meshing model of an ISLB-150 tapered beam	65
3.11	Different mode shapes of an ISLB-150 tapered beam	67
3.12	Frequency variation of an ISLB – 150 tapered beam	69
3.13	The comparison of various frequency of all four beams	70
4.1	Block diagram of experimental set up for modal analysis	87
4.2	Block diagram with input and output response.	88
4.3	Picture of the experimental set up of an impact experiment	89
4.4	Photograph of specimens of Glass-Epoxy rectangular composite specimens	89

5.1	Combined influence of positive taper ratio $\beta$ and negative ratio $\alpha$ –first mode	100
5.2	The combined influence of positive taper ratios $\beta$ and negative taper ratio $\alpha$ on the first three frequencies of vibration-second mode	101
5.3	The combined influence of positive taper ratios $\beta$ and negative taper ratio $\alpha$ on the first three frequencies of vibration-third mode	101
6.1	First mode	112
6.2	Second Mode	112
6.3	Third Mode	113
6.4	Fourth mode	114
6.5	Mode shapes for $W_k = 0.01$	115
6.6	Mode shapes for $W_k = 0.1$	115
6.7	Mode shapes for $W_k = 1.0$	116
7.1	Definition of coordinates in thin-walled open section	121
7.2	Geometry of a thin-walled doubly symmetric Composite I-beam.	130
8.1	Thin-walled I-section composite beam	137
8.2	SHELL99, Linear Layered Structural Shell	139
8.3	Variation of the non-dimensional natural frequencies of a simply supported composite beam with respect to fibre angle change in flanges	146
8.4	Variation of the non-dimensional natural frequencies of a simply supported composite beam with respect to fibre angle change in the web	152
8.5	Mode shapes of the composite beams with unidirectional fibre.	155
8.6	Mode shapes of the composite beams with fibre angle $30^\circ$ in the web.	157
8.7	Variation of the non-dimensional natural frequencies of a simply Supported composite beam with respect to modulus ratio	158
8.8	Variation of the non-dimensional natural frequencies of fixed composite beam with respect to modulus ratio	159
8.9	Variation of the non-dimensional natural frequencies of a simply supported composite beam with height-to-thickness ratio.	160
8.10	Variation of the non-dimensional natural frequencies of a fixed composite beam with height-to-thickness ratio	161

8.11	Frequency Vs. Amplitude for fibre angle rotation in two flanges.	162
8.12	Frequency Vs. Amplitude for various elastic modulus ratios	163
8.13	Frequency Vs. Amplitude for various beam height to thickness ratios	164
9.1	Tapered composite I- beam with layers	167
9.2	Variation of the non-dimensional natural frequencies of a tapered cantilever composite beam with small end fixed with respect to fibre angle change in flanges	170
9.3	Mode shapes of the tapered composite beam with fibre angle $45^{\circ}$ in top and bottom flanges	171
9.4	Variation of the non-dimensional natural frequencies of a Tapered Cantilever composite beam with small end fixed with respect to fibre angle change in web.	172
9.5	Variation of the non-dimensional natural frequencies of a Tapered Cantilever composite beam with small end fixed with respect to fibre angle.	173
9.6	Frequency Vs. Displacement for fibre angle rotation in two flanges	176
9.7	Frequency vs. displacement for fibre angle rotation in web	177
9.8	Frequency Vs. displacement for various modular ratios	178
10.1	Variation of the non-dimensional natural frequencies of a tapered cantilever composite beam with big end fixed with respect to fibre angle change in flanges	181
10.2	Mode shapes of the tapered composite beam with fibre angle $45^{\circ}$ in top and bottom flanges	183
10.3	Variation of the non-dimensional natural frequencies of a Tapered Cantilever composite beam with big end fixed with respect to fibre angle change in web.	184
10.4	Variation of the non-dimensional natural frequencies of a Taper cantilever composite beam with big end fixed with respect to modulus ratio.	185
10.5	Frequency vs. Displacement for fibre angle rotation in two flanges	186
10.6	Frequency vs. Displacement for fibre angle rotation in web	187
10.7	Frequency vs. Amplitude for various modular ratios.	188
10.8	Uniform composite I-beam with circular holes in web	189

10.9	Variation of the non-dimensional natural frequencies of a cantilever Composite beam with circular holes in web with fibre angle change in flanges	190
10.10	Mode shapes of the Cantilever composite beam with circular holes in web with fibre angle $45^0$ in top and bottom flanges	192
10.11	Variation of the non-dimensional natural frequencies of a Cantilever composite beam with circular holes in web with to fibre angle change in flanges	193
10.12	Variation of the non-dimensional natural frequencies of a Cantilever composite beam with circular holes in web with elastic modular ratio	194
10.13	Frequency vs. Displacement for fibre angle rotation in two flanges	195
10.14	Frequency vs. Displacement for fibre angle rotation in web.	196
10.15	Frequency vs. Displacement for various modular ratios.	197

## LIST OF TABLES

<b>Table No</b>	<b>Description</b>	<b>Page No</b>
3.1	Furnishes the frequencies of first 10 mode shapes of ISLB-150	53
3.2	The frequencies of first 10 mode shapes of an ISJB-150	58
3.3	The frequencies of first 10 mode shapes of ISJB-150 tapered beam.	63
3.4	The frequencies of first 10 mode shapes of ISLB-150 tapered beam	68
4.1	Material properties	75
4.2	Numerical results obtained from FEM	90
4.3	Experimental results for two cases	91
4.4	Percentage Variation in natural frequencies for case 1	92
4.5	Percentage Variation in natural frequencies for case 2	93
8.1	Non-dimensional natural frequencies w.r.t to fibre angle change in the flange	141
8.2	Percentage variation in natural frequencies of a simply supported composite beam w.r.t to fibre angle change in the flange	142
8.3	Percentage variation in second natural frequencies of a simply supported composite beam with respect to fibre angle change in flanges	143
8.4	Percentage variation in third natural frequencies of a simply supported composite beam with respect to fibre angle change in flanges	144
8.5	Percentage variation in fourth natural frequencies of a simply supported composite beam with respect to fibre angle change in flanges	145
8.6	Nondimensional natural frequencies with respect to the fibre angle change in the web.	147
8.7	Percentage variation in first natural frequencies of a simply supported composite beam with respect to fibre angle change in web	148
8.8	Percentage variation in natural frequencies of a simply supported composite beam with respect to fibre angle change in web	149
8.9	Percentage variation in natural frequencies of a simply supported composite beam with respect to fibre angle change in web	150
8.10	Percentage variation in natural frequencies of a simply supported composite beam with respect to fibre angle change in web	151



## NOMENCLATURE

$[K]$	Element Stiffness matrix
$[M]$	Element Mass matrix
$[F]$	Element Force Matrix
$\{U\}$	Displacement matrix
$U_x, U_y, U_z$	Deformation along X, Y, and Z direction
$ROT_x, ROT_y, ROT_z$	Rotations along X, Y, and Z-direction
$R$	Radius
$M_x, M_y, M_z$	Moments about X, Y, and Z-direction
$\rho$	Density
$\omega$	Natural frequency
$E$	Young's modulus of Elasticity
$G$	Modulus of Rigidity
$\nu$	Poisson's Ratio
$L$	Length of the beam
$A$	Cross section Area of Beam
$I$	Moment of Inertia
$J$	Polar Moment of Inertia
$W$	Width of the beam
$t$	Thickness
$\theta$	Fibre angle of orientation
$\gamma$	Shear strain
$\phi$	Rotation angle about the pole axis
$\tau$	Kinetic energy of the system
$\Pi$	Total potential energy of the system
$m$	Inertia coefficients

$\overline{Q}_{ij}$	Transformed reduced stiffness matrices
$N_z$	Axial force
$A_{ij}$	Extensional stiffness matrices
$B_{ij}$	Coupling stiffness matrices
$D_{ij}$	Bending stiffness matrices
$\Psi_j$	Lagrange interpolation function
$\phi_j$	Hermite-cubic interpolation function
$[M]$	Global mass matrix
$[C]$	Global damping matrix
$[K]$	Global stiffness matrix
$\{F(t)\}$	Global forces vector
$[M]_{(e)}$	Element mass matrix
$[N]$	Interpolation function matrix
$[K]_{(e)}$	Element stiffness matrix
$[B]$	Displacement matrix (based on shape functions)
$[D]$	Laminate elasticity matrix (orthotropic case)
$[C]_e$	Element damping matrix
$\{\ddot{a}\}$	Global displacements vector
$\{\dot{a}\}$	Global velocities vector
$\{\ddot{a}''\}$	Global accelerations vector
$\rho_c$	Composite density
$\hat{u}_r$	Natural frequency
$\{\ddot{O}r\}$	Mode shapes of the system
$T_k$	kinetic energy of the strained bar
$U$	Total strain energy
$W$	The potential energy of the external force
$t_0, t_1$	Fixed constants.
$G$	Shear modulus
$C_s$	Torsion constant for the cross section,
$\phi(z, t)$	The angle of twist
$b$	Width of the flanges

$t_f$	Thickness of flanges
$h$	Height between the centre lines of the flanges.
$t_w$	Thickness of the web
$M$	Moment
$X$	Displacement of the top flange centre line,
$E$	Young's modulus,
$I_f$	Moment of inertia of each flange area about y-axis
$Q$	The shear force
$T_w$	Torque due to warping
$T_t$	The total torque
$I_p$	The polar moment of inertia of the cross section
$\rho$	The mass density of the material of the beam
$P$	Compressive load acting at the centroid
$A$	The area of the cross section
$Z$	The non-dimensional beam length
$k_2$	Warping rigidity parameter
$\nabla$	Axial load parameter
$\gamma$	Foundation parameter
$\lambda_n$	The dimensionless torsional frequency parameter
$\lambda_n$	The dimensionless torsional frequency parameter
$W$	Weight per meter
$h$	Depth of Section
$b_f$	Width of Flange
$t_f$	Thickness of Flange
$t_w$	Thickness of Web
$E$	Young's Modulus
$\nu$	Poisson's Ratio
$\alpha$	The taper ratios in the width of the flanges
$\beta$	The taper ratios in the depth of the web
$u$	The warping displacement, in the flanges
$h(z)$	The height between centrelines of the flanges
$T$	The torque induced in the beam
$\theta_e$	Torsional amplitudes over each element

$A_{f0}$	The flange area
$I_{f0}$	Moment of inertia
$[A]$	The stiffness matrix
$[B]$	Mass matrix
$\{\delta\}$	The eigenvector
$\lambda$	The frequency parameter
$I_f$	The flange moment of inertia
$\bar{\varepsilon}_z$	Mid surface axial strain
$\bar{k}_z$	Biaxial curvature of the shell
$\bar{k}_{sz}$	Biaxial curvature of the shell
$\varepsilon_z$	Axial strain
$k_x$	Biaxial curvatures in the x direction
$k_y$	Biaxial curvatures in the y direction
$k_\omega$	Warping curvature with respect to the shear centre
$k_{sz}$	Twisting curvature in the beam
$\Pi$	The total potential energy of the system
$N_z$	Axial force
$M_x$	Bending moments in x direction
$M_y$	Bending moments in y direction
$M_\omega$	Warping moment (bi moment) with respect to centroid
$m_0, m_c, m_s, m_\omega, m_p, m_2$	Inertia coefficients
$\bar{Q}_{ij}$	Transformed reduced stiffness
$N_z$	Axial force
$E_{ij}$	Stiffness of the thin-walled composite
$A_{ij}$	Extensional stiffness matrices
$B_{ij}$	Coupling stiffness matrices
$D_{ij}$	Bending stiffness matrices
$(EA)_{com}$	Axial rigidity
$(EI_x)_{com}$	Flexural rigidities with respect to x axis

$(EI_y)_{com}$	Flexural rigidities with respect to y axis
$(EI_\omega)_{com}$	Warping rigidities of the thin-walled composite
$(GJ)_{com}$	Torsional rigidities of the thin-walled composite
$\{ \Delta \}$	The eigenvector of nodal displacements

# CONTENTS

<b>Preliminaries</b>	<b>Page No.</b>
Certificate	ii
Acknowledgement	v
Abstract	vii
List of Papers brought out of the present work	ix
List of figures	xii
List of tables	xvi
Nomenclature	xvii

<b>Chapter No</b>	<b>Description</b>	<b>Page No.</b>
1	<b>INTRODUCTION</b>	
1.1	Introduction to thin walled beams	2
1.2	Convergence Criterion	3
1.3	Criterion of Finite Element Selection:	4
1.4	Defining the Layered Configuration	4
1.4.1	Specifying Individual Layer Properties	5
1.4.1.1	Material Properties	5
1.4.1.2	Layer orientation angle	6
1.4.1.3	Layer thickness	6
1.4.2	Defining the Constitutive Matrices	6
1.5	Sandwich and Multiple-Layered Structures	7
1.5.1	Node offset	7
1.5.2	Specifying failure criteria	8
1.6	Introduction to composites	8

1.6.1	Selection of material for matrix	9
1.6.2	Materials for the reinforcement	9
1.6.3	Manufacturing process	10
1.6.4	Advantages of composites	10
1.7	Classifieds of materials	11
1.8	Properties of composites	12
1.8.1	Fibre volume fraction	12
1.8.2	Areal weight of a fabric	12
1.8.3	Rules of Mixtures	12
1.8.4	Stacking sequence	13
1.8.5	Young's modulus	14
1.8.6	The fibre length distribution factor (FLDF)	14
1.8.7	Critical length	15
1.8.8	Fibre orientation distribution factor	15
1.8.9	Shear modulus	16
1.8.10	Poisson's ratio	17
1.8.11	Bulk modulus	17
1.9	Research problem and objectives	17
1.9.1	Objectives	18
1.10	Scope of The Current Research Work	18
1.11	Flow chart showing the numerical and experimental Plan	20
1.12	Flow chart showing the study and analysis of orthotropic I-beams by different methods	21
1.13	Flow chart showing the detailed plan of thesis	22
1.14	Flow chart to show the Procedure to do Modal analysis using ANSYS	23

1.15	Flow chart to show the Procedure to do Harmonic analysis of a Cantilever beam using ANSYS	25
1.16	Organisation of the thesis	27
2	<b>LITERATURE REVIEW</b>	31
3	<b>VIBRATIONS OF A THIN-WALLED I-BEAM RESTING ON ELASTIC FOUNDATION</b>	
3.1	Introduction	39
3.2	Derivation of basic differential equation	39
3.3	Natural boundary conditions	42
3.4	Time dependent boundary conditions	43
3.5	Analysis of various terms	44
3.6	Non-Dimensionalization and General Solution of Equation of Motion	45
3.7	Frequency Equations and Modal Functions	47
3.7.1	Boundary conditions	47
3.8	Simply Supported Beam	47
3.9	Finite element simulation	48
3.9.1	Meshing model of an ISJB-150.	49
3.9.1.1	Different mode shapes of an ISJB-150.	50
3.9.2	Meshing model of an ISLB-150.	55
3.9.2.1	Different mode shapes of an ISLB-150	56
3.9.3	Meshing model of an ISJB-150 tapered beam	60
3.9.3.1	Different mode shapes of an ISJB-150	61
3.9.4	Meshing model of an ISLB-150 tapered beam.	65



3.9.4.1	Different mode shapes of an ISLB-150 tapered beam	66
3.10	Results and Discussion	70
4	<b>EXPERIMENTAL ANALYSIS OF GLASS-EPOXY RECTANGULAR COMPOSITE BEAMS</b>	
4.1	Introduction	72
4.2	Manufacturing of Glass-Epoxy Composites	72
4.3	Dimensions of the rectangular glass –epoxy composite beam	74
4.4	Modal Analysis by Finite Element method	76
4.5	Mode shapes	76
4.5.1	Mode shapes for first case	76
4.5.2	Mode shapes for second case	81
4.6	Experimental analysis of Glass-Epoxy composite Rectangular laminated beams	87
4.7	Background	88
4.8	Comparison of experimental results with numerical results	90
4.9	Results and Discussions	93
5	<b>GALERKIN FINITE ELEMENT ANALYSIS OF FREE TORSIONAL VIBRATION OF TAPERED</b>	
5.1	Introduction	95
5.2	Governing equations of torsional motion	96
5.3	Finite element formulation	98
5.4	Numerical results and Discussion	100
5.5	Results and Discussion	

6	<b>TORSIONAL VIBRATIONS AND BUCKLING OF THIN-WALLED BEAMS ON ELASTIC FOUNDATION</b>	
6.1	Introduction	104
6.2	Formulation and analysis	105
6.3	Dynamic stiffness matrix	106
6.4	Method of solution	110
6.5	Results and discussion	110
6.6	Concluding Remarks	117
7	<b>MATHEMATICAL MODELING OF COMPOSITE I-BEAM</b>	
7.1	Introduction to composites	119
7.2	Laminated composites	119
7.2.1	Lamina and laminate	120
7.3	Mathematical Modeling of Composite I-Beam	121
7.3.1	Kinematics	121
7.3.2	Variational formulation	124
7.3.3	Constitutive equations	126
7.3.4	Equations of motion	131
7.3.5	Finite Element Model	133
8	<b>EFFECT OF VARIOUS PARAMETERS ON VIBRATIONS OF UNIFORM COMPOSITE I-BEAM</b>	

8.1	Material Properties	138
8.1.1	Element used	138
8.2	Model analysis	139
8.2.1	Effect of Fibre angle rotation in top and bottom flanges	139
8.3	Percentage variation of frequencies closed form Vs FEM Solutions	142
8.4	Effect of Fibre angle rotation in Web	147
8.5	Mode shapes	153
8.5.1	Effect of Elastic modulus ratio	158
8.6	Effect of Height-to-thickness ratio for simply supported beams	158
8.6.1	Effect of Height-to-thickness ratio	160
8.6.2	Harmonic analysis	162
8.6.2.1	Effect of fibre angle rotation in top and bottom flanges	162
8.6.2.2	Effect of Elastic modulus ratio	163
8.6.2.3	Effect of Height-to-thickness ratio	163
9	<b>MODAL &amp; HARMONIC ANALYSIS OF TAPERED COMPOSITE I- BEAM WITH A SMALL END FIXED</b>	
9.1	Modal Analysis	168
9.1.1	Effect of fibre angle rotation in top and bottom Flanges	169
9.1.2	Mode shapes	171
9.1.3	Effect of fibre angle rotation in web	172
9.1.4	Effect of modular ratio	173
9.2	Harmonic analysis	174
9.2.1	Effect of fibre angle rotation in flanges	176

	9.2.2	Effect of fibre angle rotation in web	177
	9.2.3	Effect of Elastic modulus ratio	178
10		<b>TAPERED COMPOSITE I- BEAM WITH BIG END FIXED</b>	
10.1		Modal Analysis	180
	10.1.1	Effect of fibre angle rotation in top and bottom Flanges	180
	10.1.2	Mode shapes	181
	10.1.3	Effect of fibre angle rotation in web	184
	10.1.4	Effect of modular ratio	185
	10.1.5	Harmonic analysis	186
	10.1.6	Effect of fibre angle rotation in top and bottom Flanges	187
	10.1.7	Effect of fibre angle rotation in web	187
	10.1.8	Effect of modular ratio	188
10.2		Composite I-beam with three circular holes in web	189
	10.2.1	Modal Analysis	190
	10.2.1.1	Effect of fibre angle rotation in top and bottom Flanges	190
	10.2.1.2	Mode shapes	191
	10.2.1.3	Effect of fibre angle rotation in web	193
	10.2.1.4	Effect of Elastic modular ratio	194
10.3		Harmonic Analysis	195
	10.3.1	Effect of fibre angle rotation in top and bottom Flanges	195
	103.2	Effect of fibre angle rotation in web	196
	10.3.3	Effect of modular ratio	197

<b>DISCUSSION ON RESULTS</b>	199
<b>CONCLUSIONS</b>	201
<b>SCOPE OF FUTURE WORK</b>	204
<b>AUTHOR'S INDEX</b>	206
<b>REFERENCES</b>	210

## **Chapter 1**

# **INTRODUCTION**

# INTRODUCTION

### 1.1. Introduction to thin- walled beams

For intricate structures such as space craft, beams of standard cross sections may not be the most efficient or convenient structural members to use. Thin walled beams of open sections are frequently employed for their structural efficiency. When the dimensions of cross sections of a beam are very small compared to length of the beam, the beam is referred as Thin-walled beam. Thin- walled beams of open sections such as I, Z, Channel and angle sections are frequently used for intricate structures in spacecrafts. The thin-walled beams of open sections are widely used in engineering industry and space vehicles due to their low torsional rigidity and stability. With the improved versions of extrusion methods in metal forming, beams of different shapes of cross sections can be formed to order. However, it has been known that a beam with nonsymmetrical cross sections under loads will not only deflect but also twist. Only under special loading along the flexure axis, beam will deflect without twist.

Currently, fibre-reinforced laminated composite structures are being used extensively in a variety of industrial products and structures such as air craft, automobiles, marine vessels, rocket launchers, pressure vessels and pipes owing to their strength, high stiffness, low weight and good resistance to fatigue and corrosion. The most common problem is delamination along ply interfaces which may arise due to fabrication defects and impact loading. The present work particularly deals with dynamic analysis of lengthy uniform thin-walled I-beams of open section, particularly composite beams. In the present thesis, the analytical model developed by Lee and Kim [11] is taken as reference and the dynamic behaviour of a thin-walled I-section composite beam is studied in detail. This model accounts for the coupling of flexural and torsional modes for arbitrary laminate stacking sequence configuration, i.e. symmetric as well as unsymmetric, and various boundary conditions are also discussed in detail.

**Some of the following basic assumptions made in this study are**

- The thin-walled beam has uniform open cross section along its length.

- Strains are assumed to remain within the elastic limit and the curvature and twist of the beam are considered to be small.
- The material of the beam is homogeneous and isotropic and obeys Hook's Law as in the case of conventional beams.
- The centroid and shear centre of the cross-section coincide.
- Shearing strains of the middle surface due to shear and warping effects and axial strains are considered to be negligibly small.
- Longitudinal inertia effects are considered to be very small.
- Damping forces are not considered.
- Distortion of cross section in their own planes is not considered.

The need for high performance to weight ratio structures in the most advanced engineering applications leads to massive usage of composite materials for critical applications. The thin-walled composite I- beams are modelled and modal and harmonic analysis is done to know the effects of fibre angle, modulus ratio, height-to-thickness ratio on the vibration frequencies and mode shapes of the composites by using ANSYS, general purpose software. The different terminology used in analysis software is discussed below.

## **1.2. Convergence Criterion**

The solution should converge to the correct result, if the following three conditions are achieved or satisfied.

- The displacement function must be continuous within the element choosing polynomial for displacement model.
- The displacement function must be capable of representing rigid body displacement of the element i.e. When the nodes are given such displacement corresponds to a rigid body motion, the element should not experience any strain and hence leads to zero nodal forces. The constant terms in polynomials used for the displacement models would usually ensure this condition.
- The displacement function must be capable of representing constant strain states within the element when the body or structure is divided to smaller and smaller element. As the number of elements increases to infinity the strains in each element also approach to constant value.



Hence the assumed displacement function should include terms for representing constant strain states. For 1D, 2D, and 3D elasticity problems, the linear terms present in the polynomial satisfy the requirement.

### **1.3 Criterion of Finite Element Selection**

Element to be used is dependent on physical problem itself. Following are important considerations in the selection of type of element.

1. Number of degrees of freedom required.
2. Expected accuracy.
3. Easy in formulating the necessary equation.
4. Degree to which the physical structures can be modelled without approximation.

### **1.4 Defining the Layered Configuration**

The most important characteristic of a composite material is its layered configuration. Each layer may be made of a different orthotropic material and may have its principal directions oriented differently. For laminated composites, the fibre directions determine layer orientation.

Two methods are available to define the layered configuration:

1. By specifying individual layer properties
2. By defining constitutive matrices that relate generalized forces and moments to generalized strains and curvatures (available only for SOLID46 and SHELL99 )

### 1.4.1 Specifying Individual Layer Properties

With this method, the layer configuration is defined layer-by-layer from bottom to top. The bottom layer is designated as layer 1, and additional layers are stacked from bottom to top in the positive Z (normal) direction of the element coordinate system.

Occasionally, a physical layer will extend over part of the model only. In order to model continuous layers, these dropped layers may be modelled with zero thickness. A layered model showing dropped layer model with four layers, the second of which is dropped over part of the model, as shown in figure 1.1.

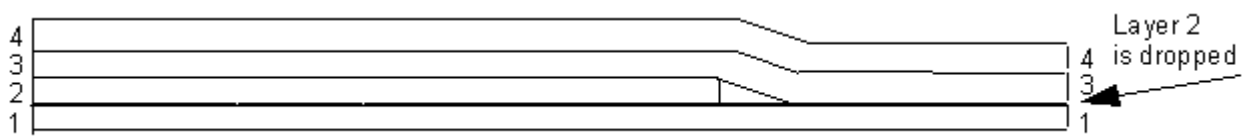


**Figure 1.1. Layered model showing dropped layer**

For each layer, the following properties are specified in the element real constant table of ANSYS, (Main Menu> Pre-processor> Real Constants) (accessed with REAL attributes).

- Material properties (via a material reference number MAT)
- Layer orientation angle commands
- Layer thickness

#### 1.4.1.1. Material Properties

As with any other element, the material properties command (Main Menu> Pre-processor> Material Props> Material Models > Structural > Linear > Elastic> Isotropic or Orthotropic) is used to define the linear material properties, and the TB command is used to define the nonlinear material data tables. The only difference is that the material attribute number for each layer of an element is specified in the element's real constant table. The linear material properties for each layer may be either isotropic or orthotropic. Typical fibre-reinforced composites contain orthotropic materials and these properties are most often supplied in the major Poisson's ratio form. Material property directions are parallel to the layer coordinate system, which is defined by the element coordinate system and the layer orientation angle and is described below.

#### **1.4.1.2. Layer Orientation Angle**

This defines the orientation of the layer coordinate system with respect to the element coordinate system. It is the angle (in degrees) between X-axes of the two systems. By default, the layer coordinate system is parallel to the element coordinate system. All elements have a default coordinate system which can be changed using the ANSYS element attribute (Main Menu> Pre-processor > Meshing > Mesh Attributes > Default Attributes).

#### **1.4.1.3. Layer Thickness**

If the layer thickness is constant, then specify the thickness at node. Otherwise, the thicknesses at the four corner nodes must be given as input. Dropped layers may be represented with zero thickness.

#### **1.4.2. Defining the Constitutive Matrices**

This is an alternative to specify the individual layer properties and is available as an option [KEYOPT (2)] for SOLID46 and SHELL99. The matrices, which represent the force-moment and strain-curvature relationships for the element, must be calculated outside the ANSYS program.

The main advantages of the matrix approach are:

1. It allows you to incorporate an aggregate composite material behaviour.
2. A thermal load vector may be supplied.
3. The matrices may represent an unlimited number of layers.

The terms of the matrices are defined as real constants. Mass effects are incorporated by specifying an average density for the element. If the matrix approach is used, detailed results in each layer cannot be obtained since individual layer information is not input.

## 1.5. Sandwich and Multiple-Layered Structures

Sandwich structures have two thin faceplates and a thick which is relatively weak core and the same is illustrated in Figure 1.2 .

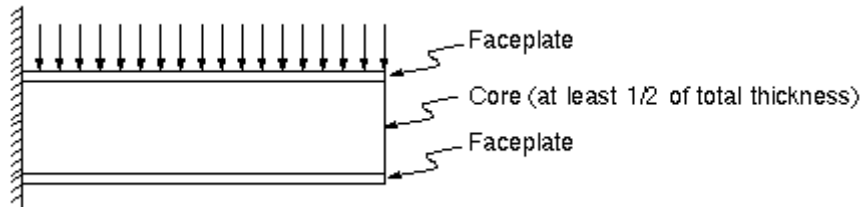


Figure 1.2. Sandwich Construction

The sandwich structures can be modelled with SHELL63, SHELL91, or SHELL181; SHELL63 has one layer but permits sandwich modelling through the use of real constants.

### 1.5.1. Node Offset

For SHELL91 and SHELL99 the node offset option locates the element nodes at the bottom, middle or top surface of the shell. The figures 1.3 shows layered shell with nodes at mid plane and Figure 1.4 shows the layered shell with nodes at bottom surface, and these surfaces are aligned.

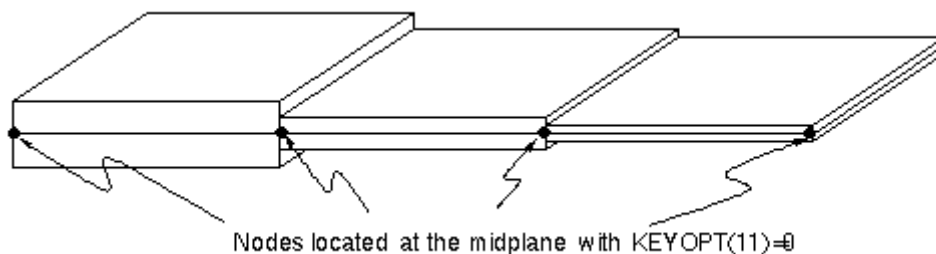


Figure. 1.3. Layered shell with nodes at mid plane

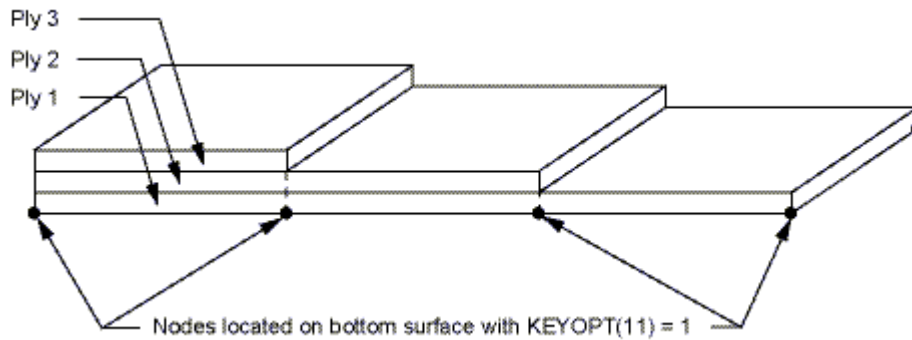


Figure 1.4. Layered Shell with Nodes at Bottom Surface

### 1.5.2. Specifying Failure Criteria

Failure criteria are used to learn if a layer has failed due to the applied loads. The failure criteria can be chosen from three predefined criteria.

The three predefined criteria are:

1. Maximum Strain Failure Criterion, which allows nine failure strains.
2. Maximum Stress Failure Criterion, which allows nine failure stresses.
3. Tsai-Wu Failure Criterion, which allows nine failure stresses and three additional coupling coefficients.

## 1.6. Introduction to Composites

Composite materials are formed by combining two or more materials that have quite different properties. The different materials work together to give the composite unique properties, but within the composite, the different materials are apart and they do not dissolve or blend into each other. Technically, the composite has both good [compressive strength](#) and good [tensile strength](#).

The threads of glass in fibreglass are very strong under tension but they are also brittle and will snap if bent sharply. The matrix not only holds the fibres together, it also protects them from damage by sharing any [stress](#) among them. The matrix is soft enough to be shaped with tools, and can be softened by suitable solvents to allow repairs to be made. Any deformation of a sheet of fibreglass necessarily stretches some of the glass fibres, and they are able to resist this, so even a thin sheet is very strong. It is also quite light, which is an advantage in many applications.

Over recent decades many new composites have been developed, some with very valuable properties. By carefully choosing the reinforcement, the matrix, and the manufacturing process that brings them together, engineers can tailor the properties to meet specific requirements. They can also select properties such as resistance to heat, chemicals, and weathering by choosing an appropriate matrix material.

### **1.6.1 Selection of material for Matrix**

For the matrix, many modern composites use thermosetting or thermosoftening plastics (also called resins). The use of plastics in the matrix explains the name 'reinforced plastics' commonly given to composites. The plastics are [polymers](#) that hold the reinforcement together and help to determine the physical properties of the end product. Thermosetting plastics are liquid when prepared but harden and become rigid (ie, they *cure*) when they are heated. The setting process is irreversible, so that these materials do not become soft under high temperatures. These plastics also resist wear and attack by chemicals making them very durable, even when exposed to extreme environments. Thermosoftening plastics, as the name implies, are hard at low temperatures but soften when they are heated. Ceramics, carbon and metals are used as the matrix for some highly specialised purposes. For example, ceramics are used when the material is going to be exposed to high temperatures in heat exchangers and carbon is used for products that are exposed to friction and wear in bearings and gears.

### **1.6.2 Materials for the reinforcement**

Although glass fibres are by far the most common reinforcement, many advanced composites now use fine fibres of pure carbon. Carbon fibres are much stronger than glass fibres, but are also more expensive to produce. Carbon fibre composites are light as well as strong. They are used in aircraft structures and in sporting goods (such as golf clubs), and increasingly are used instead of metals to repair or replace damaged bones. Even stronger (and more costly) than carbon fibres are threads of boron. Polymers are not only used for the matrix, they also make a good reinforcement material in composites. For example, Kevlar is a polymer fibre that is immensely strong and adds toughness to a composite. It is used as the reinforcement in composite products that require lightweight and reliable construction i.e., in structural body parts of an aircraft. Composite materials were not the original use for Kevlar

– it was developed to replace steel in radial tyres and is now used in bullet proof vests and helmets.

### **1.6.3. Manufacturing process**

Making an object from a composite material usually involves some form of mould. The reinforcing material is first placed in the mould and then semi-liquid matrix material is sprayed or pumped in to form the object. Pressure may be applied to force out any air bubbles, and the mould is then heated to make the matrix set solid. The moulding process is often done by hand, but automatic processing by machines is becoming more common. One of the new methods is called [pultrusion](#) (a term derived from the words 'pull' and 'extrusion'). This process is ideal for manufacturing products that are straight and have a constant cross section, such as bridge beams.

In many thin structures with complex shapes, such as curved panels, the composite structure is built up by applying sheets of woven fibre reinforcement, saturated with the plastic matrix material, over an appropriately shaped base mould. When the panel has been built to an appropriate thickness, the matrix material is then cured.

In many advanced composites, the structure may consist of a honeycomb of plastic sandwiched between two skins of carbon-fibre reinforced composite material. Such sandwich composites combine high strength, and particularly bending stiffness, with low weight and cost.

### **1.6.4. Advantages of composites**

- The greatest advantage of composite materials is strength and stiffness combined with lightness. By choosing an appropriate combination of reinforcement and matrix material, manufacturers can produce properties that exactly fit the requirements for a particular structure for a particular purpose.

- Composites are less likely to break up completely under stress than metals (such as aluminium). A small crack in a piece of metal can spread very rapidly with very serious consequences (especially in the case of aircraft). The fibres in a composite act to block the widening of any small crack and to share the stress around.
- The right composites also stand up well to heat and corrosion.
- Another advantage of composite materials is that they provide design flexibility.  
Example: a surfboard or a boat hull.

## 1.7. Classification of materials

Degree of anisotropy	Principal axes	Properties	Example
Isotropic	Orthogonal	Constant regardless of direction	Metals
Square symmetric	Orthogonal	Two different principal axes	Unidirectional fibres or woven cloth
Orthotropic	Orthogonal	Three different principal axes	Unidirectional weave with light weft
Anisotropic	Any angle	Constant relative to axes	Filament wound tube : Many crystals
Aeolotropic	Any angle	May change with position	Timber



## 1.8. Properties of composites

The different properties of the composites are listed below.

### 1.8.1. Fibre volume fraction ( $V_f$ ):

It is calculated by using the formula

$$V_f = \frac{nA_F}{\rho_f t}$$

where:

$n$  = the number of layers,

$A_F$  = the areal weight of the fabric,

$\rho_f$  = density of the fibre, and

$t$  = the thickness of the laminate

### 1.8.2. Areal Weight of a Fabric ( $A_F$ )

It is calculated by formula

$$A_F = 2N_f N_T \pi r_f^2 \rho_f$$

where, for a balanced fabric, the parameters are:

$N_f$  = number of filaments per tow

$N_T$  = number of tows in unit width of fabric

$r_f$  = radius of the fibre cross-section

$\rho_f$  = density of the fibre

### 1.8.3. Rule of Mixtures

The properties of composite can be calculated from rule of mixtures. It is given by

$$E_c = \eta_l \eta_o V_f E_f + V_m E_m$$

where

$E_c$  = Young's modulus of the composite

$E_f$  = Young's modulus of the fibre

$E_m$  = Young's modulus of the matrix

$V_f$  = fibre volume fraction

$V_m$  = matrix volume fraction ( $1 - V_f - V_v$ )

$V_v$  = void volume fraction

$\eta_l =$  [fibre length distribution factor](#)

$\eta_o =$  [fibre orientation distribution factor](#)

#### 1.8.4. Stacking sequence

There are a number of ways in which fibres can be arranged in order of increasing stiffness and strength.

- 3-D random: e.g. injection moulding grades.
- planar random: e.g. moulding compounds, chopped strand mat and continuous random swirl.
- quasi-isotropic: e.g. continuous fibres oriented at 0°/-45°/90°/+45° or 0°/60°/120°.
- bidirectional: e.g. woven fabrics or cross-ply unidirectional at 0°/90°.
- unidirectional: e.g. pultrusions and aligned fibre laminates.

The normal way to concisely record a laminate stacking sequence is as follows:

$$[0^\circ/+45^\circ/-45^\circ/90^\circ]_{ns}$$

where the subscripts are:

$n$  is the number of times the sequence is repeated

$s$  means the laminate is symmetric

$T$  is the total number of plies, and

overbar denotes that the laminate is symmetric about the mid-plane of the ply

Thus for  $n = 2$ , when  $*$  denotes the line of symmetry, the sequence will be:

$$0^\circ/+45^\circ/-45^\circ/90^\circ/0^\circ/+45^\circ/-45^\circ/90^\circ * 90^\circ/-45^\circ/+45^\circ/0^\circ/90^\circ/-45^\circ/+45^\circ/0^\circ$$

### 1.8.5. Young's modulus

Hooke's Law originally stated that the stress ( $\sigma$ ) is proportional to the strain ( $\epsilon$ ) with the constant of proportionality known as Young's modulus ( $E$ ), so that  $\sigma = E\epsilon$ . Traditional structural engineering materials are isotropic and hence the value of  $E$  is independent of direction. However, the Young's modulus of a composite material is anisotropic (varies with direction) and can be estimated using the rule-of-mixtures. The variation of young's modulus for fibre orientation is as shown in figure 1.1

$$E_c = \eta_l \eta_o V_f E_f + V_m E_m$$

where:

$E_c$  = Young's modulus of the composite

$E_f$  = Young's modulus of the fibre

$E_m$  = Young's modulus of the matrix

$V_f$  = fibre volume fraction

$V_m$  = matrix volume fraction ( $1 - V_f - V_v$ )

$V_v$  = void volume fraction

$\eta_l$  = fibre length distribution factor

$\eta_o$  = fibre orientation distribution factor

### 1.8.6. The fibre length distribution factor (FLDF)

It assumes that the matrix and fibre remain elastic and the interface bond is perfect, the shear stress at the fibre ends is maximum and falls to zero after half the "critical length", and the tensile stress at the fibre ends is zero and rises to a maximum after half the "critical length".

FLDF can be calculated using equation :

$$\eta_l = 1 - \frac{\tanh(\beta L / 2)}{(\beta L / 2)}$$

where

$$\beta = \frac{2\pi G_m}{E_f A_f \ln(R/R_f)}$$

$G_m$  = the shear modulus of the matrix,

$L$  = the fibre length,

$A_f$  = the cross sectional area of the fibre,

$R_f$  = the radius of the fibre and

$R$  = the mean separation of the fibres.

### 1.8.7. Critical length

The critical length (when there is no debonding) is given by the expression

$$l_c = \frac{R_f \sigma_{11}}{\sigma'_{12}}$$

where  $R$  = the fibre radius,

$\sigma_{11}$  = the tensile stress in the fibre and

$\sigma'_{12}$  = the shear strength (of the interface or of the matrix as appropriate).

### 1.8.8. Fibre orientation distribution factor

The fibre orientation distribution factor can be calculated

$$\eta_o = \sum_{i=0^\circ}^{180^\circ} V_f \cos^4 \theta_i$$

For a unidirectional ply, the rule-of-mixtures does assume that the fibres are continuous with uniform cross-section and lie parallel to each other. There is perfect bonding between the fibre and the matrix.

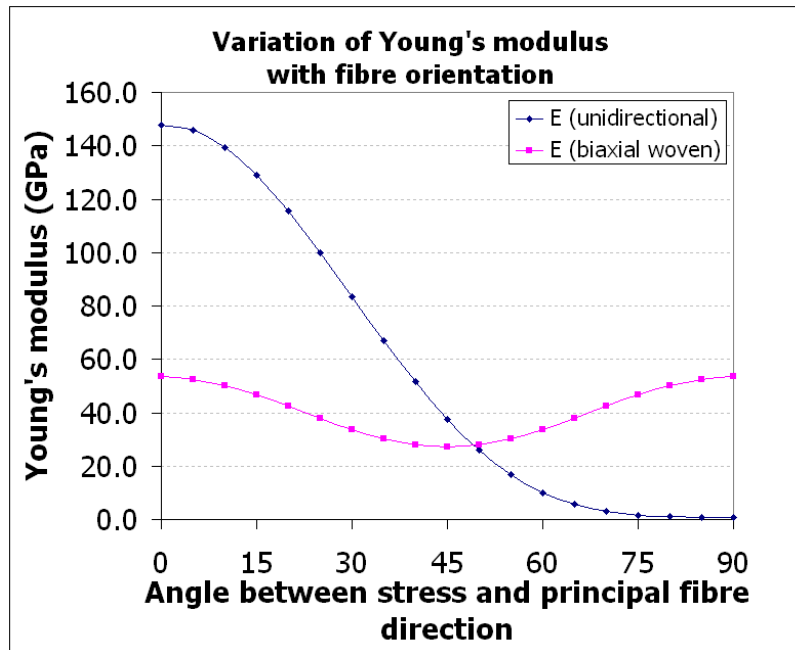


**Fig.1.1. Variation of young's modulus with fibre orientation.**

### 1.8.9. Shear modulus

The inter-relationship of the elastic constants for isotropic materials is given by

$$G = E/2(1+\nu)$$

$$K = E/3(1-2\nu)$$

where E = the Young's modulus,

G = the shear modulus,

K = the bulk modulus and

$\nu$  = Poisson's ratio.

For orthotropic materials within a single plane, the shear modulus is

$$G_{12} = \frac{\sqrt{E_1 E_2}}{2(1 + \sqrt{\nu_{12} \nu_{21}})}$$

### 1.8.10. Poisson's ratio

Poisson's ratio is denoted by the Greek letter  $\nu$ . It has a value determined by:

$$\nu = -(\text{strain normal to the applied strain})/(\text{strain parallel to the applied strain}).$$

Tensile deformation is taken as positive and compressive deformation is taken as negative. The minus sign in the definition of Poisson's ratio normally results in positive values of Poisson's ratio and a thermodynamic constraint which restricts the values to  $-1 < \nu < 1/2$ .

### **1.8.11. Bulk modulus**

The bulk modulus for a square symmetric material can be found by the following equation

$$K = \frac{\sqrt[3]{E_1 E_2 E_3}}{3(1 - 2\sqrt[3]{\nu_{12} \nu_{31} \nu_{23}})}$$

This equation reduces to the isotropic form when  $E_1 = E_2 = E_3$  and  $\nu_{12} = \nu_{21} = \nu_{23}$ .

## **1.9. Research problem and objectives:**

Besides the applications in the aeronautical and automobile industry, the application of composite materials has been enlarged, including new areas such as nautical industry, sporting goods, civil and aerospace construction. In order to find the right combination of material properties and in service performance, their dynamic behaviour of the composites need to be studied. To avoid structural damages caused by undesirable vibrations, it is important to determine the natural frequencies of the structure to avoid resonance, the mode shapes to reinforce the most flexible points and the right positions to reduce weight. With respect to these dynamic aspects, the composite materials represent an excellent possibility to design beams with requirements of dynamic behaviour.

### **1.9.1. Objectives:**

- The main objective of this thesis is to contribute for a better understanding of the dynamic behaviour of doubly symmetric composite I- beams.
- To know the influence of fibre orientation, elastic moduli and height to thickness ratio on natural frequencies of composite I- beams for uniform and tapered beams for various boundary conditions.
- To investigate the dynamic behaviour of the beams, experimental studies and numeric analysis using Finite element method have been carried out and the results are presented in detail. The experimental results of a cantilever glass-epoxy rectangular composite beam are used to validate the results obtained from finite element analysis .

### **1.10. Scope of the Current Research Work**

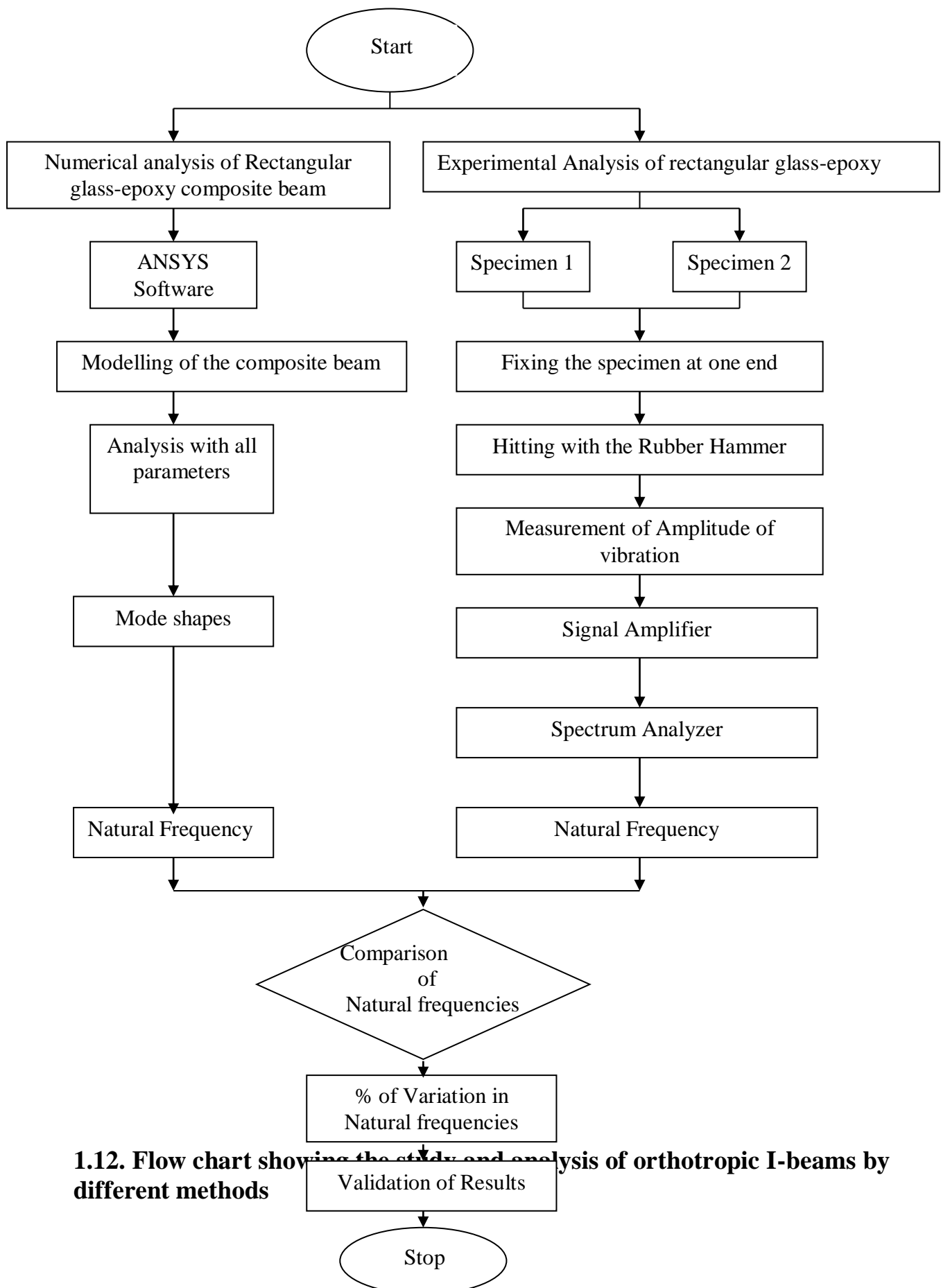
Since many years, the combination of different materials has been used to achieve better performance requirements. Although the benefits brought by the composite materials known , the present focuses the behaviour of composite I-beams is dealt in detail, and the influence of fibre orientation, elastic moduli and height to thickness ratio on natural frequencies of composite beams. The modal analysis and harmonic analysis is done by changing the fibre angle in top and bottom flanges, the effect of fibre angle rotation in web of simply supported composite I-beams. The effect of Elastic modulus ratio and height to thickness ratio of composite beams on the natural frequencies for a simply supported and clamped composite beams were investigated with the stacking sequence of the top and bottom flanges at  $[0/90]$  keeping the web unidirectional.

Further, the study was extended to know the effects of fibre orientation, modulus ratio for a cantilever composite I – beam with a small end fixed on natural frequencies and mode shapes. The natural frequencies and mode shapes of the same cantilever I beam were obtained when its bigger end is fixed, with the same parameters. The dynamic analysis is extended to know the behaviour and mode shapes of a composite I-beam with circular holes in web with the same dimensions, parameters and boundary conditions.

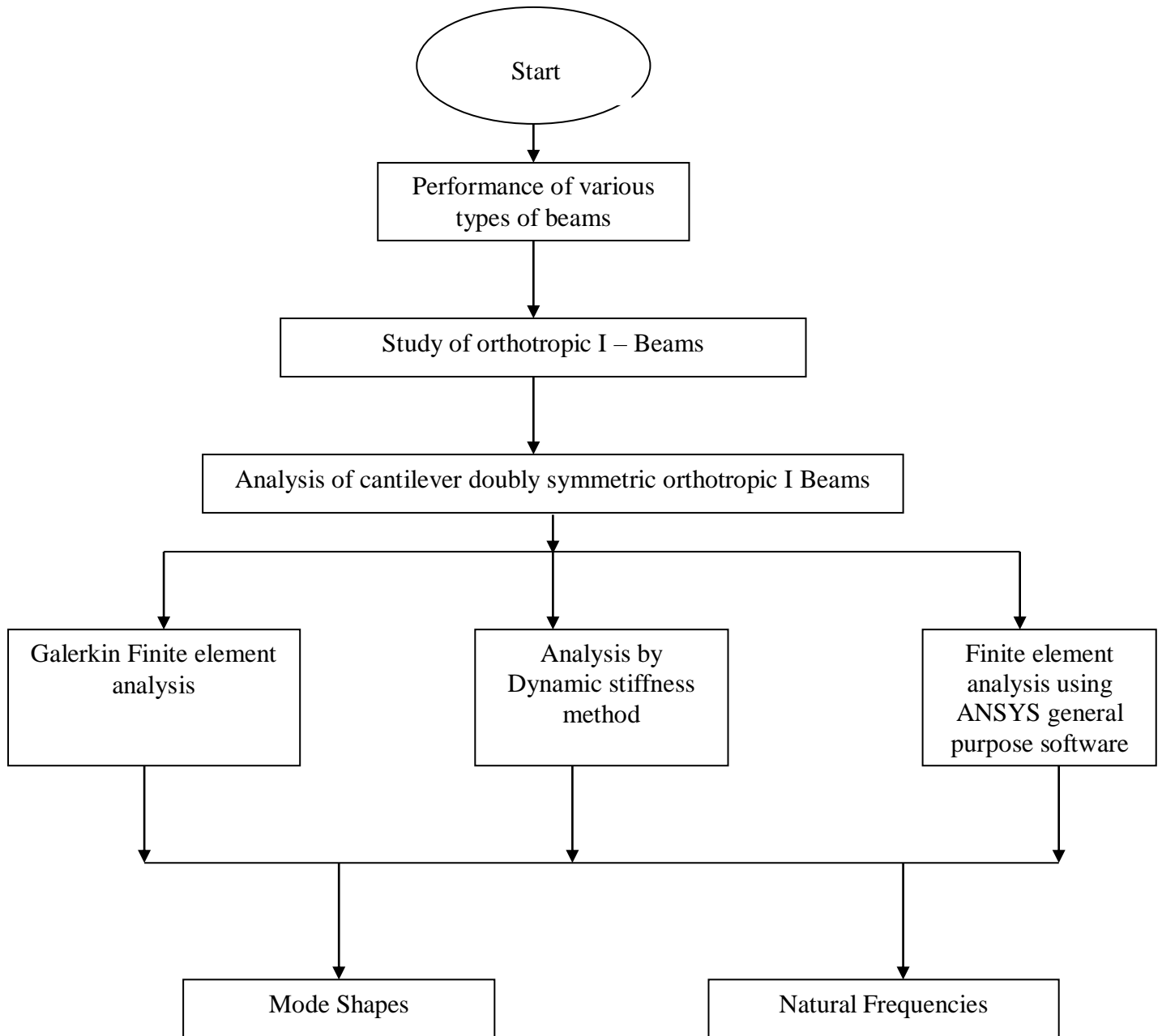
The flow charts 1.8 shows the numerical analysis and experimental analysis plan of verifying the results and validation for rectangular glass-epoxy composite laminates. The flow chart 1.9 shows the study of orthotropic I-beams by different methods namely Galerkin Finite Element Analysis, Dynamic stiffness method and Finite element analysis using ANSYS with various boundary conditions. The flow chart 1.10 shows the detailed plan of total research work in thesis.



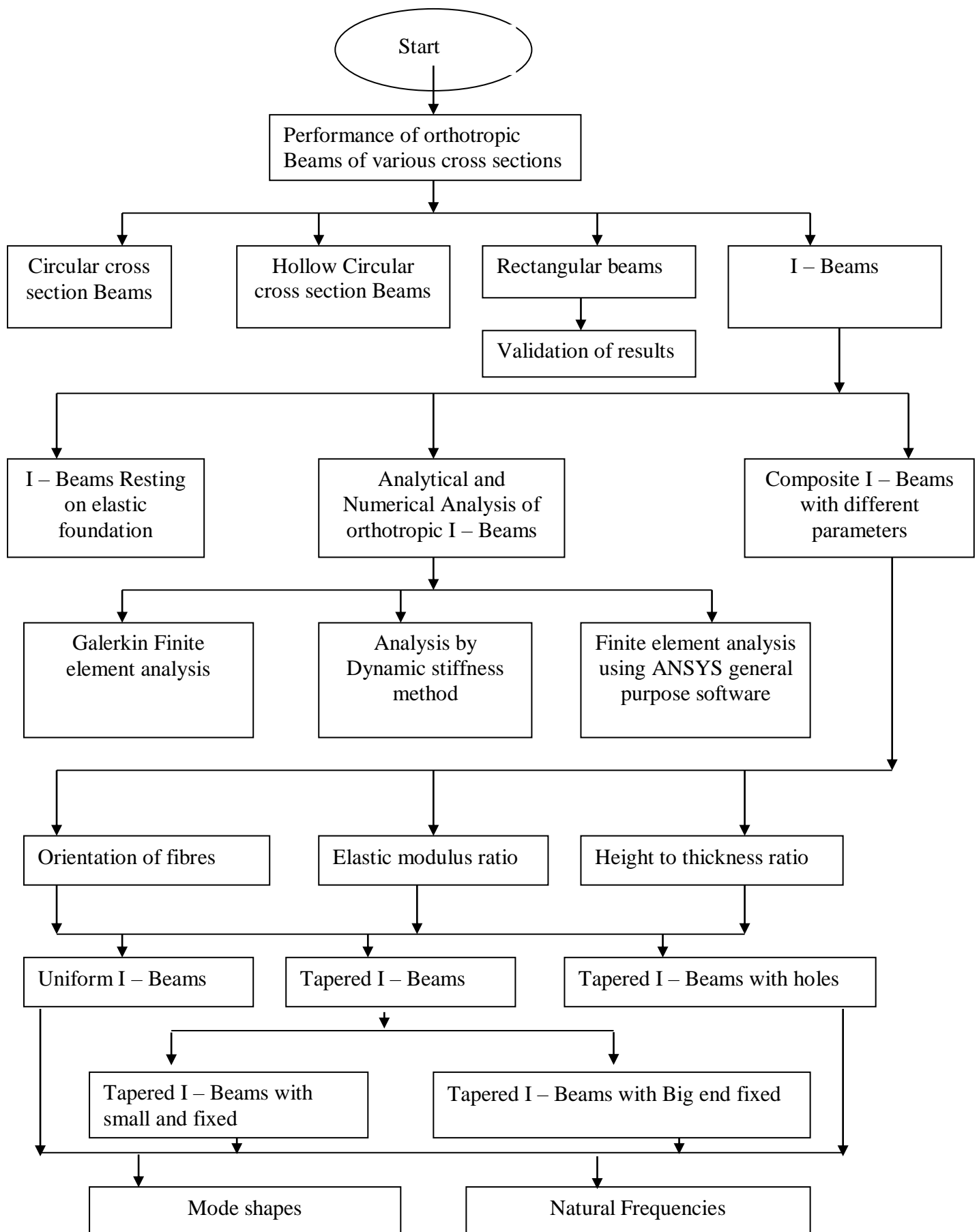
### 1.11. Flow chart showing the numerical and experimental plan



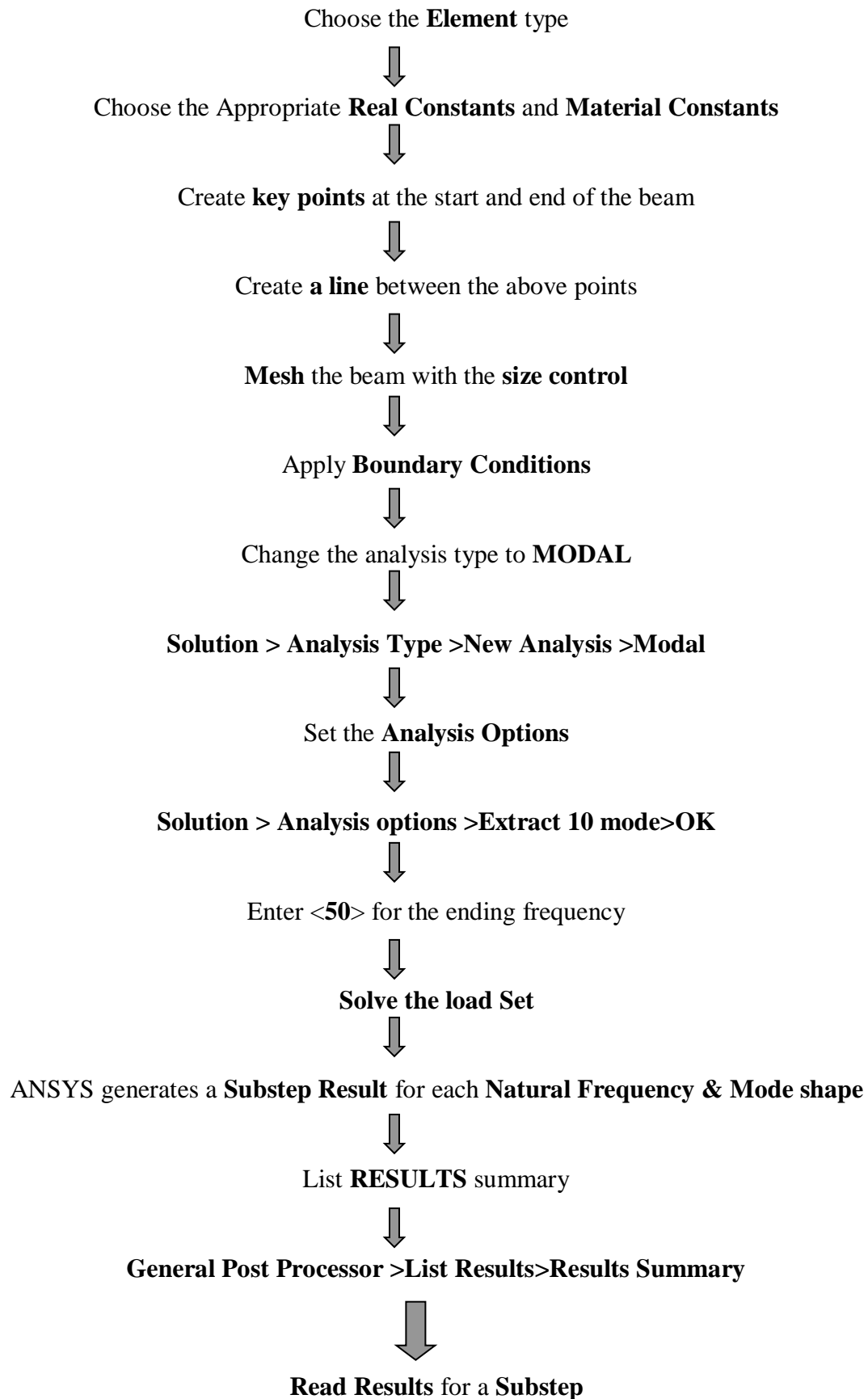
### 1.12. Flow chart showing the study and analysis of orthotropic I-beams by different methods



### 1.13. Flow chart showing the detailed plan of thesis



### 1.14. Flow chart to show the Procedure to do Modal analysis using ANSYS





**General Post Processor > Read results > First Set**



**PLOT deformed geometry**

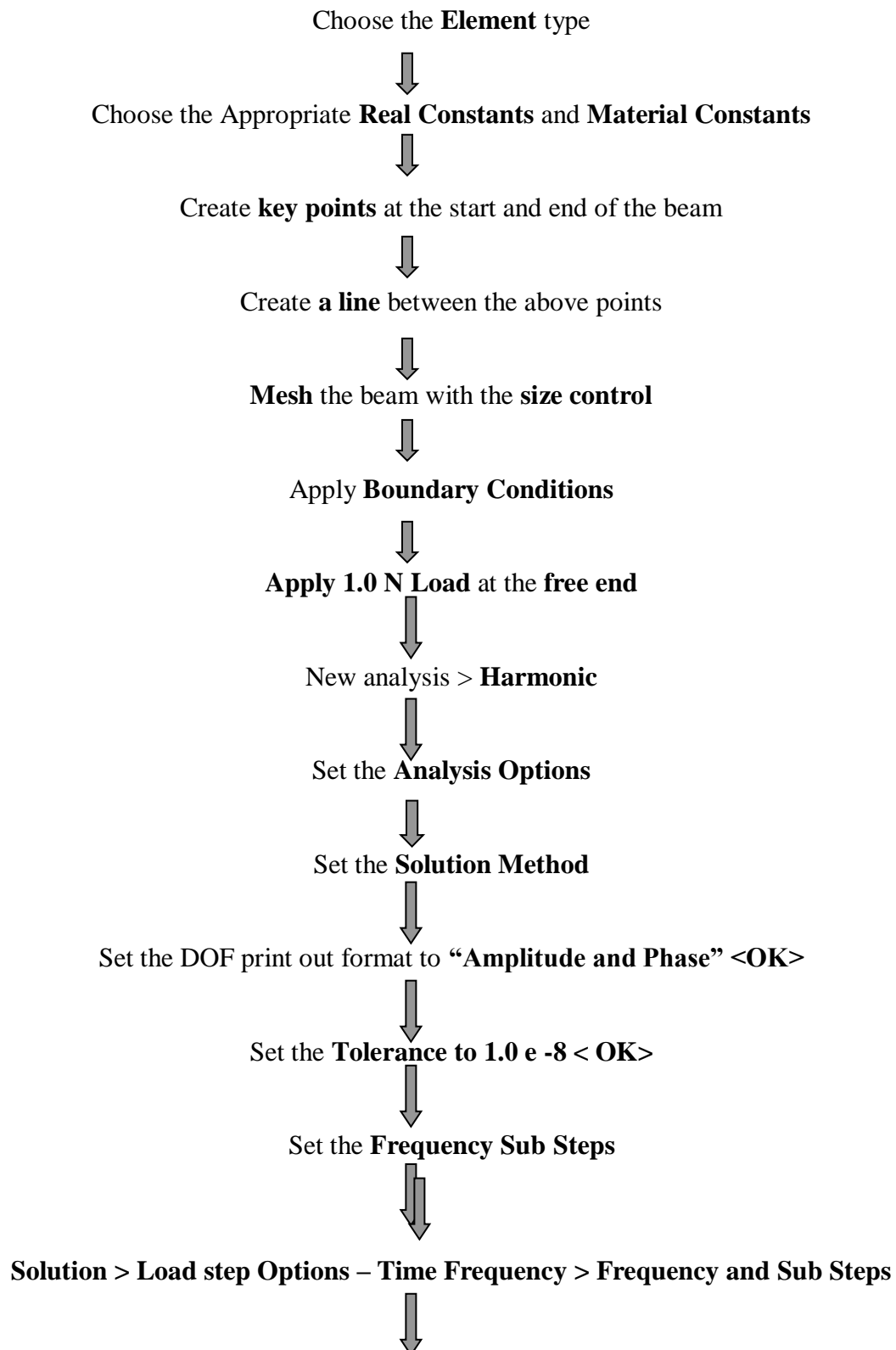


**Read Results for Next Substep**



**General Post Processor > Read results > Next Set**

### 1.15. Flow chart to show the Procedure to do Harmonic analysis of a Cantilever beam using ANSYS



**Set the Harmonic Frequency Range 0-50 Hz**



**Set the Number of Sub steps to 100**



**Set to be Stepped**



**SOLVE the model**

## 1.16. Organisation of the thesis

The thesis is organized in the following manner.

**Chapter-1** covers the importance, background and the present status of research in the fields relevant to the present work. It starts with the importance of thin walled isotropic beams, assumptions made to develop a model for composite beams in particular for I-section. The flow charts clearly explain the steps adopted for experimental analysis , orthotropic I-beams by different methods, presentation of work in thesis, modal and harmonic analysis of cantilever beams.

**Chapter-2** presents the literature survey on finite element modeling and simulations and vibrations of composite beams of open and closed section including isotropic and composite beams. This chapter reviews the extent of literature that is relevant to the problem, which the author intends to investigate. About 131 papers were referred and are given in reference section at the end of the thesis. In particular, the literature pertaining to composite beams of open and closed sections was considered.

**Chapter-3** covers the scope of the research work which includes modelling of isotropic beams resting on elastic foundation. Basic governing equations for various boundary conditions are derived in this chapter. The mode shapes for Indian standard I- beams (uniform and tapered) are modelled using ANSYS and are shown.

**Chapter 4** illustrates the experimental set up to conduct impact test for cantilever rectangular glass-epoxy composite laminated beam .The experiment is conducted with glass-epoxy specimens with different stacking and results are obtained and tabulated. These results are validated by finding the percentage variation with numerical results obtained by ANSYS .Therefore the numerical values are in good agreement with experimental results. Hence, the research work was extended for composite I-beams (both uniform and tapered beams) assuming the above validation.

**Chapter 5** emphasises Galerkin's finite element formulation of orthotropic I-beams and governing equations for tapered cantilever isotropic I-beam. Analytical results are presented for various different conditions.



**Chapter 6** presents a dynamic stiffness matrix method has been developed for computing the natural frequencies and buckling loads of thin-walled beams resting on continuous elastic foundation and can be applied for treating beams non-uniform cross section and also non-classical boundary conditions.

**Chapter 7** presents mathematical modeling of composite I-Beam and the Stiffness Equation of a  $K^{\text{th}}$  orthotropic lamina in the laminate coordinate system are developed and explicit expressions for I-section are given. Finite element formulation and the closed form expressions for vibration frequencies of a simply supported anisotropic beam, expressions for axial frequency, flexural frequencies in x and y directions, and the torsional vibration frequency are presented.

**Chapter 8** covers the effect of various parameters namely fibre orientation, modular ratio and height to thickness ratio on natural frequencies of composite I- beams and mode shapes are shown for cantilever boundary condition. The harmonic analysis is done for doubly symmetric composite I-beam.

**Chapter 9** deals with modelling of tapered composite I-beam with its small end fixed and modal and harmonic analysis are carried out using ANSYS R10.0, the analysis software. The results obtained are presented in graphical form.

**Chapter 10** deals with modelling of tapered composite I-beam with its small end free and big end fixed .Modal and harmonic analysis are carried out using ANSYS R10.0, the analysis software. In this chapter, a case study is done for a cantilever composite I-beam with three holes of diameter 32 mm in web. Modal and harmonic analysis is done and compared.

At the end of the thesis, discussion on results, conclusions, future scope of work, author's index, and references are presented.

**Chapter 2**  
**LITERATURE REVIEW**

# LITERATURE REVIEW

In the literature survey, it is found that thin-walled beams of open cross-section, such as I-section beams, are susceptible to instability in a variety of modes, but a few publications have dealt with dynamic behaviour of such members. Closed-form solution for flexural and torsional natural frequencies of isotropic thin-walled beams is found in the literature [4-6]. However, the research was limited to doubly symmetric beams with simply supported boundary conditions. Free vibration of thin-walled beams with variable I-section by finite element method was studied by Wekezer [4,5]. Ohga et al. [7] presented an analytical procedure to estimate the natural frequencies and mode shapes of thin-walled members using the transfer matrix method and various types of cross-sections of thin-walled members including C-section, box-section and I-section were analyzed.

The literature mentioned in the list dealt with free vibration of isotropic metallic thin-walled beams. For composite thin-walled beams, the flexural and torsional vibrations are fully coupled in general, even for a doubly symmetric cross-section due to their material anisotropy. Only a few works have addressed the dynamic behaviour of composite thin-walled members. Bauld and Tzeng [8] extended Vlasov's thin-walled bar theory [9] to symmetric fibre-reinforced laminates to derive buckling equations of composite thin-walled beams. In addition, the differential equations for the general case of tapered wide-flanged beam columns have been derived using the Vlasov's method [9] for uniform beams. An experimental investigation of the elastic stability of tapered beam columns has also been investigated. Song and Librescu [10] proposed an analytical model to predict free vibration behavior of laminated composite thin-walled beams of open sections. They investigated natural frequency and mode shape with respect to the fibre orientation for composite box-section beams. Recently Lee and Kim [11] presented a general analytical model to predict buckling loads and mode shapes of thin-walled composites.

Xi-Xian Wu and C.T. Sun [13] gave the simplified theory for composite beams in 1992. Torsional vibrations of beams and cracked beams were dealt in detail by J.M. Gere [14]. Pratyosh Gupta, Wang S.T., Blandford, G.E. [15] gave the detailed study of Torsional Buckling of Non-Prismatic I-Beam and derived the equations for various boundary conditions.

Shakourzadeh ,et al [16] deduced torsion bending element for thin-walled beams with open and closed cross sections. He also studied the torsional vibration of beams with doubly symmetric cross section for which the shear centre and centroid coincide and analysed the effect of warping on the frequencies of torsional vibrations and shapes of the normal modes of vibration for bars of single span with various conditions. Derivation of the fundamental theory of strength and stability of thin-walled members was performed Xie (20) presented nonlinear normal modes of a clamped –clamped beam for large amplitude displacements. Naidu ,chen,Banerjee [21-24] have studied the free vibration of thin walled beams with axial loading and extended this to beams subjected to torsion and bending. Banerjee [25] has developed the dynamic stiffness matrix method for an axially loaded Timoshenko beam element. He has considered the case of coupled bending and torsion for the beam in his basic governing differential equations. The detailed procedure for analysis of orthotropic and anisotropic beams using various elements listed in ANSYS [26] library.

The results obtained for the fundamental normal mode are compared with the corresponding reported experimental and theoretical studies. Godier, Timoshenko,Vlasov and others. Free Torsional Vibrations of Tapered Cantilever I-beams and its formulation is given by Kameswara rao and Mirza [38].Timoshenko[52] initiated the concept of non uniform torsion and considered warping of cross sections of a symmetrical I-beam subjected to torsional moment. Wagner [53] generalised the Timoshenko torsion theory. The finite element method has been shown by Barsoum [54], and Barsoum and Gallagher [62] ,to be completely general, in that they had provided results that are sufficiently accurate for engineering purposes.

Gere and Carter[57] obtained the critical buckling loads for tapered columns. A finite element formulation using Galerkin's method for the buckling problem of tapered members was presented by Morrel and Lee. Gere and Lin [56] generalised the theory of vibrations of thin-walled beams of an arbitrary open section. Goodier [58] published a series of studies in which he simplified and proved some of the assumptions proposed by earlier investigations. Nowinski[60] and Panovko[61] have studied several literature papers related to the theories of thin-walled beams in which they have focussed on optimum design of tapered thin-walled beams.

H.N.Lee [63] presented an analysis of non-uniform torsion of tapered I-beam in 1956, the taper being only of a restrictive type. Using the finite element technique, Krajcinovic[ 64] ,

developed a formulation for thin-walled members based on the hyperbolic functions to express the twist. These functions which are the solutions to the exact differential equation for twist, lead to complicated stiffness expressions in torsional and warping constants. It does not include the effects of instabilities due to torque. The formulation is only applicable to solid beams where the shear centre coincides with the centre of gravity. The investigations done prior to the year 1945 related to lateral stability and flexural –torsional stability of uniform thin-walled beams were compiled and consolidated by Timoshenko [68]. Valsov's extensive investigations of thin-walled elastic members were published in book form in 1940. A new edition containing comprehensive study of equilibrium, stability and vibrations of thin-walled members of arbitrary cross sections was published in 1958.

Static torsional response and lateral-torsional stability of tapered I-beams has been investigated by many researchers [65-72]. Hamaychi [66], Lee and Szabo [67], Wilde [68] presented basic derivations for a comprehensive theory of non-uniform torsion of tapered I-beams. Among these, Massey and McGuire [70] studied the lateral stability of stepped cantilever beams of rectangular and I-cross-section using a Runge Kutta integration procedure. The problem of lateral-torsional buckling of tapered I-beams has been studied by Kitipornchai and Trahair [71], Brown [72], Culver and Preg [46] and Shiomi and Kurata [47]. In these studies, solutions were obtained for simply supported and cantilever beams using finite-difference or finite-integral methods. A review of the literature clearly shows that very few studies [73-74, 38] have been conducted on the free vibration characteristics of non-uniform thin-walled beams. Several investigations [84-86] have been reported on torsional vibrations and stability of long uniform thin-walled open section beams, such as I-beams.

Wiedemann (76) was presented generalised method and analytical solution is also presented for the natural frequencies ,mode shapes and orthogonality conditions of an arbitrary system of Euler-Bernowli's beams inter connected by arbitrary joints and subjected to boundary conditions. Prokic (77) derived the governing equations for coupled bending and torsional vibrations for simply supported beams. Claeysen (79) determined the modes of uniform beam described by Euler-Bernoulli model with axial force or Timoshenko Model in a unified manner with the use of a fundamental free response. Several authors have studied vibration of beams masses. Goel (80) investigated the free vibration of a beam –mass system hinged at either end by rotational springs and arbitrarily located heavy mass. Chang (82)

analysed the vibrations of a mass loaded system with a heavy tip mass by using Laplace Transform.

Lin (83) derived the exact governing equations for linear vibrations of a rotating Timoshenko beam by the d'Alemberts principle and Virtual Work Principle, on the assumptions that the beam is linear elastic and the steady state axial strain is small. Prokic(84) considered the problem of thin walled beams of closed sections by means of exact solution and the differential equations are derived from the principle of virtual work due to variation of displacements, for the case of simply supported beam. Gurgose (84) studied the natural frequencies of restrained beam and rods with point masses. Dynamic stiffness matrix of a moving beam is developed and investigated the free flexural vibration characteristics by Banarjee(85),

Law, S.S., (86) investigated the dynamic behaviour of a bolted joint which has flexibility in both the tangential & rotational directions the joint is prestressed with a axial tension in the bolt shank. The formulation of a hybrid beam column element including the end springs is presented, and the dynamic behaviour of a cantilevers beam with nonlinear semi rigid joint is studied, The natural frequencies & node shapes remain relatively unchanged only for a limited range of the joint stiffness. Mei, C. (88) presented the wave vibration analysis of axially loaded bending torsion coupled composite beam structures, including the effects of axial force, shear deformation and rotary inertia & this study was limited for a axially loaded Timoshenko composite beam. The study also includes the material coupling between the bending tensional modes of deformation that is usually present in laminated composite beam due to ply orientation.

The classical single-mode elliptic function frequency solutions for simply supported beams and square plates are assessed and the characteristics of non linear response are studied. Magadi Mohareb,M(89) , developed a finite element formulation that captures both the St.Venant and warping torsional effects of open sections. The formulation is applicable to prismatic thin-walled open sections commonly used in steel construction and is able to represent general torsional and warping end restraints. Gere,J.M.(90) studied the free torsional vibrations of bars of thin walled open cross section for which the shear centre and centroid coincide, for I-beams and Z-sections. The differential equations for torsional vibrations are derived including the effect of warping. The effects of warping on frequency of vibration are

determined for bars of single span with various end conditions. For a simply supported bar, a formula for the principal torsional frequencies and an expression for mode shape are derived.

Prasad, K.S.R.K.,(91) studied the analysis of Eigen value problems such as free vibration problems, and exact solutions of the governing differential equations are possible only in special cases and presented a comparative study of some commonly used approximate methods. A comparative study of Raleigh Ritz method and iterative type approximate methods for the evaluation of Eigen values has been made with the aid of examples. Kwok-Tung Chen (92) derived the equation of free transverse vibration of beams with two sections of partially distributed mass and its exact solution has been obtained. Experimental data for a cantilever beam are given to verify the computational results. Yuchengshi(93), presented a multimode time-domain modal formulation based on the finite element method for large amplitude free vibrations of thin composite plates. Banerjee (94) presented an exact stiffness matrix for a composite Beamed including the effects of shear deformation and rotatory inertia, for a Timoshenko beam. An explicit analytical expression for each of the elements of the dynamic stiffness matrix is derived by use of REDUCE computing package. Hamed, E (95) investigated analytically dynamic behaviour of reinforced concrete (RC) beams strengthened with externally bonded composite materials. The equations of motion along with the boundary & continuity conditions are derived using Hamilton's variational Principle and the Kinematic relations of small deformations the mathematical formulation also includes the constitutive laws that are based on beam & laminations theories, and the two – dimensional elasticity representation of the adhesive layer including the closed form solution of its stresses displacement.

Banerjee[95] has developed the exact dynamic stiffness matrix method of approach for composite Timoshenko beams and has considered all boundary conditions. Arpaci,A(96) presented an exact analytical method for predicting natural frequencies of beams with thin-walled open cross sections having no axis of symmetry. The governing equations give a characteristic equation of the 12<sup>th</sup> order with real coefficients. The roots are found numerically and the exact boundary conditions are considered especially for free ends to obtain natural frequencies. Li [97] has studied the free torsional vibrations of open cross section and also derived expressions including the effect of warping. Abbas[98] has extended the study of vibrations of Timoshenko beams with elastically restrained ends and Lee S Y[99] extended his study for non uniform beams with elastically restrained ends. Bishop and Price



(100), and Banerjee and Williams (101) have taken into the effects of rotary inertia and transverse shear. Warping stiffness has been neglected in both works. A recent study carried on by Bercin and Tanaka (102) has included the effect of warping in doubly coupled vibration analysis of Timoshenko beams with monosymmetric open cross sections. In case of triple coupling, where the flexural vibrations in two mutually perpendicular directions and the torsional vibrations are all coupled is dealt with by Arpacı and Bozdağ(103). This is experienced when the cross sections of no symmetry are of concern.

Kameswara Rao [104-112] has studied the torsional vibrations and stability of lengthy thin walled beams on elastic foundation. He has developed the governing equations for the short wide flanged thin walled beams of open sections. He also studied the effects of longitudinal inertia and shear deformation. He has derived the equations to find vibration frequencies and mode shapes for generally restrained Bernouli beams. Then, he deduced the equations for frequency analysis of Clamped-Clamped uniform beams with intermediate elastic support. The same concept was extended to two span uniform Euler-Bernouli beams. He has also considered non linear torsional vibration of thin walled beams of open sections.

To avoid structural damage caused by undesirable vibrations and resonance, it is important to determine the natural frequencies of the structure. The mode shapes must also be determined in order to reinforce the most flexible points or to determine the right positions where is necessary to reduce weight or to increase damping [113]. Sahu and Asha (2005) [114], used eight-noded isoparametric quadratic shell element to develop the finite element procedure, to investigate the vibration and stability behaviour of pretwisted panels, the effect of various geometrical parameters like angle of twist, aspect ratio, lamination parameters, shallowness ratio are studied. Tita (2003) [115] worked on the theoretical and experimental dynamic analysis of reinforced epoxy resin. He used laminates in his study. The laminates were fabricated by hand-lay-up process and cut to beam shape specimens. The specimens were used as free-end beams in the vibration measurements. He calculated the mechanical properties of the composite analytically and used them in his simulations of the dynamic properties. He presented his ANSYS® simulation results in contour format showing the mode types and shapes.

Colakoglu (2006) [116] performed vibration experiments on 10-layer beam specimens of glass polyethylene composite at a range of temperatures. The vibration was induced by the impact of spherical steel ball hammer. ANSYS® numerical simulations were also used to

obtain the frequency response. Teng and Hu (2001) [117] analyzed the design parameters for constrained layer damping structures by employing the Ross-Kerwin-Ungar (RKU) model. They also discussed the effects of temperature, frequency and the dimensions of damped structures on vibration damping characteristics.

### **Chapter 3**

# **VIBRATIONS OF A THIN-WALLED I-BEAM RESTING ON ELASTIC FOUNDATION**

# VIBRATIONS OF A THIN-WALLED I-BEAM RESTING ON ELASTIC FOUNDATION

### 3.1. Introduction

Static and dynamic analysis of beams resting on elastic foundation occupies a prominent place in contemporary structural mechanics. The vibrations and buckling of continuously supported finite and infinite beams resting on elastic foundation has an application in the design of highway pavements, aircraft runways and in the use of metal rails for rail road tracks. The vibrations of beams resting on elastic foundation have been investigated by a number of investigators. In these studies, it has been mostly assumed that the foundation reacts in tension as well as compression. Various types of foundation models such as Winkler, Pasternak, Vlasov, Filonenko-Borodich, etc., have been used in the analysis of structures on elastic foundation. Among these, the Winkler model, in which the medium is taken into account as a system composed of infinitely close linear springs, is the simplest and is adopted for analysis. It assumes that the foundation applies only a reaction normal to the beam that is proportional to the beam deflection.

### 3.2. Derivation of basic differential equation:

As the cross sectional dimensions are assumed to be small compared to the length in thin-walled beams, the second order effects such as longitudinal inertia and shear deformation can be treated as negligible.

In this work, based on Timoshenko's torsion theory, the governing differential equation of free motion of a doubly symmetric thin-walled I-beam on elastic foundation subjected to a time- invariant axial compressive load is derived based on Hamilton's principle.

According to Hamilton's principle,

$$(\dot{T}_k - \dot{U} + \dot{W})dt = 0 \quad (3.1)$$

Where  $T_k$  = kinetic energy of the strained bar,

$U$  = total strain energy,

$W$  = the potential energy of the external force, and

$t_0, t_1$  are fixed constants.

According to Saint-Venant, the cross- sections are assumed to rotate about the

Centroid –shear centre 'O', giving rise to a torsional couple,

$$T_s = G C_s (\partial\phi/\partial z) \quad (3.2a)$$

Where  $G$  = shear modulus,

$C_s$  = torsion constant for the cross section,

$\phi(z,t)$  = the angle of twist

The torsion constant for an I- section is

$$C_s = (2bt_f^3 + ht_w)/3 \quad (3.2b)$$

Where  $b$  = width of the flanges,

$t_f$  = thickness of flanges

$h$  = height between the centre lines of the flanges.

$t_w$  = thickness of the web.

The strain energy  $U_1$  at any instant  $t$  in the beam of length  $L$  due to saint - Venant torsion is

$$U_1 = (1/2) \int_0^L G C_s (\partial\phi/\partial z)^2 dz \quad (3.2c)$$

Accompanying the rotation in a warping of the section which is assumed constant in each piece of cross- section having a moment  $M$ . and the X- displacement of the top flange

center line,  $U$ , is given by,  $U = (h/2) \phi$  (3.2d)

And hence the moment  $M$  in the top flange is given by

$$M = E I_f (\partial^2 u / \partial z^2) = E I_f (h/2) (\partial^2 \phi / \partial z^2) \quad (3.2e)$$

Where  $E$  = Young's modulus,

$I_f$  = moment of inertia of each flange area about y-axis.

The shear force  $Q$  due to the bending of the flanges is given by

$$Q = (\partial M / \partial z) = E I_f (h/2) (\partial^3 \phi / \partial z^3) \quad (3.2f)$$

The equal and opposite shear forces  $Q$ , a distance  $h$  apart in the top and bottom flanges, give rise to torque due to warping,  $T_w$ , is given by

$$T_w = - Q_h = - E I_f (h^2/2) (\partial^3 \phi / \partial z^3) = - E C_w (\partial^3 \phi / \partial z^3) \quad (3.2g)$$

where  $C_w = I_f (h^2/2)$  = warping constant for an I-section

The total torque,  $T_t$ , on the cross section is given by

$$T_t = T_s + T_w = GC_s (\partial\phi/\partial z) - E C_w (\partial^3\phi/\partial z^3) \quad (3.2h)$$

If  $U_2$  is the strain energy of the two flanges due to warping, then

$$U_2 = \frac{1}{2} \int 2EI_f (\partial^2\phi/\partial z^2)^2 dz = \frac{1}{2} \int E C_w (\partial^2\phi/\partial z^2)^2 dz \quad (3.2i)$$

The strain energy  $U_3$  due to the Winkler type elastic foundation, is given by

$$U_3 = \frac{1}{2} \int K_t (\phi)^2 dz \quad (3.2j)$$

Hence the total strain energy  $U$ , at any instant  $t$  becomes

$$U = U_1 + U_2 + U_3 = \frac{1}{2} \int [GC_s (\partial\phi/\partial z)^2 + E C_w (\partial^2\phi/\partial z^2)^2 + K_t (\phi)^2] dz \quad (3.2)$$

The kinetic energy of rotation of the cross section at the corresponding instant  $t$  is given as:

$$T = \frac{1}{2} \rho I_p (\partial\phi/\partial t)^2 dz \quad (3.3)$$

Where  $I_p$  is the polar moment of inertia of the cross section and

$\rho$  the mass density of the material of the beam.

The potential energy due to the external time – invariant axial compressive load,  $P$ , acting at the centroid of the cross section at the corresponding instant  $t$  is given by

$$W = \frac{1}{2} \int (PI_p / A) (\partial\phi/\partial z)^2 dz \quad (3.4)$$

Where  $A$  is the area of the cross section

Substituting for  $T_k$ ,  $U$  and  $W$  from the above equations in the equation (1), taking the variations of the integrand and integrating the first term by parts with respect to 't' and the next four terms with respect to 'z', we get,

$$\left. \begin{aligned} & \int \int \left\{ \int \left[ GC_s - \rho I_p / A \right] \left( \frac{\partial^2 \phi}{\partial z^2} \right) - EC_w \left( \frac{\partial^4 \phi}{\partial z^4} \right) - K_t (\phi) - \rho I_p \left( \frac{\partial^2 \phi}{\partial t^2} \right) \right\} \delta \phi dz dt \\ & + \int \rho I_p \left( \frac{\partial \phi}{\partial t} \delta \phi \right) dz - \int EC_w \left( \frac{\partial^2 \phi}{\partial z^2} \right) \delta \left( \frac{\partial \phi}{\partial z} \right) dt \\ & - \int \left\{ (GC_s - PI_p / A) \left( \frac{\partial \phi}{\partial z} \right) - EC_w \left( \frac{\partial^3 \phi}{\partial z^3} \right) \right\} \delta \phi dt = 0 \end{aligned} \right\} \quad (3.5)$$

Assuming that the values of  $\phi$  given at the two fixed instants, the second integral vanishes. If the boundary conditions are such that the third and fourth integrals also vanish, then the associate differential equation of motion is given by:

$$\left( GC_s - \rho I_p / A \right) \left( \partial^2 \phi / \partial z^2 \right) - EC_w \left( \partial^4 \phi / \partial z^4 \right) - Kt(\phi) - \rho I_p \left( \partial^2 \phi / \partial t^2 \right) = 0 \quad (3.6)$$

### 3.3. Natural boundary conditions

In deriving the basic differential equation of motion (6) from equation.(5) it was assumed that the expressions

$$EC_w \left( \partial^2 \phi / \partial z^2 \right) \delta \left( \partial \phi / \partial z \right) \text{ and } \int \left[ \left( GC_s - \rho I_p / A \right) \left( \partial \phi / \partial z \right) - EC_w \left( \partial^3 \phi / \partial z^3 \right) \right] \delta \phi$$

Vanish at the ends  $z = 0$  and  $z = L$ . these conditions are satisfied if at the two ends

$$\left( \partial^2 \phi / \partial z^2 \right) \delta \left( \partial \phi / \partial z \right) = 0 \quad (3.7)$$

$$\text{and} \left[ \left( GC_s - \rho I_p / A \right) \left( \partial \phi / \partial z \right) - EC_w \left( \partial^2 \phi / \partial z^2 \right) \right] = 0 \quad (3.8)$$

Equations (3.7) and (3.88) give the natural boundary conditions for the finite bar, and are satisfied if the end conditions are taken as

$$(1) \phi = 0 \text{ and } \left( \partial^2 \phi / \partial z^2 \right) = 0 \quad (3.9)$$

These conditions imply restraint against rotation but not against warping; that is, the end of the bar does not rotate but is free to warp. This is the case of a “simple support”.

$$(2) \phi = 0 \text{ and } (\partial\phi/\partial z) = 0 \quad (3.10)$$

These conditions imply restraint not only against rotation but also against any warping of the end cross section this means that the end of the bar is built in rigidly so that no deformation of the end cross section can take place. These conditions define a “fixed support”.

$$(3) \left( \frac{\partial^2 \phi}{\partial z^2} \right) = 0$$

$$\text{and} \left[ (GCs - \rho I p / A) \left( \frac{\partial \phi}{\partial z} \right) - EC_w \left( \frac{\partial^3 \phi}{\partial z^3} \right) \right] = 0 \quad (3.11)$$

these conditions imply no restraint of any kind at the end of the bar. This requires that the bending moment in the flange ends and torque acting on the end cross-section must be zero. These correspond to a “free end”.

$$(4) \left( \frac{\partial \phi}{\partial z} \right) = 0 \text{ and } \left[ (GCs - \rho I p / A) \left( \frac{\partial \phi}{\partial z} \right) - EC_w \left( \frac{\partial^3 \phi}{\partial z^3} \right) \right] = 0$$

$$\left. \begin{array}{l} (4) \text{ or} \\ \left( \frac{\partial \phi}{\partial z} \right) = 0 \text{ and } \left( \frac{\partial^3 \phi}{\partial z^3} \right) = 0 \end{array} \right\} \quad (3.12)$$

The later conditions imply no warping and zero shear forces in the end flanges. These conditions are useful for finding symmetric modes of vibration in simply supported, fixed-fixed and free-free beams.

### 3.4. Time- dependent boundary conditions

The homogeneous boundary conditions discussed above, give the free vibrations of bars. For forced vibrations produced by the motion of boundaries, approximate time dependent end conditions are given by prescribing at each end one member of each of the Products:

$$EC_w \left( \frac{\partial^2 \phi}{\partial z^2} \right) \delta \left( \frac{\partial \phi}{\partial z} \right) \quad \text{and} \quad [(GCs - \rho I p / A) \left( \frac{\partial \phi}{\partial z} \right) - EC_w \left( \frac{\partial^3 \phi}{\partial z^3} \right)]$$

Or equivalent of  $M \delta (\partial \phi / \partial z)$  and  $T_t \delta \phi$  respectively.

Of the many conditions thus obtained, the following are of more theoretical interest:

1. Twisting moment  $T_t$  prescribed, flange bending moment  $M = 0$  or  $(\partial \phi / \partial z) = 0$ .
2.  $\phi$  or  $(\partial \phi / \partial t)$  prescribed, flange bending moment  $M = 0$  or  $(\partial \phi / \partial z) = 0$ .



3. Flange bending moment  $M$  prescribed, twisting moment  $T_t = 0$ ,  $\phi = 0$ ,  
 $(\partial\phi/\partial z)$  or  $(\partial^2\phi/\partial z\partial t)$  prescribed, twisting moment  $T_t = 0$  or  $\phi = 0$ .

In the case of semi-finite beams, conditions need be prescribed at one end since all physical quantities at any instant are zero at the free end.

### 3.5. Analysis of various terms

1. If  $K_t = P = 0$  and  $C_w = 0$ , equation (6) becomes

$$GC_s \left( \frac{\partial^2 \phi}{\partial z^2} \right) - \rho I_p \left( \frac{\partial^2 \phi}{\partial t^2} \right) = 0 \quad (3.13)$$

This equation represents Saint Venant's torsion theory for slender beams and does not include warping of the cross section shear deformation and or longitudinal inertia effects.

2. IF  $K_t = P = 0$  The EQN.(6) reduces to

$$GC_s \left( \frac{\partial^2 \phi}{\partial z^2} \right) - EC_w \left( \frac{\partial^4 \phi}{\partial z^4} \right) - \rho I_p \left( \frac{\partial^2 \phi}{\partial t^2} \right) = 0 \quad (3.14)$$

This equation represents Timoshenko's torsion theory which includes the effect of warping of the cross section.

3. If  $K_t = 0$ , Equation.(6) reduces to

$$(GC_s - \rho I_p / A) \left( \frac{\partial^2 \phi}{\partial z^2} \right) - EC_w \left( \frac{\partial^4 \phi}{\partial z^4} \right) - \rho I_p \left( \frac{\partial^2 \phi}{\partial t^2} \right) = 0 \quad (3.15)$$

This Equation represents the effect of an axial time- invariant compressive load added to Timoshenko's torsion theory.

4. If  $P = 0$ , Equation.(6) reduces to

$$GCL^2 \left( \frac{\partial^2 \phi}{\partial z^2} \right) - EC_w \left( \frac{\partial^4 \phi}{\partial z^4} \right) - K_t(\phi) - \rho I_p \left( \frac{\partial^2 \phi}{\partial t^2} \right) = 0 \quad (3.16)$$

This equation represents the effect of Winkler type constant modulus elastic foundation added to Timoshenko's torsion theory.

### 3.6. Non-Dimensionalization and General Solution of Equation of Motion

For mathematical simplification, it is convenient to reduce equation (6) to a non-dimensional form, simultaneously introducing some dimensionless parameters having physical interpretations.

Introducing,  $Z = z/L$ , the non-dimensional beam length, and

$$T_1 = (EC_w)/(\rho I_p L^4) t, \text{ the dimensionless time variable,}$$

Equation (3.16) in non-dimensional form can be written as:

$$\left( \frac{\partial^4 \phi}{\partial Z^4} \right) - (K^2 - \nabla^2) \left( \frac{\partial^2 \phi}{\partial Z^2} \right) + 4\gamma^2(\phi) + \left( \frac{\partial^2 \phi}{\partial T_1^2} \right) = 0 \quad (3.17)$$

$$\text{Where } k_2 = (GCL^2)/(EC_w), \text{ warping rigidity parameter} \quad (3.18)$$

$$\nabla^2 = (P I_p L^2)/(AEC_w), \text{ axial load parameter} \quad (3.19)$$

$$\text{and } \gamma^2 = (K_t L^4)/(4EC_w), \text{ foundation parameter,} \quad (3.20)$$

the general solution of equation.(3.14) can be obtained by using the standard method of separation of variables. Thus, by taking  $\phi$  in the form

$$\phi = X(Z) T(T_1) \quad (3.21)$$

and then substituting into equation.(3.14), separating the variables, and setting the resulting expressions equal to  $\lambda n^2$ , we obtain

$$T = A_n \cos \lambda_n t_1 + B_n \sin \lambda_n t_1 \quad (3.22)$$

The expression for a normal mode of vibration is then

$$\phi = X(A_n \cos \lambda_n t_1 + B_n \sin \lambda_n t_1) \quad (3.23)$$

in which  $X$  is the normal function giving the shape of the mode of vibration.

$\lambda_n$  is the dimensionless torsional frequency parameter given by

$$\lambda_n^2 = (\rho I_p L^4 p_n^2)/(EC_w) \quad (3.24)$$

$\lambda_n$  is the dimensionless torsional frequency parameter. Any actual motion of the vibrating beam can be obtained by a summation of normal modes, so that in the general case

$$\phi = \sum X_n (A_n \cos \lambda_n t_l + B_n \sin \lambda_n t_l) \quad (3.25)$$

in which the coefficients  $A_n$  and  $B_n$  are found from the initial conditions of the vibration. The equation for determining the normal function  $X$ , found by substituting equation (3.24) into differential equation (3.14), then

$$\left( \frac{\partial^4 X}{\partial z^4} \right) - (k^2 - \nabla^2) \left( \frac{\partial^2 X}{\partial z^2} \right) + (4\gamma^2 - \lambda_n^2) X = 0 \quad (3.26)$$

The general solution of this equation may be found by taking the normal function  $X$  in the form:

$$X = D e^{nz} \quad (3.27)$$

The equation (3.27) yields the auxiliary algebraic equation.

$$\eta^4 - (k^2 - \nabla^2) (\eta^2) + (4\gamma^2 - \lambda_n^2) = 0 \quad (3.28)$$

The four roots of the equation are

$$\eta_1 = +\alpha_1; \quad \eta_2 = -\alpha_1; \quad \eta_3 = +i\beta_1; \quad \eta_4 = -i\beta_1 \quad (3.29)$$

In which  $\alpha_1$  and  $\beta_1$  are the positive, real quantities given by

$$\alpha_1 = (1/\sqrt{2}) \{ (k^2 - \nabla^2) + (k^2 - \nabla^2)^2 + 4(\lambda_n^2 - 4\gamma^2) \}^{1/2} \quad (3.30)$$

$$\beta_1 = (1/\sqrt{2}) \{ -(k^2 - \nabla^2) + (k^2 - \nabla^2)^2 + 4(\lambda_n^2 - 4\gamma^2) \}^{1/2} \quad (3.31)$$

The general solution of equation (26) then becomes either

$$X = D_1 e^{\alpha_1 z} + D_2 e^{-\alpha_1 z} + D_3 e^{\beta_1 z} + D_4 e^{-\beta_1 z}$$

or

$$X = D_1 \cosh \alpha_1 z + D_2 \sinh \alpha_1 z + D_3 \cos \beta_1 z + D_4 \sin \beta_1 z \quad (3.32)$$

There are four arbitrary constants in this expression, which must be determined so as to satisfy the particular boundary conditions of the problem. For any beam there will be two boundary conditions at each end and these four conditions determine the frequency equation and the ratios of three of the constants to the fourth constant. Solving the frequency equation

then determines the principal frequency of vibration. With the frequencies and normal functions determined, the solution is essentially complete.

### 3.7. Frequency Equations and Modal Functions

Because of the complexity of the frequency equations, the study is limited the case of simply supported beam.

#### 3.7.1. Boundary conditions

In terms of non-dimensional parameters, the boundary conditions can be written as:

**1. Simple support:**

$$X = 0, \quad d^2X/dZ^2 = 0, \quad (3.33)$$

**2. Fixed support:**

$$X = 0, \quad dX/dZ = 0, \quad (3.34)$$

**3. Free end:**

$$d^2X/dZ^2 = 0, \quad (k^2 - \nabla^2)dx/dz - d^3x/dz^3 = 0 \quad (3.35)$$

### 3.8. Simply Supported Beam:

The present study is limited to simply supported beams only. The boundary conditions are applied and frequency equations and mode shapes for simply supported beam are established in detail. From the boundary conditions

$$X = d^2X/dZ^2 = 0 \text{ at } Z=0, \text{ and } X = d^2X/dZ^2 = 0 \text{ at } Z = 1.$$

For the conditions at  $z=0$ , equation (32) gives:

$$D_3 + D_1 = 0,$$

$$\text{and } D_1(\alpha_1^2 + \beta_1^2) = 0.$$

Since the  $(\alpha_1^2 + \beta_1^2)$  is not equal to zero, it follows that  $D_3 = D_1 = 0$ .

From the second pair of conditions, equation (32) gives:

$$D_2 \sinh \alpha_1 + D_4 \sin \beta_1 = 0, \text{ and } D_2 \alpha_2 \sinh \alpha_1 - D_4 \beta_2 \sin \beta_1 = 0,$$

The characteristic equation is  $(\alpha_1^2 + \beta_1^2) \sinh \alpha_1 \sin \beta_1 = 0$

The frequency equation is  $\sin \beta_1 = 0$ , Therefore  $\beta_1 = n\pi$ , where  $n=1, 2, 3 \dots$

The frequency parameter is

$$\lambda_n = \left| n^2 \pi^2 (n^2 \pi^2 + k^2 - \Delta^2) + 4\gamma^2 \right|^{1/2}$$

### 3.9. Finite Element Simulation

Finite Element modelling and analysis is used to analyze natural frequencies and mode shapes of Indian Standard Junior Beam (ISJB - 150), Indian Standard Light Beam (ISLB – 150) and tapered beams with following dimensions by using Finite Element Analysis.

#### Problem description of an ISJB –150 Beam

Weight per meter,  $W = 7.1 \text{ kg-f}$

Sectional Area,  $a = 9.01 \text{ cm}^2$

Depth of Section,  $h = 150 \text{ mm}$

Width of Flange  $b_f = 50 \text{ mm}$

Thickness of Flange,  $t_f = 4.6 \text{ mm}$

Thickness of Web,  $t_w = 3.0 \text{ mm}$

Young's Modulus,  $E = 2E5$

Poison's Ratio = 0.3

#### Problem description of an ISLB –150 Beam:

Weight per meter,  $W = 14.2 \text{ kg-f}$

Sectional Area,  $a = 18.08 \text{ cm}^2$

Depth of Section,  $h = 150 \text{ mm}$

Width of Flange,  $b_f = 80 \text{ mm}$

Thickness of Flange,  $t_f = 6.8 \text{ mm}$

Thickness of Web,  $t_w = 4.8 \text{ mm}$

Young's Modulus,  $E = 2E5$

Poison's Ratio = 0.3

### **3.9.1 Meshing model of an ISJB-150.**

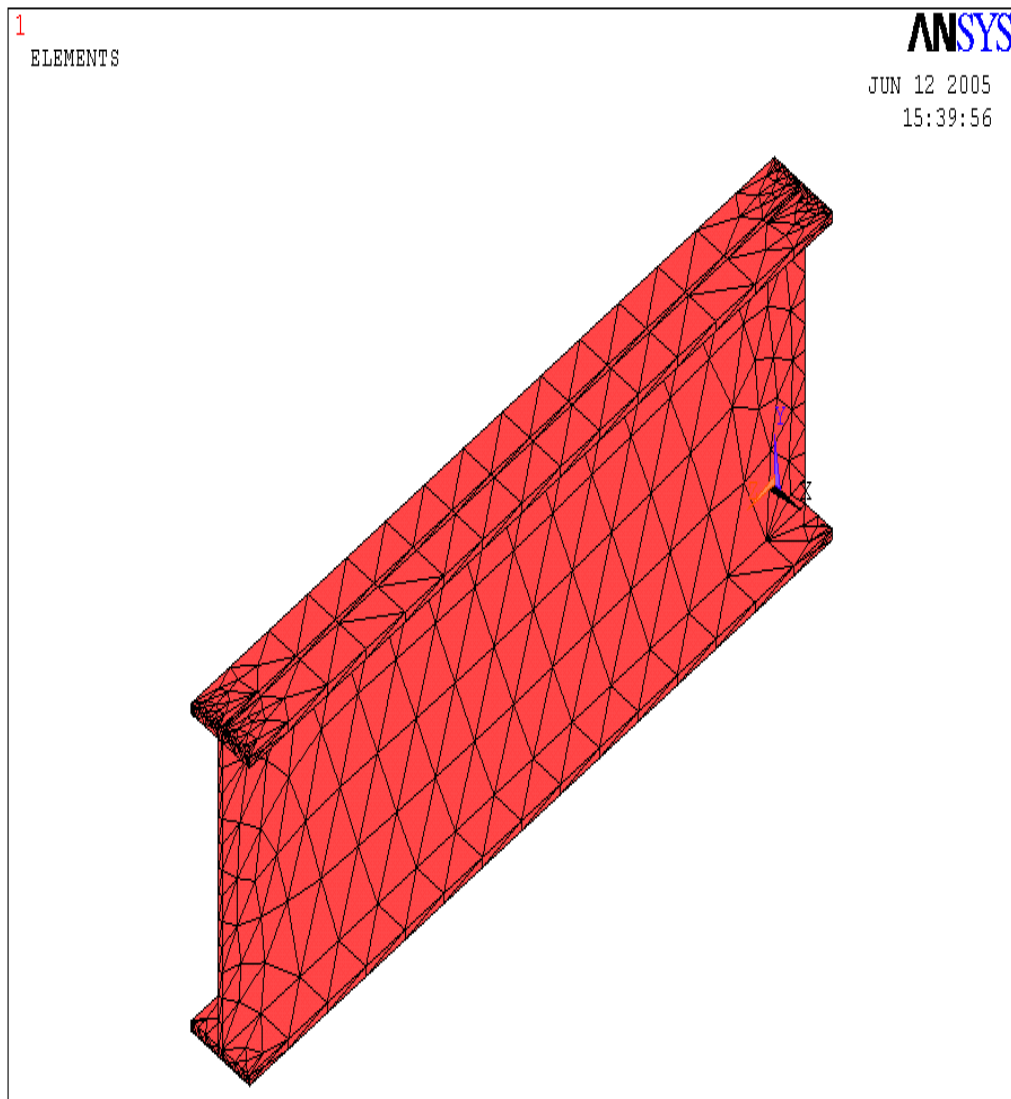


**Fig.3.1** Meshing model of an ISJB-150

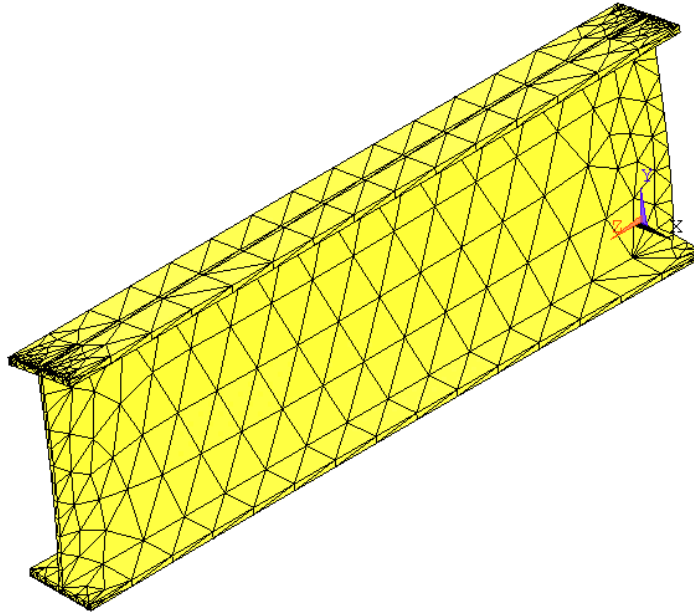
**3.9.1.1. Different mode shapes of an ISJB-150.**

1

DISPLACEMENT  
STEP=1  
SUB =1  
FREQ=.009379  
DMX =.005

ANSYS

JUN 12 2005  
15:43:49



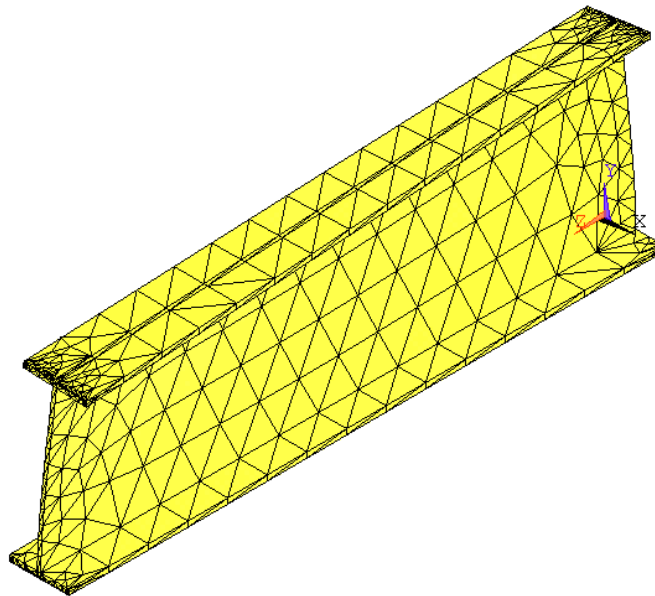
**First mode shape**

1

DISPLACEMENT  
STEP=1  
SUB =2  
FREQ=.019775  
DMX =.008345

ANSYS

JUN 12 2005  
15:44:23

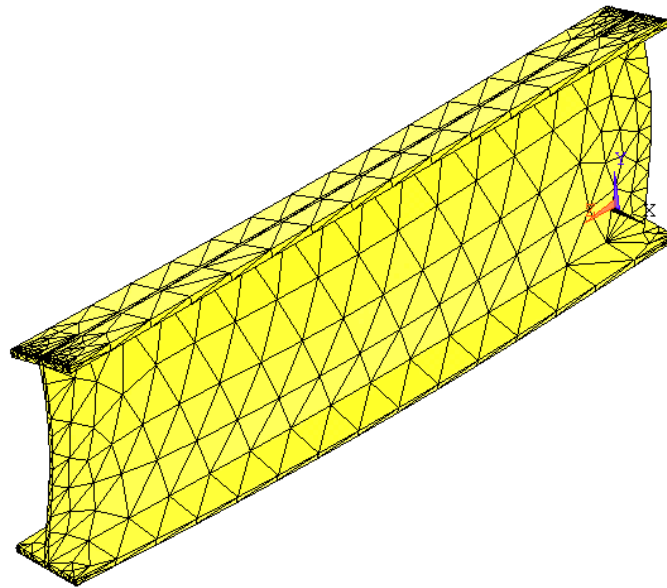


**Second mode shape**



1  
DISPLACEMENT  
STEP=1  
SUB =3  
FREQ=.075295  
DMX =.006279

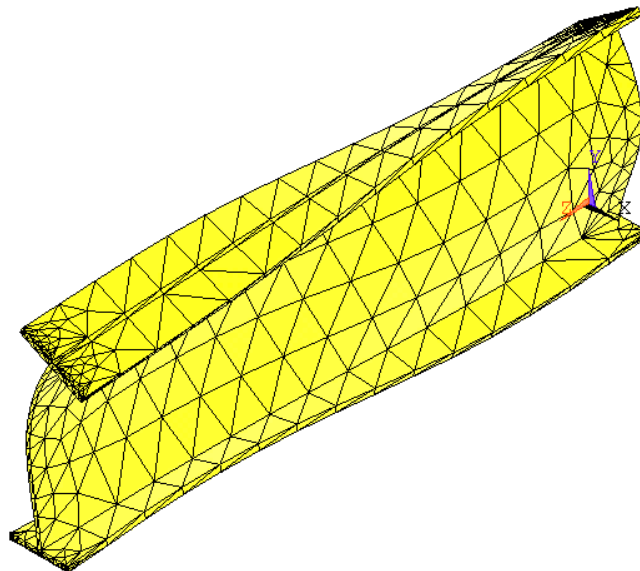
ANSYS  
JUN 12 2005  
15:44:50



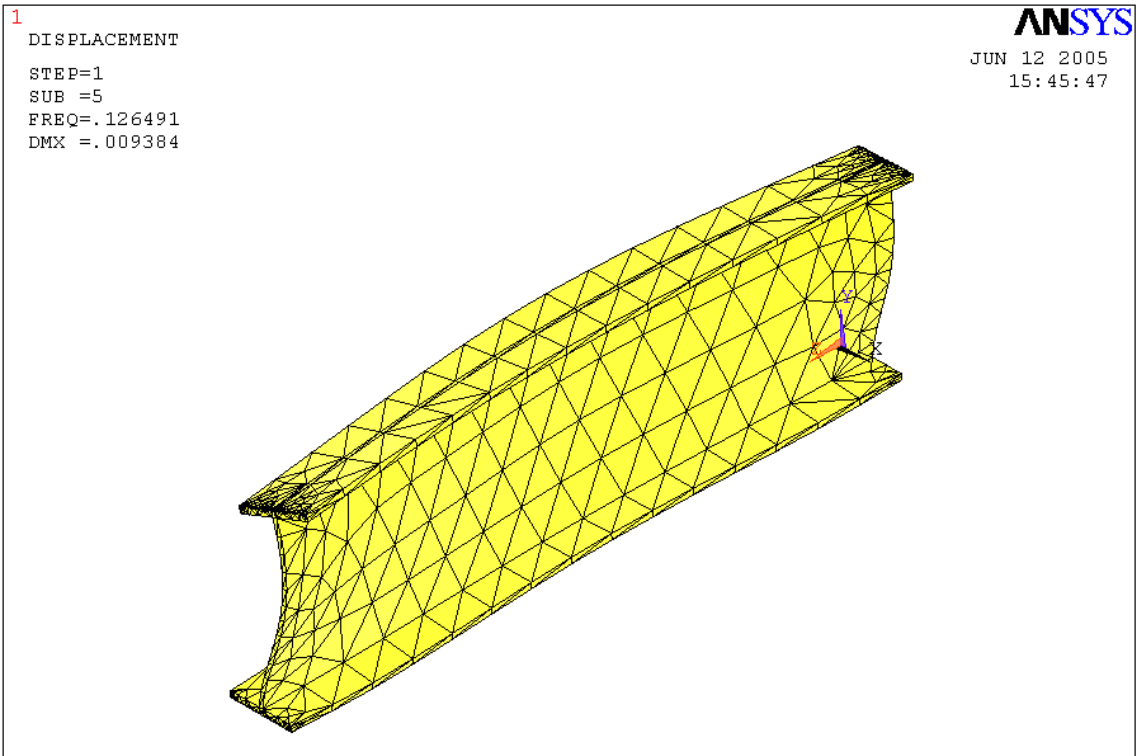
**Third mode shape**

1  
DISPLACEMENT  
STEP=1  
SUB =4  
FREQ=.116304  
DMX =.006635

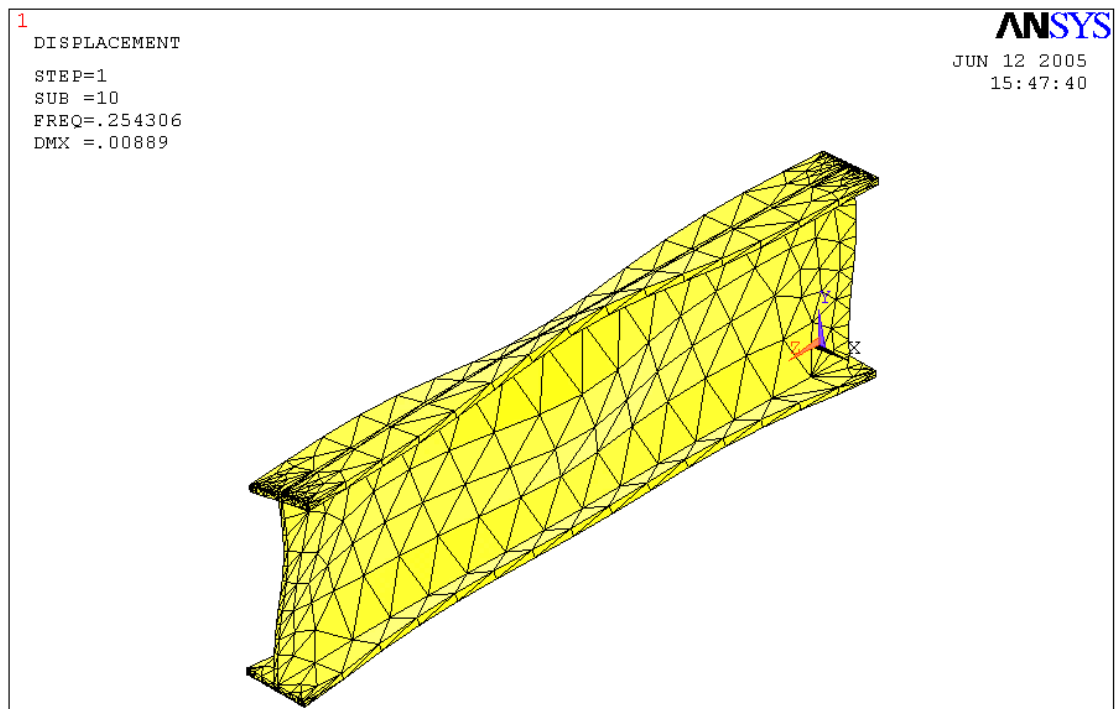
ANSYS  
JUN 12 2005  
15:45:22



**Fourth mode shape**



**Fifth mode shape**



**Tenth mode shape**

**Fig.3.2 Mode shapes of an ISJB-150**

**Table.3.1. furnishes the frequencies of first 10 mode shapes of an ISJB-150.**

<b>SET</b>	<b>FREQUENCY Hz</b>
1	0.93486E-02
2	0.19445E-01
3	0.45295E-01
4	0.11630
5	0.12649
6	0.14440
7	0.20126
8	0.20654
9	0.22584
10	0.25431

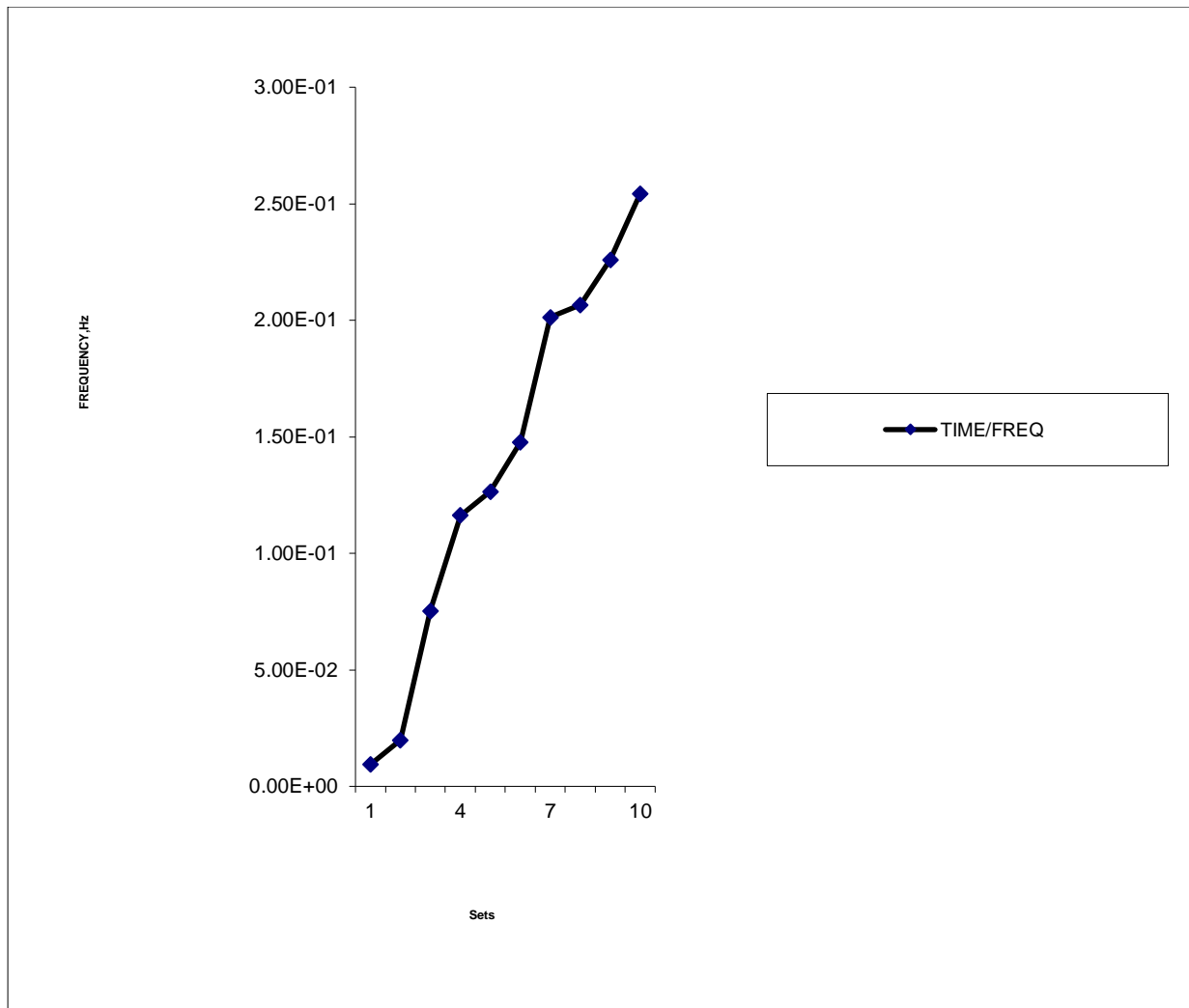


**Fig. 3.3. Frequency Variation of an ISJB - 150 Beam Over Different Set**

### 3.9.2. Meshing model of an ISLB-150.

1  
ELEMENTS

ANSYS

JUN 12 2005  
15:54:44

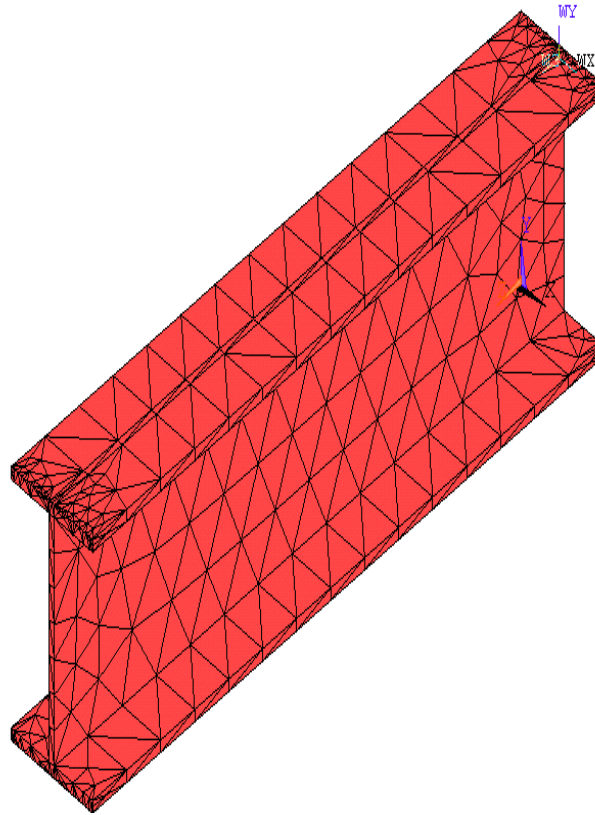


**Table 3.3. The frequencies of first 10 mode shapes of ISJB-150 tapered beam.**

<b>SET</b>	<b>FREQUENCY, Hz</b>
1	0.14934E-01
2	0.28969 E-01
3	0.42584 E-01
4	0.68405 E-01
5	0.10413
6	0.11395
7	0.14493
8	0.16825
9	0.16956
10	0.23494

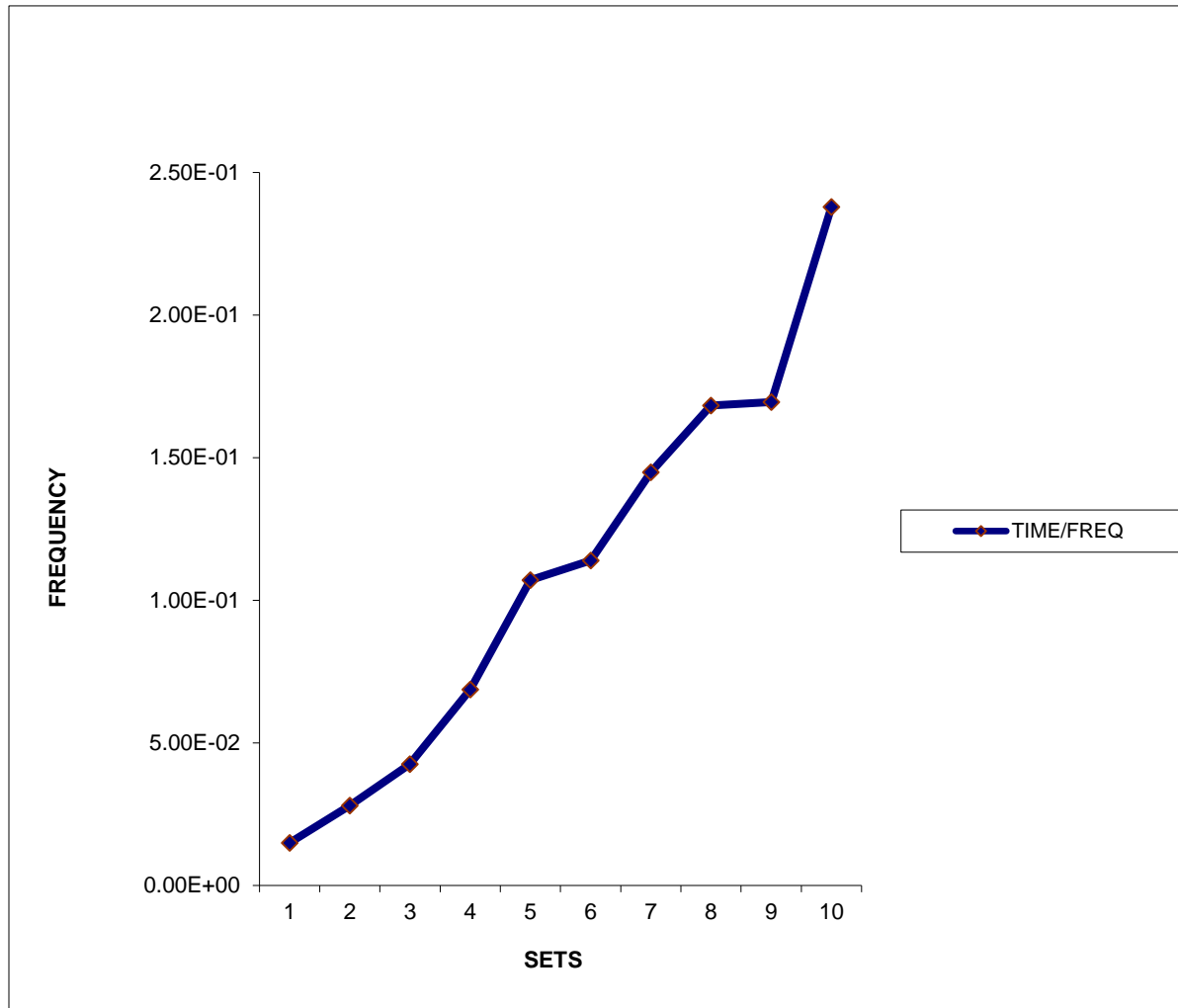


**Fig. 3.9 shows frequency variation of an ISJB – 150 tapered beam.**

#### 3.9.4. Meshing model of an ISLB-150 tapered beam.

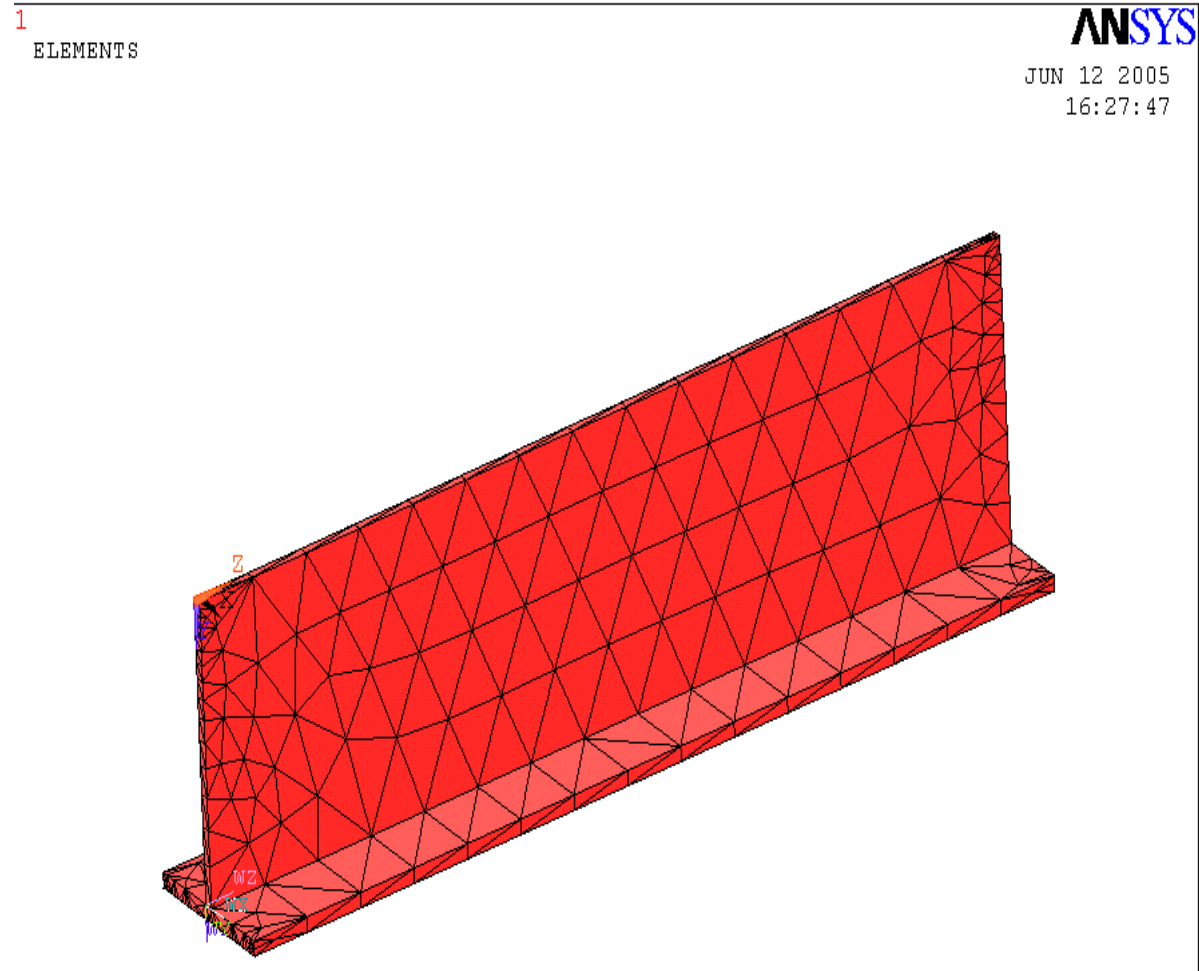
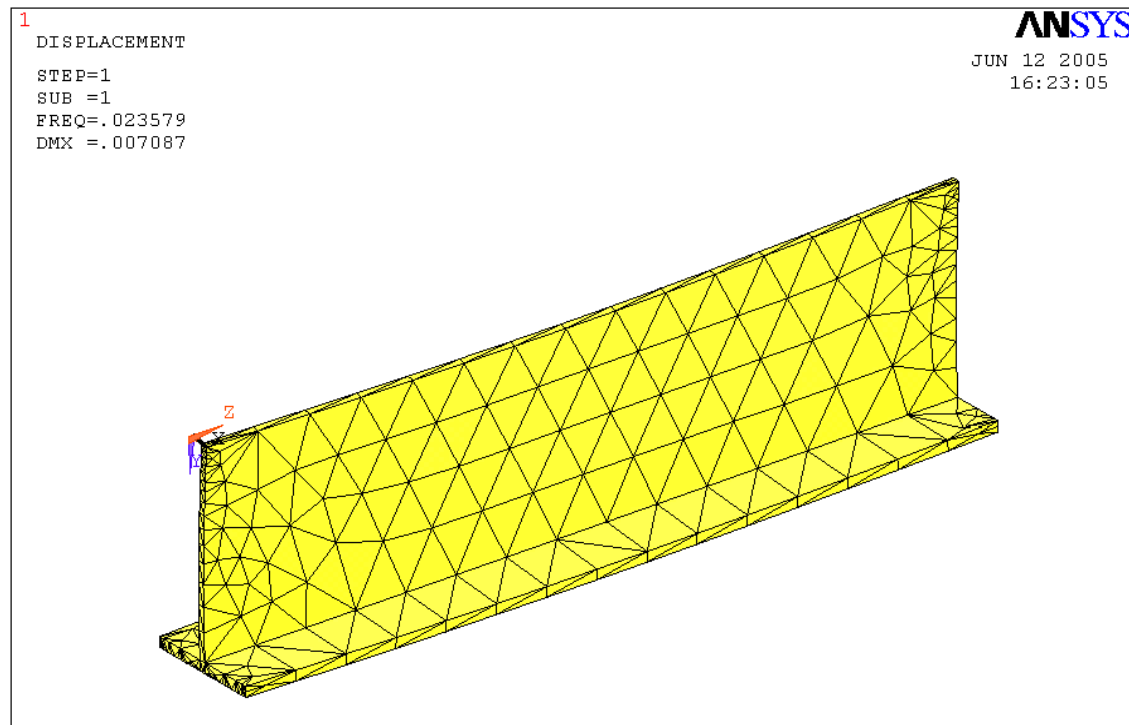


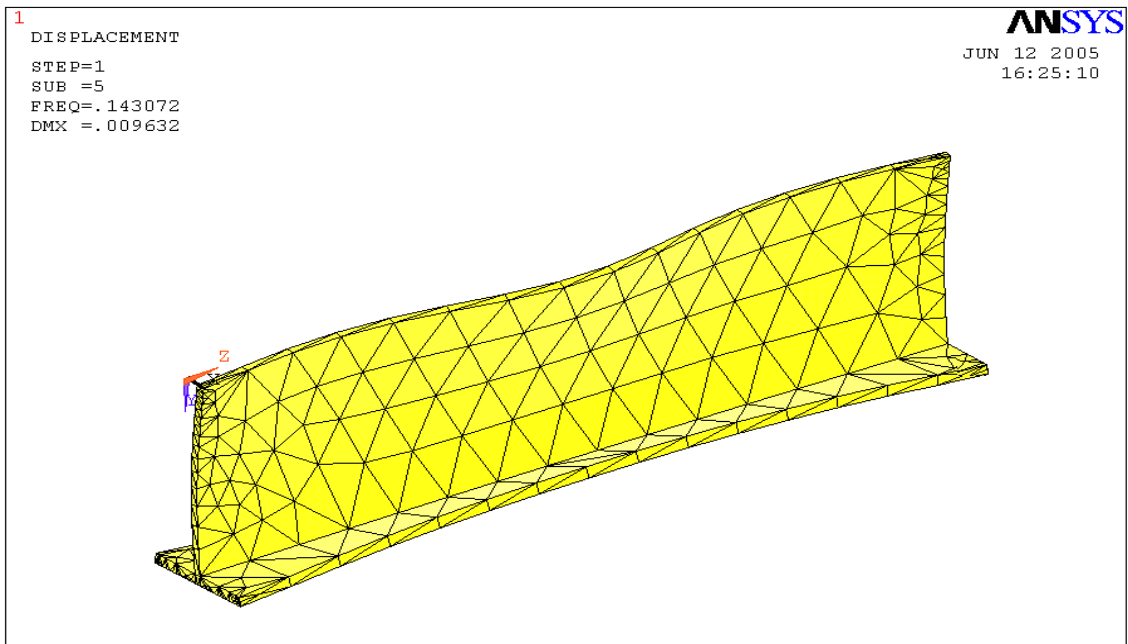
**Fig.3.10 Meshing model of an ISLB-150 tapered beam.**



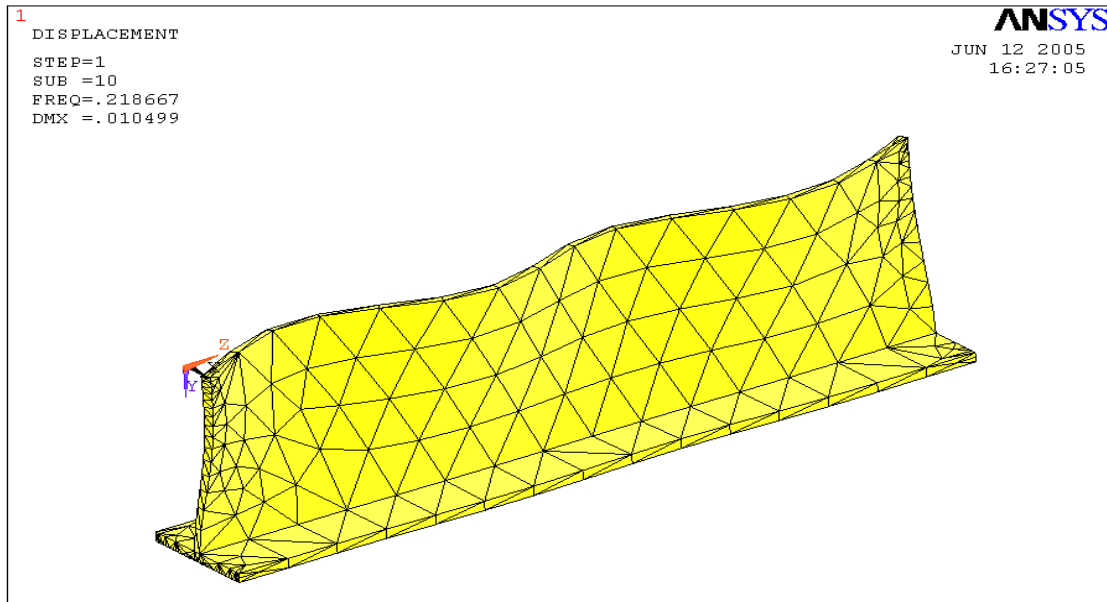
### 3.9.4.1. Different mode shapes of an ISLB-150 tapered beam:



**First mode shape**



**Fifth mode shape**



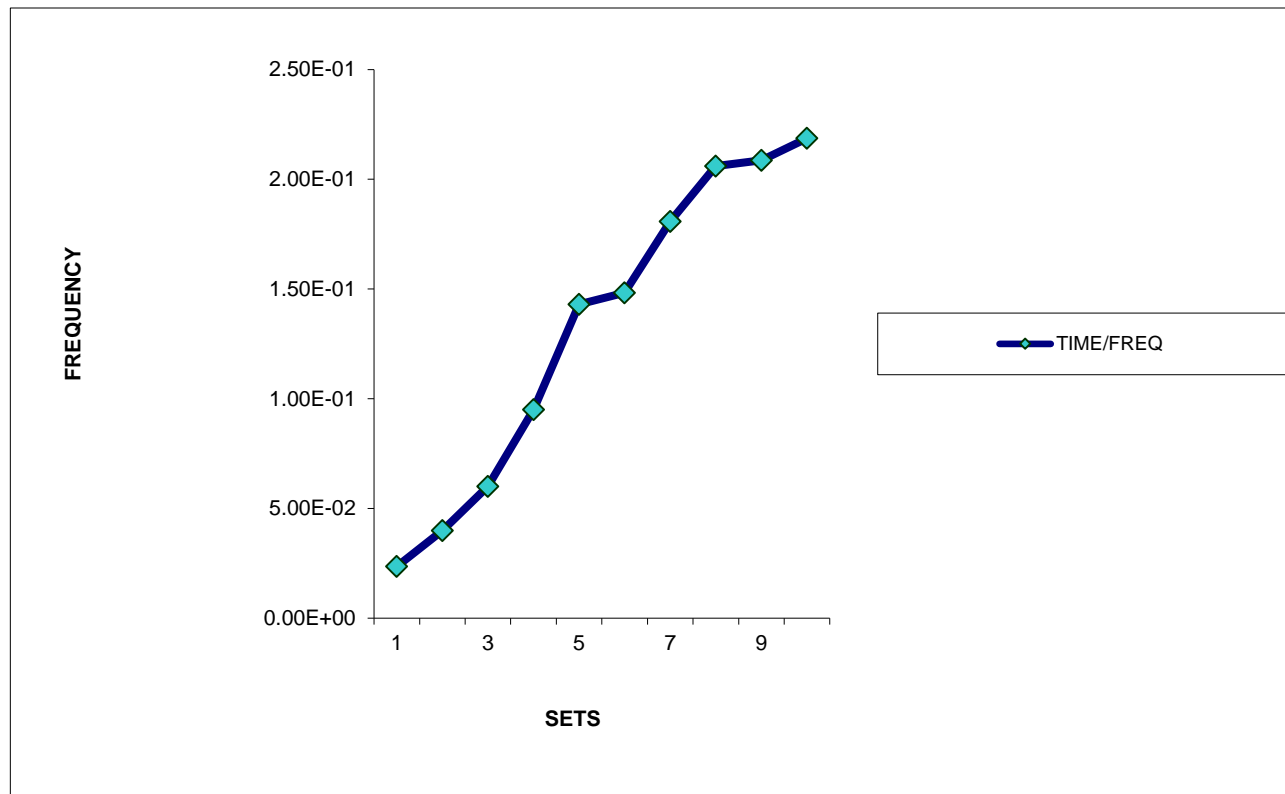
**Tenth mode shape**

**Fig.3.11 Different mode shapes of an ISLB-150 tapered beam**

**Table 3.4. The frequencies of first 10 mode shapes of ISLB-150 tapered beam.**

<b>SET</b>	<b>FREQUENCY, Hz</b>
1	0.23549E-01
2	0.40699 E-01
3	0.60454 E-01
4	0.95891 E-01
5	0.14304
6	0.14833
7	0.18048
8	0.20608
9	0.20863
10	0.21864

**Figure. 3.12** shows frequency variation of an ISLB – 150 tapered beam



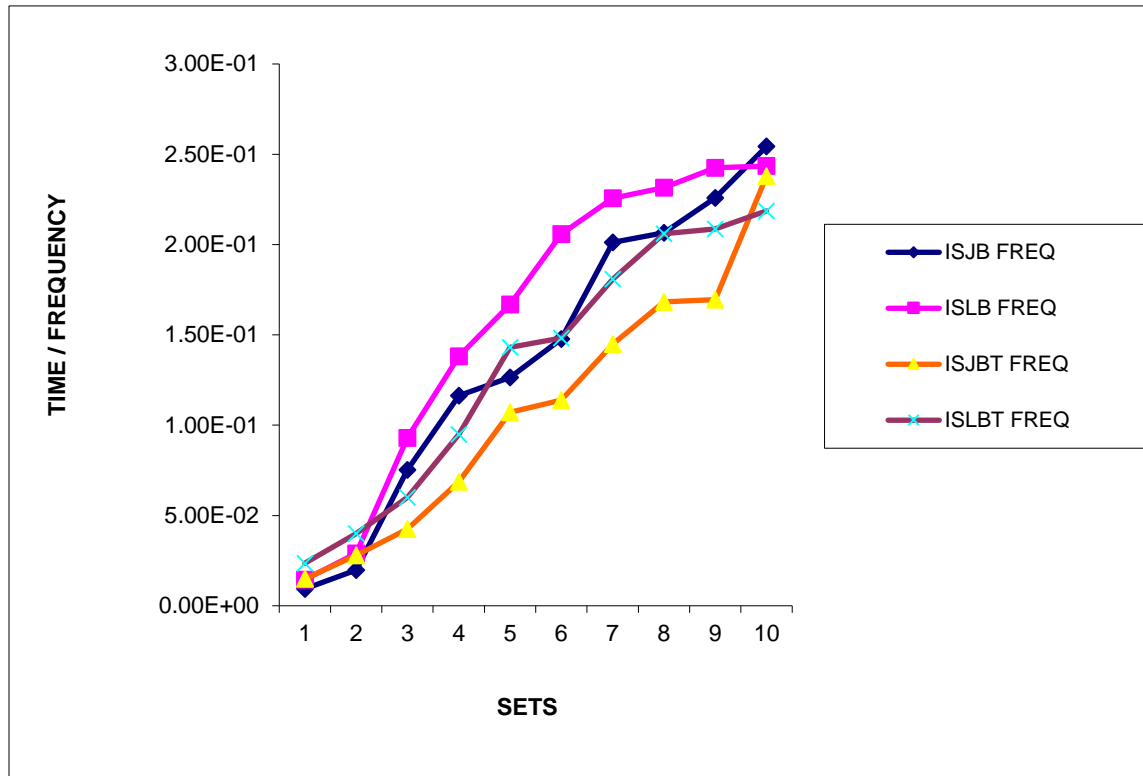


**Fig. 3.13 shows the comparison of variation of frequency over different sets of all four beams.**

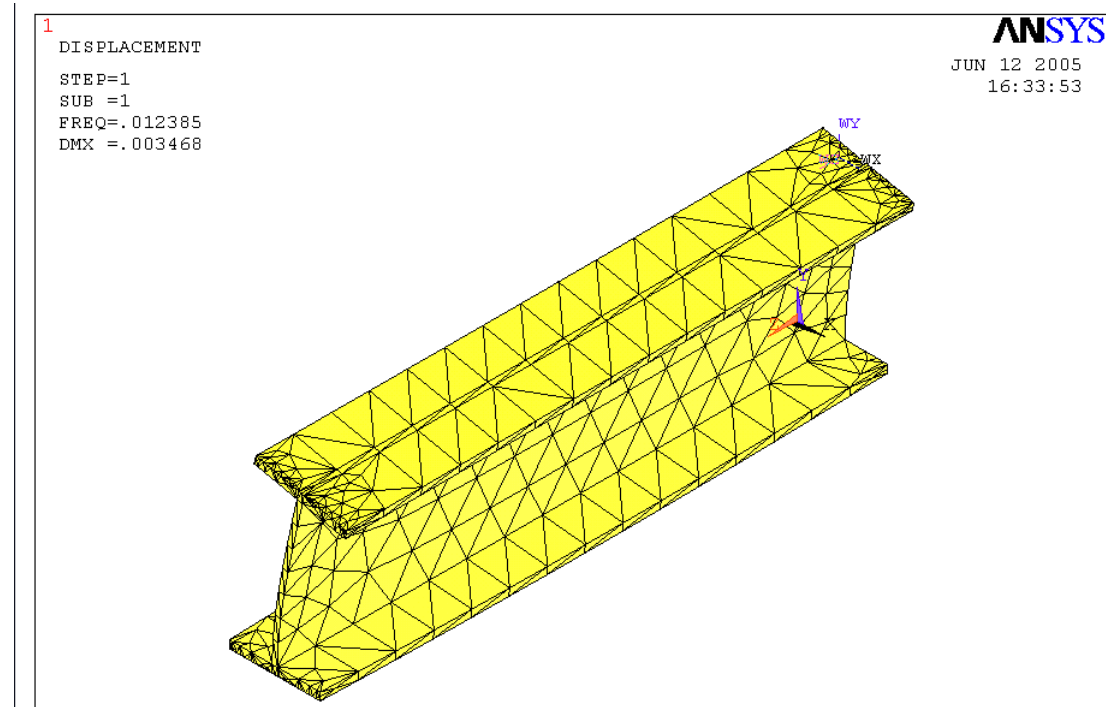
### **3.10. RESULTS AND DISCUSSIONS**

It has found that the frequencies of standard beams are higher than that of tapered beams, the frequencies of individual beams gradually increases over different sets and also numerical results obtained from the ANSYS software are almost nearer to the theoretical values obtained by using Wittrick.W.H. & Williams, E.W., Algorithm.

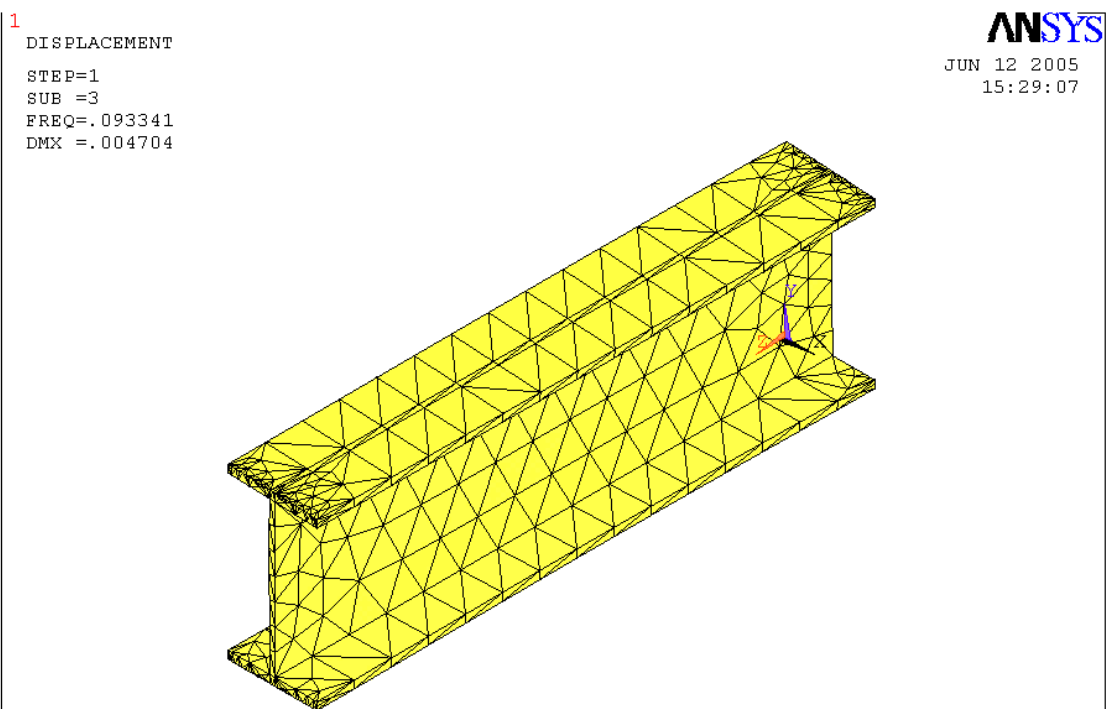




### 3.9.2.1. Different mode shapes of an ISLB-150:



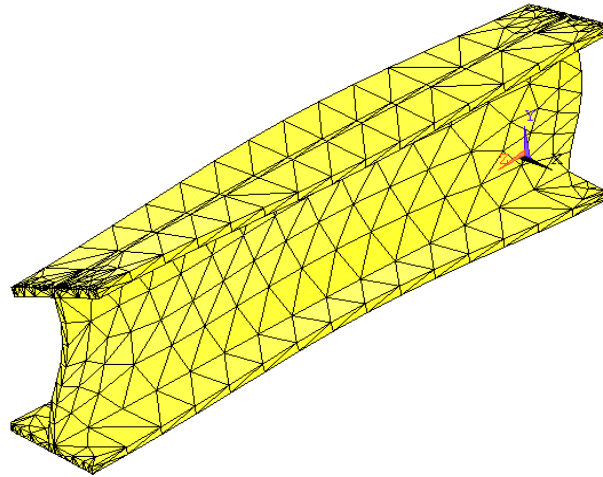
First mode shape



Third mode shape

1  
DISPLACEMENT  
STEP=1  
SUB =5  
FREQ=.166767  
DMX =.007172

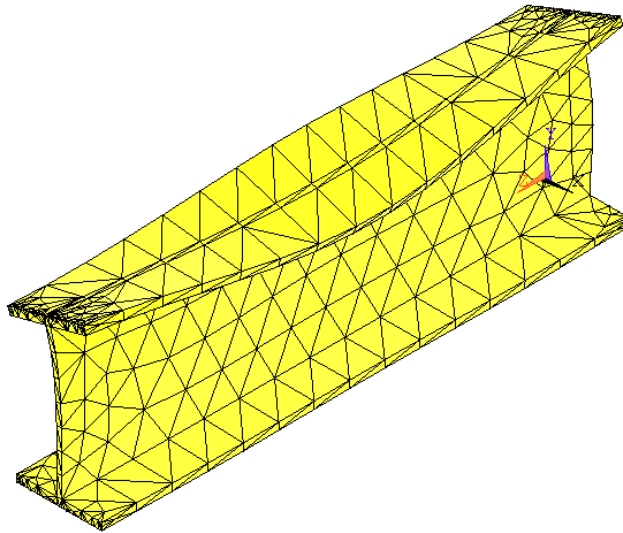
ANSYS  
JUN 12 2005  
15:30:30



**Fifth mode shape**

1  
DISPLACEMENT  
STEP=1  
SUB =10  
FREQ=.243514  
DMX =.00831

ANSYS  
JUN 12 2005  
15:32:49



**Tenth mode shape**

**Fig.3.5 Mode shapes of an ISLB-150**

**Table 3.2. The frequencies of first 10 mode shapes of ISLB-150.**

SET	TIME/FREQ
1	0.14501E-01
2	0.29164 E-01
3	0.93341 E-01
4	0.13815
5	0.16644
6	0.20584
7	0.22566
8	0.23144
9	0.24260
10	0.24351

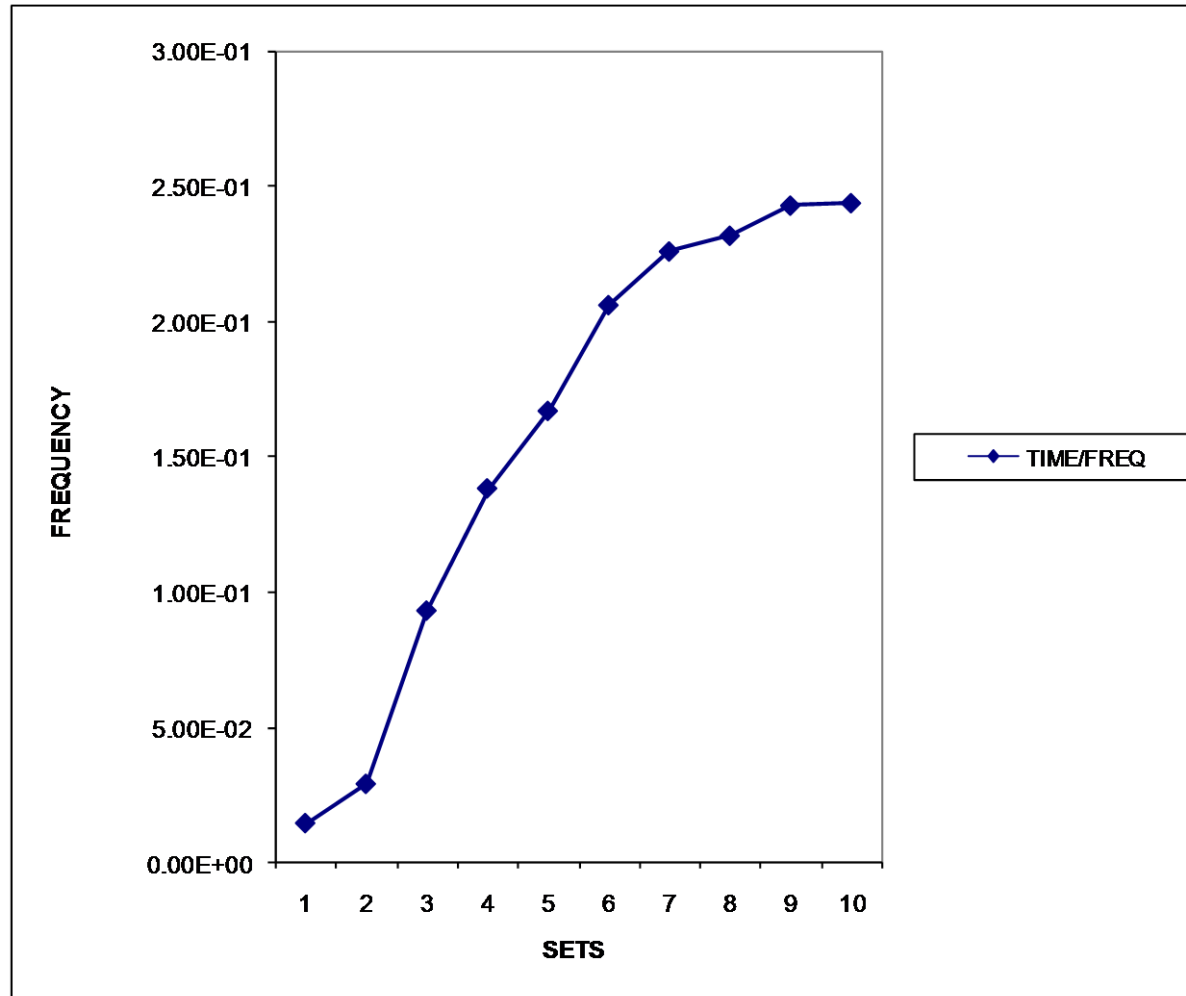


**Figure 3.6. Frequency variation of an ISLB - 150 Beam over different sets**

### 3.9.3. Meshing model of an ISJB-150 tapered beam:

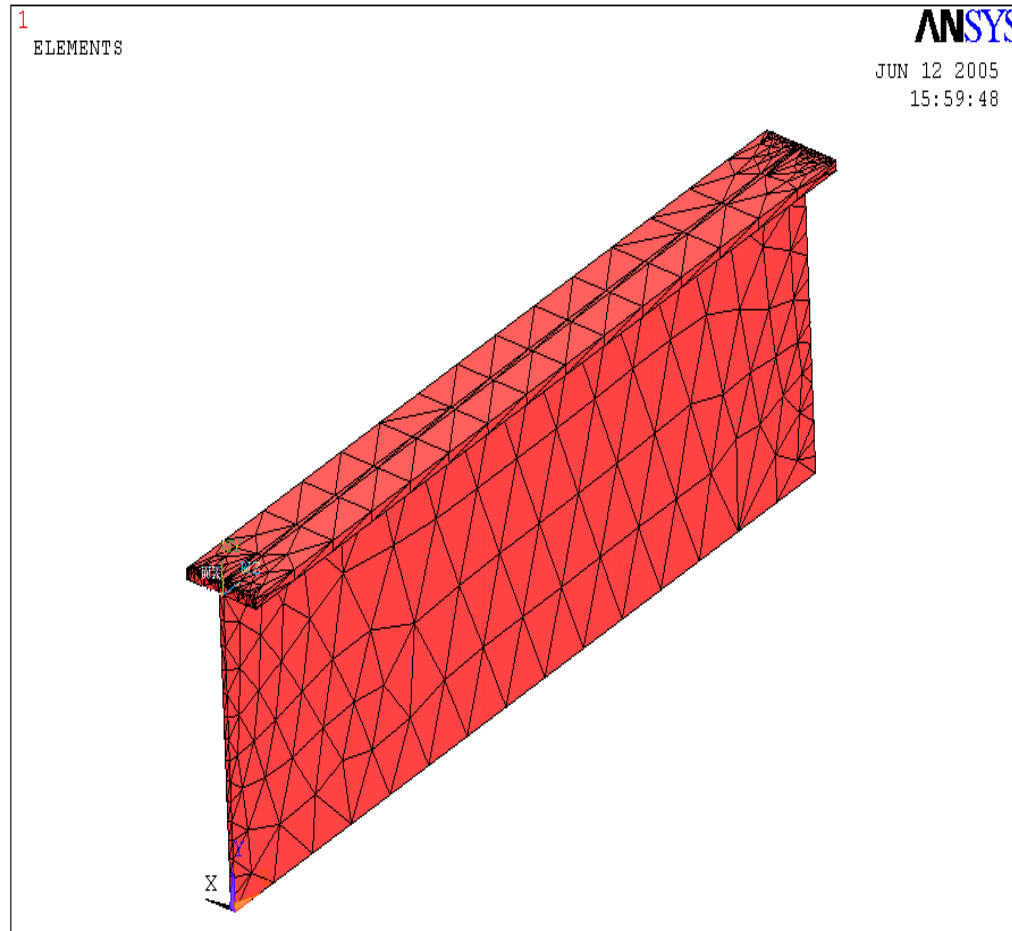
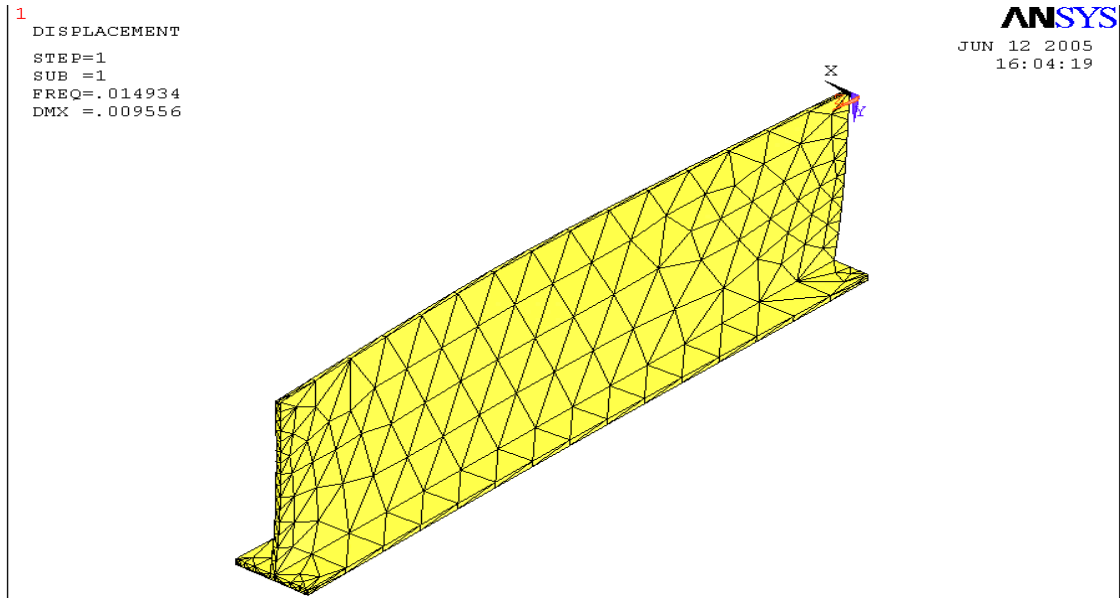
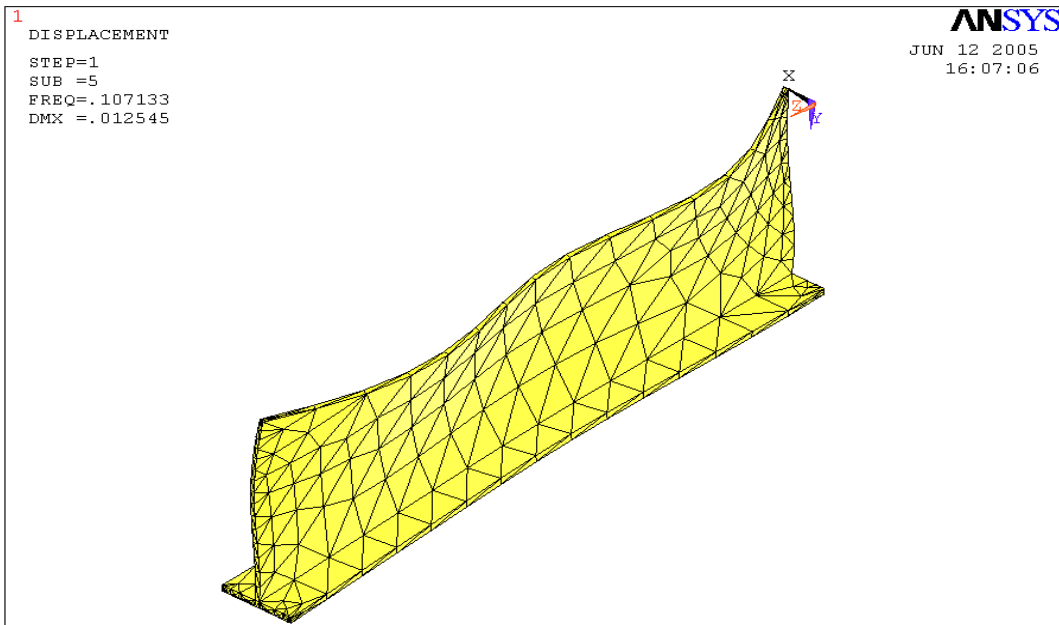


**Fig.3.7 Meshing model of an ISJB-150 tapered beam**

### 3.9.3.1. Different mode shapes of an ISJB-150 tapered beam:



**First mode shape**



**Fifth mode shape**

1

DISPLACEMENT

STEP=1

SUB =10

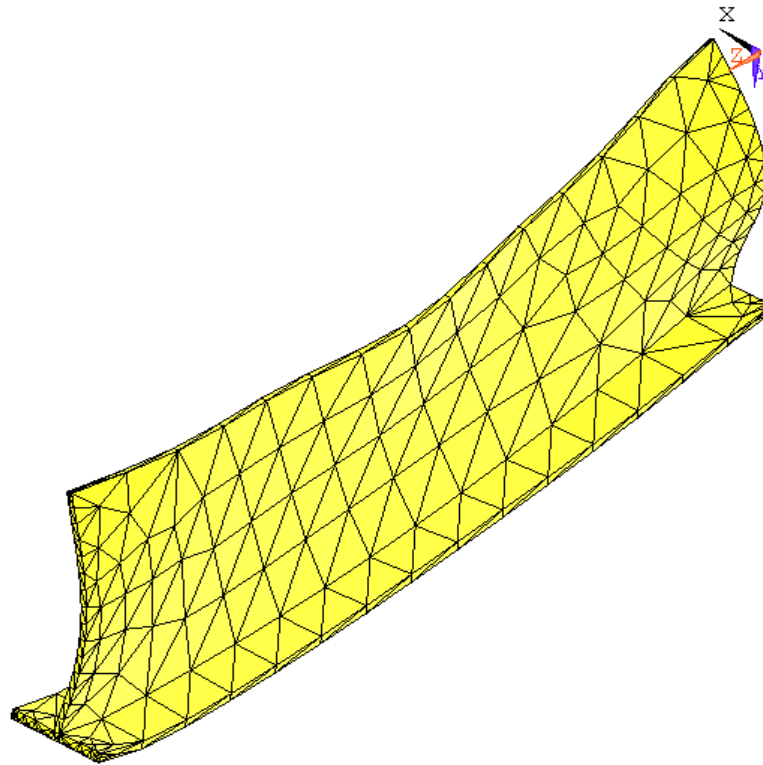
FREQ=.237936

DMX =.005543

ANSYS

JUN 12 2005

16:09:10



**Tenth mode shape**



## **Chapter 4**

# **EXPERIMENTAL ANALYSIS OF GLASS-EPOXY COMPOSITE RECTANGULAR LAMINATED BEAMS**

## **EXPERIMENTAL ANALYSIS OF GLASS-EPOXY COMPOSITE RECTANGULAR LAMINATED BEAMS**

### **4.1. Introduction**

It is known from dynamic systems that a structure temporarily excited by an external force will vibrate at a frequency defined as the natural frequency. The natural frequency is characteristic of the entire structure and its boundary conditions. An external excitation applied to the structure at the same frequency as the structure's natural frequency will result in resonance. At resonance, the structure will vibrate at higher than normal amplitude levels. Depending upon the overall system design, the amplitude of vibration at resonance can cause unwanted operating conditions as well as a catastrophic failure. This type of system failure can be avoided by determining the structure's natural frequency and maintaining the overall system at an operating condition which will not induce resonance. The natural frequencies of a structure can be determined by measuring frequency response. One means of measuring the frequency response is to impact test the structure. Impact testing is a measurement of the ratio of the beam's transient response to the excitation impulse versus frequency.

### **4.2. Manufacturing of Glass-Epoxy Composites:**

Manufacturing of composite materials involves distinct operations that may vary depending upon available technology, existing facilities and skilled persons. The manufacturing process may also vary due to wide variety of composite materials and their applications. Factors considered for selection of most efficient manufacturing process are

- User needs
- Performance requirements
- Labour
- Surface complexity
- Volume of the production
- Size of the product
- Appearance
- Production rate
- Tooling/assembly
- Equipment

The main goals of the composite manufacturing process are

- To achieve a consistent product by controlling fibre thickness, fibre volume and fibre direction.
- To minimise voids.
- Reduce internal residual stresses.
- Economy of process

The hand lay-up method is used for manufacturing the glass – epoxy composite specimens for conducting the experiments. Even though the method has been replaced with automated techniques, the lay-up of preimpregnated material by hand is the oldest and most common fabrication method for advanced composite structures. The following steps illustrate the adopted manufacturing process for glass epoxy specimens.

1. The surface of the tool is cleaned and release agent is applied. The release agent can be in liquid or solid form.
2. An optical sacrificial layer is laid upon the tool surface. This layer is usually a fibre glass fibre made with the same resin system as the composite laminate. The sacrificial layer protects the laminate from surface abrasion and surface irregularities during manufacturing.
3. A peel ply is placed on top of the sacrificial layer. The peel ply is removed after processing.
4. The preimpregnated plies are cut according to design specifications. They can be cut by hand using shears or a steel blade knife. However, automated cutting machines have largely replaced hand cutting.
5. The first prepeg ply is oriented and placed upon the tool or mold. Subsequent plies are placed one upon another; a roller is used to compact the plies and remove entrapped air that could later lead to voids.
6. A flexible resin dam is anchored to the sacrificial layer approximately 3mm from the edge of the laminate. The dam prevents resin flow out of the laminate, in the plane of the laminate.
7. Another peel ply is placed on top of the laminate to protect the laminate surface.
8. A sheet of porous release film is laid over the dam and the laminate. The porous release film will serve as a barrier to prevent bonding of the composite laminate to the secondary materials to follow.
9. Next, bleeder plies are laid up over the release film. The bleeder plies extend to the edge of the laminate.
10. Another porous release ply is next laid up over the bleeder plies.
11. Caul plates are sometimes placed on the top of lay-up. The caul plate is steel or aluminium plate that protects the surface from sharp temperature increases (it acts as a heat sink) and it gives a smooth non-waxy surface texture.

Obviously, hand lay-up represents an extreme that can not be scaled to high volume or large components. There is a significant amount of skilled labour necessary for the hand lay-up of composite parts. Each step has a specific purpose and function. This type of fabrication is the most time-consuming, but it is also the most flexible manufacturing process.

### 4.3 Dimensions of the rectangular glass –epoxy composite beam

Two different symmetrical laminates with twenty layers each is manufactures by laying one layer over another by pressure.

Type 1: [45/-/45/45/-45/45/-45/45/-45/0/90]<sub>s</sub>

Type 2:[0/90/0/90/0/90/0/90/0/90]<sub>s</sub>

The details of the Rectangular beam considered for both experimental and simulation by ANSYS R10.0 are :

Beam length = 40 cm ,

Width of the beam = 25mm,

Thickness of the beam = 1.6mm, and

Total mass of the beam =  $28 \times 10^{-3}$  kg.

The rectangular cantilever beam is modelled and analysed using ANSYS R 10.0 with the above data using SHELL99, for both the types of stacking of layers.

**Material used:** glass fibre and Epoxy resin (HY -956)

**Table 4.1.Material properties**

Material	Properties	Symbol	Value
Glass fibre	Elastic modulus	$E_f$	$76 \times 10^9$
	Density	$\rho_r$	$2.56 \times 10^3$

	Poisson's ratio	$\nu_{12}$	0.22
Epoxy resin	Elastic modulus	$E_{11}$	$4.0 \times 10^9$
	Density	$\rho_m$	$1.3 \times 10^3$
	Poisson's ratio	$\nu_m$	0.40
Laminate { orthotropic)	Elastic modulus Fibre direction	$E_{11}$	$44.8 \times 10^9$
	Normal to fibre	$E_{22} = E_{33}$	$11.27 \times 10^9$
	Density	$\rho_c$	1780
	Shear modulus	$G_{12} = G_{13}$	$4.86 \times 10^9$
		$G_{23}$	$4.45 \times 10^9$
	Poisson's ratio	$\nu_{12}$	0.28
	Fibre volume fraction	$V_f$	

#### **4.4. Modal Analysis by Finite Element method**

The glass –epoxy composite rectangular beam with above dimensions is modelled using SHELL99. This beam is discretized into 50 elements and analysis is done by ANSYS software by fixing one end. The analysis is carried out for two different symmetrical laminates with twenty layers each by laying one layer over another with following orientations.

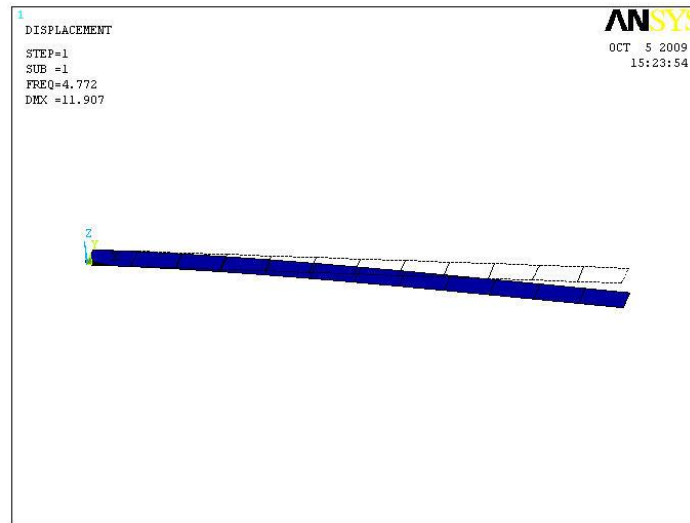
Type 1:  $[45/-45/45/-45/45/-45/45/-45/0/90]_s$

Type 2:  $[0/90/0/90/0/90/0/90/0/90]_s$

#### **4.5. Mode shapes:**

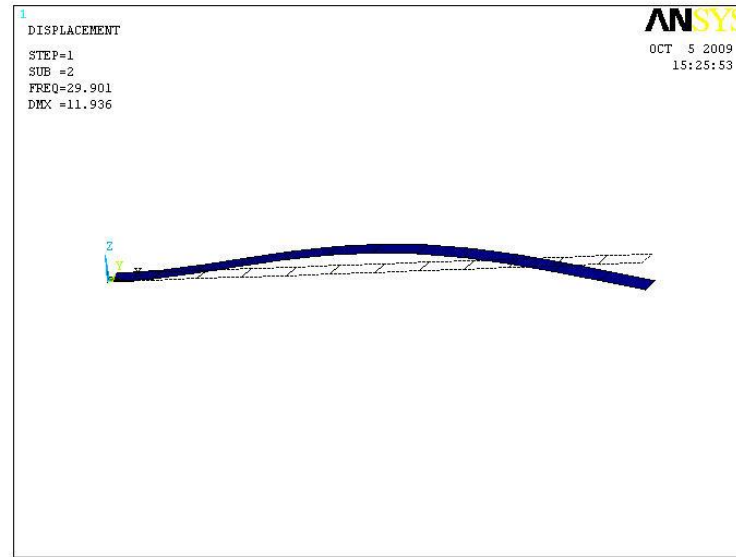
Few of the mode shapes obtained from Finite Element Analysis are shown below for both the cases.

##### **4.5.1. Mode shapes for first case:**

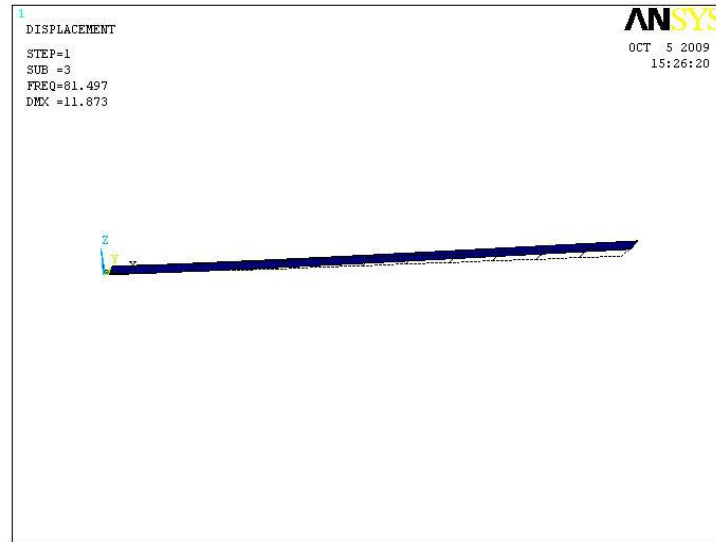


Case 1---First mode

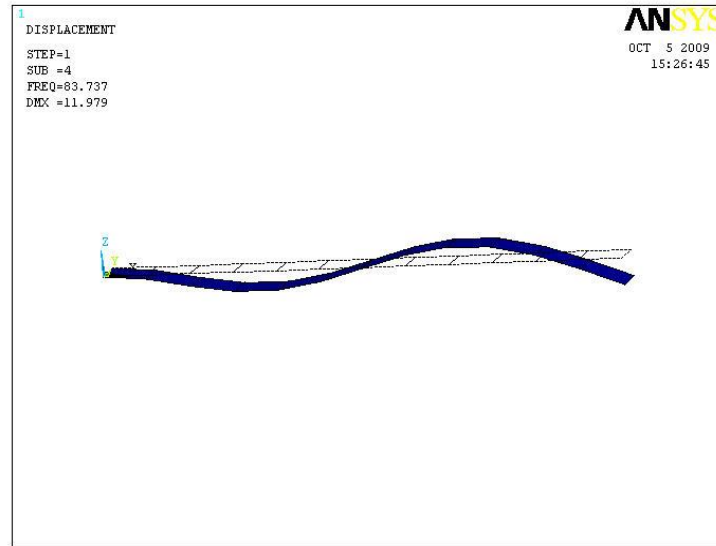




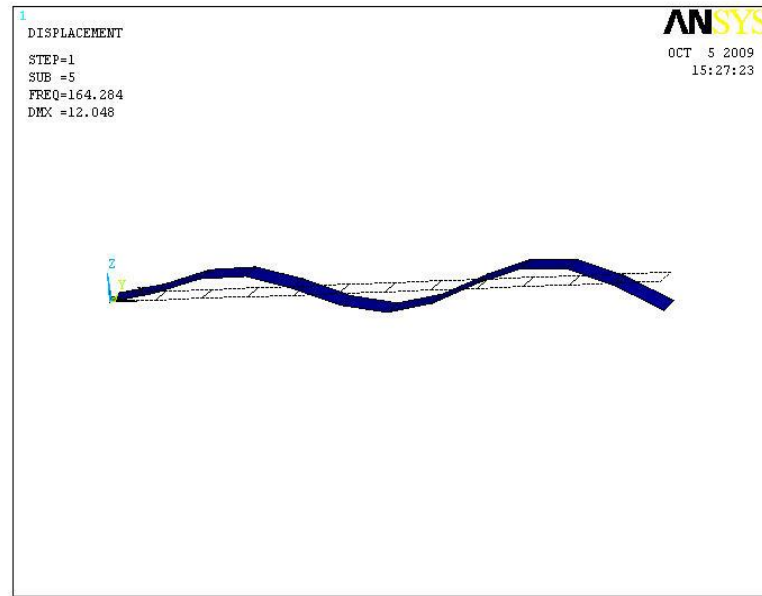
Case 1---Second mode



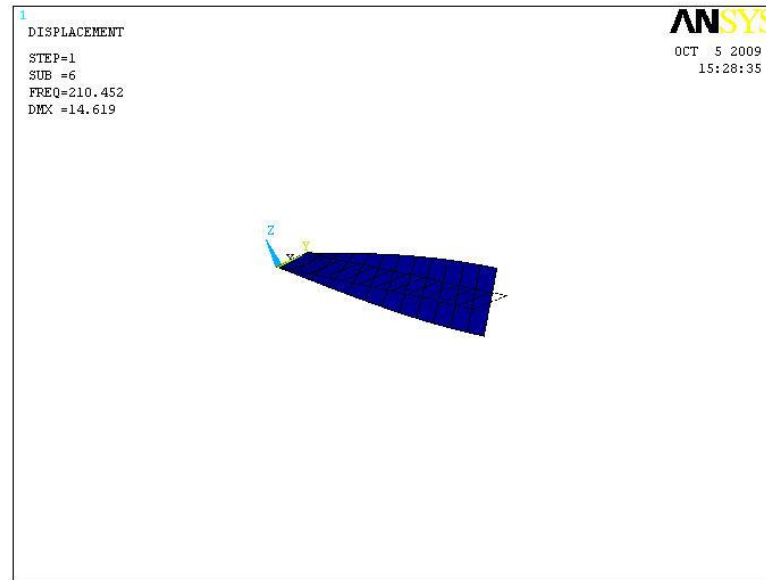
Case 1---Third mode



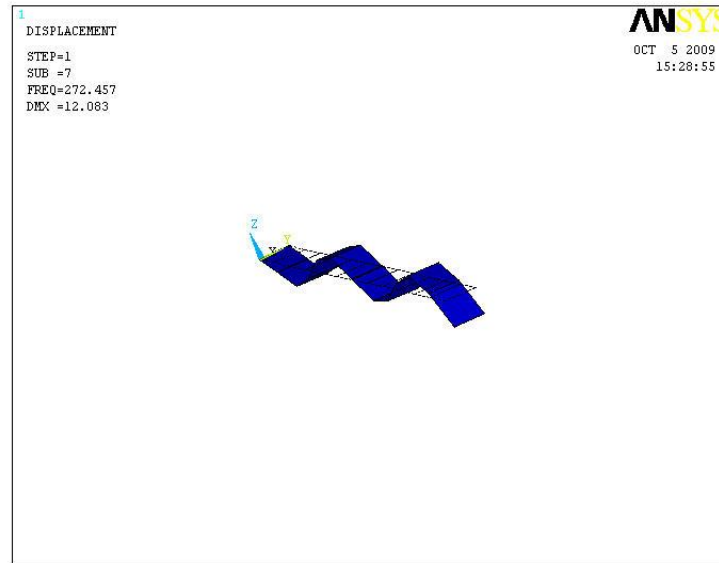
Case 1--Fourth mode



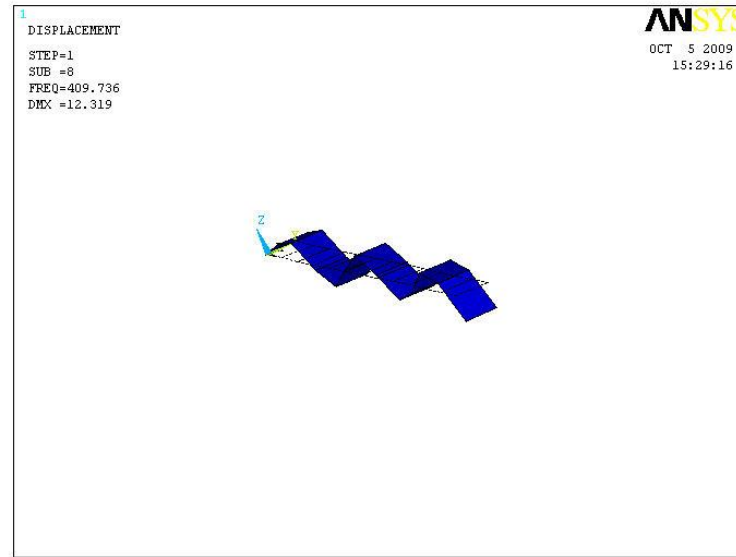
Case 1--Fifth mode



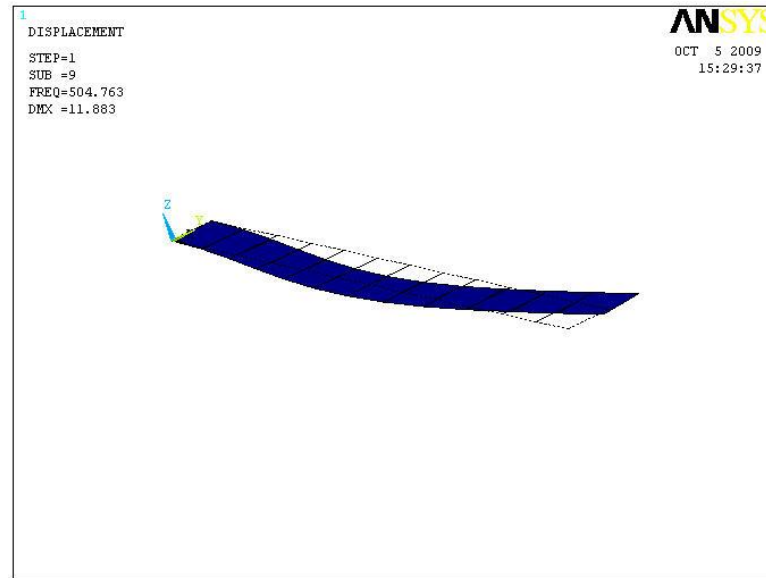
Case 1Sixth mode



Case 1 Seventh mode

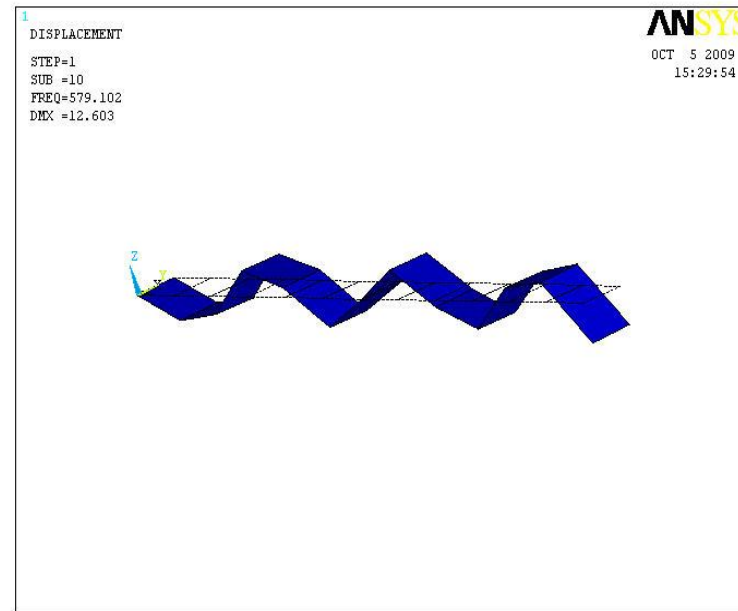


Case 1 Eighth mode



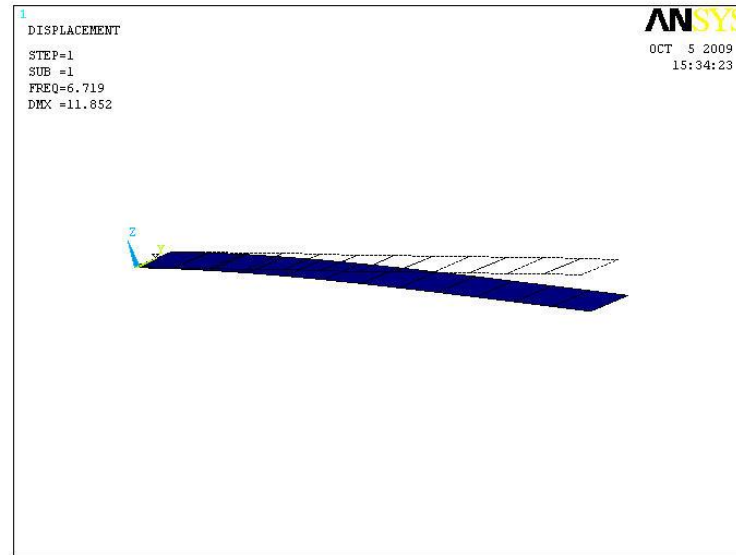
Case 1 Ninth mode



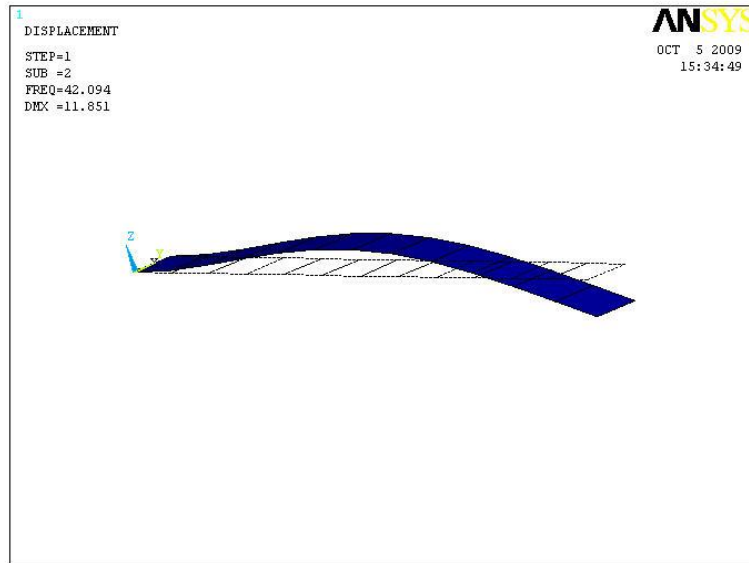


Case 1--Tenth mode

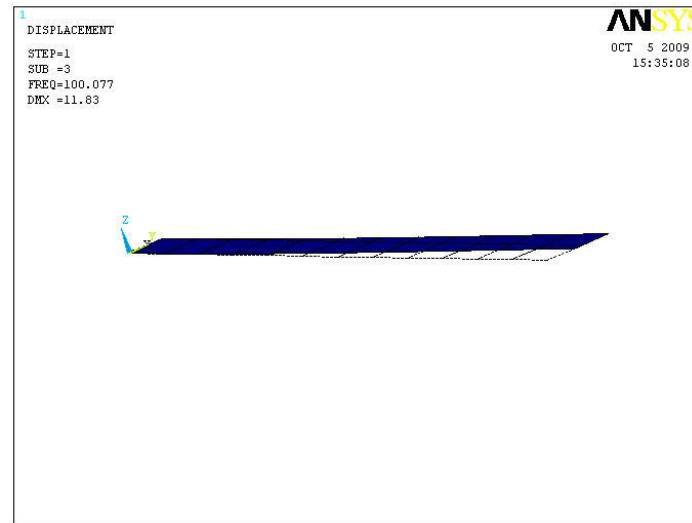
#### 4.5.2. Mode shapes for second case



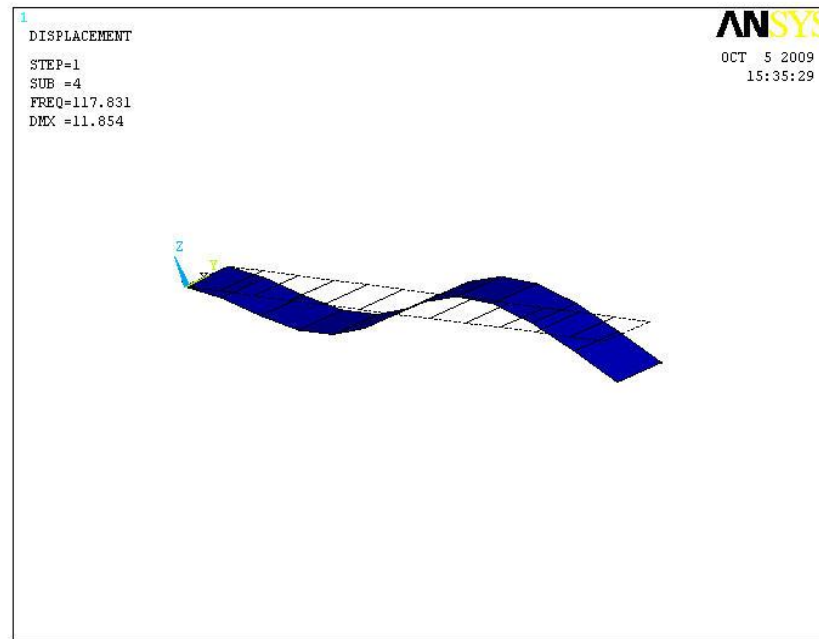
Case 2--First mode



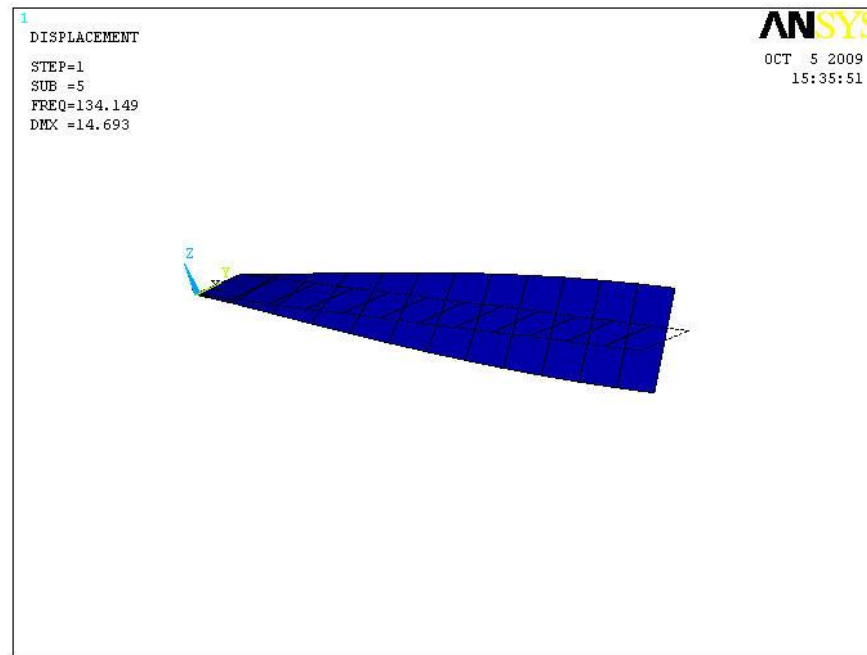
Case 2--Second mode



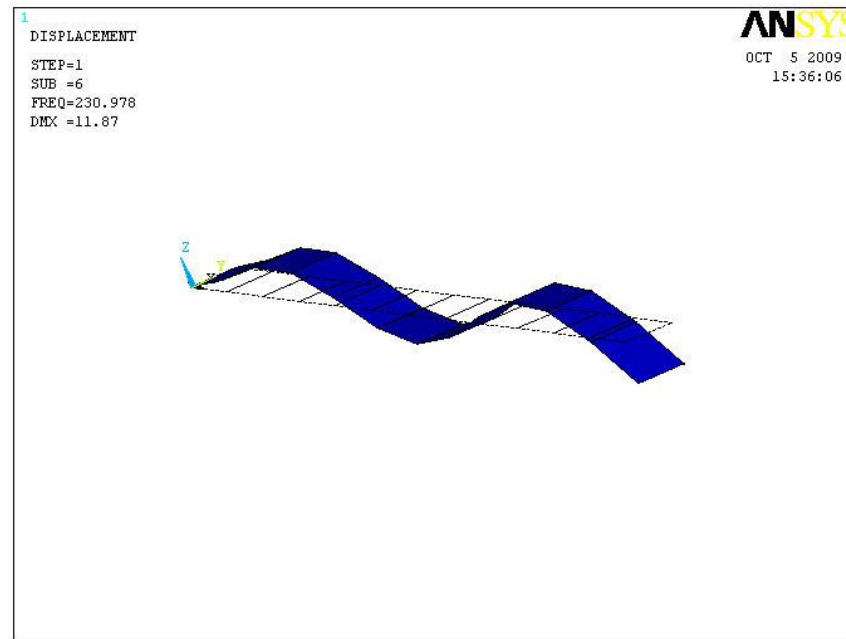
Case 2--Third mode



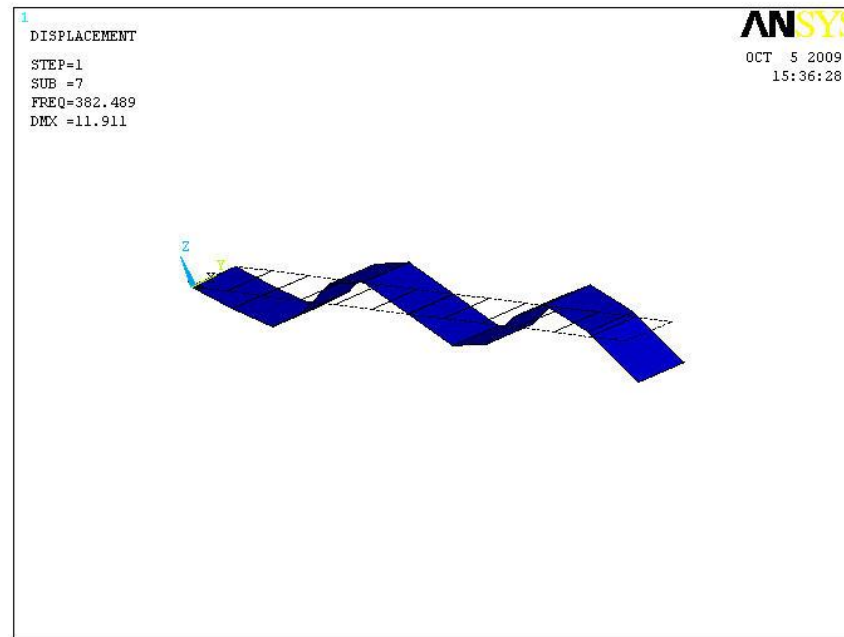
Case 2--Fourth mode



Case 2--Fifth mode

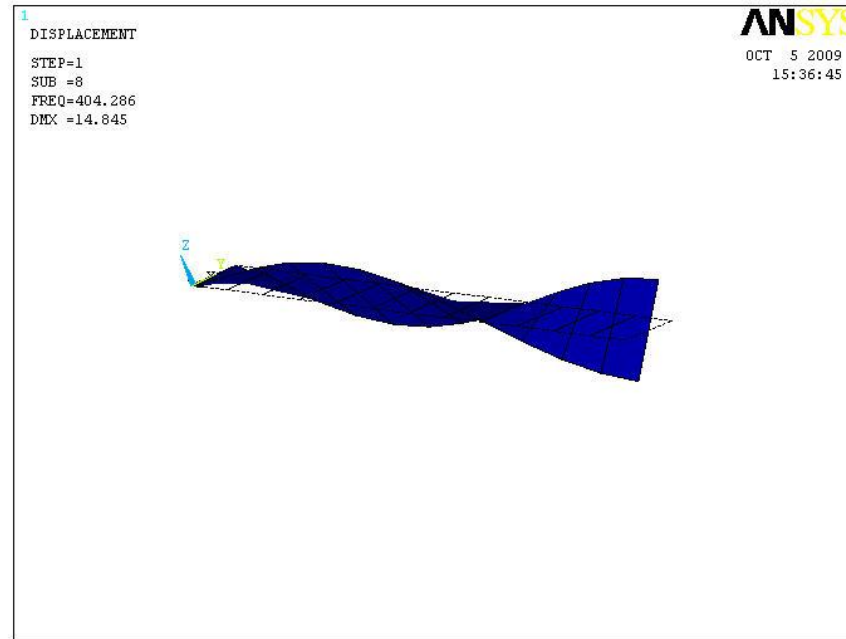


Case 2--Sixth mode

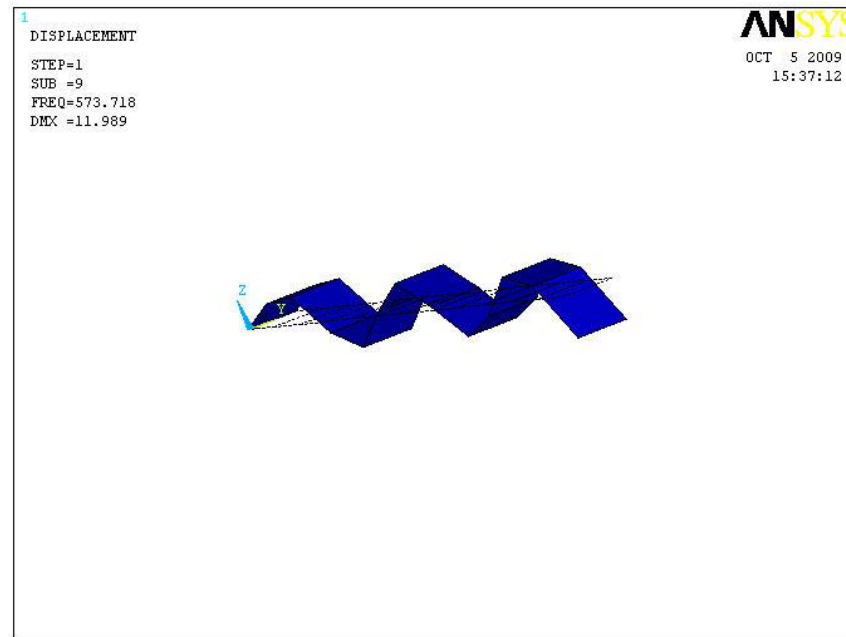


Case 2--Seventh mode

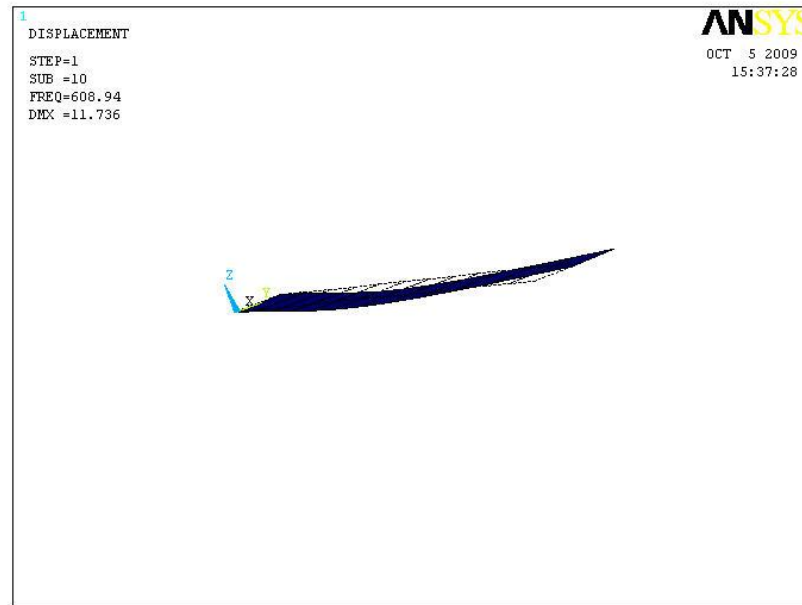




Case 2--Eighth mode



Case 2--Ninth mode

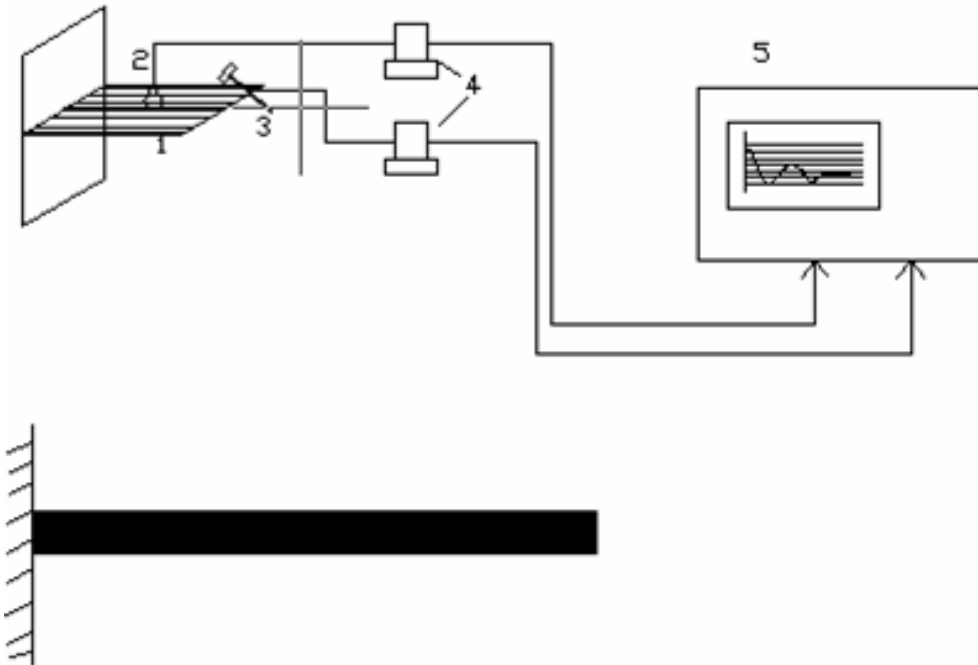


Case 2--Tenth mode

#### 4.6. Experimental analysis of Glass-Epoxy composite Rectangular

##### laminated beams:

The experiment is conducted by fixing the specimen in a rigid support with other end free to vibrate, as a cantilever beam. The impact hammer was used to give impact to the specimen, and the Spectral analyzer was set from 0-400 Hz. This output was captured by using accelerometer connected to the sensor which is fixed to the beam and amplified. The Frequency response function (FRF) is analysed using the spectrum analyzer. After the measurement of the FRF (Amplitude and phase), the natural frequencies were evaluated. The block diagram of the experimental set up is as shown in figure 4.1.



1. Cantilever beam   2. Accelerometer   3. Impact hammer with piezoelectric cells
4. Power Amplifier   5. Spectrum Analyzer.

**Figure.4.1. Block diagram of experimental set up for modal analysis**

## 4.7. Background

Frequency response measurements are a type of modal testing which can be used to determine the resonant frequencies of a structure. Frequency response testing is accomplished by exciting a system with a known input and simultaneously measuring the corresponding output response. Figure 4.2 is a block diagram which represents a system with one input (single-point excitation) and the output response.

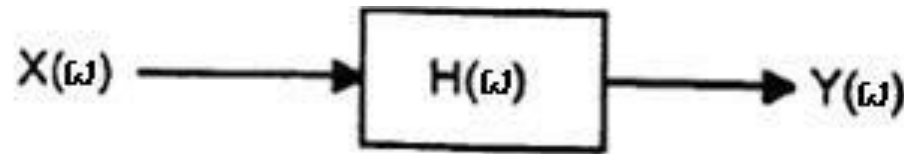


**Fig. 4.2. Block diagram with input and output response.**

Where  $X(\omega)$  is the excitation supplied to the structure,  $Y(\omega)$  is the system's response, and  $H(\omega)$  is the physical system being analyzed. The ratio of response to excitation versus frequency is defined as the frequency response. Figure 4.3 shows the instruments that can be used to conduct frequency response measurements by impact test of a beam and utilizing digital data acquisition and set up is shown. The fig. 4.4. shows the photograph of two specimens of Glass-Epoxy rectangular composite specimens, which are used for conducting the experiments to find the natural frequencies. These specimens are manufactured by following the steps mentioned in this chapter.



IMPACT TEST EXPERIMENTAL SET UP

**Fig.4.3.**Picture of the experimental set up of an impact experiment.



**Fig.4.4. photograph of specimens of Glass-Epoxy rectangular composite specimens.**



#### 4.8. Comparisons of experimental results with numerical results

The rectangular laminated beam is analysed by ANSYS for a cantilever boundary condition and numerical results are listed in table 4.2 for both the cases. The rectangular laminated beam is fixed at one end in the impact experimental setup and results are tabulated in table 4.3 for both cases of beams.

**Table: 4.2 Numerical results obtained from FEM**

Case 1 [45/-45/45/-45/45/-45/45/-45/0/90]		Case 2 0/90/0/90/0/90/0/90/0/90	
Mode	Frequency in Hz	Mode	Frequency in Hz
1 <sup>st</sup> Flexural Mode	4.2	1 <sup>st</sup> Flexural Mode	5.3
2 <sup>nd</sup> Flexural Mode	26.2	2 <sup>nd</sup> Flexural Mode	34.1
3 <sup>rd</sup> Flexural Mode	74	3 <sup>rd</sup> Flexural Mode	96.5

4 <sup>th</sup> Flexural Mode	143	4 <sup>th</sup> Flexural Mode	107.2
1 <sup>st</sup> Torsional Mode	176	1 <sup>st</sup> Torsional Mode	193
5 <sup>th</sup> Flexural Mode	241.2	5 <sup>th</sup> Flexural Mode	310.2

**Table: 4.3.Experimental results for two cases**

<b>Case 1</b> <b>[45/-45/45/-45/45/-45/45/-45/0/90]</b>		<b>Case 2</b> <b>0/90/0/90/0/90/0/90/0/90</b>	
Mode	Frequency in Hz	Mode	Frequency in Hz
1 <sup>st</sup> Flexural Mode	4	1 <sup>st</sup> Flexural Mode	5.9
2 <sup>nd</sup> Flexural Mode	27	2 <sup>nd</sup> Flexural Mode	36
3 <sup>rd</sup> Flexural Mode	74	3 <sup>rd</sup> Flexural Mode	97
4 <sup>th</sup> Flexural Mode	149	4 <sup>th</sup> Flexural Mode	109
1 <sup>st</sup> Torsional Mode	181	1 <sup>st</sup> Torsional Mode	197
5 <sup>th</sup> Flexural Mode	237	5 <sup>th</sup> Flexural Mode	326

The natural frequencies obtained from numerical analysis and experimental are compared separately and the percentage variation is calculated and listed in table 4.4 and table 4.5 for case 1 and case 2 of rectangular laminated composite beams. This is to

validate the results obtained from numerical analysis. It is found that the natural frequencies obtained from ANSYS are in good agreement with the experimental results. The same is assumed to be valid for the cases of uniform composite I-beam and tapered composite I-beam and the study of these beams is carried out in subsequent chapters.

**Table: 4.4.Percentage Variation in natural frequencies for case 1**

Case 1 [45/-45/45/-45/45/-45/45/-45/0/90]			Difference	% Variation
Mode	Frequency in Hz from FEM	Frequency in Hz from experiment		
1 <sup>st</sup> Flexural Mode	4.2	4	0.2	4.7619
2 <sup>nd</sup> Flexural Mode	26.2	27	0.8	3.053
3 <sup>rd</sup> Flexural Mode	74	74	0.0	0.0
4 <sup>th</sup> Flexural Mode	143	149	6.0	4.196

1 <sup>st</sup> Torsional Mode	176	181	5.0	2.841
5 <sup>th</sup> Flexural Mode	241.2	237	4.2	1.7413

**Table: 4.5.Percentage Variation in natural frequencies for case 2**

Case 2 0/90/0/90/0/90/0/90/0/90			Difference	% Variation
Mode	Frequency in Hz	Frequency in Hz		
1 <sup>st</sup> Flexural Mode	5.3	5.9	0.6	11.321
2 <sup>nd</sup> Flexural Mode	34.1	36	1.9	5.572
3 <sup>rd</sup> Flexural Mode	96.5	97	0.5	0.518
4 <sup>th</sup> Flexural Mode	107.2	109	1.8	1.679
1 <sup>st</sup> Torsional Mode	193	197	4	2.073
5 <sup>th</sup> Flexural Mode	310.2	326	15.8	5.093

## **4.9. Results and Discussions**

The natural frequency values for the composite glass-epoxy rectangular laminated beams are shown in the above tables 4.2 and 4.3 .These results are compared with the numerical results obtained from ANSYS and the percentage variation is found to be the in good agreement with the experimental values of frequencies.



## **Chapter 5**

# **Galerkin Finite Element Analysis of Free Torsional Vibrations of Tapered Cantilever I - Beams**

## **Galerkin Finite Element Analysis of Free Torsional Vibrations of Tapered Cantilever I - Beams**

### **5.1. Introduction**

It is commonly believed that material saving can be accomplished by using non-uniform beams. Non-uniform thin-walled beams are quite commonly used in aircraft, bridges and several other industrial structures. In view of the current emphasis on structural optimization, there is an urgent need to obtain a proper understanding of the vibration characteristics of non-prismatic structural members. Several investigations [84-86] have been reported on torsional vibrations and stability of long uniform thin-walled open section beams, such as I-beams.

Static torsional response and lateral-torsional stability of tapered I-beams has been investigated by many researchers [65-72]. Among these, Hamaychi [66], Lee [67], Wilde [68], presented basic derivations for a comprehensive theory of non-uniform torsion of tapered I-beams and they have also studied the lateral stability of stepped cantilever beams of rectangular and I-cross-section using a Runge Kutta integration procedure. The problem of lateral-torsional buckling of tapered I-beams has been studied by Kitipornchai and Trahair [71], Brown [72], Culver and Preg [46] and Shiomi and Kurata [47]. In these studies, solutions were obtained for simply supported and cantilever beams using finite-difference or finite-integral methods.

A review of the literature clearly shows that very few studies [73-74, 75] have been conducted on the free vibration characteristics of non-uniform thin-walled beams. It can be also seen that especially little progress has been made in the area of torsional vibrations of I-beams with taper along their depth.

In this chapter, the governing differential equation for torsional vibrations of tapered doubly symmetric I-beams is derived and solved for the case of a cantilever I-beam fixed at its bigger end and free at the larger end by utilizing the Galerkin finite element method. The governing differential equation for torsional vibrations of tapered doubly symmetric I-beams was derived and solved and analysed for cantilever I-beam. The individual as well as combined effects of linear taper in the width of flanges and the depth of the web on torsional natural frequencies were investigated.

This chapter deals with the case of cantilever I-beams with uniform linear taper in web height ( $\beta$ ), flange width ( $\alpha$ ) and flange thickness ( $\gamma$ ) with the bigger end fixed and smaller end free.

## 5.2. Governing equation of torsional motion

Consider free torsional vibrations of a doubly symmetric thin-walled I-beam of variable cross-section and of length  $L$ . the variations in the width of the flanges and the depth of the web are respectively assumed to be of the form

$$b(z) = b_0 (1 - \alpha/L), \quad (5.1)$$

$$d(z) = d_0 (1 - \beta z/L), \quad (5.2)$$

where  $z$  is the distance along the length of the beam, and  $\alpha$  and  $\beta$  are the taper ratios in the width of the flanges and depth of the web, respectively. The values with subscript zero are those at the bigger end of the beam .

When the beam is executing torsional vibration, the bending moment,  $M$ , induced in the flanges is given by equation 5.3.

$$M(z) = EI_f(z) \partial^2 u / \partial z^2. \quad (5.3)$$

In equation (5.3), the warping displacement,  $u$ , in the flanges is given by

$$U(z) = [h(z)/2]\phi, \quad (5.4)$$

Where  $h(z)$  is the height between centrelines of the flanges. Hence,

$$H(z) = d(z) + t_f. \quad (5.5)$$

Substituting equation (5.4) in equation (5.3) gives

$$M(z) = EI_f(z) \partial^2 / \partial z^2 [(h(z)/2) (\partial^2 u / \partial z^2)] \quad (5.6)$$

The torque,  $T$ , induced in the beam is given by (5.6)

$$T(z) = Gc_s(z) \frac{\partial \phi}{\partial z} - h(z) \frac{\partial M(z)}{\partial z} + M(z) \frac{dh(z)}{dz}. \quad (5.7)$$

For free torsional vibrations, the static torque is replaced by the inertia torque which has an intensity of  $\rho I_p(z) \frac{\partial^2 \phi}{\partial t^2}$ , in which  $I_p$  is the polar moment of inertia and  $\rho$  is the mass density of the material of the beam. Thus,

$$\frac{\partial T(z)}{\partial z} = \rho I_p(z) \frac{\partial^2 \phi}{\partial t^2}. \quad (5.8)$$

Substituting equation (5.7) in equation (5.8) gives

$$\begin{aligned} \frac{\partial}{\partial z} [Gc_s(z) \frac{\partial \phi}{\partial z}] - \frac{\partial^2}{\partial z^2} [EI_f(z)h(z) \frac{\partial^2}{\partial z^2} ((h(z)/2)(\phi))] \\ + 2(\frac{\partial}{\partial z})[EI_f(z) (dh(z)/dz)/dz (\frac{\partial^2}{\partial z^2} (h(z)/2) \phi)] = \rho I_p(z) (\frac{\partial^2 \phi}{\partial t^2}) \end{aligned} \quad (5.9)$$

For harmonic vibration the angle of twist  $\phi$  can be written in the form

$$\phi(z,t) = \theta(z) \sin \omega t. \quad (5.10)$$

Substituting equation (5.10) in equation (5.4) gives

$$\partial/\partial z [Ec_w(z) d^2/dz^2 (h(z)/2) \theta] - d/dz [Gc_s(z) d\theta/dz]$$

$$-2(d/dz)[EI_f(z) (dh(z)/dz)/dz (d^2/dz^2 (h(z)/2) \theta)] - \rho I_p(z) \omega^2 \theta = 0 \quad (5.11)$$

When expanding the differential equation (5.11), terms containing  $d^2h(z)/dz^2$  are neglected as the depth taper considered in this study is linear.

Equation (5.11) is a fourth order differential equation with variable coefficients and a Galerkin-finite element method has been utilized in this study in obtaining the solutions for cantilever beams.

### 5.3. Finite Element Formulation

In the Galerkin-finite element formulation, the domain of the beam is subdivided into a number of elements. A third degree polynomial for angle of twist in  $z$  is assumed over the element. The variation of Torsional amplitudes  $\theta_e$  over each element, in terms of nodal degrees of freedom  $\theta$  and  $\theta'$ , is given by

$$\{\theta_e\} = [x]\{\delta_e\} \quad (5.12)$$

Where  $\{x\}$  is the row matrix of shape functions

$$\{\delta\}_e = [\theta_1, \theta'_1, \theta_2, \theta'_2]^T \quad (5.13)$$

Here primes denote differentiation with respect to  $z$  and subscripts 1 and 2 denote the two ends of the element.

Substituting equation (5.12) in equation (5.11) gives the residual  $R_e$  for the element as

$$R_e = EI_f h [h/2]'' [X]'' \{\delta\}_e - [Gc_s X] \{\delta\}_e - 2 EI_f h' [h/2]'' [X]'' \{\delta\}_e - \rho I_p \omega^2 x \{\delta\}_e \quad (5.14)$$

Where  $E$  = Young's modulus,

$I_f$  = Moment of Inertia of flange

$h$  = height of the beam,

$[h/2]''$  = second derivative of  $h$  w.r.t  $z$

$[X]''$  = second derivative of  $X$  w.r.t  $z$

$h'$  = first derivative of  $h$  w.r.t  $z$

In the Galerkin - finite element method, the weighted residual is minimized by setting

$$\frac{\partial}{\partial \{\delta\}_e} \int_0^L R_e \theta_e dz = 0 \quad (5.15) \quad \frac{\partial \{\delta\}_e}{\partial \{\delta\}_e} = 0$$

This procedure is repeated for all elements and after the usual assembly procedure; the final matrix equation governing free vibration is obtained as



$$[A]\{\delta\} - \lambda_n^2 [B]\{\delta\} = 0. \quad (5.16)$$

where

$$\lambda_n^2 = A_{f0} \omega^2 L^4 / EI_{f0} \quad (5.17)$$

the quantities  $A_{f0}$  and  $I_{f0}$  are the flange area and moment of inertia respectively at the fixed end. Also,  $[A]$  is the stiffness matrix,  $[B]$  the mass matrix and  $\{\delta\}$  the eigenvector. Equation (5.16) can be solved by using any standard eigenvalue algorithm to obtain the eigenvalues and eigenvectors  $\{\delta\}$ .

## 5.4. Numerical Results

Numerical results of the frequency parameter  $\lambda$  have been obtained, by dividing the beam into a sufficient number of elements, for the case of a tapered cantilever I-beam. It is found that 12 elements are sufficient to yield convergence. The boundary conditions considered at the fixed end are  $\theta = \theta' = 0$ .

The values of  $\lambda$  for various combinations of taper ratios  $\alpha$  and  $\beta$  for the first three modes of vibration are presented in the figures Graph 5.1., Graph 5.2. and Graph 5.3 (first, second and third modes respectively). The combined influence of positive taper ratio  $\beta$  and negative taper ratio  $\alpha$  on the first three frequencies of vibration are shown in the figures.

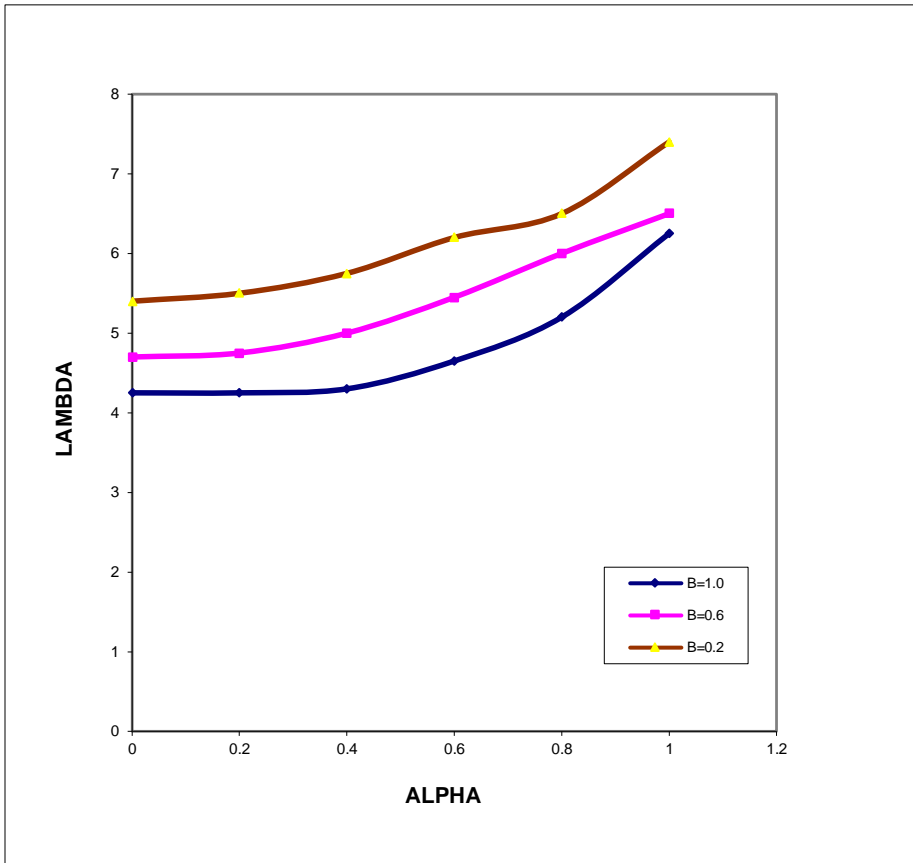


**Fig. 5.1. Combined influence of positive taper ratio  $\beta$  and negative ratio  $\alpha$   
(FIRST MODE)**

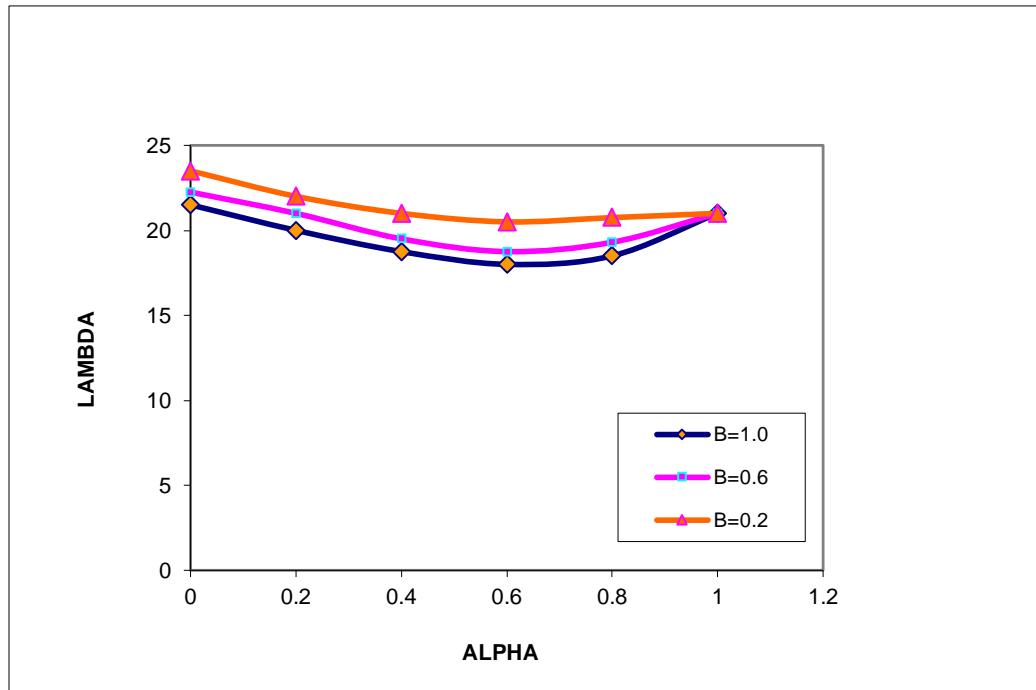
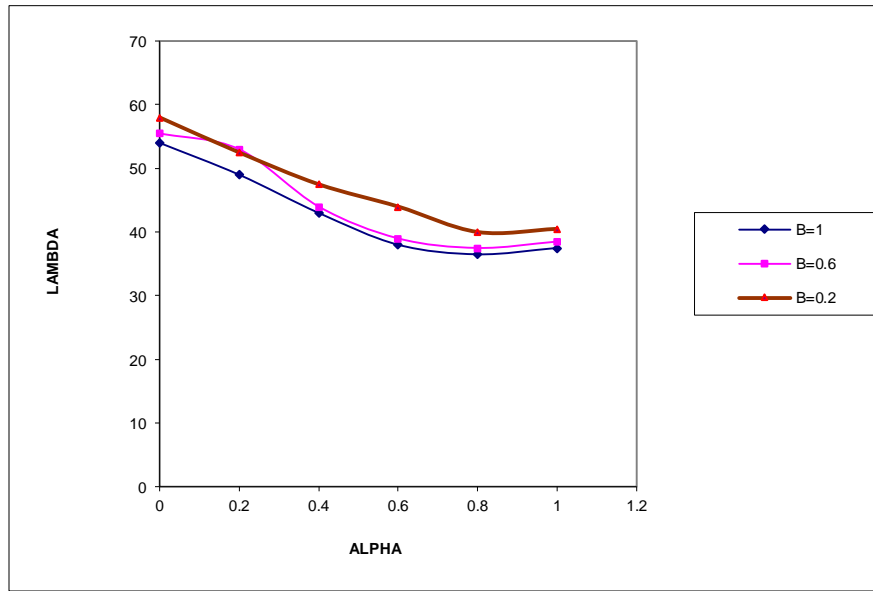


**Fig.5.2 Combined influence of positive taper ratio  $\beta$  and negative ratio  $\alpha$**



**(SECOND MODE)**

**Fig. 5.3 Combined influence of positive taper ratio  $\beta$  and negative ratio  $\alpha$   
(THIRD MODE)**

## 5.5. Results and discussion

The torsional frequencies of first three modes of vibration are increasing significantly by increasing values of taper ratio  $\beta$  and marginally for increasing values of taper ratios  $\alpha$  and  $\lambda$ .

The torsional frequencies of first three modes of vibration are significantly increasing for increasing values of taper ratios  $\beta$  and  $\lambda$  and are decreasing drastically for increasing values of taper ratio  $\alpha$  in second mode and third modes of vibration only.

The torsional frequency increases significantly for increasing values of combined influence of negative taper ratios  $\alpha$  and  $\beta$  in first mode. In second and third modes of vibrations the torsional natural frequency gradually decreases to certain value and then starts increasing.

## **Chapter 6**

# **Torsional Vibrations and Buckling of Thin-Walled Beams on Elastic Foundation-Dynamic Stiffness method**

# Torsional Vibrations and Buckling of Thin-Walled Beams on Elastic Foundation- Dynamic Stiffness Method

## 6.1. Introduction

The problem of free torsional vibration and buckling of doubly symmetric thin-walled beams of open section, subjected to an axial compressive static load and resting on continuous elastic foundation, is discussed in this chapter. An analytical method based on the dynamic stiffness matrix approach is developed including the effect of warping. The resulting transcendental equation is solved for thin-walled beams clamped at one end and simply supported at the other. The dynamic stiffness matrix can be used to compute the natural frequencies and mode shapes of either a single beam with various end conditions or an assembly of beams. When several elements are to be used the overall dynamic stiffness matrix of the complete structure must be assembled. The associated natural frequencies and mode shapes are extracted using Wittrick-Williams algorithm (36). The algorithm guarantees that no natural frequency and its associated mode shape are missed. This is, of course, not possible in the conventional finite element method. Numerical results for natural frequencies and buckling load for various values of warping and elastic foundation parameter are obtained and presented.

The vibrations and buckling of continuously – supported finite and infinite beams on elastic foundation have applications in the design of aircraft structures, base frames for rotating machinery, rail road tracks, and etc. several studies have been conducted on this topic, and valuable practical methods for the analysis of beams on elastic foundation have been suggested. A discussion of various foundation models was presented by Kerr.

While there are a number of publications on flexural vibrations of rectangular beams and plates on elastic foundation, the literature on torsional vibrations and buckling of beams on elastic foundation is rather limited. Free torsional vibrations and stability of doubly-symmetric long thin-walled beams of open section were investigated by Gere , Krishna Murthy and Joga Rao and Christiano and Salmela , Kameswara Rao et al., used a finite element method to study the problem of torsional vibration of long thin-walled beams of open section resting on elastic foundations. In another publication Kameswara Rao and Appala satyam developed approximate expressions for torsional frequency and buckling loads for thin walled beams resting on Winkler-type elastic foundation and subjected to a time invariant axial compressive force.

It is known that higher mode frequencies predicted by approximate methods are generally in considerable error. In order to improve the situation, a large number of elements or terms in the series have to be included in the computations to get values with acceptable accuracy. In view of the same, more and more effort is being put into developing frequency dependent ‘exact’ finite elements or dynamic stiffness and mass matrices. In the present chapter, an improved analytical method based on the dynamic stiffness matrix approach is developed including the effects of Winkler – type elastic foundation and warping torsion. The resulting transcendental frequency equation is solved for a beam clamped at one end and simply supported at the other. Numerical results for torsional natural frequencies and buckling loads for some typical values of warping and foundation parameters are presented. The approach presented in this chapter is quite general and can be utilised in analyzing continuous thin – walled beams also.

## **6.2. Formulation and analysis:**

Consider a long doubly-symmetric thin walled beam of open section of length  $L$  and resting on a Winkler –type elastic foundation of torsional stiffness  $K_s$ . The beam is subjected to a constant static axial compressive force  $P$  and is undergoing free torsional vibrations. The corresponding differential equation of motion can be written as



$$EC_w \partial^4 \phi / \partial z^4 - (GC_s - \rho I_p / A) \partial^2 \phi / \partial z^2 + K_s \phi + \rho I_p \partial^2 \phi / \partial t^2 \quad 6.1$$

In which E, the modulus of elasticity;  $C_w$ , the warping constant; G, the shear modulus;  $C_s$ , the torsion constant;  $I_p$ , the polar moment of Inertia; A, the area of cross section;  $\rho$ , the mass density of the material of the beam;  $\phi$ , the angle of twist; Z, the distance along the length of the beam and t, the time.

For the torsional vibrations, the angle of twist  $\phi(z,t)$  can be expressed in the form

$$\phi(z,t) = x(z)e^{ipt} \quad 6.2$$

in which  $x(z)$  is the modal shape function corresponding to each beam torsion natural frequency p.

The expression for  $x(z)$  which satisfies equation(6.1) can be written as:

$$x(z) = A \cos \alpha z + B \sin \alpha z + C \cosh \beta z + D \sinh \beta z \quad 6.3$$

in which

$$\alpha L, \beta L = (1/\sqrt{2}) \{ \sqrt{(k^2 - \Delta^2)} + [(k^2 - \Delta^2)^2 + 4(\lambda^2 - 4\gamma^2)]^{1/2} \}^{1/2} \quad 6.4$$

$$K^2 = L^2 GC_s / EC_w, \Delta^2 = \rho I_p L^2 / AEC_w \quad 6.5$$

$$\text{And } \lambda^2 = \rho I_p L^4 p^2 / EC_w \quad \gamma^2 = K_s L^4 / 4EC_w \quad 6.6$$

From equation (4), the following relation between  $\alpha L$  and  $\beta L$  is obtained.

$$(\beta L)^2 = (\alpha L)^2 + K^2 - \Delta^2 \quad 6.7$$

Knowing  $\alpha$  and  $\beta$ . The frequency parameter  $\lambda$  can be evaluated using the following equation:

$$\lambda_2 = (\alpha L)(\beta L) + 4\gamma^2 \quad 6.8$$

The four arbitrary constants A, B, C, and D in equation (6.3) can be determined from the boundary equation of the beam. For any single span beam, there will be two boundary conditions at each end and these four conditions then determine the corresponding frequency and mode shape expressions.

### 6.3. DYNAMIC STIFFNESS MATRIX:

In order to proceed further, we must first introduce the following nomenclature: the variation of angle of twist  $\phi$  with respect to  $z$  is denoted by  $\theta(z)$ ; the flange bending moment and the total twisting moment are given by  $M(z)$  and  $T(z)$ . Considering clockwise rotations and moments to be positive, we have,

$$\theta(z) = d\phi/dz, \quad 6.9$$

$$hM(z) = -EC_w (d^2\phi/dz^2)$$

and

$$T(z) = -EC_w (d^3\phi/dz^3) + (GC_s - \rho I_p/A) d\phi/dz \quad 6.10$$

Where  $ECw = I_f h/2$ ,

$I_f$  = the flange moment of inertia and

$h$  = the distance between the centre lines of flanges of a thin-walled I-beam.

Consider a uniform thin-walled I-beam element of length  $L$  as shown **in fig.1**.

By combining the equation (6.3) and (6.9), the end displacements  $\phi(0)$  and  $\theta(0)$  and end forces,  $hM(0)$  and  $T(0)$  of the beam at  $z = 0$ , can be expressed as :

$$\begin{Bmatrix} \phi(0) \\ \theta(0) \\ hM(0) \\ T(0) \end{Bmatrix} = \begin{Bmatrix} 1 & 0 & 1 & 0 & A \\ 0 & \alpha & 0 & \beta & B \\ ECw\alpha^2 & 0 & -ECw\beta^2 & 0 & C \\ 0 & ECw\alpha\beta^2 & 0 & -ECw\alpha^2\beta & D \end{Bmatrix}$$

Equation (6.11) can be written in an abbreviated form as follows:

$$\delta(0) = V(0)U \quad 6.11$$

in a similar manner , the end displacements ,  $\phi(L)$  and  $\theta(L)$  and end forces  $hM(L)$  and  $T(L)$ , of the beam where  $z = l$  can be expressed as follows:

$$\delta(L) = V(L)U$$

where

$$\{\delta(L)\}_T = \{\phi(L), \theta(L), hM(L), T(L)\}$$

$$\{U\}_T = \{A, B, C, D\}$$

and

$$[V(L)] = \begin{Bmatrix} \begin{matrix} c & s & C & S \\ -\alpha s & \alpha c & \beta S & \beta C \end{matrix} \\ \begin{matrix} ECw\alpha^2 c & ECw\alpha^2 s & -ECw\beta^2 C & -ECw\beta^2 S \\ -ECw\alpha\beta^2 s & ECw\alpha\beta^2 c & -ECw\alpha^2 \beta S & -ECw\alpha^2 \beta C \end{matrix} \end{Bmatrix}$$

in which  $c = \text{Cos}\alpha L$ ;  $s = \text{Sin}\alpha L$ ;  $C = \text{Cosh}\beta L$ ;  $S = \text{Sinh}\beta L$ .

By eliminating the integration constant vector  $U$  from equation (11) and (12), and designating the left end of the element as  $i$  and the right end as  $j$ . the equation relating the end forces and displacements can be written as:

$$\begin{Bmatrix} T_i \\ \vdots \end{Bmatrix} = \begin{Bmatrix} j_{11} & j_{12} & j_{13} & j_{14} & \varphi_i \end{Bmatrix}$$

$$\begin{array}{cccccc}
H M_i & & j_{21} & & j_{22} & & j_{23} & & j_{24} & & \theta_i \\
T_j & = & j_{31} & & j_{32} & & j_{33} & & j_{34} & & \phi_j \\
H M_j & & j_{41} & & j_{42} & & j_{43} & & j_{44} & & \theta_j
\end{array}$$

Symbolically it is written

$$\{F\} = [J] \{U\} \quad (6.12)$$

where

$$\{F\}^T = \{T_i, h M_i, T_j, h M_j\}$$

$$\{U\}^T = \{\phi_i, \theta_j, \phi_j, \theta_j\}$$

In the above equations the matrix  $[J]$  is the ‘exact’ element dynamic stiffness matrix, which is also a square symmetric matrix.

The elements of  $[J]$  are given by:

$$j_{11} = H[(\alpha^2 + \beta^2)(\alpha C_s + \beta S_c]$$

$$j_{12} = -H[(\alpha^2 - \beta^2)(1 - Cc) + 2\alpha\beta Ss]$$

$$j_{13} = -H[(\alpha^2 + \beta^2)(\alpha s + \beta S)]$$

$$j_{14} = -H[(\alpha^2 + \beta^2)(C - c)]$$

$$j_{22} = -(H/\alpha\beta)[(\alpha^2 + \beta^2)(\alpha Sc - \beta Cs)] \quad \text{-----}(6.13)$$

$$j_{24} = (H/\alpha\beta)[(\alpha^2 + \beta^2)(\alpha S - \beta s)]$$

$$j_{23} = -j_{14}$$

$$j_{33} = j_{11}$$

$$j_{34} = -j_{12}$$

$$j_{44} = j_{22}$$

$$\text{and } H = EC_w / [2\alpha\beta(1 - Cc) + (\beta^2 - \alpha^2) Ss]$$

using the element dynamic stiffness matrix defined by equation (6.12) and (6.13). One can easily set up the general equilibrium equations for multi-span thin-walled beams, adopting the usual finite element assembly methods. Introducing the boundary conditions, the final set of equations can be solved for eigen values by setting up the determinant of their matrix to zero. For convenience in programming, the signs of end forces and end displacements used in equation are all positive and are defined as shown in fig.6.1.

#### 6.4 Method of Solution:

Denoting the assembled and modified dynamic stiffness matrix as [DS], we state that  $\det |DS| = 0$

(6.14)

Equation (6.14) yields the frequency equation of continuous thin-walled beams in torsion resting on continuous elastic foundation and subjected to a constant axial compressive force. It can be noted that equation (6.14) is highly transcendental in terms of eigen values  $\lambda$ . The roots of the equation (6.14) can, therefore, be obtained by applying the Regula-Falsi method and the Wittrick – Williams algorithm on a high speed digital computer. Exact values of frequency parameter  $\lambda$  for simply supported and built in thin-walled beams are obtained in this chapter using an error factor  $\varepsilon = 10^{-6}$ .

#### 6.5 RESULTS AND DISCUSSIONS:

The approach developed in this paper can be applied to the calculation of natural torsional frequencies and mode shapes of multi –span doubly symmetric thin-walled beams of open section such as beams of I-section. Beams with non uniform cross sections also can be handled very easily as the present approach is almost similar to the finite element method of analysis but with exact displacement shape functions. All classical and non- classical (elastic restraints) boundary conditions can be incorporated in the present model without any difficulty.

To demonstrate the effectiveness of the present approach, a single span thin walled I-beam clamped at one end ( $z=0$ ) and simply supported at the other end( $z=l$ ) is chosen. The boundary conditions for this problem can be written as:

$$\phi(0) = 0; \theta(0) = 0 \quad (6.15)$$

$$\phi(l) = 0; M(l) = 0 \quad (6.16)$$

Considering a one element solution and applying the boundary conditions defined by equation (6.15) and (6.16) gives,

$$j_{22} = 0 \quad (6.17)$$

This gives,

$$j_{22} = -(H/\alpha\beta)[(\alpha^2 + \beta^2)(\alpha S_c - \beta C_s)] = 0 \quad (6.18)$$

as  $H$  and  $(\alpha^2 + \beta^2)$  are, in general, non-zero, the frequency equation for the clamped, simply supported beam can, therefore, be written as

$$\alpha \tanh \beta L = \beta \tan \alpha L \quad (6.19)$$

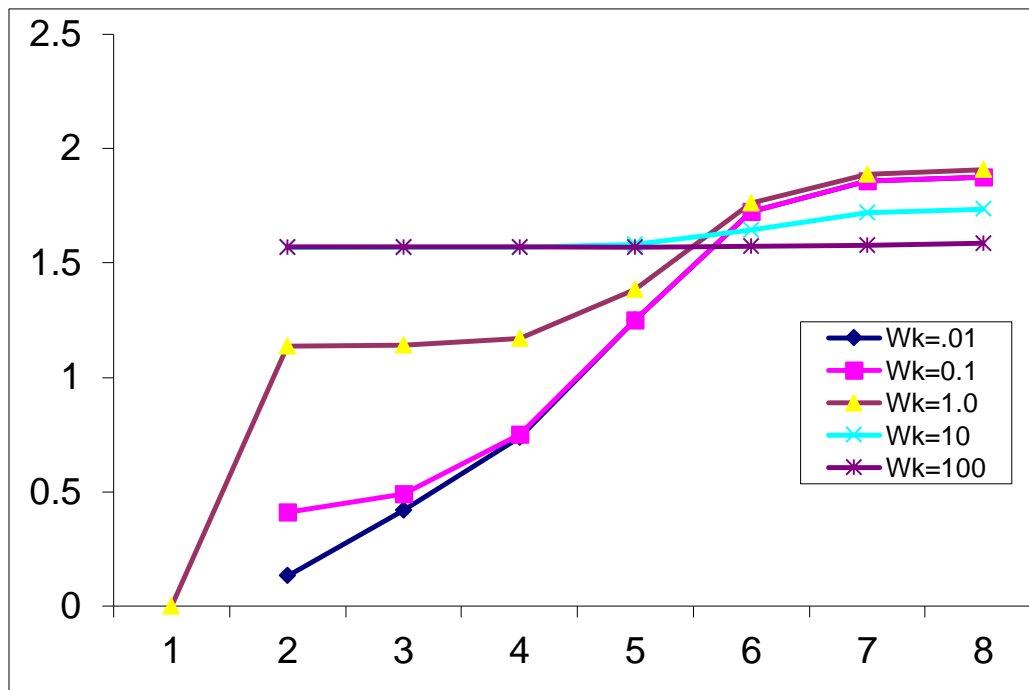
equation (6.19) is solved for values of warping parameter  $k=1$  and  $k=10$  and for various values of foundation parameter  $\gamma$  in the range 0-12.

Figures 6.2 and 6.3 show the variation of fundamental frequency and buckling load parameters with foundation parameter for values of  $k$  equal to 1 and 10 respectively. To give an idea about the accuracy of the results obtained, comparison is made with results

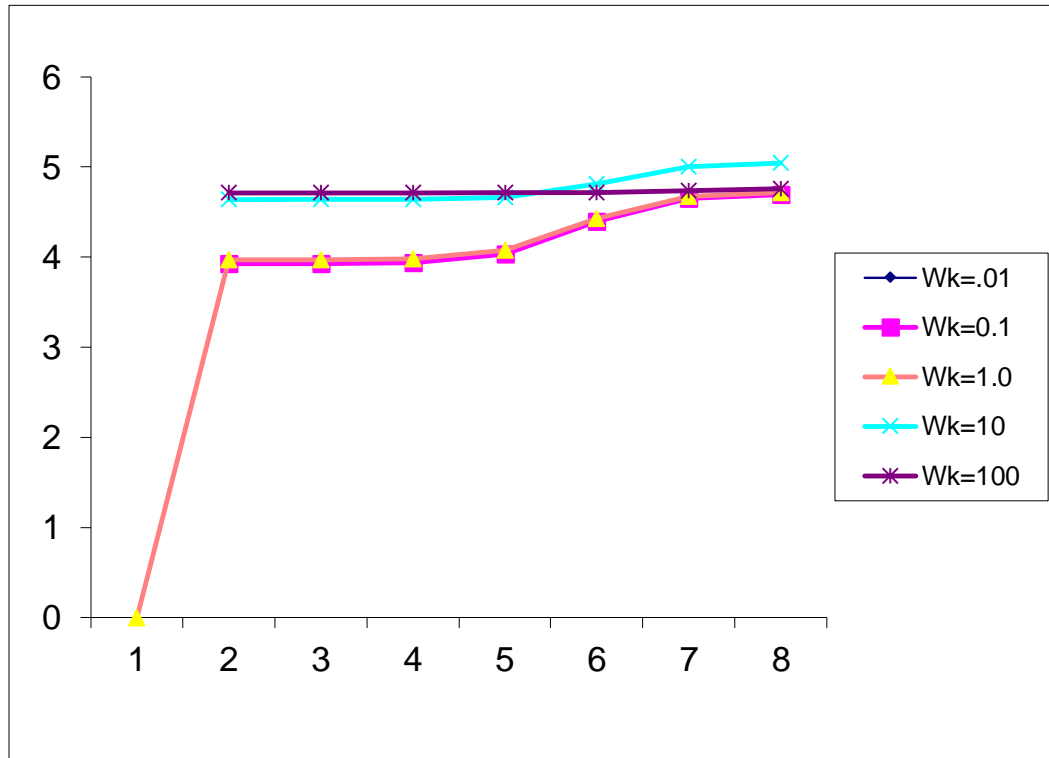


obtained using approximate methods such as Galerkin technique. It can be stated that even for the beams with non-uniform sections, multiple spans and complicated boundary conditions accurate estimates of natural frequencies can be obtained using the approach presented in this chapter.

A close look at the results presented in figures clearly reveal that the effect of an increase in axial compressive load parameter  $\Delta$  is to drastically decrease the fundamental frequency  $\lambda(N=1)$ . Further more, the limiting load where  $\lambda$  becomes zero is the buckling load of the beam for a specified value of warping parameter  $K$  and foundation parameter  $\gamma$  one can easily read the values of buckling load parameter  $\Delta_{cr}$  from these figures for  $\lambda=0$ , as can be expected, the effect of elastic foundation is found to increase the frequency of vibration especially for the first few modes. However, this influence is seen to be quite negligible on the modes higher than the third.

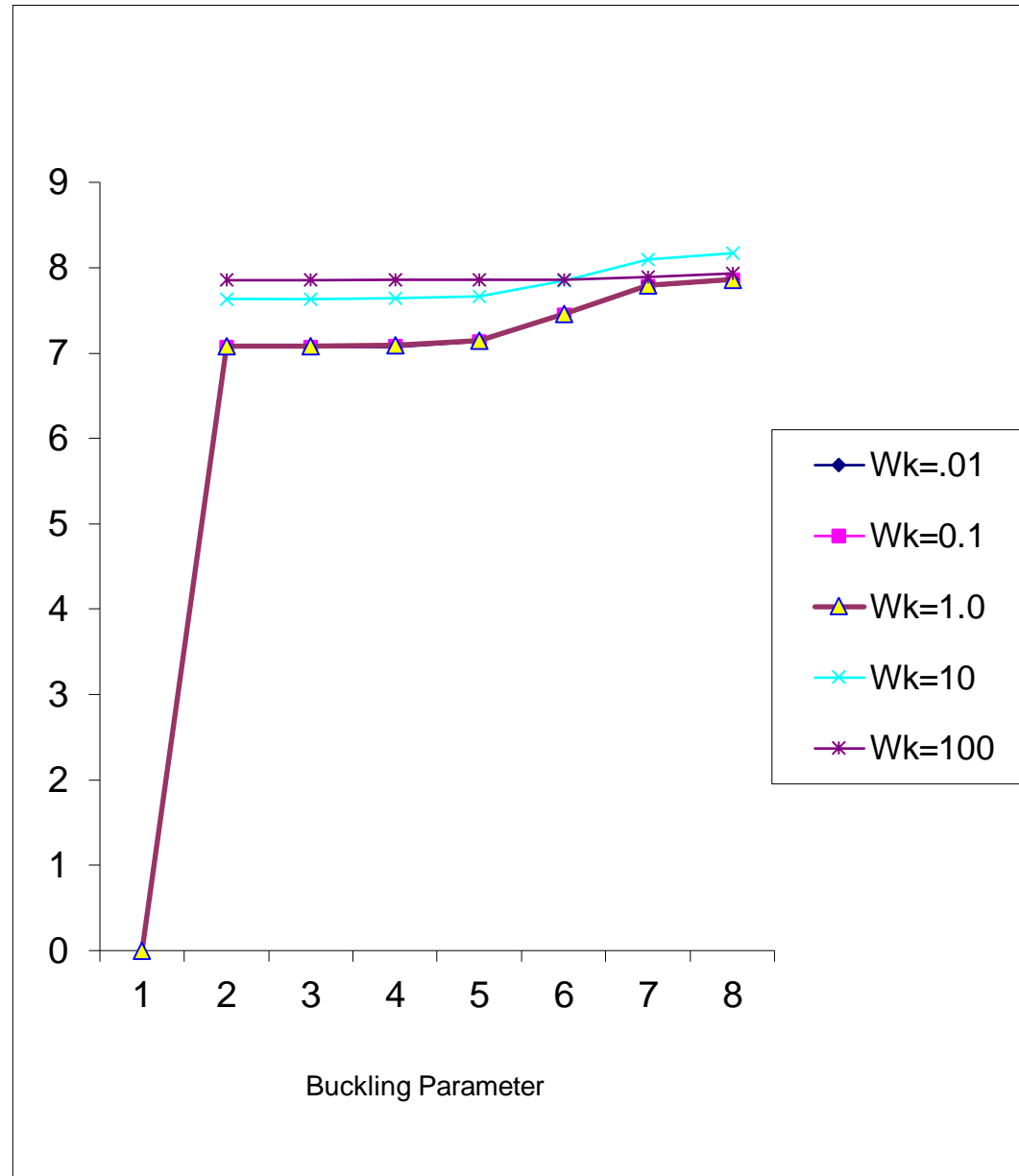


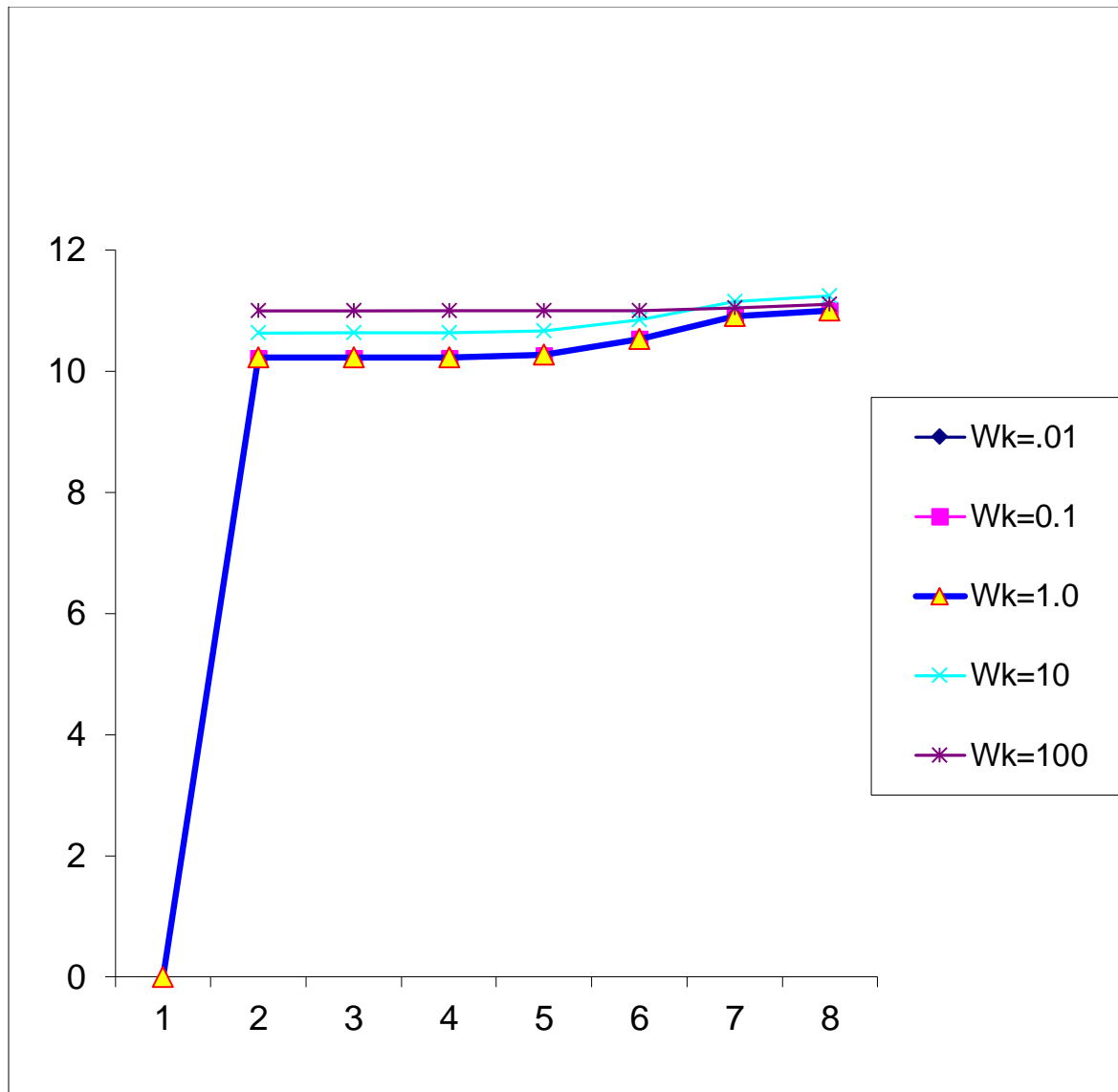
**Fig.6.1. First mode**



**Fig. 6.2 SECOND MODE**







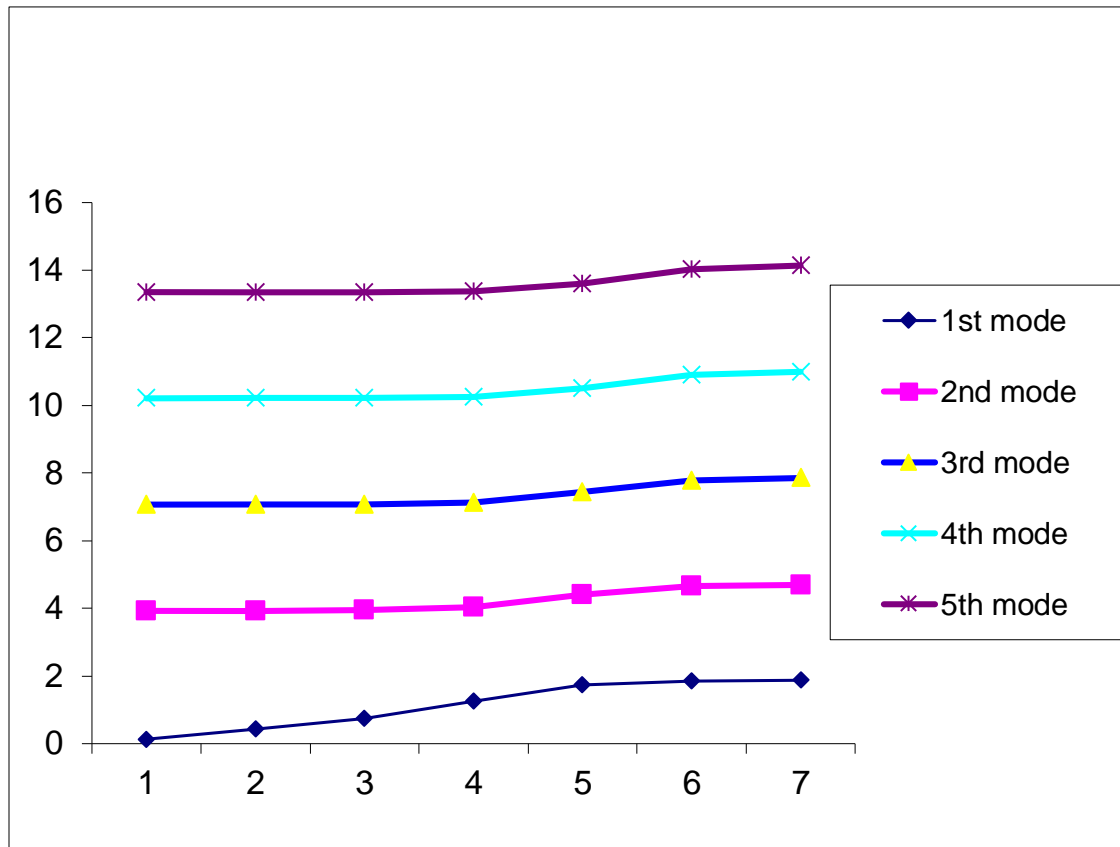


**Fig.6.4 FOUTH MODE**

**Fig. 6. 5. Mode shapes for Wk= 0.01**

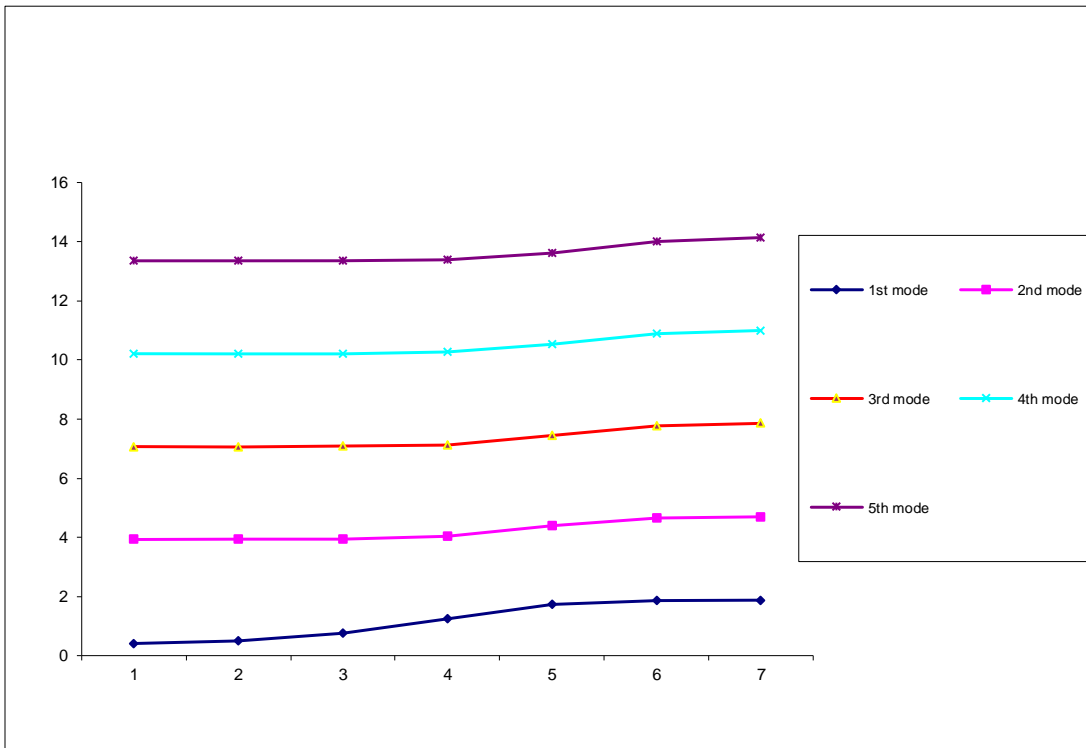


**Fig6.6. Mode shapes for  $W_k = 0.1$**



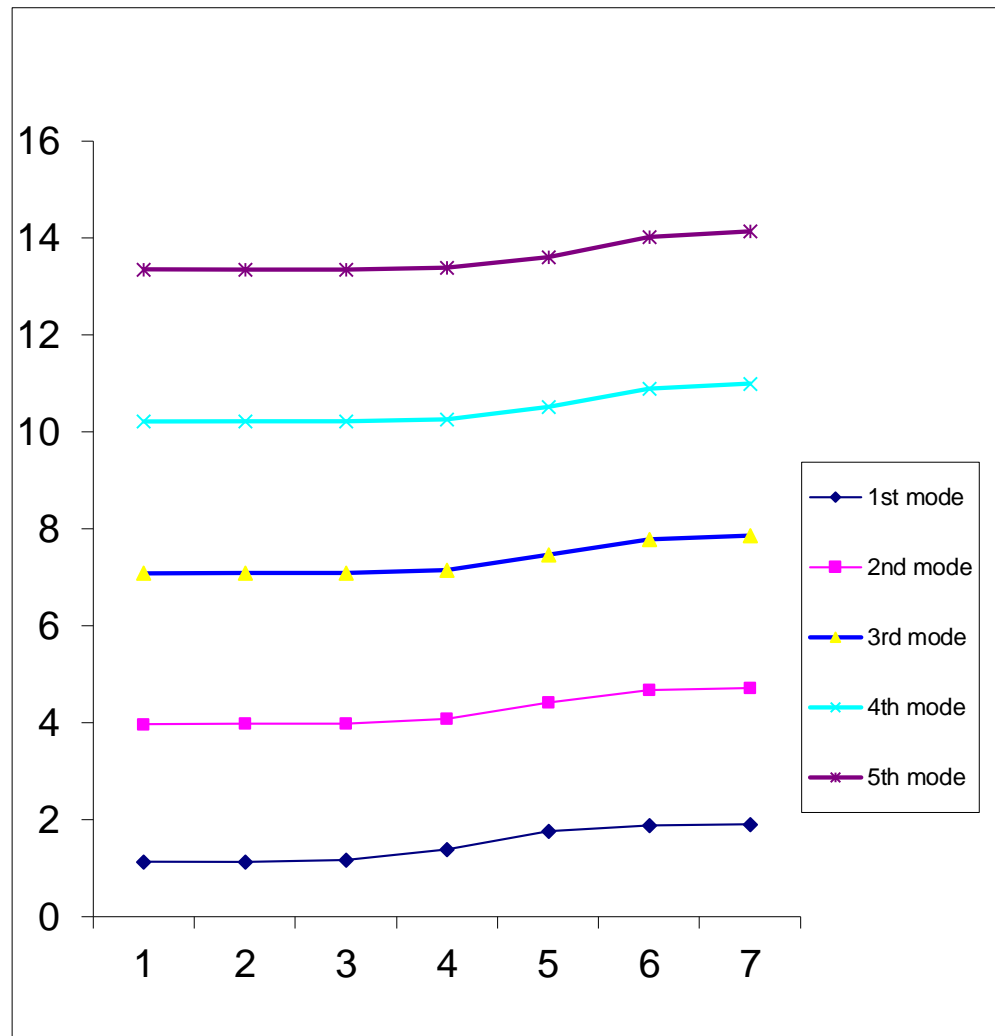


**Fig.6. 7. Mode shapes for  $W_k = 1.0$**

## 6.6 CONCLUDING REMARKS:

A dynamic stiffness matrix approach has been developed for computing the natural torsion frequencies and buckling loads of long, thin-walled beams of open section resting on continuous Winkler-Type elastic foundation and subjected to an axial time – invariant compressive load. The approach presented in this paper is quite general and can be applied for treating beams with non-uniform cross sections and also non-classical boundary conditions. Using Wittrick-Williams algorithm, a computer program has been developed to accurately determine the torsional buckling loads, frequencies and corresponding modal shapes .Results for a beam clamped at one end and simply supported at the other have been presented, showing the influence on elastic foundation, and compressive load and warping. While an increase in the values of elastic foundation parameter resulted in an increase in frequency, the effect of an increase in axial load parameter is found to be drastically decreasing the frequency to zero at the limit when the load equals the buckling load for the beam.

## **Chapter 7**

# **Mathematical Modelling of Composite I-Beam**

## **MATHEMATICAL MODELLING OF COMPOSITE I-BEAM**

### **7.1. Introduction to Composites**

The need for high performance to weight ratio structures coming from the most advanced engineering fields is the main driver of the increasing usage of composite materials for critical applications. Composite materials find application in automobile windshields (laminated glass), bimetal thermostats, and plywood. In these cases homogenous isotropic layers of materials are bonded together to form non-homogenous composite laminates.

Composite material can be defined as a multi phase material from a combination of materials, differing in form, which remain bonded together, but retain their identities and properties. The composites don't merge completely. They maintain an interface between each other and act in concert to provide improved properties not obtainable by any of the original components acting singly. The properties that can be improved by forming a composite material include strength, stiffness, corrosion resistance, wear resistance, attractiveness, reduction in weight, fatigue life, temperature dependant behavior, thermal insulation thermal conductivity, acoustical insulation etc. More recently fibre reinforced resin components that have high strength to weight and stiffness to weight ratios have become important in weight sensitive applications such as aircraft and space vehicles.

## **7.2. Laminated composites**

Consists of layers of at least two different materials that are bonded together. Lamination is used to combine the best aspects of the constituent layers in order to achieve a more useful material. The properties that can be emphasized by lamination are strength, stiffness, low weight, corrosion resistance, wear resistance, thermal insulation etc. Bimetals, clad metals, laminated glass, plastic based laminates and laminated fibrous composites fall in this category. Laminated fibrous composites are a hybrid class of composites involving both fibrous composites and lamination techniques. A more common name is laminated fibre reinforced composites. Here, layers of fibre reinforced material are built up with the fibre directions of each layer typically oriented in different directions to give different strengths and stiffness in the various directions.

### **7.2.1. Lamina and laminate:**

A lamina is a flat arrangement of unidirectional fibres in a matrix. The fibres and the matrix do not normally dissolve cohesively together but do contribute to a synergetic property change. The load bearing characteristics, the strength, and stiffness are virtually provided by these reinforced fibres while the matrix forms the body and grips or holds the reinforcement of the fibre together. The function of the matrix is to support and protect the fibres and to provide a means of distributing load among and transmitting load between the fibres. And also it provides resistance to crack propagation and damage and determines the overall service temperature limitations of the composite. Fibres generally exhibit linear elastic behaviour and resinous matrix materials are visco-elastic if not visco-plastic. Fibre reinforced composites such as boron epoxy and graphite epoxy are usually treated as linear elastic materials since the fibres provide the majority of the strength and stiffness. Refinement of that approximation requires consideration of some form of plasticity, viscoelasticity, or both. Very little work has been done to implement those idealizations of composite material behaviour in structural applications. Hence in present study, fibre reinforced composites have been treated as linear elastic materials.

A laminate is a stack of laminae with various orientations of principal material directions in the laminae. The layers of a laminate are usually bound together by the same matrix material that is used in the laminae. Laminates can be composed of different plates of different materials or, layers of fibre-reinforced laminae. The major purpose of lamination is to tailor the directional dependence of strength and stiffness of a material to match the loading environment of the structural element.

## 7.3. Mathematical Modelling of Composite I-Beam

### 7.3.1. Kinematics

The theoretical developments presented in this thesis require three sets of coordinate systems, which are mutually interrelated. The first coordinate system is the orthogonal Cartesian coordinate system  $(x, y, z)$ , for which the  $x$  and  $y$  axes lie in the plane of the cross-section and the  $z$ -axis parallel to the longitudinal axis of the beam. The second coordinate system is the local plate coordinates  $(n, s, \text{ and } z)$  as shown in Fig. 7.1, wherein the  $n$ -axis is normal to the middle surface of a plate element, the  $s$ -axis is tangent to the middle surface and is directed along the contour line of the cross-section. The  $(n, s, z)$  and  $(x, y, z)$  coordinate systems are related through an angle of orientation  $\alpha$  as defined in Fig. 7.1. The third coordinate set is the contour coordinate  $s$  along the profile of the section with its origin at any point  $O$  on the profile section. Point  $P$  is called the pole axis, through which the axis parallel to the  $z$ -axis is called the pole axis.

To derive the analytical model for a thin-walled composite beam, the following assumptions are made:

1. The contour of the thin wall does not deform in its own plane.
2. The shear strain  $\bar{\gamma}_{sz}$  of the middle surface is zero in each element.
3. The Kirchhoff-Law assumption in classical plate theory remains valid for laminated composite thin-walled beams.



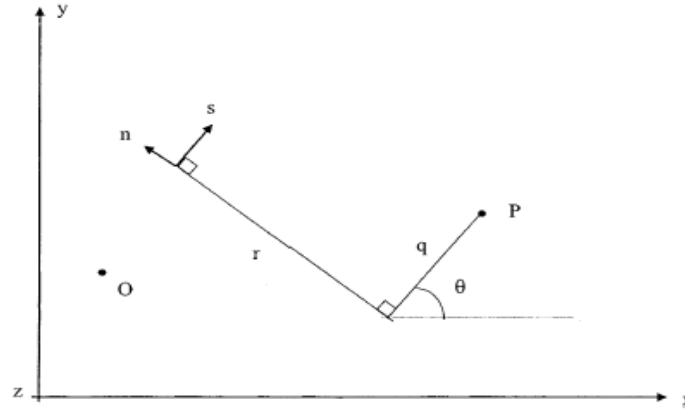


**Fig. 7.1. Definition of coordinates in thin-walled open section**

According to assumption 1, the mid surface displacement components  $\bar{u}$ ,  $\bar{v}$  at a point A in the contour coordinate system can be expressed in terms of a displacements  $U$ ,  $V$  of the pole  $P$  in the  $x$ ,  $y$  directions, respectively, and the rotation angle  $\phi$  about the pole axis

$$\bar{u}(s,z) = U(z) \sin \theta(s) - V(z) \cos \theta(s) - \phi(z)q(s), \quad (7.1a)$$

$$\bar{v}(s,z) = U(z) \cos \theta(s) + V(z) \sin \theta(s) + \phi(z)q(s). \quad (7.1b)$$

These equations apply to the whole contour. The out-of-plane shell displacement  $\bar{w}$  can now be found from assumption 2 (also known as Vlasov assumption). For each element of middle surface

$$\bar{\gamma}_{sz} = \frac{\partial \bar{v}}{\partial z} + \frac{\partial \bar{w}}{\partial s} = 0 \quad (7.2)$$

After substituting for  $\bar{v}$  from Equations (7.1a) and (7.1b), and considering the following geometric relations:

$$dx = ds \cos \theta, \quad (7.3)$$

$$dy = ds \sin \theta, \quad (7.4)$$

Eq. (7.2) can be integrated with respect to  $s$  from the origin to an arbitrary point on the contour

$$\bar{w}(s, z) = W(z) - U^1(z)x(s) - V^1(z)y(s) - \bar{\phi}(z)\omega(s), \quad (7.5)$$

Where differentiation with respect to the axial coordinate  $z$  is denoted by primes (' );  $W$  represents the average axial displacement of the beam in the  $z$ -direction;  $x$  and  $y$  are the coordinates of the contour in the  $(x, y, z)$  coordinate system; and  $\omega$  is the so-called sectorial coordinate or warping function given by

$$\omega(s) = \int r(s) ds \quad (7.6)$$

The displacement components  $u, v, w$  representing the deformation of any generic point on the profile section are given with respect to the mid surface displacements  $\bar{u}, \bar{v}, \bar{w}$  by assumption 3.

$$u(s, z, n) = \bar{u}(s, z), \quad (7.7a)$$

$$v(s, z, n) = \bar{v}(s, z) - n \frac{\partial \bar{u}(s, z)}{\partial s}, \quad (7.7b)$$

$$w(s, z, n) = \bar{w}(s, z) - n \frac{\partial \bar{u}(s, z)}{\partial z}, \quad (7.7c)$$

The strains associated with the small-displacement theory of elasticity are given by

$$\varepsilon_s = \bar{\varepsilon}_s + n\bar{k}_z, \quad (7.8a)$$

$$\varepsilon_z = \bar{\varepsilon}_z + n\bar{k}_z, \quad (7.8b)$$

$$\gamma_{sz} = n\bar{k}_{sz} \quad (7.8c)$$

Where

$$\bar{\varepsilon}_z = \frac{\partial \bar{v}}{\partial s}, \quad \bar{\varepsilon}_z = \frac{\partial \bar{w}}{\partial z}, \quad (7.9a)$$

$$\bar{k}_z = -\frac{\partial^2 \bar{u}}{\partial s^2}, \quad \bar{k}_z = -\frac{\partial^2 \bar{u}}{\partial z^2}, \quad \bar{k}_{sz} = -2\frac{\partial^2 \bar{u}}{\partial s \partial z}. \quad (7.9b)$$

All the other strains are identically zero. In equations (7.9a) and (7.9b),  $\bar{\varepsilon}_z, \bar{k}_z$  are assumed to be zero, and  $\bar{\varepsilon}_z, \bar{k}_z$  and  $\bar{k}_{sz}$  are mid surface axial strain and biaxial curvatures of the shell, respectively. The above shell strains can be converted to beam strain components by substituting Equations. (7.9a) and (7.9b)

$$\bar{\varepsilon}_z = \varepsilon_z^0 + xk_y + yk_x + \omega k_\omega, \quad (7.10a)$$

$$\bar{k}_z = k_y \sin \theta - k_x \cos \theta - k_\omega q, \quad (7.10b)$$

$$\bar{k}_{sz} = k_{sz} \quad (7.10c)$$

Where  $\varepsilon_z$ ,  $k_x$ ,  $k_y$ ,  $k_\omega$  and  $k_{sz}$  are axial strain, biaxial curvatures in the x and y directions, warping curvature with respect to the shear center, and twisting curvature in the beam, respectively, defined as

$$\varepsilon_z = W', \quad (7.11a)$$

$$k_x = -V'', \quad (7.11b)$$

$$k_y = -U'', \quad (7.11c)$$

$$k_\omega = -\phi'', \quad (7.11d)$$

$$k_{sz} = 2\phi'. \quad (7.11e)$$

The resulting strains can be obtained from Equations. (7.8a)- (7.8c) and (7.10a)- (7.10c) as

$$\varepsilon_z = \varepsilon_z^0 + (x + n \sin \theta) k_y + (y - n \cos \theta) k_x + (\omega - nq) k_\omega, \quad (7.12a)$$

$$\gamma_{sz} = nk_{sz}. \quad (7.12b)$$

### 7.3.2. Variational formulation

The total potential energy of the system can be stated as

$$\Pi = -\frac{1}{2} \int_v (\sigma_z \varepsilon_z + \sigma_{zs} \gamma_{zs}) dv \quad (7.13)$$

the variation of the total potential energy is calculated by substituting Equations (7.12a) and (7.12b) into equations (7.13)

$$\begin{aligned} \delta \Pi &= \int_v \{ \sigma_z [\delta \varepsilon_z^0 + (x + n \sin \theta) \delta k_y + (y - n \cos \theta) \delta k_x + (\omega - nq) \delta k_\omega] + \sigma_{sz} n \delta k_{sz} \} dv \\ &= \int_0^1 \{ N_z \delta \varepsilon_z^0 + M_y \delta k_y + M_x \delta k_x + M_\omega \delta k_\omega + M_t \delta k_{sz} \} dz \end{aligned} \quad (7.14)$$

Where  $N_z$ ,  $M_x$ ,  $M_y$  and  $M_\omega$  are axial force, bending moments in the x and y directions, and warping moment (bi moment) with respect to the centroid, respectively, defined by integrating over the cross-sectional area A as:

$$N_z = \int_A \sigma_z ds dn, \quad (7.15a)$$

$$M_x = \int_A \sigma_z (y - n \cos \theta) ds dn, \quad (7.15b)$$

$$M_y = \int_A \sigma_z (x + n \sin \theta) ds dn, \quad (7.15c)$$

$$M_{\omega} = \int_A \sigma_z (\omega - nq) ds dn, \quad (7.15d)$$

$$M_t = \int_A \sigma_{zs} n ds dn, \quad (7.15e)$$

The kinetic energy of the system is given

$$\tau = \frac{1}{2} \int_v \rho (\dot{u}^2 + \dot{v}^2 + \dot{w}^2) dv, \quad (7.16)$$

Where  $\rho$  is a density.

The variation of the kinetic energy is expressed by substituting the assumed displacement field into Eq. (7.16) as

$$\begin{aligned} \delta\tau = \int_v \rho \{ & \dot{U}\delta\dot{U} + \dot{V}\delta\dot{V} + \dot{W}\delta\dot{W} + (q^2 + r^2 - 2rn + n^2) \dot{\phi}\delta\dot{\phi} \\ & + (\dot{\phi}\delta\dot{U} + \dot{U}\delta\dot{\phi}) [n \cos \theta - (y - y_p)] \\ & + (\dot{\phi}\delta\dot{V} + \dot{V}\delta\dot{\phi}) [n \cos \theta - (x - x_p)] \} dv \end{aligned} \quad (7.17)$$

in Equation(7.14), the following geometric relations are used (Fig. 7.1):

$$x - x_p = q \cos \theta + r \sin \theta \quad (7.18a)$$

$$y - y_p = q \sin \theta - r \cos \theta \quad (7.18b)$$

In order to derive the equations of motion, Hamilton's principle is used

$$\delta \int_{t_1}^{t_2} (\tau - \Pi) dt = 0. \quad (7.19)$$

substituting Equations into Equations (7.19), the following weak statement is obtained:

$$\begin{aligned}
 0 = & \int_{t_1}^{t_2} \int_0^l \{ m_0 \dot{W} \delta \dot{W} + [m_0 \dot{U} + (m_c + m_0 y_p) \dot{\phi}] \delta \dot{U} \\
 & + [m_0 \dot{V} + (m_s - m_0 x_p) \dot{\phi}] \delta \dot{V} \\
 & + [(m_c + m_0 y_p) \dot{U} + (m_s - m_0 x_p) \dot{V} \\
 & + (m_p + m_2 - 2m_\omega) \dot{\phi}] \delta \dot{\phi} \\
 & - N_z \delta W' + M_y \delta U'' + M_x \delta V'' + M_w \delta \phi'' \\
 & - 2M_t \delta \phi' \} dz dt.
 \end{aligned} \quad (7.20)$$

In Equation (7.20),  $m_0$ ,  $m_c$ ,  $m_s$ ,  $m_\omega$ ,  $m_p$ ,  $m_2$  are inertia coefficients, respectively, defined by

$$m_0 = I_0 \int_s ds, \quad (7.21a)$$

$$m_c = I_1 \int_s \cos \theta \, ds, \quad (7.21b)$$

$$m_s = I_1 \int_s \sin \theta \, ds, \quad (7.21c)$$

$$m_\omega = I_1 \int_s r \, ds, \quad (7.21d)$$

$$m_p = I_0 \int_s (q^2 + r^2) \, ds, \quad (7.21e)$$

$$m_2 = I_2 \int_s ds, \quad (7.21f)$$

where

$$(I_0, I_1, I_2) = \int_n \rho(1, n, n^2) dn. \quad (7.22)$$

### 7.3.3. Constitutive equations

The constitutive equations of a  $k^{\text{th}}$  orthotropic lamina in the laminate coordinate system are given by



$$\begin{Bmatrix} \sigma_z \\ \sigma_{sz} \end{Bmatrix} = \begin{bmatrix} \bar{Q}_{11} & \bar{Q}_{16} \\ \bar{Q}_{16} & \bar{Q}_{66} \end{bmatrix}^k \begin{Bmatrix} \varepsilon_z \\ \gamma_{sz} \end{Bmatrix}, \quad (7.23)$$

where  $\bar{Q}_{ij}$  are transformed reduced stiffness[12]. Axial force  $N_z$  can now be

expressed with respect to the generalized strains ( $\varepsilon_z^0, k_y, k_x, k_\omega, k_{sz}$ ) by

combining Equations. (7.15a), (7.23) and (7.12a), (7.12b)

$$N_z = \int_A \left\{ \bar{Q}_{11} [\varepsilon_z^0 + (x + n \sin \theta) k_y + (y - n \cos \theta) k_x + (\omega - nq) k_\omega] + \bar{Q}_{16} n k_{sz} \right\}. \quad (7.24)$$

Similarly, the other stress resultants ( $M, M, M, M$ ) can also be written in terms of the generalized strains. Consequently, the constitutive equations for a thin-walled laminated composite are obtained as

$$\begin{Bmatrix} N_z \\ M_y \\ M_x \\ M_\omega \\ M_t \end{Bmatrix} = \begin{bmatrix} E_{11} & E_{12} & E_{13} & E_{14} & E_{15} \\ & E_{22} & E_{23} & E_{24} & E_{25} \\ & & E_{33} & E_{34} & E_{35} \\ & & & E_{44} & E_{45} \\ & & & & E_{55} \end{bmatrix} \begin{Bmatrix} \varepsilon_z^0 \\ k_y \\ k_x \\ k_\omega \\ k_{sz} \end{Bmatrix}, \quad (7.25)$$

*sym.*

Where  $E_{ij}$  are stiffness of the thin-walled composite, and can be defined by

$$E_{11} = \int_s A_{11} ds, \quad (7.26a)$$

$$E_{12} = \int_s (A_{11}x + B_{11} \sin \theta) ds, \quad (7.26b)$$

$$E_{13} = \int_s (A_{11}y - B_{11} \cos \theta) ds, \quad (7.26c)$$

$$E_{14} = \int_s (A_{11}\omega - B_{11}q) ds, \quad (7.26d)$$

$$E_{15} = \int_s (B_{16}) ds, \quad (7.26e)$$

$$E_{22} = \int_s (A_{11}x^2 + 2B_{11}x \sin \theta + D_{11} \sin^2 \theta) ds, \quad (7.26f)$$

$$E_{23} = \int_s (A_{11}xy + B_{11}(y \sin \theta - x \cos \theta) - D_{11} \sin \theta \cos \theta) ds, \quad (7.26g)$$

$$E_{24} = \int_s (A_{11}x\omega + B_{11}(\omega \sin \theta - qx) - D_{11}q \sin \theta) ds, \quad (7.26h)$$

$$E_{25} = \int_s (B_{16}x + D_{16} \sin \theta) ds, \quad (7.26i)$$

$$E_{33} = \int_s (A_{11}y^2 - 2B_{11}y \cos \theta + D_{11} \cos^2 \theta) ds, \quad (7.26j)$$

$$E_{34} = \int_s (A_{11}y\omega - B_{11}(\omega \cos \theta + qy) + D_{11}q \cos \theta) ds, \quad (7.26k)$$

$$E_{35} = \int_s (B_{16}y - D_{16} \cos \theta) ds, \quad (7.26l)$$

$$E_{44} = \int_s (A_{11}\omega^2 - 2B_{11}\omega q + D_{11}q^2) ds, \quad (7.26m)$$

$$E_{45} = \int_s (B_{16}\omega - D_{16}q) ds, \quad (7.26n)$$

$$E_{55} = \int_s D_{66} ds. \quad (7.26o)$$

$A_{ij}$ ,  $B_{ij}$ , and  $D_{ij}$  matrices are extensional, coupling and bending stiffness, respectively,

defined by

$$(A_{ij}, B_{ij}, D_{ij}) = \int \bar{Q}_{ij}(1, n, n^2) dn \quad (7.27)$$

It appears that the laminae stiffness  $E_{ij}$  depend on the cross-section of the composite,

and the explicit expressions for I- section are given as follows:

$$E_{11} = A_{11}^k b_k, \quad (7.28a)$$

$$E_{12} = B_{11}^3 b_3, \quad (7.28b)$$

$$E_{13} = A_{11}^\alpha b_\alpha y_\alpha - B_{11}^\alpha b_\alpha, \quad (7.28c)$$

$$E_{14} = 0, \quad (7.28d)$$

$$E_{15} = B_{16}^k b_k, \quad (7.28e)$$

$$E_{22} = A_{11}^\alpha \frac{b_\alpha^3}{12} + D_{11}^3 b_3, \quad (7.28f)$$

$$\mathbf{E}_{23} = \mathbf{O}, \quad (7.28g)$$

$$E_{24} = [A_{11}^\alpha y_\alpha - B_{11}^\alpha] \frac{b_3^3}{12}, \quad (7.28h)$$

$$E_{25} = D_{16}^3 b_3, \quad (7.28i)$$

$$E_{33} = [A_{11}^\alpha y_\alpha^2 - 2B_{11}^\alpha y_\alpha + D_{11}^\alpha] b_\alpha + \frac{b_3^3}{12} A_{11}^3, \quad (7.28j)$$

$$E_{34} = \frac{b_3^3}{12} D_{11}^3, \quad (7.28k)$$

$$E_{35} = B_{16}^\alpha y_\alpha b_\alpha - D_{16}^\alpha b_\alpha, \quad (7.28l)$$

$$E_{44} = [A_{11}^\alpha y_\alpha^2 - 2B_{11}^\alpha y_\alpha + D_{11}^\alpha] \frac{b_\alpha^3}{12} + \frac{b_3^3}{12} D_{11}^3, \quad (7.28m)$$

$$E_{45} = 0, \quad (7.28n)$$

$$E_{55} = D_{66}^{(k)} d_k, \quad (7.28o)$$

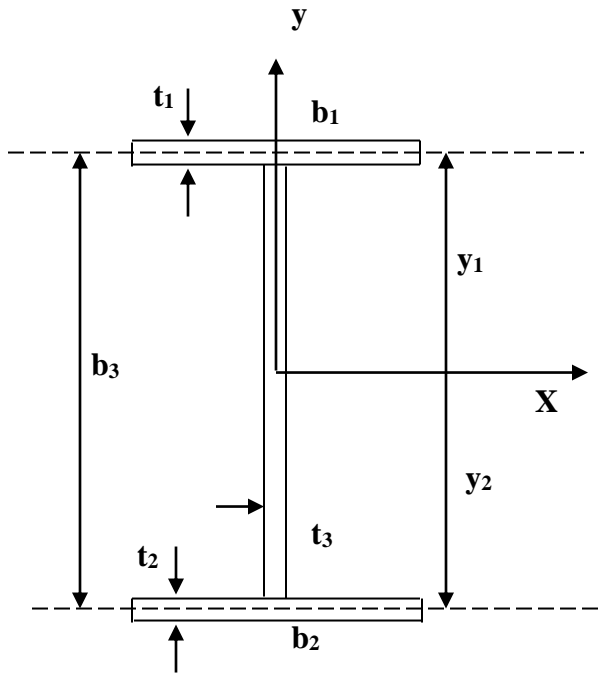


**Fig.7.2. Geometry of a thin-walled doubly symmetric Composite I-beam. ( $b_1=b_2$  and  $t_1=t_2$ )**

In the above equations, repeated index denotes summation. Index  $k$  varies from 1 to 3 whereas  $\alpha$  varies from 1 to 2 implying top and bottom flanges (1, 2) and web (3) as shown in fig.  $b_k$  denotes width of flanges and web.

Similarly , the explicit expressions of inertia coefficients for I-section are given by

$$m_o = I_o^k d_k, \quad (7.29a)$$

$$m_c = I_1^\alpha b_\alpha, \quad (7.29b)$$

$$m_s = I_1^3 b_3, \quad (7.29c)$$

$$m_\omega = I_1^\alpha y_\alpha b_\alpha, \quad (7.29d)$$

$$m_p = I_0^\alpha \left[ \frac{b_\alpha^3}{12} + y_\alpha^2 b_\alpha \right] + I_0^3 \frac{b_3^3}{12}, \quad (7.29e)$$

$$m_2 = I_2^k b_k. \quad (7.29f)$$

#### 7.3.4. Equation of motion

The equation of motion of the present study can be derived by integrating the derivatives of the varied quantities by parts and collecting the coefficients of  $\delta u$ ,  $\delta v$ ,  $\delta w$ , and  $\delta \phi$  .

$$N_z' = m_o \ddot{W}, \quad (7.30a)$$

$$M_y'' = m_o \ddot{U} + (m_c + m_o y_p) \ddot{\Phi}, \quad (7.30b)$$

$$M_x'' = m_o \ddot{V} + (m_s + m_o x_p) \ddot{\Phi}, \quad (7.30c)$$

$$M_\omega'' + 2M_t' = (m_c + m_o y_p) \ddot{U} + (m_s - m_o x_p) \ddot{V} + (m_p + m_2 - 2m_\omega) \ddot{\Phi}. \quad (7.30d)$$

The natural boundary conditions are of the form:

$$\delta W : N_z, \quad (7.31a)$$

$$\delta U : M_y', \quad (7.31b)$$

$$\delta U' : M_y, \quad (7.31c)$$

$$\delta V : M_x', \quad (7.31d)$$

$$\delta V' : M_x, \quad (7.31e)$$

$$\delta \Phi : M_\omega' + 2M_t, \quad (7.31f)$$

$$\delta \Phi' : M_\omega, \quad (7.31g)$$

The above equations are most general form for flexural-torsional vibration of a thin-walled laminated composite beam with an I-shaped section, and the dependent variables,  $u$ ,  $v$ ,  $w$  and  $\phi$  are fully coupled. If the stacking sequence of the web is symmetric,  $E_{12} = E_{34} = 0$ , and the thin-walled composite is symmetric with respect to  $z$ -axis,  $E_{13} = E_{15} = E_{24} = 0$ . Further, if both the web and flange are balanced laminates ( $\pm \theta$  pairs of layers)  $A_{i6}^k = D_{i6}^k = 0$ , and thus,  $E_{25} = 0$ . Finally, Eq. (7.30a) can be simplified to the uncoupled differential equations as:

$$(EA)_{com} W'' = \rho A \ddot{W}, \quad (7.32a)$$

$$-(EI_y)_{com} U'' = \rho A \ddot{U}, \quad (7.32b)$$

$$-(EI_x)_{com} V'' = \rho A \ddot{V}, \quad (7.32c)$$

$$-(EI_\omega)_{com} \Phi'' + (GJ)_{com} = \rho I_p \ddot{\Phi}, \quad (7.32d)$$

From the above equations,  $(EA)_{com}$  represents axial rigidity,  $(EI_x)_{com}$  and  $(EI_y)_{com}$  represent flexural rigidities with respect to  $x$  and  $y$  axes,  $(EI_\omega)_{com}$  and  $(GJ)_{com}$  represent warping and torsional rigidities of the thin-walled composite, respectively, written as

$$(EA)_{com} = E_{11}, \quad (7.33a)$$

$$(EI_y)_{com} = E_{22}, \quad (7.33b)$$

$$(EI_x)_{com} = E_{33}, \quad (7.33c)$$



$$(EI_{\omega})_{com} = EI_{44}, \quad (7.33d)$$

$$(GJ)_{com} = 4 EI_{55}, \quad (7.33e)$$

In Eqs. (7.32a)-(7.32d),  $I_p$  denotes the polar moment of inertia. It is well known that the three distinct vibration modes, flexural vibration in the x and y directions, and torsional vibration, are identified in this case, and the corresponding vibration frequencies are given by the closed form for simply supported boundary conditions[3]:

$$\omega_{z_n} = \frac{n\pi}{l} \sqrt{\frac{(EA)_{com}}{\rho A}}, \quad (7.34a)$$

$$\omega_{x_n} = \frac{n^2 \pi^2}{l^2} \sqrt{\frac{(EI_y)_{com}}{\rho A}}, \quad (7.34b)$$

$$\omega_{y_n} = \frac{n^2 \pi^2}{l^2} \sqrt{\frac{(EI_x)_{com}}{\rho A}}, \quad (7.34c)$$

$$\omega_{\omega_n} = \frac{n\pi}{l} \sqrt{\frac{1}{\rho I_p} \left( \frac{n^2 \pi^2}{l^2} (EI_{\omega})_{com} + (GJ)_{com} \right)} \quad (7.34d)$$

where  $\omega_{z_n}$ ,  $\omega_{x_n}$ ,  $\omega_{y_n}$ ,  $\omega_{\omega_n}$  are axial frequency, flexural frequencies in the x and y directions, the torsional vibration frequency, respectively

### 7.3.5. Finite Element Model

The present theory for thin-walled composite beams described in the previous section was implemented via a displacement based finite element method. The generalized displacements are expressed over each element as a linear combination of the one-dimensional Lagrange interpolation function  $\varphi_j$  and Hermite-cubic interpolation function  $\psi_j$  associated with node  $j$  and the nodal values:

$$W = \sum_{j=1}^n w_j \psi_j, \quad (7.35a)$$

$$U = \sum_{j=1}^n u_j \psi_j, \quad (7.35b)$$

$$V = \sum_{j=1}^n v_j \psi_j, \quad (7.35c)$$

$$\Phi = \sum_{j=1}^n \phi_j \psi_j, \quad (7.35d)$$

Substituting these expressions into the weak statement in Eq. (7.20), the finite element model of a typical element can be expressed as a standard Eigen value problem

$$([K] - \lambda[M])\{\Delta\} = \{0\}, \quad (7.36)$$

where  $[K]$  is the element stiffness matrix

$$[K] = \begin{bmatrix} K_{11} & K_{12} & K_{13} & K_{14} \\ & K_{22} & K_{23} & K_{24} \\ & & K_{33} & K_{34} \\ sym. & & & K_{44} \end{bmatrix} \quad (7.37)$$

and  $[M]$  is the element mass matrix

$$[M] = \begin{bmatrix} M_{11} & M_{12} & M_{13} & M_{14} \\ & M_{22} & M_{23} & M_{24} \\ & & M_{33} & M_{34} \\ sym. & & & M_{44} \end{bmatrix} \quad (7.38)$$

The explicit form of  $[K]$  and  $[M]$  are given by

$$K_{ij}^{11} = \int_0^l E_{11} \cdot \psi'_i \psi'_j dz, \quad (7.39a)$$

$$K_{ij}^{12} = \int_0^l E_{12} \cdot \psi'_i \psi''_j dz, \quad (7.39b)$$

$$K_{ij}^{13} = \int_o^l E_{13} \cdot \psi'_{\cdot i} \psi''_{\cdot j} dz, \quad (7.39c)$$

$$K_{ij}^{14} = \int_o^l 2E_{15} \cdot \psi'_{\cdot i} \psi'_{\cdot j} dz, \quad (7.39d)$$

$$K_{ij}^{32} = \int_o^l E_{22} \cdot \psi''_{\cdot i} \psi''_{\cdot j} dz, \quad (7.39e)$$

$$K_{ij}^{24} = \int_o^l E_{24} \cdot \psi''_{\cdot i} \psi''_{\cdot j} dz, \quad (7.39f)$$

$$K_{ij}^{33} = \int_o^l E_{33} \cdot \psi''_{\cdot i} \psi''_{\cdot j} dz, \quad (7.39g)$$

$$K_{ij}^{34} = \int_o^l (E_{34} \cdot \psi''_{\cdot i} \psi''_{\cdot j} - 2E_{35} \cdot \psi''_{\cdot i} \psi'_{\cdot j}) dz, \quad (7.39h)$$

$$K_{ij}^{44} = \int_o^l (E_{44} \cdot \psi''_{\cdot i} \psi''_{\cdot j} + 4E_{55} \cdot \psi'_{\cdot i} \psi'_{\cdot j}) dz, \quad (7.39i)$$

$$M_{ij}^{11} = G_{ij}^{22} = M_{ij}^{33} = \int_{jo}^l m_o \psi_i \psi_j dz, \quad (7.40a)$$

$$M_{ij}^{24} = \int_{jo}^l (m_c + m_o y_p) \psi_i \psi_j dz, \quad (7.40b)$$

$$M_{ij}^{34} = \int_{jo}^l (m_s - m_o x_p) \psi_i \psi_j dz, \quad (7.40c)$$

$$M_{ij}^{44} = \int_{j_0}^l (m_p + m_2 - 2m_\omega) \psi_i \psi_j dz, \quad (7.40d)$$

all the other components are zero.

In equations (7.36),  $\{ \Delta \}$  is the eigenvector of nodal displacements corresponding to an

$$\text{Eigen value } \{ \Delta \} = \{ w u v \phi \}^T \quad (7.41)$$

**Chapter8**

**EFFECT OF VARIOUS PARAMETERS ON VIBRATIONS OF UNIFORM  
COMPOSITE  
I-BEAM**

# **EFFECT OF VARIOUS PARAMETERS ON VIBRATIONS OF UNIFORM COMPOSITE I-BEAM**

A thin-walled composite beam with I-section and length  $L = 8$  m is considered in order to investigate the effects of various parameters namely fibre orientation, modulus ratio, height-to-thickness ratio and boundary conditions on the natural frequencies and mode shapes. The geometry of the I-section is shown in Fig. 8.1 and the following engineering constants are used for finite element analysis.

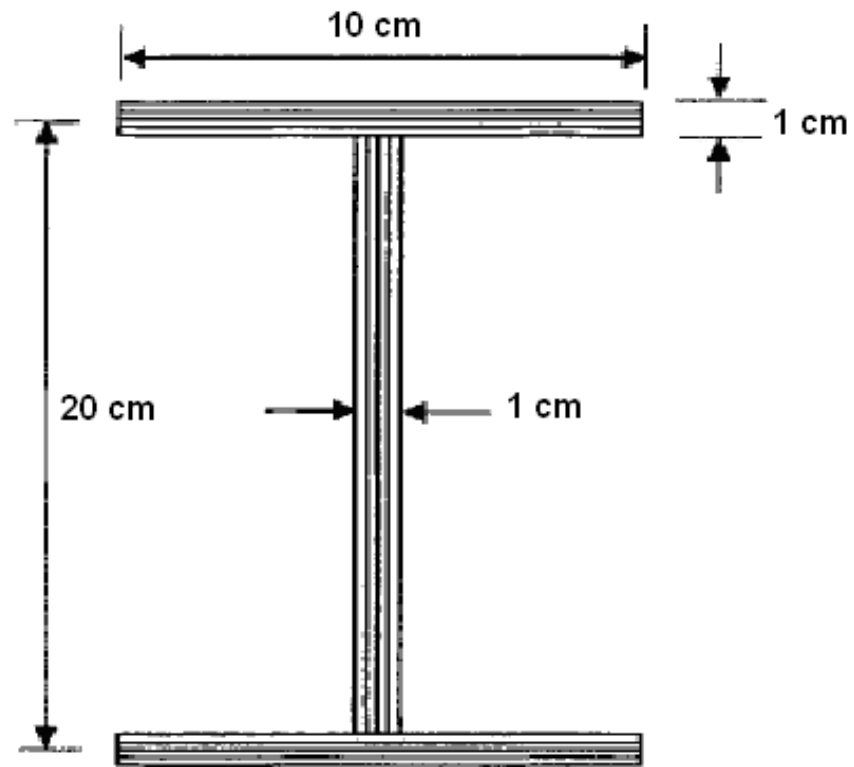


**Fig.8.1. Thin-walled composite I-beam.**



## 8.1. Material properties

Graphite-Epoxy is used for composite beam analysis. The properties of Graphite-Epoxy are

- Modulus of Elasticity  $E_1 = 1.38 \times 10^{11} \text{ N/m}^2$ ,
- Density  $\rho = 1590 \text{ Kg/m}^3$ ,
- $E_1/E_2 = 40$ ,
- $G_{12}/E_2 = 0.6$ ,  $\nu_{12} = 0.25$  Where subscripts 1 and 2 indicate fibre direction and perpendicular to fibre direction, respectively.

For convenience, the following non-dimensional natural frequency is used:

$$\varpi = \frac{\omega l^2}{b_3} \sqrt{\frac{\rho}{E_2}}$$

### 8.1.1. Element used

The element considered for the composite beam analysis is Shell99. Shell99 is used for layered applications of a structural shell model. The element has six degrees of freedom at each node, translations in the nodal x, y, and z directions and rotations about the nodal x, y, and z-axes. The element is defined by eight nodes, average or corner layer thicknesses, layer material direction angles, and orthotropic material properties. It usually has a smaller element formulation time. [Shell99](#) allows up to 250 layers. If more than 250 layers are required, a user-input constitutive matrix is available. The figure 8.2 shows Shell99, Linear Layered Structural Shell.



### 8.2.1 Effect of Fibre angle rotation in top and bottom flanges

First, the top and bottom flanges are considered as angle-ply laminates  $[\theta/-\theta]$ , and the web laminate is assumed to be unidirectional in I-beam. In addition, the stacking sequence of the beam is symmetric with respect to x-axis. The coupling stiffnesses  $E_{12}$ ,  $E_{13}$ ,  $E_{15}$ ,  $E_{24}$  and  $E_{25}$  become zero, but  $E_{35}$  does not vanish due to unsymmetric stacking sequence of each flange.

Accordingly, flexural vibration in the y-direction is uncoupled, whereas the flexural vibration in the x-direction and the torsional vibration are coupled. The lowest four non-dimensional natural frequencies by the finite element analysis and the orthotropic closed-form solutions, which neglects the coupling effects obtained from equations (7.34a) to (7.34d) for each mode are given in Table 8.1. For unidirectional fibre orientation, the lowest four natural frequencies by the finite element analysis exactly correspond to the first flexural mode in the x-direction, torsional mode, second flexural mode in the x-direction, and flexural mode in the y-direction by the orthotropic closed-form solution, respectively. As the fibre angle changes, the variation in natural frequencies is illustrated in Fig. 8.3, and the results by finite element analysis and closed form solution show slight discrepancy. This is because of the coupling stiffnesses which are neglected in the closed-form analysis.

**Table 8.1: Non-dimensional natural frequencies with respect to the fibre angle change in the flanges.**

	Closed form				FEM			
Natural freq Fibre angle	$\omega_{x1}$	$\omega_o$	$\omega_{x2}$	$\omega_y$	$\omega_1$	$\omega_2$	$\omega_3$	$\omega_4$
0	15.859	19.481	39.419	41.085	15.859	19.48	39.419	41.085
15	12.163	25.562	36.564	38.504	12.214	22.365	36.294	38.042
30	6.4308	30.126	23.386	32.381	6.4315	23.146	24.142	31.452
45	3.1165	34.536	16.498	29.365	3.1165	13.599	25.465	24.143

60	2.865	30.052	14.635	24.912	2.865	15.415	25.946	24.102
45	2.356	20.542	11.546	26.546	2.356	10.946	19.512	26.451
90	2.152	14.512	10.562	26.469	2.152	10.562	14.512	22.643

### 8.3. Percentage variation of frequencies closed form Vs FEM Solutions

The difference and variation between FEM and closed form solution is presented from table 8.2 to table 8.5, for a simply supported beam with respect to the fibre angle change in flanges.

**Table 8.2.** Percentage variation in first natural frequencies of a simply supported composite beam with respect to fibre angle change in flanges

Fibre Angle	Closed form Natural Frequencies	FEM Natural Frequencies	difference	% variation
	$\omega_{x1}$	$\omega_1$		
0	15.859	15.859	0.0	0.0
15	12.163	12.214	-0.051	0.42
30	6.4308	6.4315	-0.0004	0.01
45	3.1165	3.1165	0.0	0.0

60	2.865	2.865	0.0	0.0
45	2.356	2.356	0.0	0.0
90	2.152	2.152	0.0	0.0

**Table 8.3.** Percentage variation in second natural frequencies of a simply supported composite beam with respect to fibre angle change in flanges

<b>Fibre Angle</b>	<b>Closed form Natural Frequencies</b>	<b>FEM Natural Frequencies</b>	<b>Difference</b>	<b>% Variation</b>
------------------------	--	--	-------------------	--------------------

	$\omega_o$	$\omega_2$		
0	19.481	19.48	0.001	0
15	25.562	22.365	3.197	12.5
30	23.126	23.146	-0.02	0.086
45	34.536	33.599	0.937	2.713
60	30.052	25.946	4.106	13.66
45	20.542	20.946	-0.404	1.966
90	14.512	14.512	0.0	0



**Table 8.4.** Percentage variation in third natural frequencies of a simply supported composite beam with respect to fibre angle change in flanges

<b>Fibre Angle</b>	<b>Closed form Natural frequencies</b>	<b>FEM Natural Frequencies</b>	<b>Difference</b>	<b>%Variation</b>
	$\omega_{x2}$	$\omega_3$		
0	39.419	39.419	0.0	0.0
15	36.564	36.294	0.27	0.738
30	23.386	24.142	-0.756	3.232
45	26.498	25.465	1.033	3.898
60	14.635	15.415	-0.78	5.329

45	14.546	19.512	-4.966	0.341
90	10.562	10.562	0.0	0.0

**Table 8.5.** Percentage variation in fourth natural frequencies of a simply supported composite beam with respect to fibre angle change in flanges

Fibre Angle	Closed form Natural Frequencies $\omega_y$	FEM Natural Frequencies $\omega_4$	Difference	% Variation
0	41.085	41.085	0.0	0.0
15	38.504	38.042	0.462	0.011
30	32.381	31.452	0.929	0.0286
45	29.365	24.143	2.222	0.045
60	24.912	24.102	0.80	0.0286

45	26.546	26.451	0.095	0.0035
90	26.469	22.643	3.826	0.1445

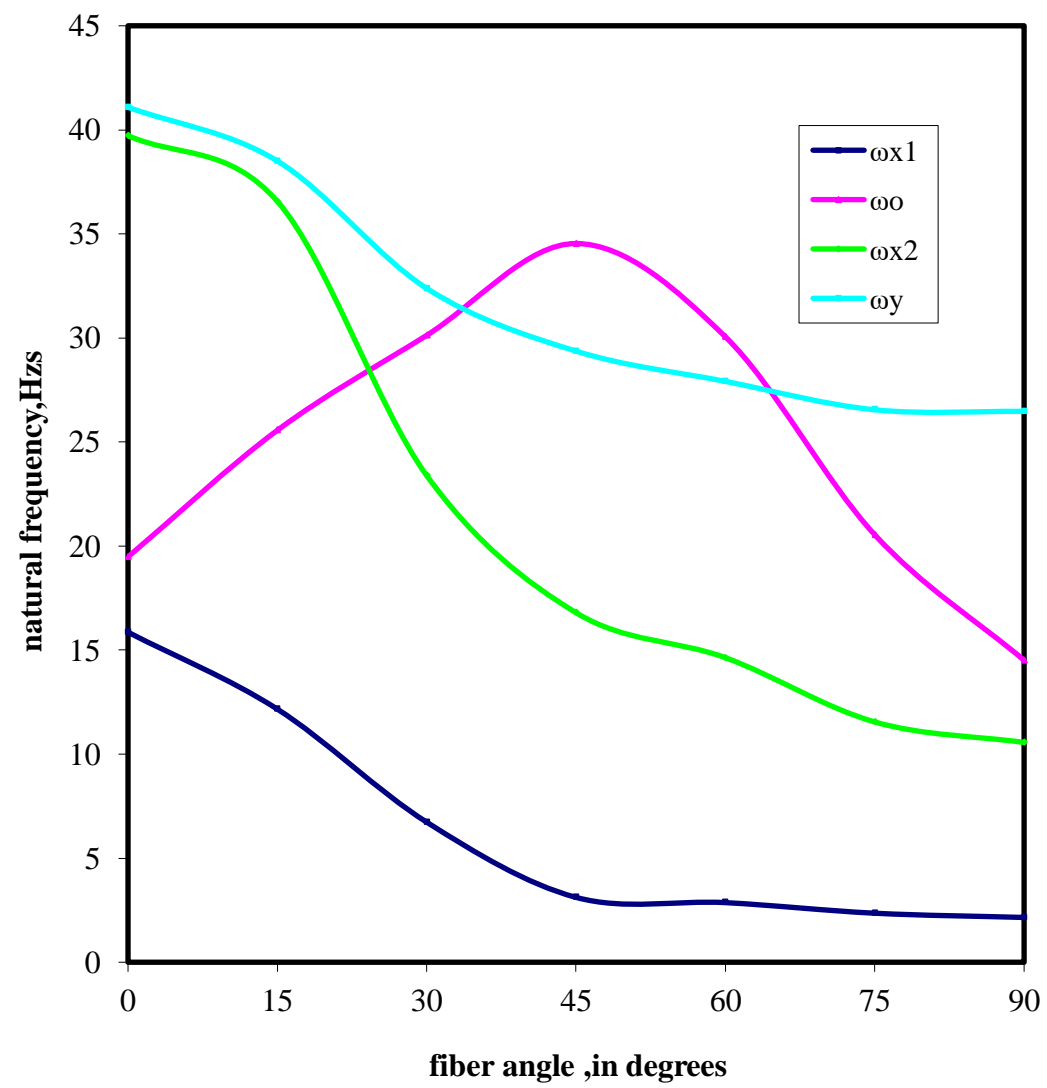


**Fig.8.3.**Variation of the non-dimensional natural frequencies of a simply supported composite beam with respect to fibre angle change in flanges

The variation of natural frequencies of a simply supported composite beam by orthotropic closed-form solution with fibre angle change in the flanges for the lowest four vibration mode shapes are shown in Fig.8.3. It is seen that the mode shape corresponding to the lowest natural frequency is the first flexural mode in z-direction ( $\omega_{x1}$ ), which is well below the other three types of modes. In general,  $\omega_{x1}$ ,  $\omega_{x2}$  and  $\omega_y$  decrease as the fibre angle increases. In torsional vibration, however, the laminate torsional rigidity,  $\{GJ\}_{com}$ , has an important effect on vibration characteristics. Thus, placing the fibre angle at  $\pm 45^\circ$  leads to considerable improvement in the torsional vibration frequency as can be seen for the compressive load-carrying capacity in the in the paper [11].

#### **8.4. Effect of Fibre angle rotation in Web:**

The fibre angle is rotated in the web instead of the flanges for the same composite I-beam referred in fig.8.1. The variations of natural frequencies for various modes by finite element solution with respect to the fibre angle variation in the web are shown in Fig. 8.4.

**Table 8.6:** Nondimensional natural frequencies with respect to the fibre angle change in the web.

	Closed form				FEM			
Natural freq Fibre angle	$\omega_{x1}$	$\omega_o$	$\omega_{x2}$	$\omega_y$	$\omega_1$	$\omega_2$	$\omega_3$	$\omega_4$
0	15.859	19.481	39.419	41.085	15.859	19.481	39.419	41.085
15	15.494	21.68	39.614	38.421	15.804	20.968	38.83	39.524
30	15.483	26.296	39.564	36.689	15.491	24.148	36.542	38.562
45	15.446	24.953	39.463	35.569	14.158	25.053	35.231	34.024
60	15.448	24.804	39.452	35.365	14.058	24.481	30.941	35.21
45	15.485	21.126	39.253	35.286	14.022	22.142	29.146	34.462
90	15.499	19.458	38.984	35.252	13.966	14.165	28.125	33.912

**Table 8.7.** Percentage variation in first natural frequencies of a simply supported composite beam with respect to fibre angle change in web

Fibre Angle	Closed form	FEM	Difference	% Variation
	Natural Frequencies	Natural Frequencies		
	$\omega_{x1}$	$\omega_1$		
0	15.859	15.859	0.0	0.0
15	15.494	15.804	0.31	0.02
30	15.483	15.491	0.008	0.0005
45	15.446	14.158	1.288	0.083
60	15.448	14.058	1.39	0.0589
45	15.485	14.022	1.463	0.0944



90	15.499	13.966	1.533	0.0989
----	--------	--------	-------	--------

**Table 8.8.** Percentage variation in natural frequencies of a simply supported composite beam with respect to fibre angle change in web

Fibre Angle	Closed form	FEM	Difference	% Variati on
	Natural Frequencies	Natural Frequencies		
	$\omega_o$	$\omega_2$		
0	19.481	19.481	0.0	0.0
15	21.68	20.968	0.712	0.032841
30	26.296	24.148	2.148	0.081685

45	24.953	25.053	0.1	0.004008
60	24.804	24.481	0.323	0.013022
45	21.126	22.142	1.016	0.048092
90	19.458	14.165	5.293	0.272022

**Table 8.9.** Percentage variation in natural frequencies of a simply supported composite beam with respect to fibre angle change in web

Fibre Angle	Closed form	FEM	Difference	% Variation
	Natural Frequencies	Natural Frequencies		
	$\omega_{x2}$	$\omega_3$		
0	39.419	39.419	0.0	0.0
15	39.614	38.83	0.784	0.019791
30	39.564	36.542	3.022	0.076383
45	39.463	35.231	4.232	0.10724

60	39.452	30.941	8.511	0.215731
45	39.253	29.146	10.107	0.257484
90	38.984	28.125	10.859	0.27855

**Table 8.10.** Percentage variation in natural frequencies of a simply supported composite beam with respect to fibre angle change in web

Fibre Angle	Closed form	FEM	Difference	% Variation
	Natural Frequencies	Natural Frequencies		
	$\omega_y$	$\omega_4$		
0	41.085	41.085	0.0	0.0

15	38.421	39.524	-1.103	0.028
30	36.689	38.562	0.124	0.003
45	35.569	34.024	-1.455	0.039
60	35.365	35.21	0.155	0.004
45	35.286	34.462	-0.0146	0.004
90	35.252	33.912	1.34	0.038

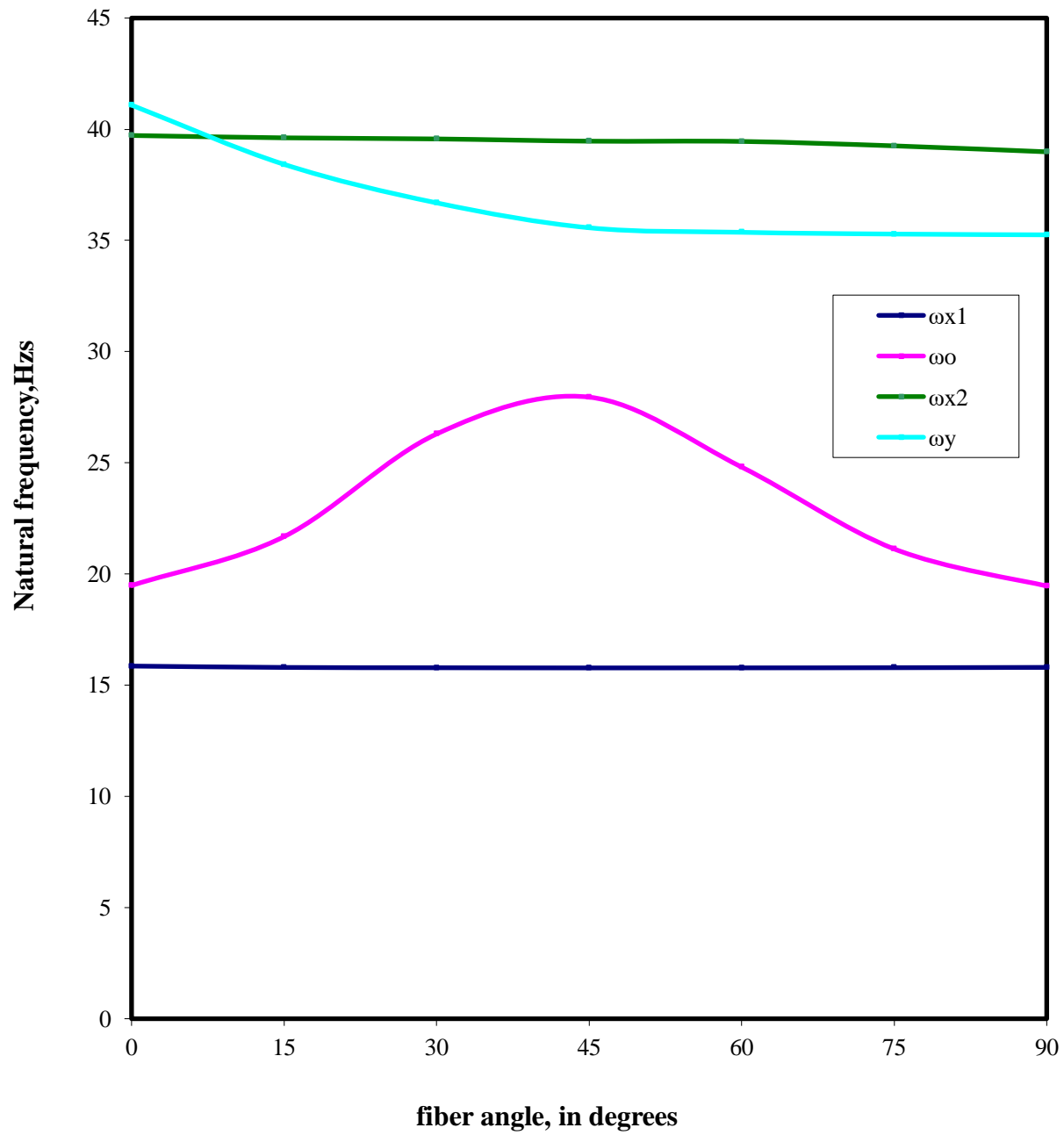


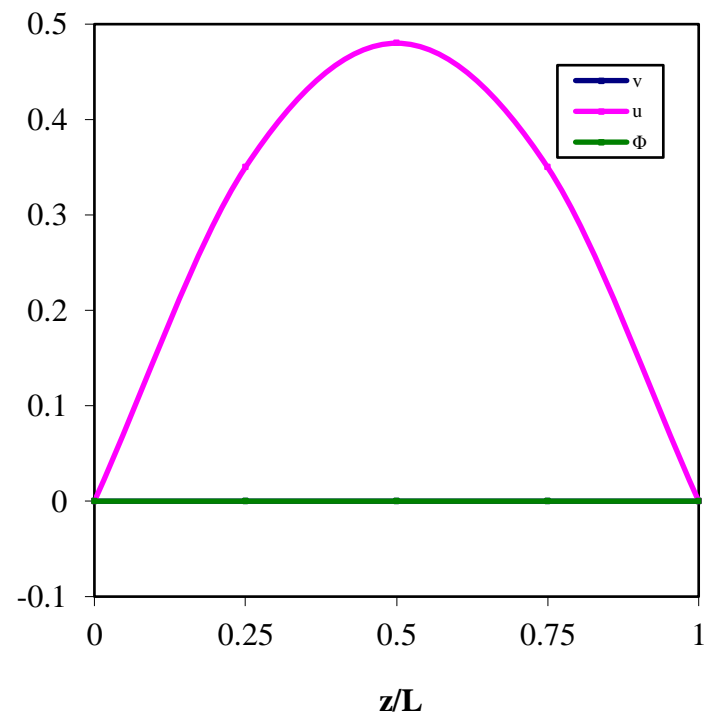
Figure.8.4.Variation of the non-dimensional natural frequencies of a simply supported composite beam with respect to fibre angle change in the web

It is seen that the natural frequencies corresponding to the first and second flexural modes in the z-direction ( $\omega_{x1}, \omega_{x2}$ ) are almost invariant for entire range of fibre angle variation in the web. The torsional frequency reaches its maximum near  $\theta = 45^\circ$  showing similar trends as for the previous case.

In order to investigate the coupling effect further, the top flange is considered as an angle-ply laminate  $[\theta/-\theta]$ , while the bottom flange and web are unidirectional. In this case, the thin-walled composite beam is unsymmetric with respect to z-axis. As the fibre angle changes, the results by the finite element analysis and the orthotropic closed form solution show significant discrepancy implying that the coupling effects in this case become no longer negligible.

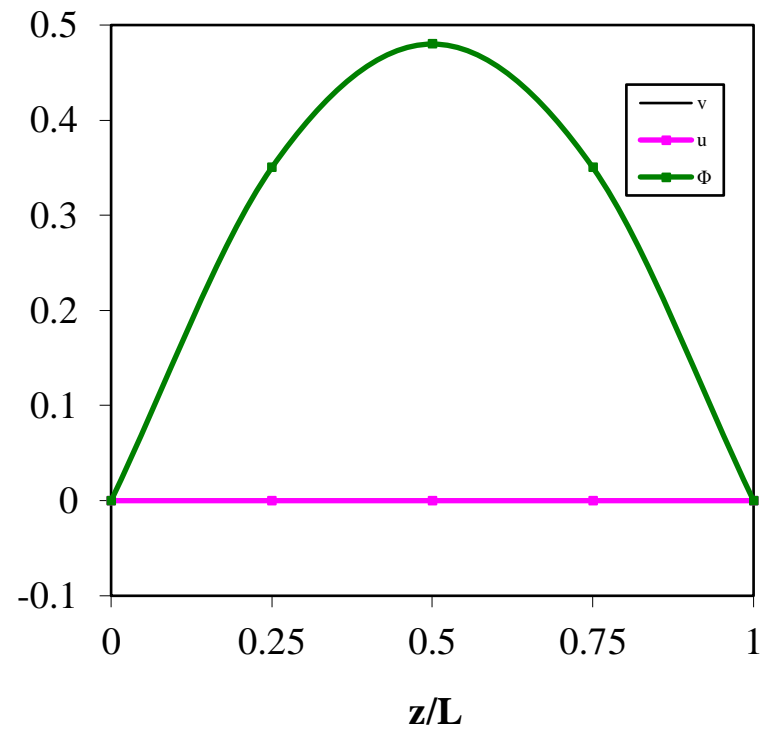
## 8.5. Mode shapes

The mode shapes corresponding to the first four lowest modes with unidirectional fibre and with fibre angle  $30^\circ$  in the top flange are illustrated in Figs. 8.5 and 8.6. It can be readily seen that the beam with fibre angle  $30^\circ$  in the top flange exhibits strong flexural-torsional coupling. In fact, the coupling stiffnesses  $E_{12}$  and  $E_{25}$  vanish while  $E_{13}, E_{15}, E_{24}$  and  $E_{35}$  do not vanish due to globally unsymmetric lay up. That is, the orthotropic solution is no longer valid for unsymmetric laminated beams, and fully coupled flexural-torsional vibration should be considered for accurate analysis.

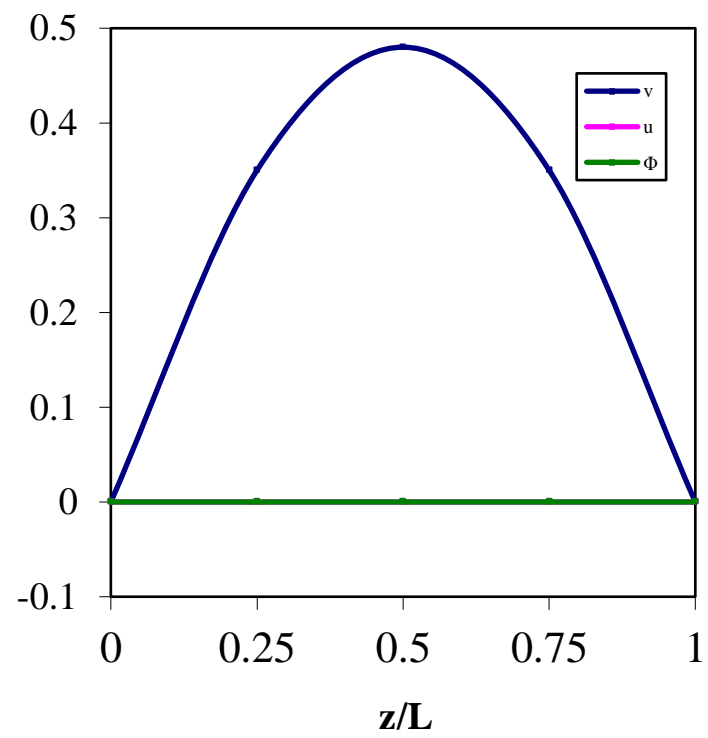


(a) Mode 1

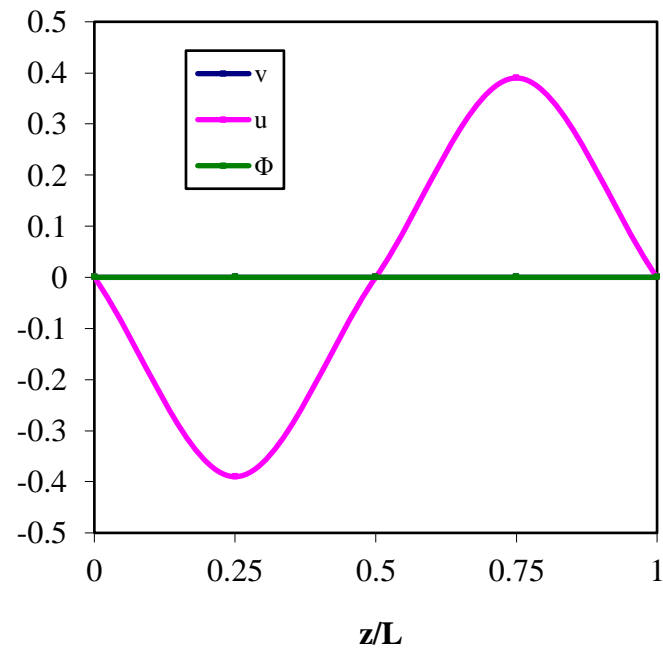




(b) Mode 2

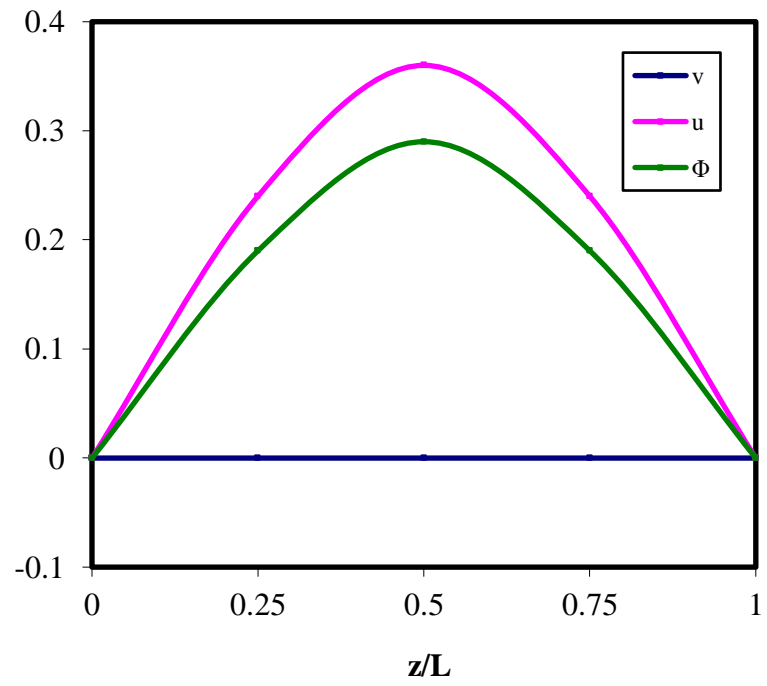


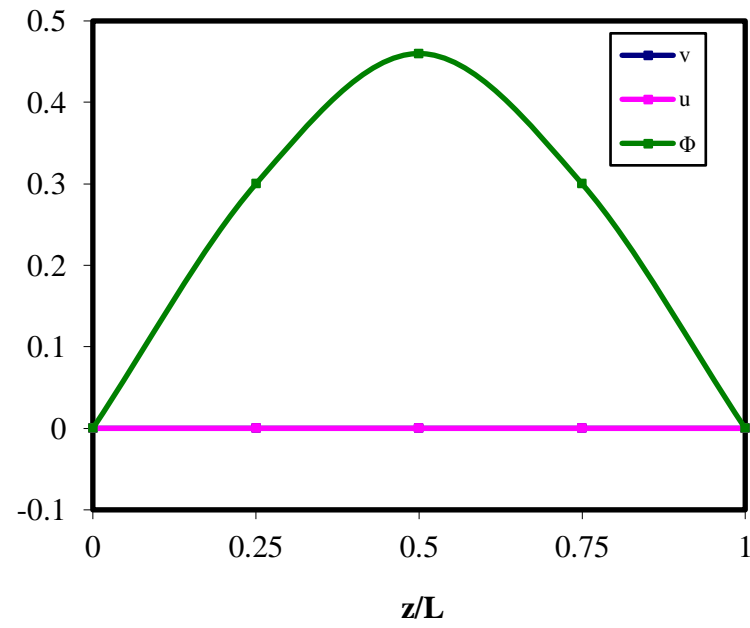
(c) Mode 3



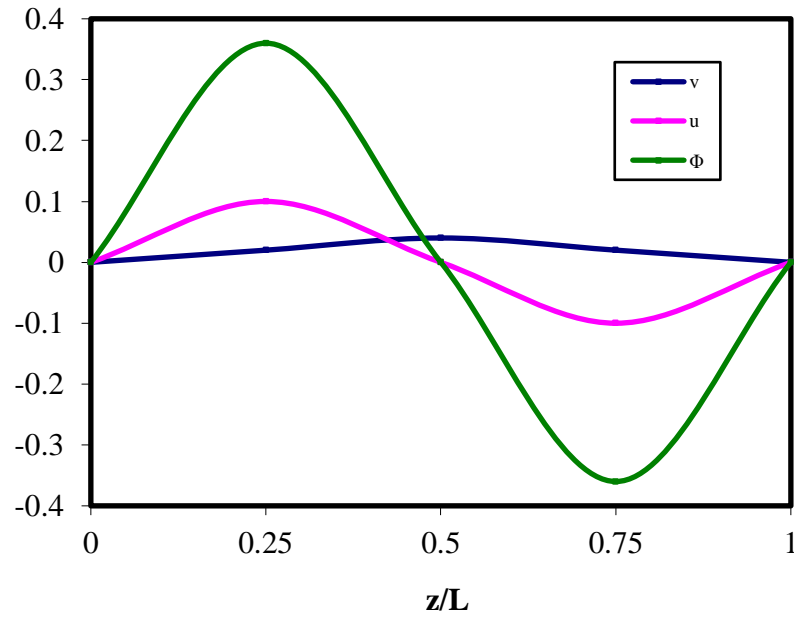
(d) Mode 4

Fig.8.5. Mode shapes of the composite beams with unidirectional fibre.

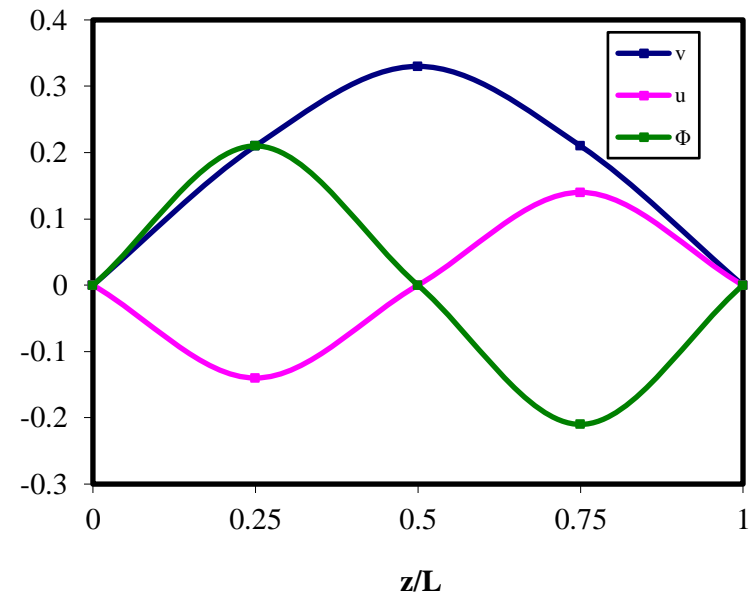




(a) Mode 1 (b) Mode 2



(c) Mode 3



(d) Mode 4

Fig.8.6. Mode shapes of the composite beams with fibre angle  $30^\circ$  in the web.

### **8.5.1. Effect of Elastic modulus ratio**

The next case study shows the effects of modulus ratio ( $E_1/E_2$ ) of composite beams on the natural frequencies and mode shapes for simply supported and clamped composite beams (Figs. 8.7 and 8.8). The stacking sequence of the top and bottom flanges are  $[0/90]_s$ , and web is unidirectional. It is observed that the natural frequencies increase with increasing orthotropy ( $E_1/E_2$ ) for both simply supported and fixed boundary conditions.

### **8.6. Effect of Height-to-thickness ratio:**

The effects of the height-to-thickness ratio ( $b_3/t$ ) of thin-walled composite beams on the natural frequencies and mode shapes are illustrated in Fig. 8.7 and fig. 8.8 for simply supported and clamped boundary conditions. Torsional frequency is found to be very sensitive to height-to-thickness ratio while the other frequencies almost invariant for both boundary conditions.

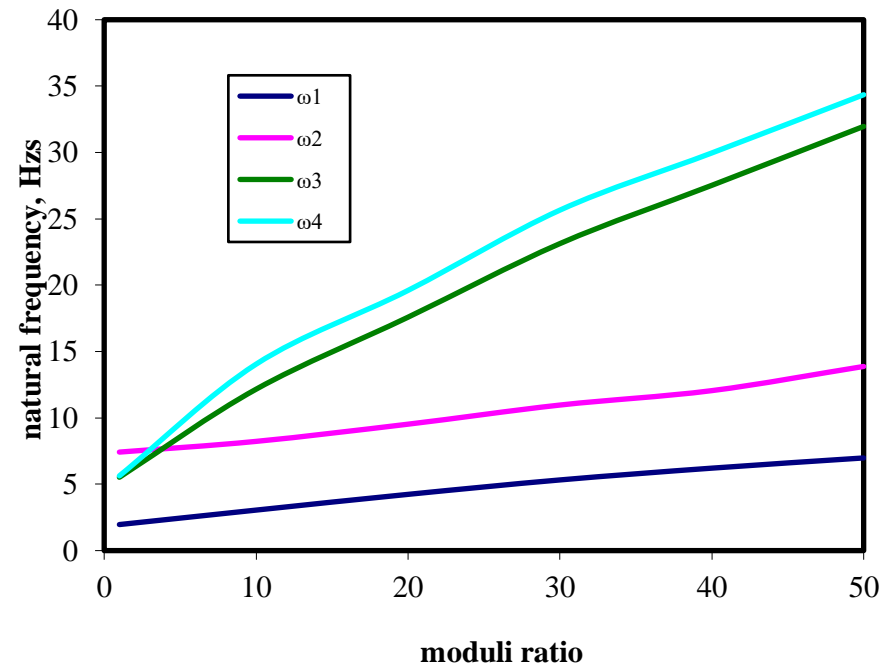


Fig.8.7. Variation of the non-dimensional natural frequencies of a simply Supported composite beam with respect to modulus ratio



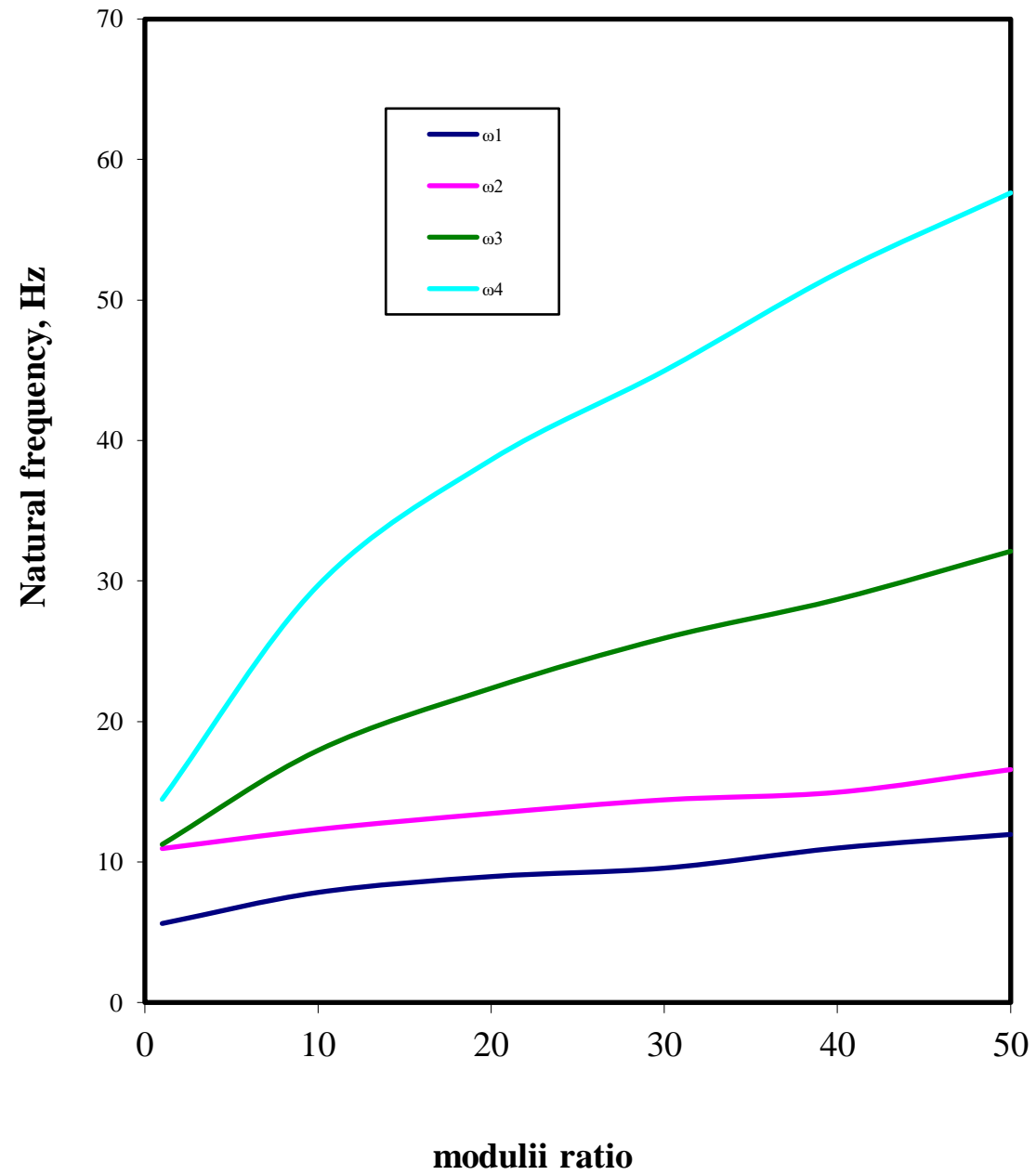


Fig.8.8.Variation of the non-dimensional natural frequencies of fixed composite beam with respect to modulus ratio

### **8.6.1. Effect of Height-to-thickness ratio**

The variation of the non-dimensional natural frequencies of a simply supported composite beam and fixed beam with respect to height-to-thickness ratio are shown in figure 8.9 and 8.10..

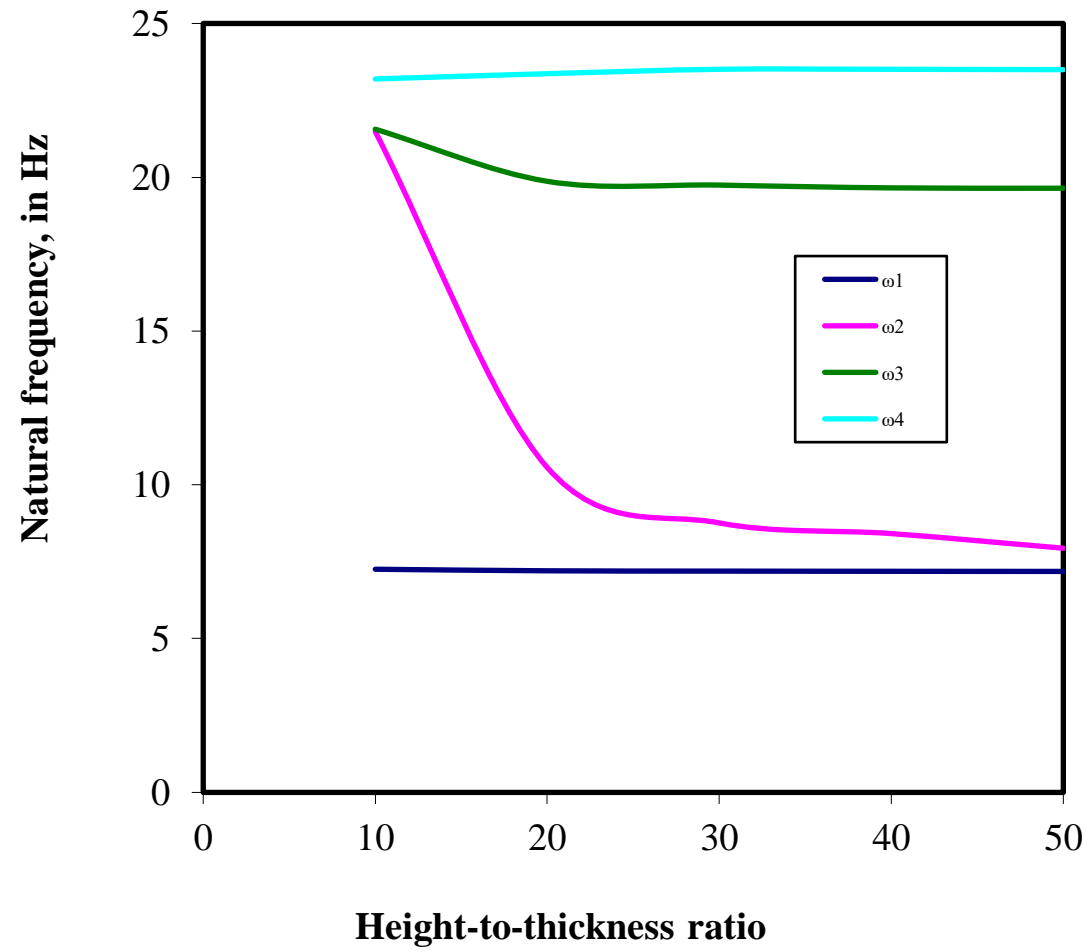


Fig.8.9.Variation of the non-dimensional natural frequencies of a simply supported composite beam with height-to-thickness ratio.

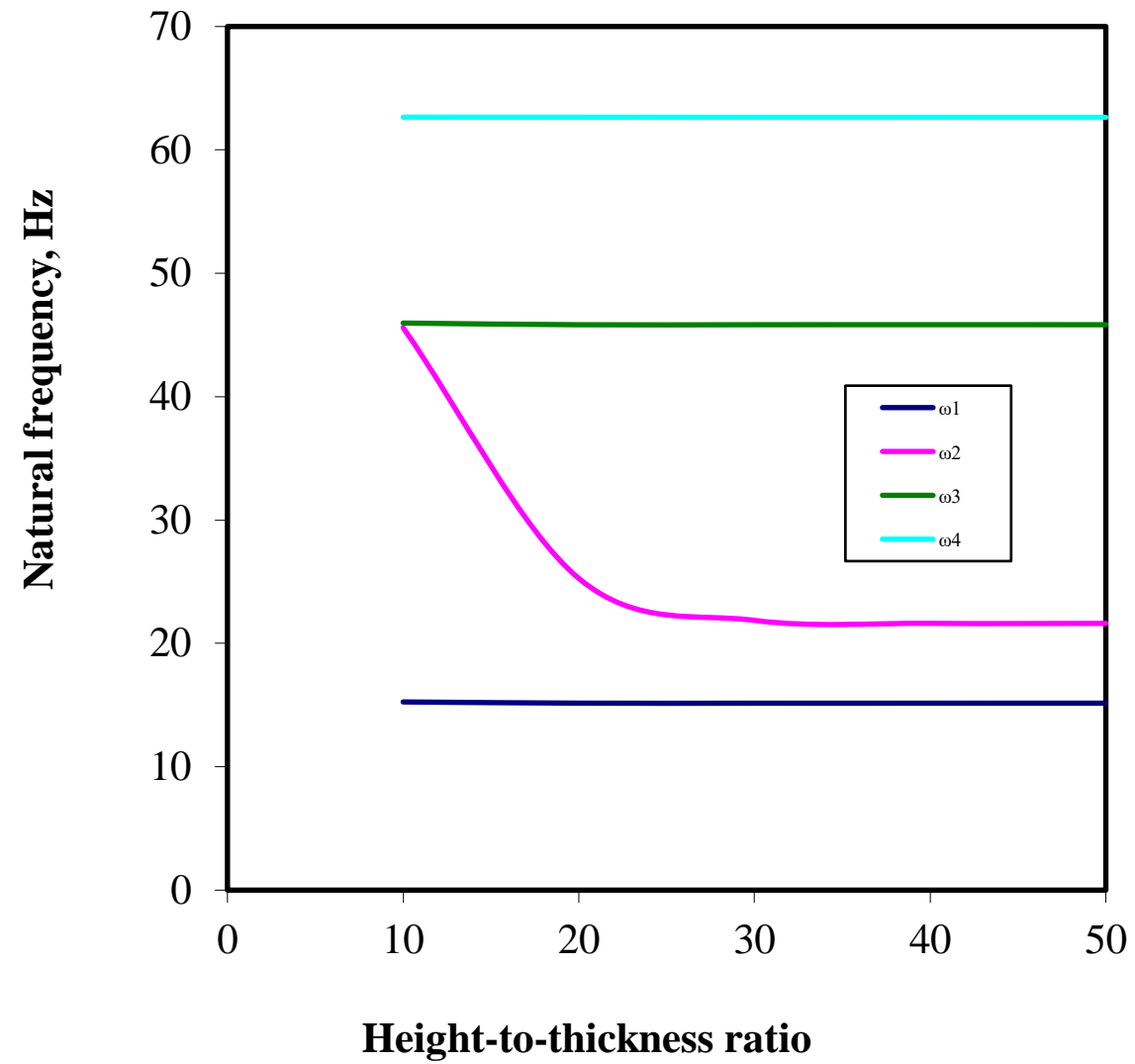


Fig.8.10.Variation of the non-dimensional natural frequencies of a fixed composite beam with height-to-thickness ratio.

### **8.6.2. Harmonic analysis.**

The harmonic analysis is carried out for a cantilever doubly symmetric composite I-beam by applying a load of 1 Newton at free end. The analysis is carried out by varying fibre angle rotation in top and bottom flanges of I- beam, elastic modular ratio and height to thickness ratio of I- beam and results are obtained and presented in the tabular form. These results are also depicted in the graphical form as Frequency Vs. Amplitude in figures 8.11, 8.12 and 8.13.

#### **8.6.2.1. Effect of fibre angle rotation in top and bottom flanges**

In this example the top and bottom flanges are considered as angle-ply laminates  $[\theta/ -\theta]$ , and the web laminate is assumed to be unidirectional. The numbers (0-90) shown in graph are fibre angle rotations  $[\theta/ -\theta]$  in degrees.



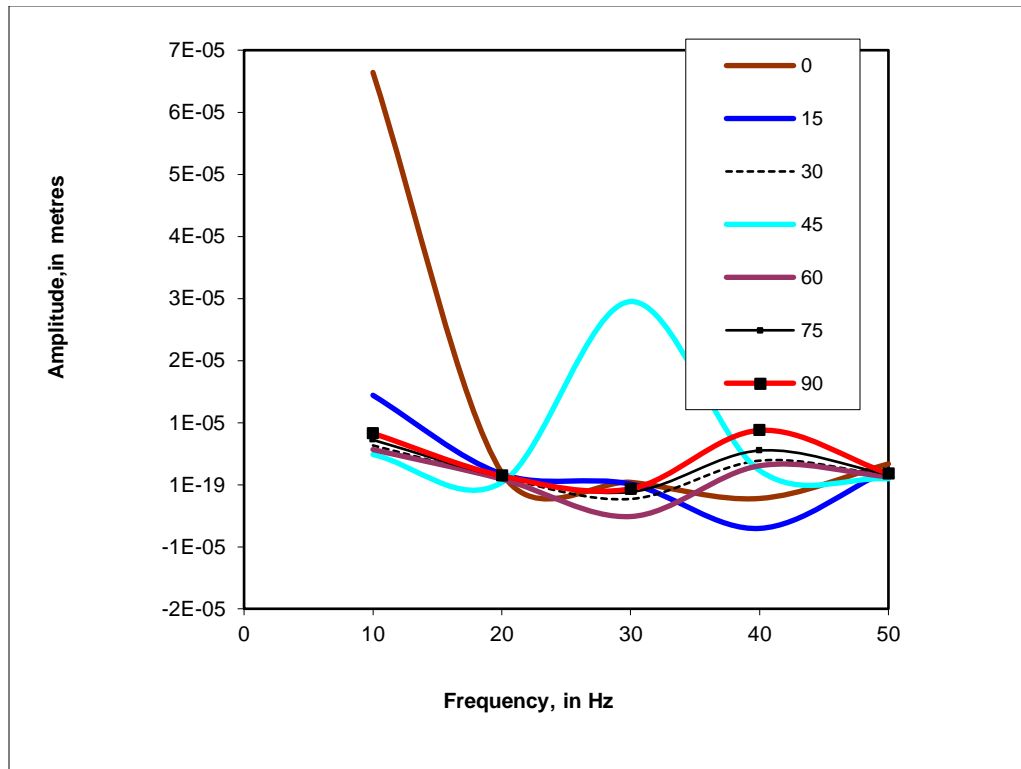


Fig.8.11. Frequency Vs. Amplitude for fibre angle rotation in two flanges.

From the Fig.8.11, for unidirectional fibre (zero fibre angle rotation), the amplitude of vibration is maximum at 10 Hz and decreases suddenly and slowly increases after wards. For a 45 degree fibre angle rotation, the value of the amplitude increases from 20-30 Hz and decreases afterwards.

#### **8.6.2.2. Effect of Elastic modulus ratio**

This analysis shows the effects of modulus ratio ( $E_1/E_2$ ) of composite beams on the harmonic response for cantilever composite I-beams. The stacking sequence of the top and bottom flanges are  $[0/90]_s$ , and web is unidirectional is considered in this analysis. The figure 8.12 shows the variation of natural frequencies Vs amplitude for elastic modular ratios ( $E_1/E_2$ ) from 1 to 40.

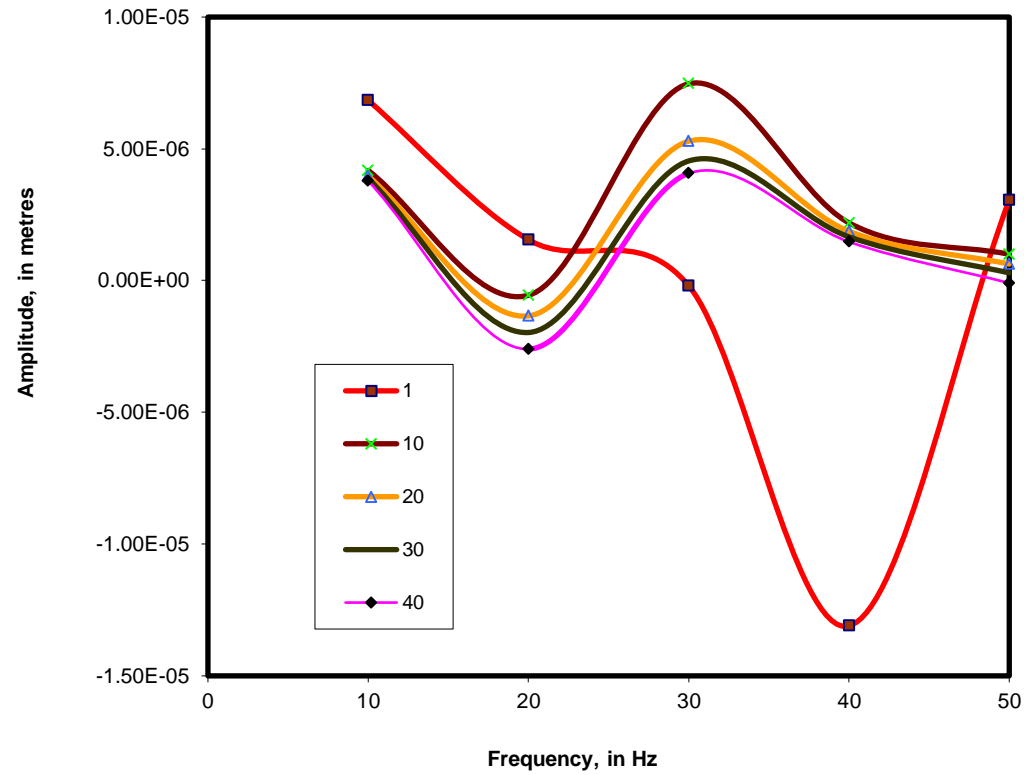


Fig.8.12. Frequency Vs. Amplitude for various elastic modulus ratios

From the fig.8.12, it is clear that as the frequency increases, the value of the amplitude of vibration for a cantilever composite beam follows sinusoidal curve, for all modular ratios from 10-40 , except for modular ratio one and the values of amplitude of vibration decreases in frequency step 10-20 Hz and gradually increases for next step 20-30Hz and then decreases.

### 8.6.2.3. Effect of Height-to-thickness ratio

The effects of the height-to-thickness ratio ( $b_3/t$ ) of thin-walled composite beams on the Harmonic response illustrated in Fig.8.13 for cantilever boundary conditions for the different values of height-to-thickness ratio ( $b_3/t$ ) of 10 to 40.

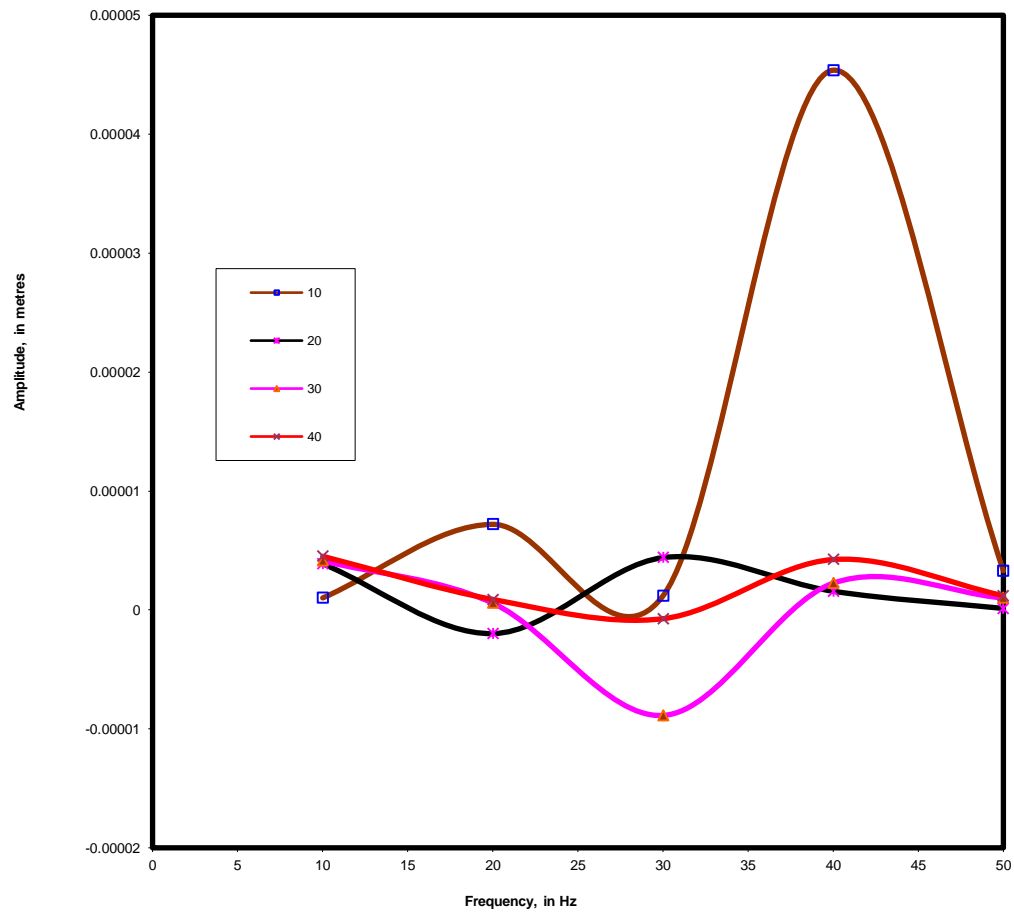


Fig. 8.13. Frequency Vs. Amplitude for various beam height to thickness ratios

From the fig. 8.13, it shows that the amplitude of vibration is maximum for frequency of 40 Hz. for a height to thickness ratio of 10. For other height to thickness ratios, it is almost constant for all other values of frequencies. It clearly shows that the amplitude of vibration decreases by increasing the height to thickness ratio at all frequencies.

## **Chapter 9**

# **MODAL AND HARMONIC ANALYSIS OF TAPERED COMPOSITE I-BEAM WITH A SMALL END FIXED**

# **MODAL AND HARMONIC ANALYSIS OF TAPERED COMPOSITE I- BEAM WITH A SMALL END FIXED**

A thin-walled tapered composite beam with I-section and length  $L = 8$  m is considered in order to investigate the effects of fibre orientation and modulus ratio on the natural frequencies and mode shapes for a cantilever boundary condition. The Finite Element model of a tapered I-beam is shown in Fig. 9.1. The engineering constants and element used is same as in the case of a uniform I-beam, mentioned in 8.1 and 8.1.1. In this case, the thickness of the flanges and web is constant but the height and width of the beam is tapered to half of the actual size from one end to another. The smaller end is fixed and another end is free. For Harmonic analysis 1 Newton load is applied at free end of the cantilever composite I-beam and results are obtained are presented in graphical form.



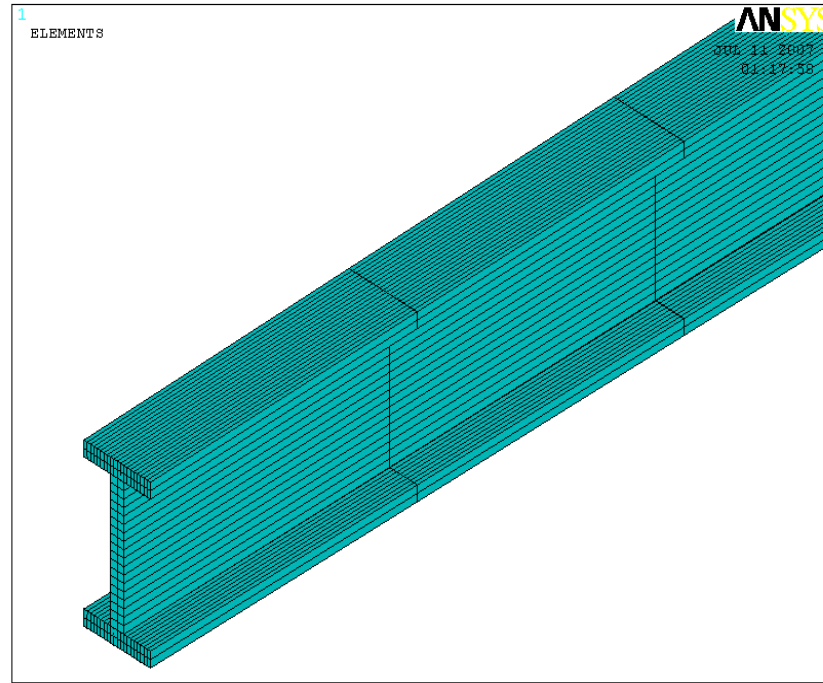


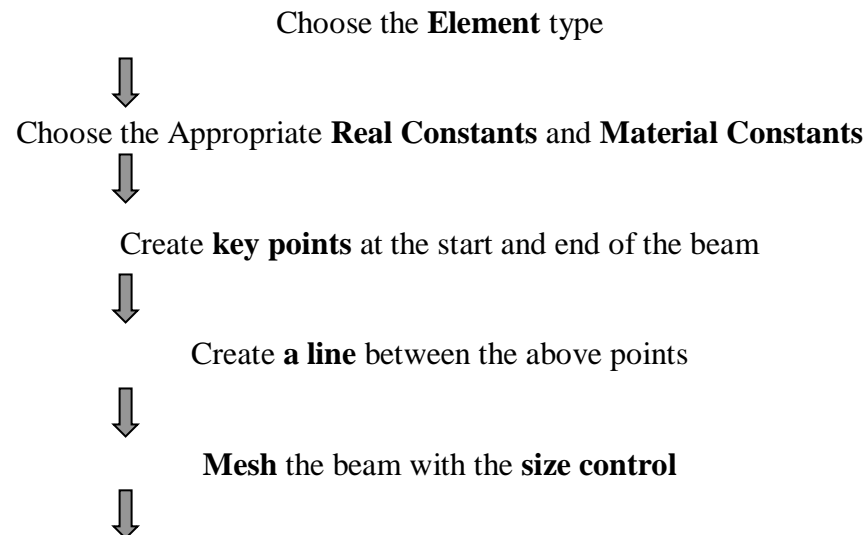
**Fig9.1. Tapered composite I- beam with layers**

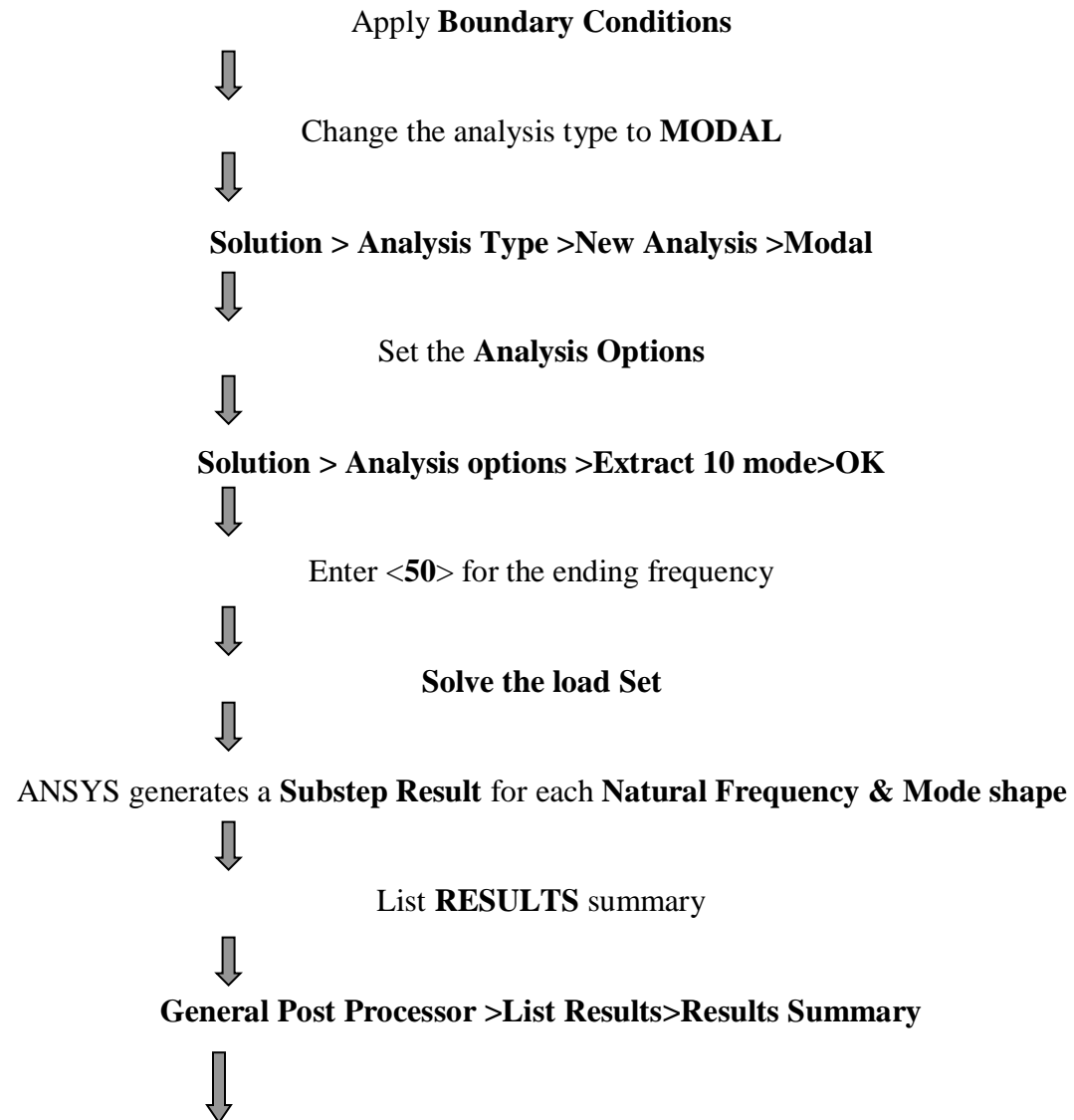
## 9.1. Modal Analysis

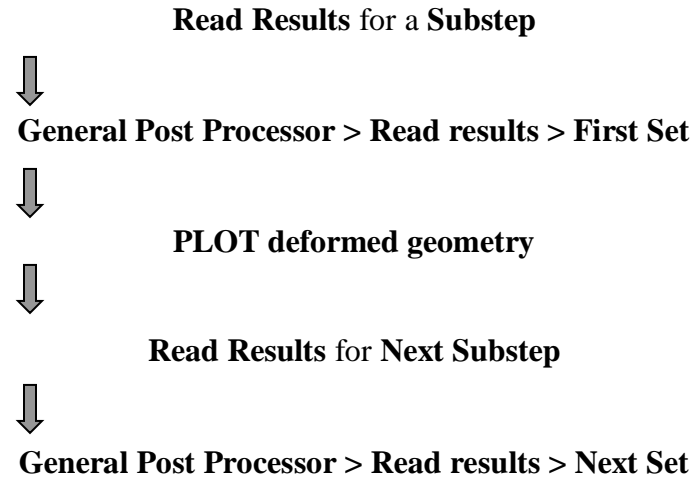
The modal analysis of a cantilever I-beam is done using ANSYS and the steps involved to do modelling and analysis to get the natural frequencies and mode shapes is shown below in the form of flow chart. The different mode extraction methods in ANSYS are

- Sub space
- Block Lanczos
- Power dynamics
- Reduced
- unsymmetric

### Flow chart to show the Procedure to do Modal analysis using ANSYS







#### **9.1.1. Effect of fibre angle rotation in top and bottom Flanges:-**

The top and bottom flanges are considered as angle-ply laminates  $[\theta/ -\theta]$ , and the web laminate is assumed to be unidirectional. In this case, the lowest four natural frequencies by the finite element analysis exactly correspond to the first flexural mode in the x-direction, and flexural mode in the y-direction, second flexural mode in the x-direction, torsional mode by the orthotropic closed-form solution, respectively. It is shown that from fig.9.2, the natural frequencies are increasing with increasing fibre angle rotation. Up to  $45^\circ$  fibre angle, very small variation in the natural frequencies for first three modes.

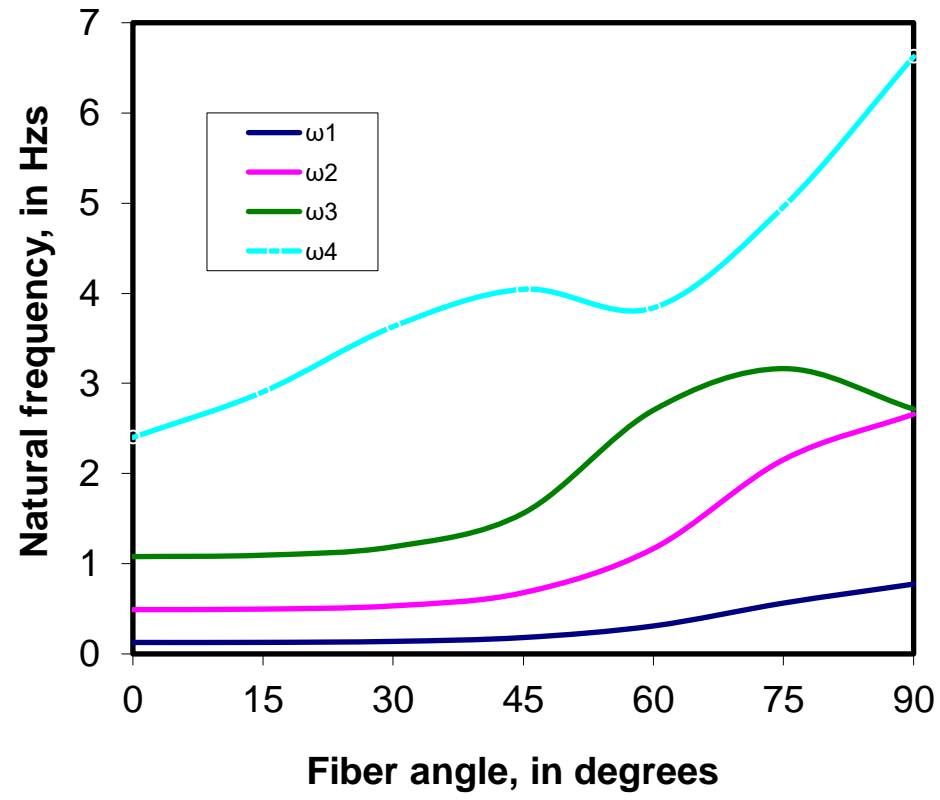
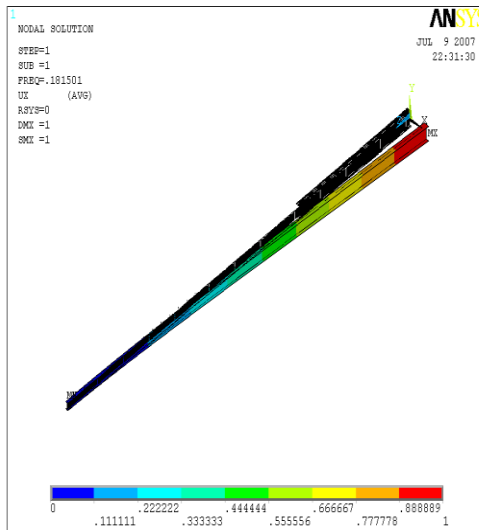


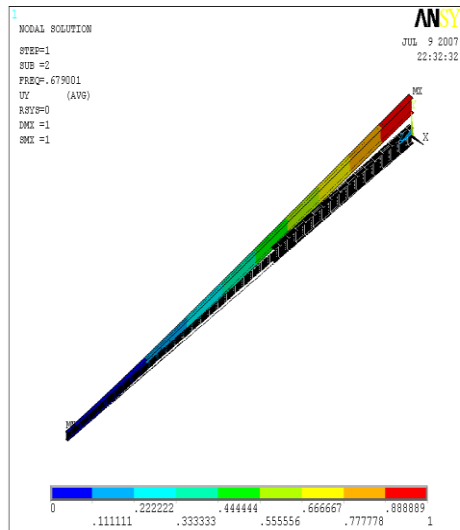
Fig 9.2. Variation of the non-dimensional natural frequencies of a tapered cantilever composite beam with small end fixed with respect to fibre angle change in flanges

### 9.1.2. Mode shapes

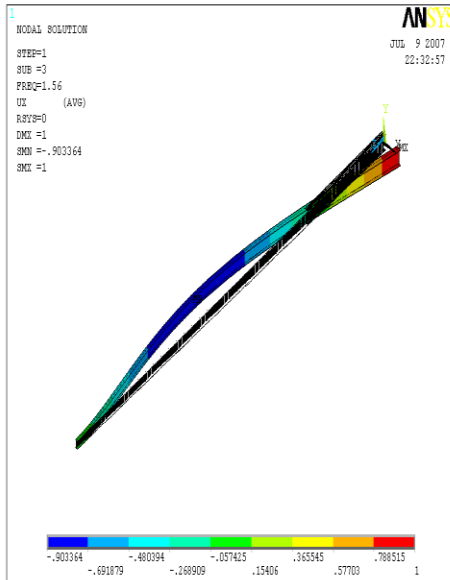
The mode shapes corresponding to the first four lowest modes with unidirectional fibre in web and fibre angle  $45^\circ$  in the top and bottom flanges are illustrated in Figs.9.3.



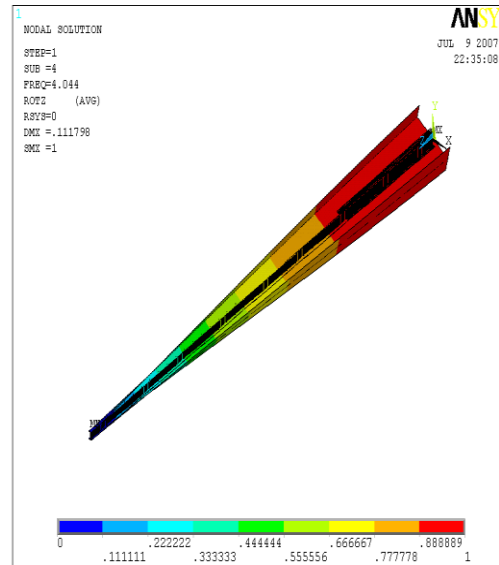
(a). Mode 1



(b). Mode 2



(a). Mode 3



(b). Mode 4

**Fig. 9.3. Mode shapes of the tapered composite beam with fibre angle  $45^\circ$  in top and bottom flanges**

### 9.1.3. Effect of fibre angle rotation in web

In this case the natural frequencies for first mode are constant for all fibre angles as shown in fig.9.4. For second and third modes frequency is constant from fibre angle  $0^\circ$  to  $60^\circ$  and after that a small increment is observed. For fourth mode, natural frequency is increased up to fibre angle  $60^\circ$  and then decreases.

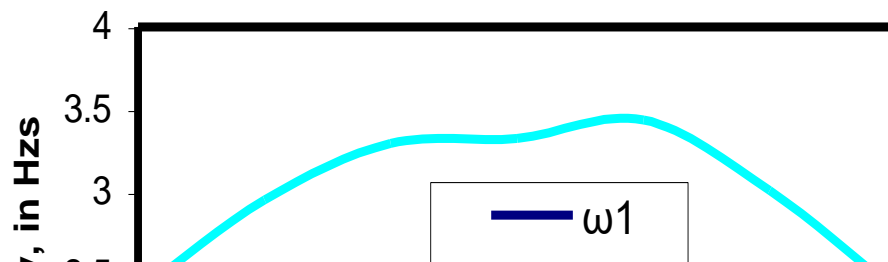


Fig. 9.4. Variation of the non-dimensional natural frequencies of a Tapered Cantilever composite beam with small end fixed with respect to fibre angle change in web.



#### 9.1.4. Effect of modular ratio

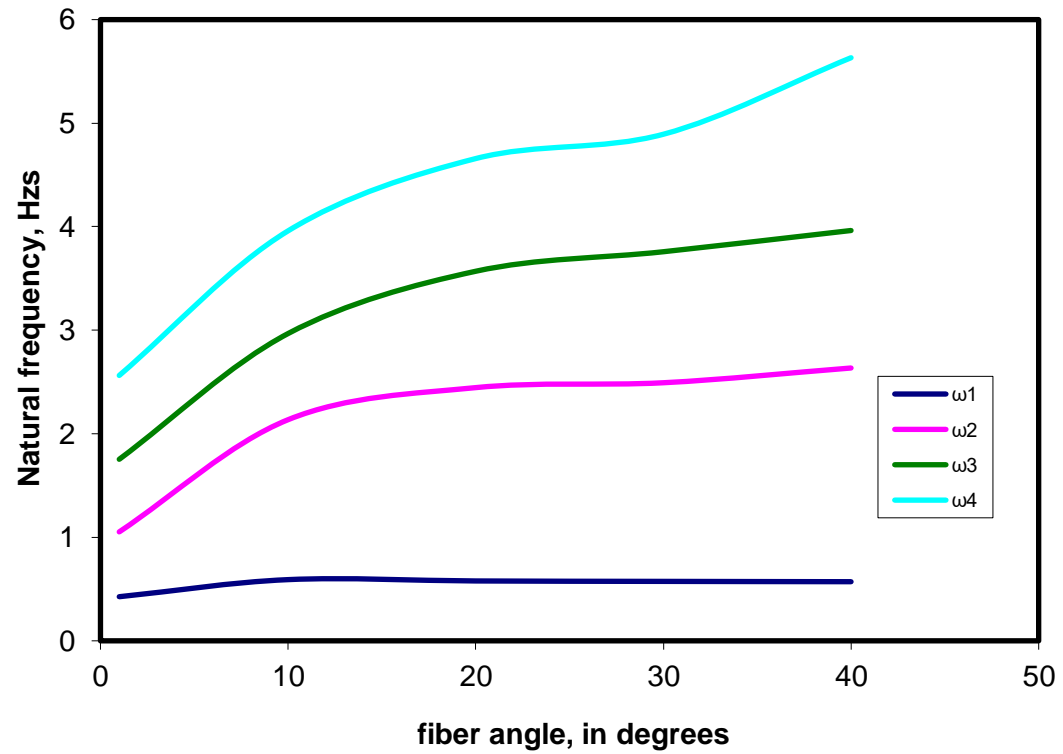


Fig.9.5. Variation of the non-dimensional natural frequencies of a Tapered Cantilever composite beam with small end fixed with respect to fibre angle.

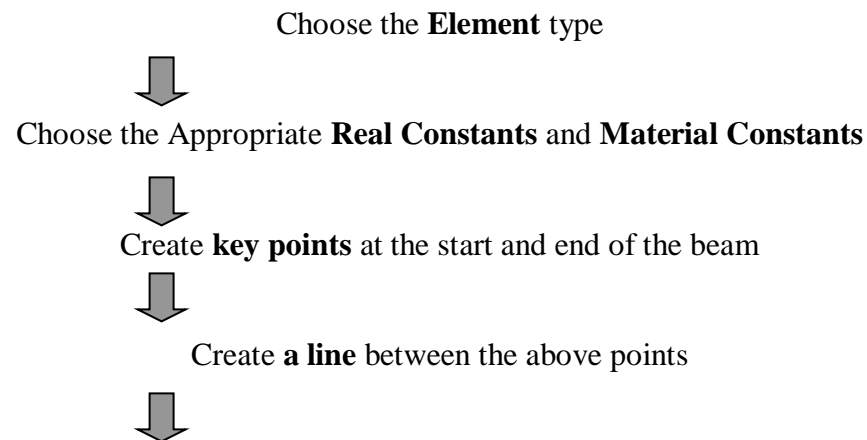
The next analysis shows the effects of modulus ratio ( $E_1/E_2$ ) of composite beams on the natural frequencies and mode shapes for tapered Cantilever composite I- beam. The stacking sequence of the top and bottom flanges are  $[0/90]_s$ , and web is unidirectional is considered for analysis. It is observed that the natural frequencies increase with increasing orthotropy ( $E_1/E_2$ ).

## 9.2. Harmonic analysis

Any sustained cyclic load will produce a sustained cyclic response in a structural system. In order to predict the sustained dynamic behaviour of a structure, Harmonic response analysis can verify whether or not a designed structure will successfully overcome resonance, fatigue and other harmful effects of forced vibration.

The harmonic response analysis was applied to a composite cantilever beam and its structural response was investigated. A load of 1.0 N at a frequency 0-50 Hz. is applied at free end and was used to examine the composite beam to laminates stacking. The pulse was localised at the centre node in the free edge. The study is carried out by varying fibre angle rotation in top and bottom flanges of I-beam and elastic modular ratio and results are obtained and represented in the graphical format as Frequency vs. Amplitude. The detailed steps involved in harmonic analysis of a beam using ANSYS are shown in flow chart form.

### Flow chart to show the Procedure to do Harmonic analysis of a Cantilever beam using ANSYS



**Mesh** the beam with the **size control**



Apply **Boundary Conditions**



Apply **1.0 N Load** at the **free end**



**New analysis > Harmonic**



Set the **Analysis Options**



Set the **Solution Method**



Set the DOF print out format to **“Amplitude and Phase” <OK>**



Set the **Tolerance to 1.0 e -8 < OK>**



Set the **Frequency Sub Steps**



**Solution > Load step Options – Time Frequency > Frequency and Sub Steps**



**Set the Harmonic Frequency Range 0-50 Hz**



**Set the Number of Sub steps to 100**



**Set to be STEPPED**



**SOLVE** the model

### **9.2.1. Effect of fibre angle rotation in top and bottom Flanges**

From the fig.9.6, it is clear that as the frequency increases, the value of the amplitude of vibration for a cantilever composite beam follows sinusoidal curve, for all fibre angles. For fibre angle  $60^0$ , the value of amplitude of vibration is high at frequency of 5 Hz.

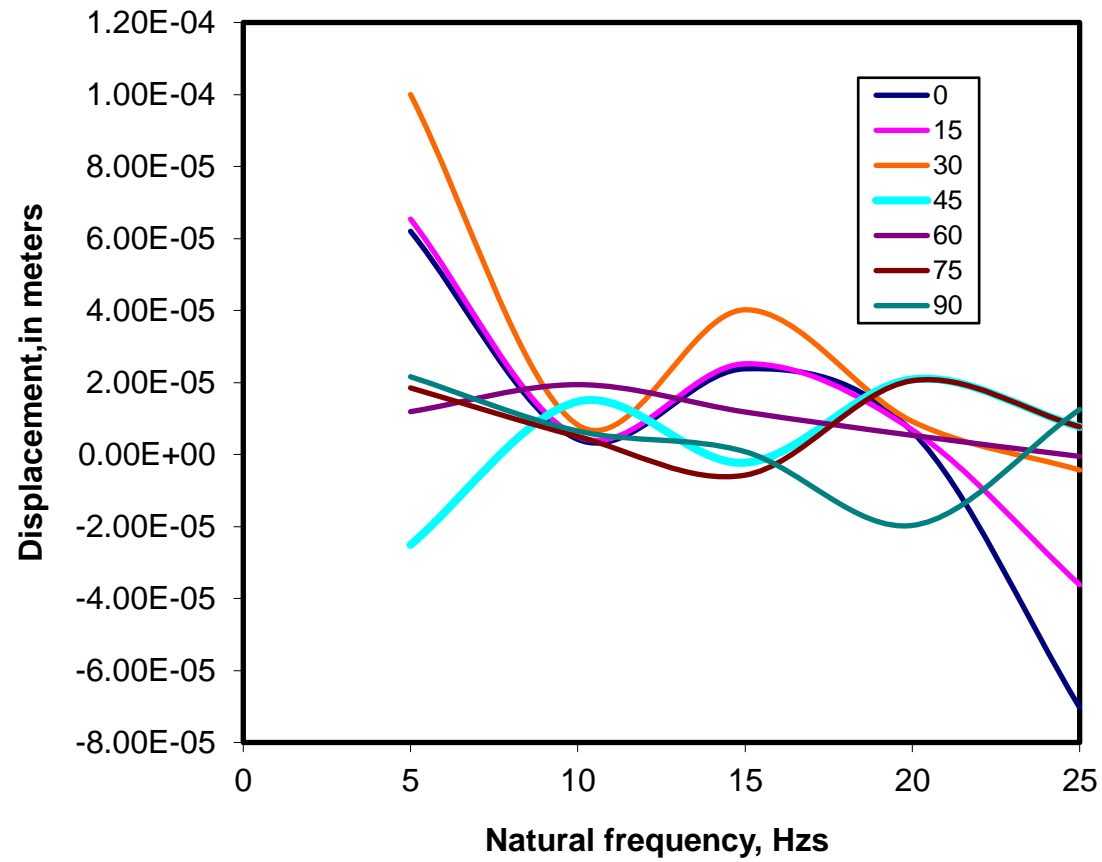


Fig.9.6. Frequency Vs. Displacement for fibre angle rotation in two flanges

### 9.2.2 .Effect of fibre angle rotation in web

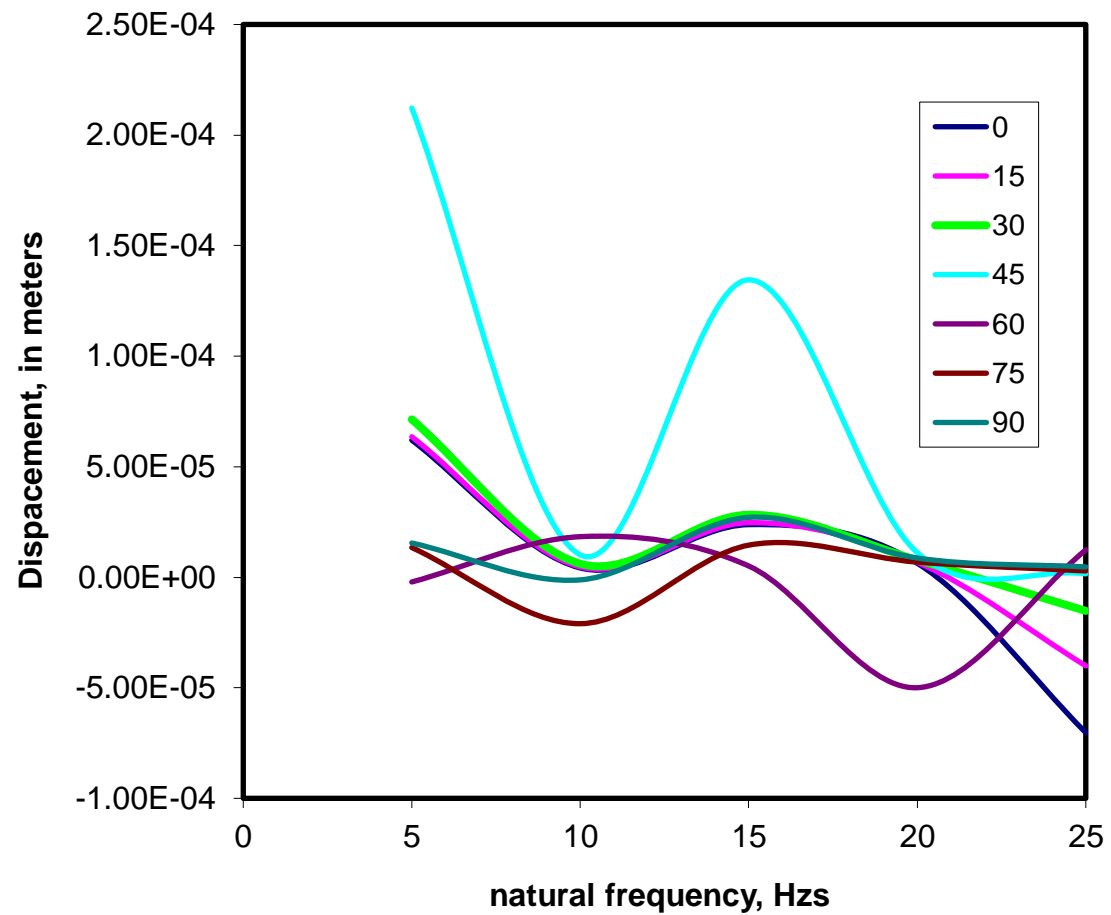


Fig.9.7. Frequency vs. displacement for fibre angle rotation in web



From the fig.9.7, it is seen that as the frequency increases, the value of the amplitude of vibration for a cantilever composite beam follows sinusoidal curve, for all fibre angles , same as above case, and for fibre angle  $45^0$ , the value of amplitude of vibration is high at frequency of 5 Hz .

### 9.2.3. Effect of modular ratio

As shown in fig.9.8, a small variation in amplitude of vibration for all modular ratios except modular ratio of 30. For modular ratio of 30, the minimum displacement is at frequency of 20 Hz.

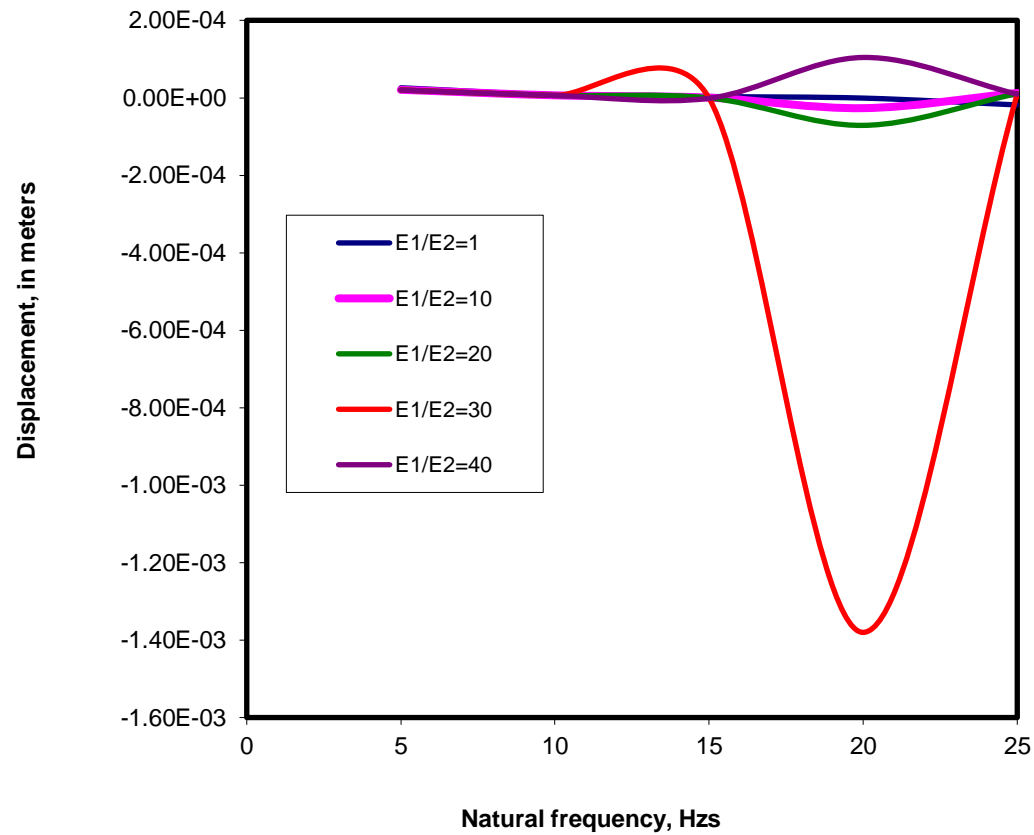


Fig.9.8. Frequency Vs. displacement for various modular ratios

## **Chapter 10**

# **MODAL AND HARMONIC ANALYSIS OF TAPERED COMPOSITE I- BEAM WITH BIG END FIXED**

# MODAL AND HARMONIC ANALYSIS OF TAPERED COMPOSITE I- BEAM WITH BIG END FIXED

In this case the same tapered beam is taken and the big end is fixed and small end is free instead of small end fixed and big end free as in previous case. The same engineering constants and element are used as for previous case. For harmonic analysis 1.0 N load is applied at free end of the cantilever beam and other end is kept free. The results obtained are presented in graphical form with displacement Vs natural frequency.

## 10.1. Modal Analysis

A composite cantilever I-beam is modelled with element shell99 and the material properties are taken as discussed in 8.1. Modal analysis is done by fixing the big end and kept smaller end free. The effect of fibre angle rotation in top and bottom flanges, elastic moduli and height to thickness ratio on natural frequencies and mode shapes are discussed below.

### 10.1.1. Effect of fibre angle rotation in top and bottom Flanges

The top and bottom flanges are considered as angle-ply laminates  $[\theta/-\theta]$ , and the web laminate is assumed to be unidirectional. In this case, the lowest four natural frequencies by the finite element analysis exactly correspond to the first flexural mode in the x-direction, flexural mode in the y-direction, second flexural mode in the x-direction, and torsional mode by the orthotropic closed-

form solution, respectively. It is clear that from fig.10.1, the natural frequencies are increasing with increase in fibre angle rotation. Very small variation in the natural frequencies for first three modes is observed from  $0^\circ$  and up to fibre angle  $45^\circ$ .

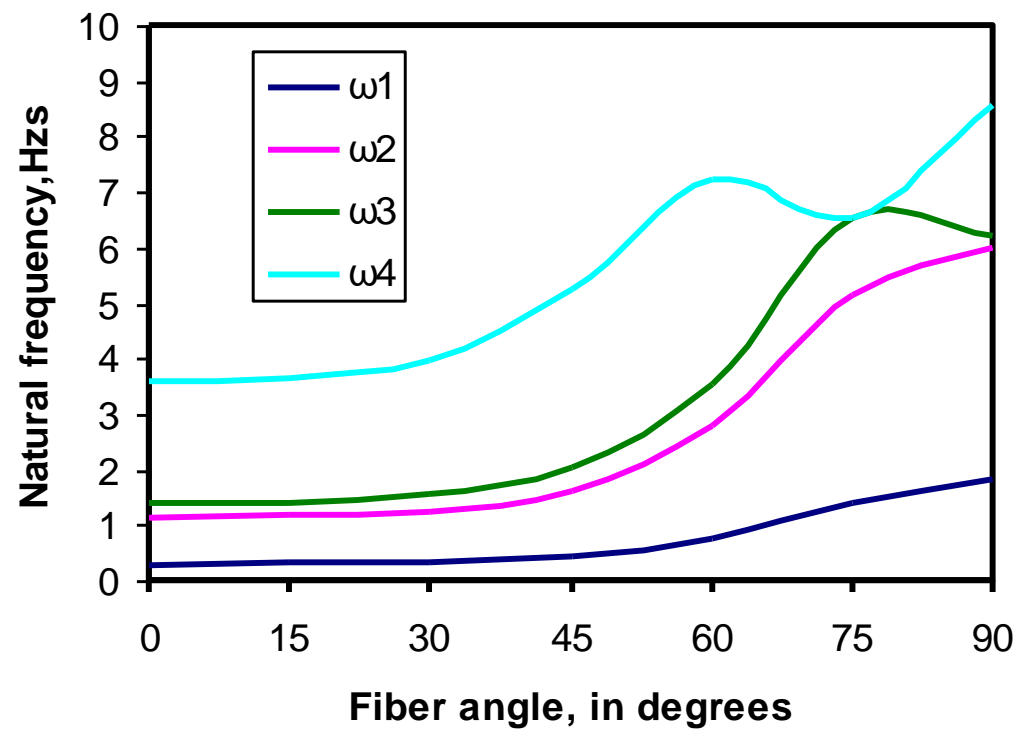
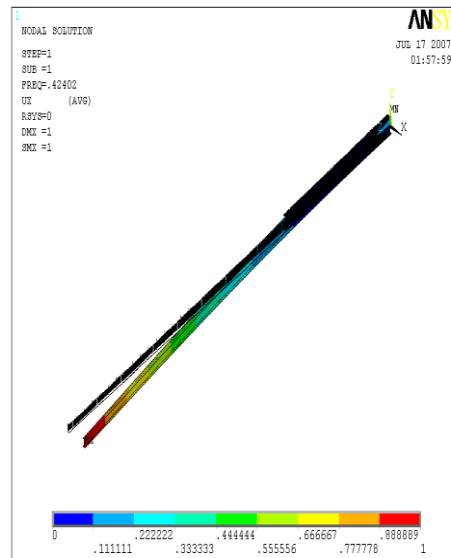


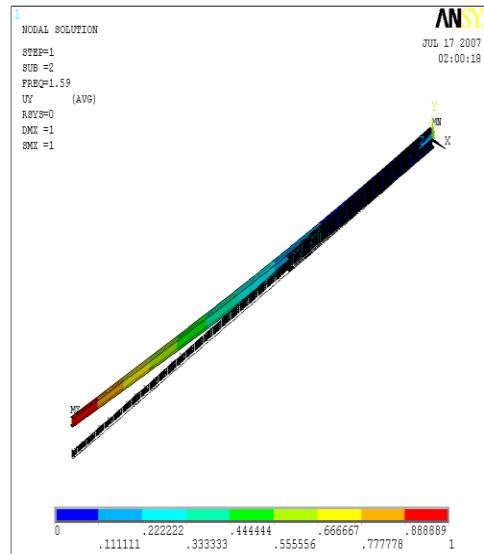
Fig10.1. Variation of the non-dimensional natural frequencies of a tapered cantilever composite beam with big end fixed with respect to fibre angle change in flanges

### 10.1.2. Mode shapes

The mode shapes corresponding to the first four lowest modes with unidirectional fibre in web and fibre angle  $45^\circ$  in the top and bottom flanges are illustrated in fig.10.2.

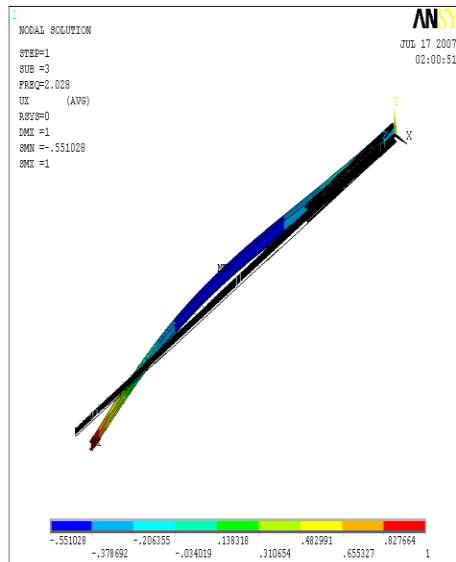


(a).Mode 1

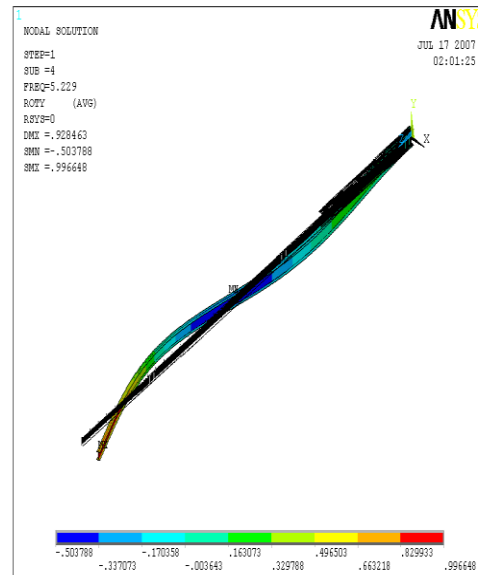


(b). Mode 2





(a).Mode 3



(b). Mode 4

Fig.10.2. Mode shapes of the tapered composite beam with fibre angle  $45^{\circ}$  in top and bottom flanges

### 10.1.3. Effect of fibre angle rotation in web

In this case the natural frequencies for first mode are constant for all fibre angles as shown in fig.10.3. For second, third and fourth modes frequency is constant from fibre angle 0- 45° and a small increment in each mode is observed .

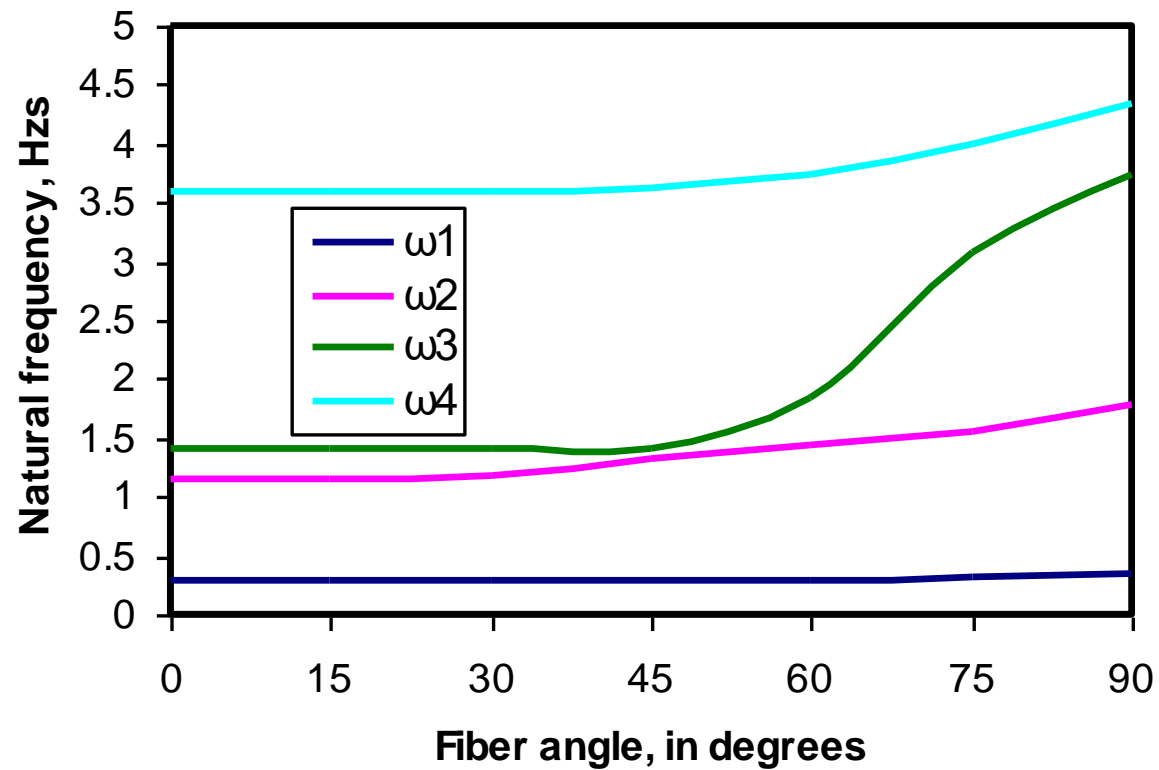


Fig10.3. Variation of the non-dimensional natural frequencies of a Tapered cantilever composite beam with big end fixed with respect to fibre angle change in web.

#### 10.1.4. Effect of modular ratio

The effects of modulus ratio ( $E_1/E_2$ ) of composite beams on the natural frequencies and mode shapes for Tapered Cantilever composite beam is shown below.

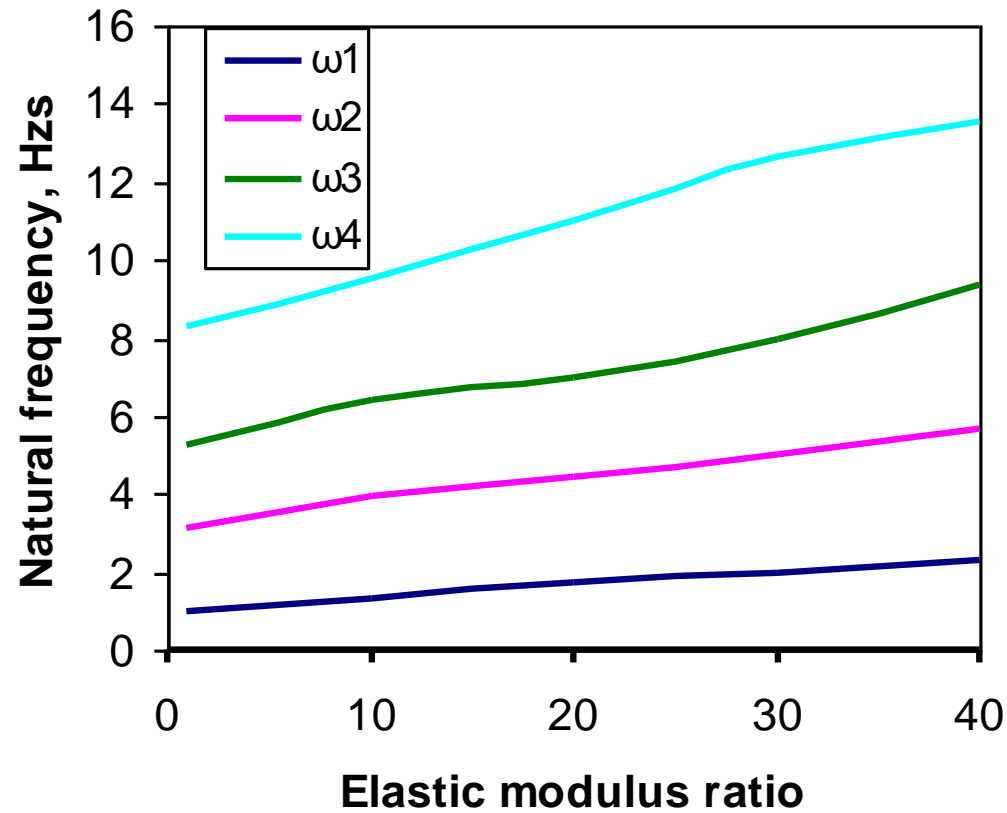


Fig. 10.4. Variation of the non-dimensional natural frequencies of a Taper cantilever composite beam with big end fixed with respect to modulus ratio.

The stacking sequence of the top and bottom flanges are  $[0/90]_s$ , and web is unidirectional. It is observed that the natural frequencies increase with increasing orthotropy ( $E_1/E_2$ ).

### 10.1.5. Harmonic analysis

The harmonic analysis is carried out for a tapered cantilever composite I-beam and load of 1.0 N is applied at free end. The study is carried out by varying fibre angle rotation in top and bottom flanges of I- beam and elastic modular ratio and results are obtained and represented in the graphical form as Frequency Vs. Displacement.

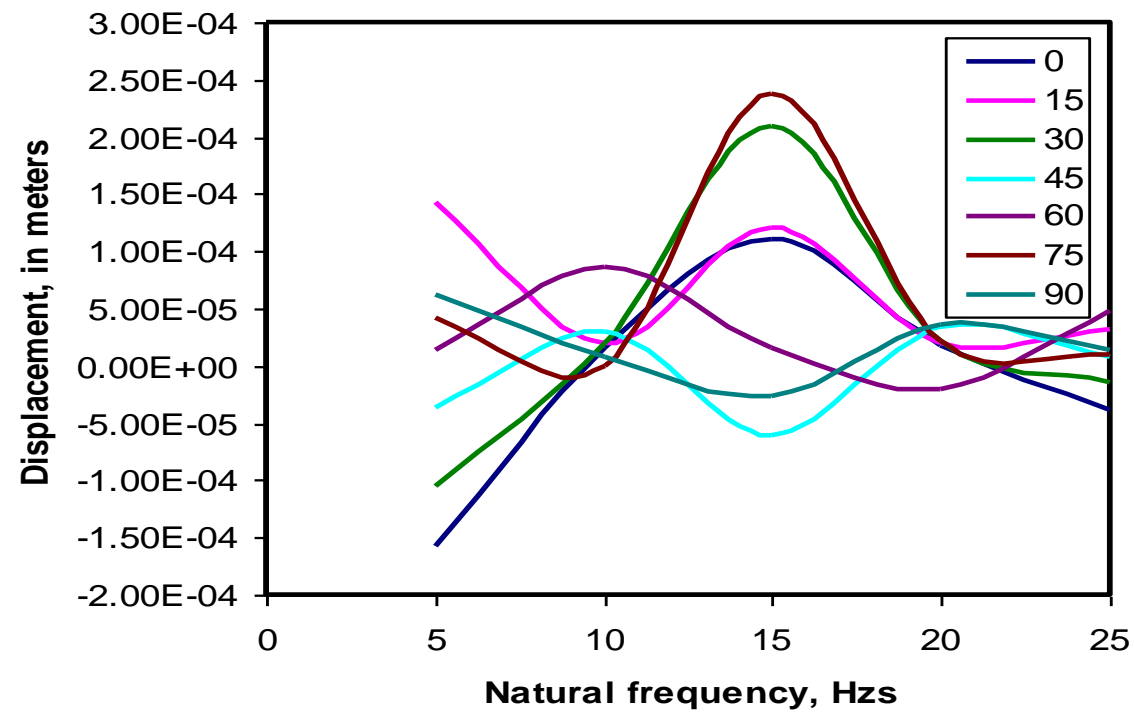


Fig10.5. Frequency vs. Displacement for fibre angle rotation in two flanges

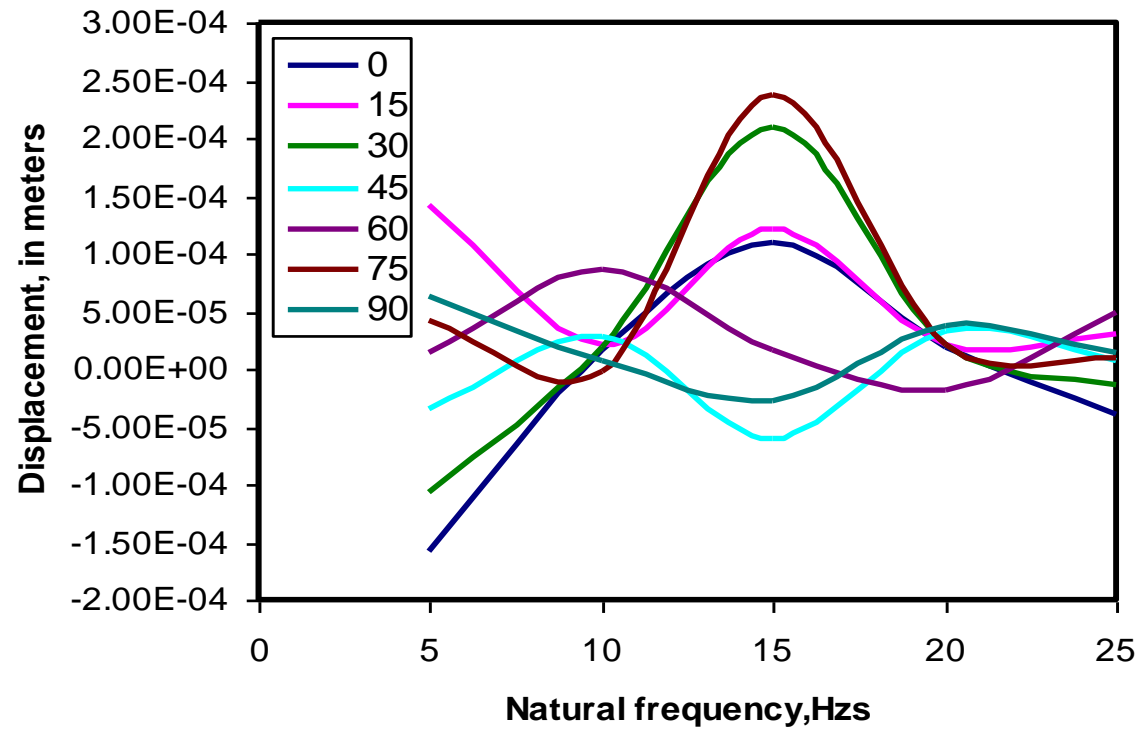


Fig.10.6. Frequency vs. Displacement for fibre angle rotation in web

#### 10.1.6. Effect of fibre angle rotation in top and bottom Flanges



From the fig.10.5, it is clear that as the frequency increases, the value of the amplitude of vibration for a cantilever composite beam follows sinusoidal curve, for all fibre angles. For fibre angle  $45^0$ , the value of amplitude of vibration is high at frequency of 5 Hz .

#### **10.1.7. Effect of fibre angle rotation in web**

From the fig.10.6, it is seen that as the frequency increases, the value of the amplitude of vibration for a cantilever composite beam follows sinusoidal curve, for all fibre angles same as above case.

#### **10.1.8. Effect of modular ratio**

From the fig.10.7, it is evident that there is a small variation in amplitude of vibration for all modular ratios except for modular ratio of 40. For modular ratio of 40, the minimum displacement is at frequency of 20 Hz.

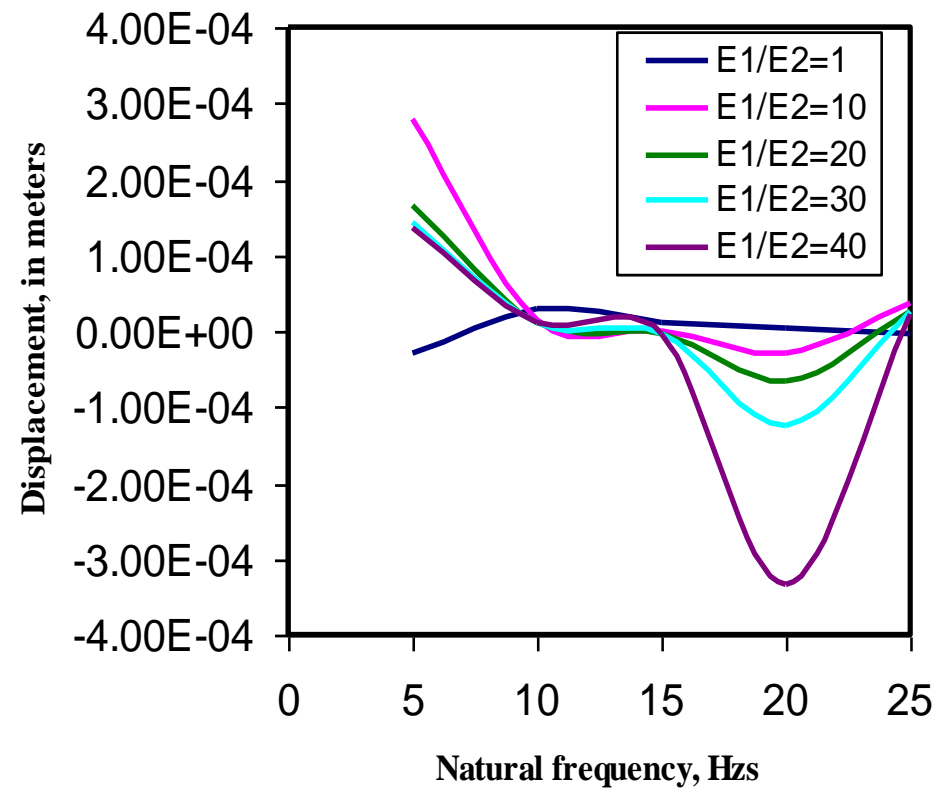
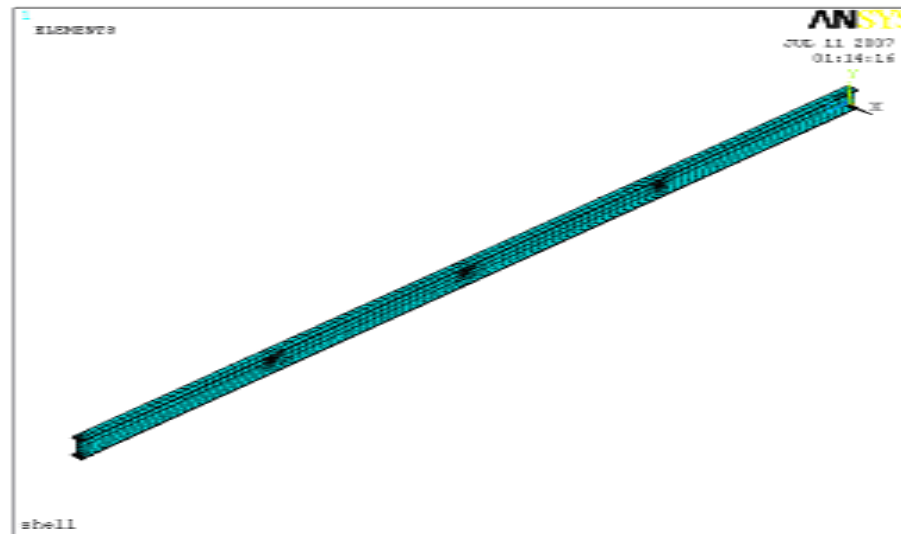


Fig.10.7. Frequency vs. Amplitude for various modular ratios.

## 10.2. Composite I-beam with three circular holes in web

In this case, uniform I- beam is considered and three circular holes are made in the web at 2m apart with holes diameter of 32 mm as shown in fig.10.8. The beam is modeled using ANSYS with the same material properties mentioned in the chapter 8. Modal and harmonic analysis is done for a cantilever boundary condition. Harmonic analysis is carried out by applying a load of 1.0 N at free end and nodal results at free end are obtained in the form of amplitude Vs natural frequency graphs for various fibre angle rotations and modular ratios. The Finite element model of a uniform doubly symmetric composite I-beam with holes in web is shown in fig.10.8.



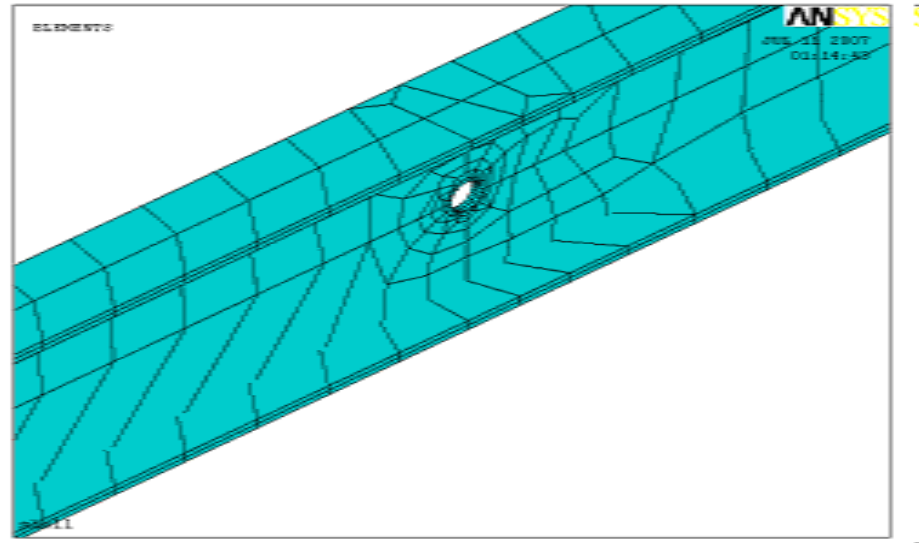


Fig.10.8. Uniform composite I-beam with circular holes in web

### 10.2.1. Modal Analysis

The modal analysis is carried out with the top and bottom flanges as angle-ply laminates  $[\theta/-\theta]$ , and the web laminate is assumed to be unidirectional in I beam. In this case, the lowest four natural frequencies by the finite element analysis exactly correspond to the first flexural mode in the x-direction, and flexural mode in the y-direction, second flexural mode in the x-direction, torsional mode by the orthotropic closed-form solution, respectively.

#### 10.2.1.1. Effect of fibre angle rotation in top and bottom Flanges

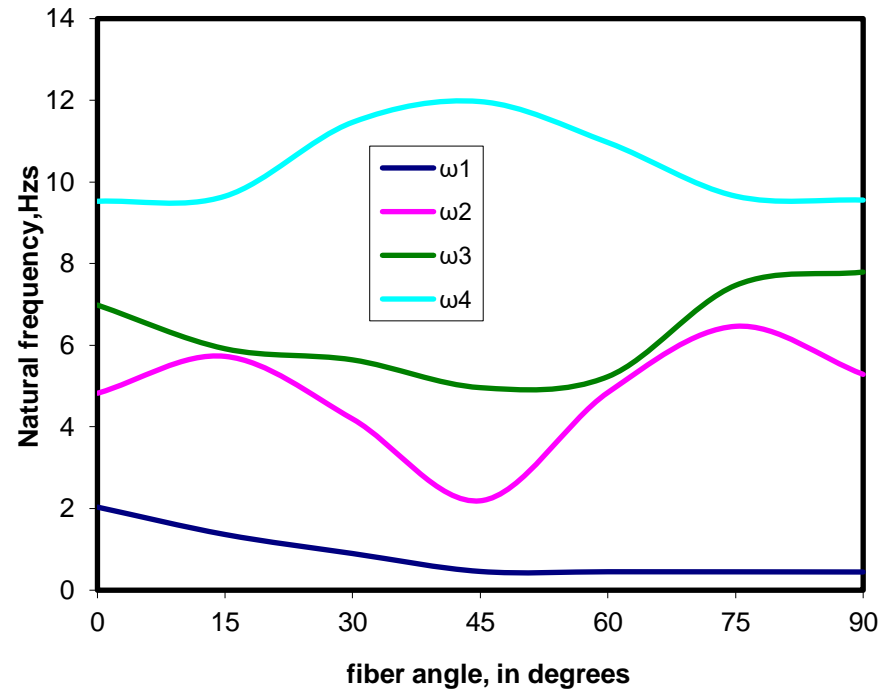
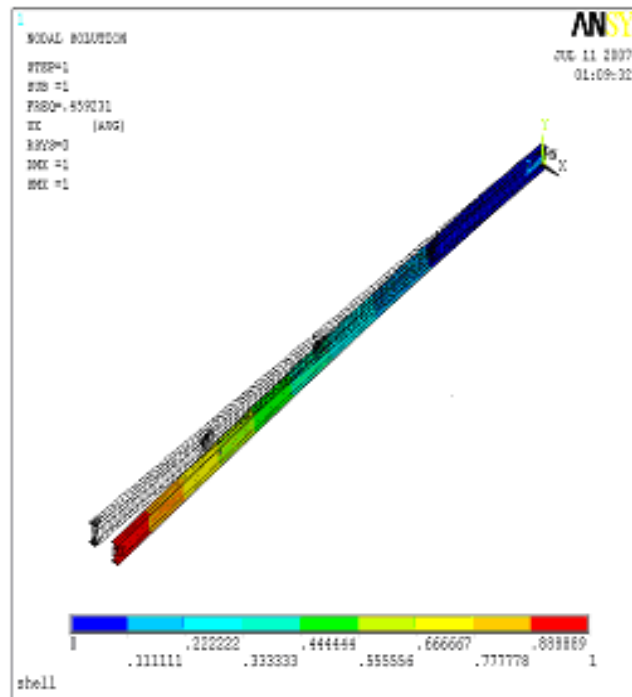


Fig.10.9. Variation of the non-dimensional natural frequencies of a cantilever Composite beam with circular holes in web with fibre angle change in flanges

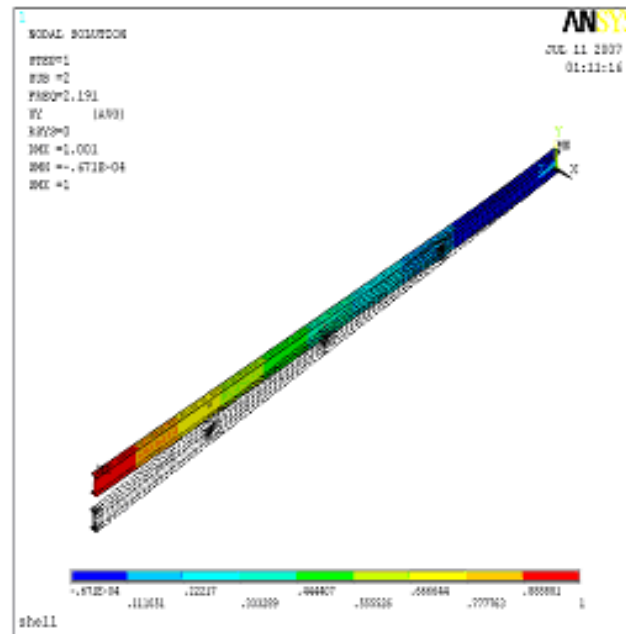
From fig.10.9, it is clear that natural frequencies for fourth mode increases with increasing fibre angle from 0 to 45<sup>0</sup> , maximum at 45<sup>0</sup> and then decreases afterwards. In second mode, the natural frequency at 45<sup>0</sup> fibre angle found to be minimum.

### 10.2.1.2. Mode shapes

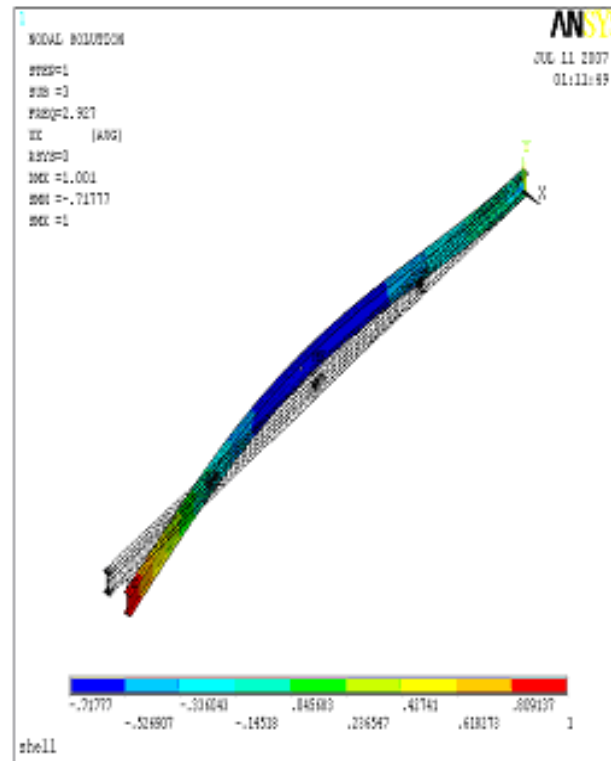
The mode shapes corresponding to the first four lowest modes with unidirectional fibre in web and fibre angle  $45^\circ$  is taken in the top and bottom flanges are illustrated in Fig.10.10.



(a).Mode 1

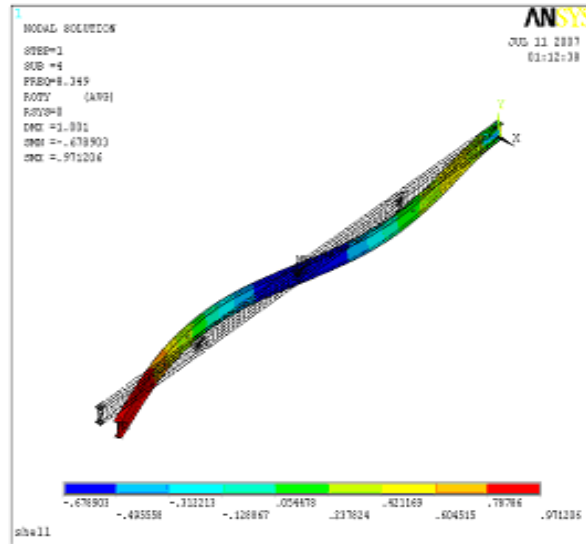


(b) Mode 2



(c) Mode 3





(d) Mode 4

Fig. 10.10. Mode shapes of the Cantilever composite beam with circular holes in web with fibre angle  $45^{\circ}$  in top and bottom flanges

### 10.2.1.3. Effect of fibre angle rotation in web

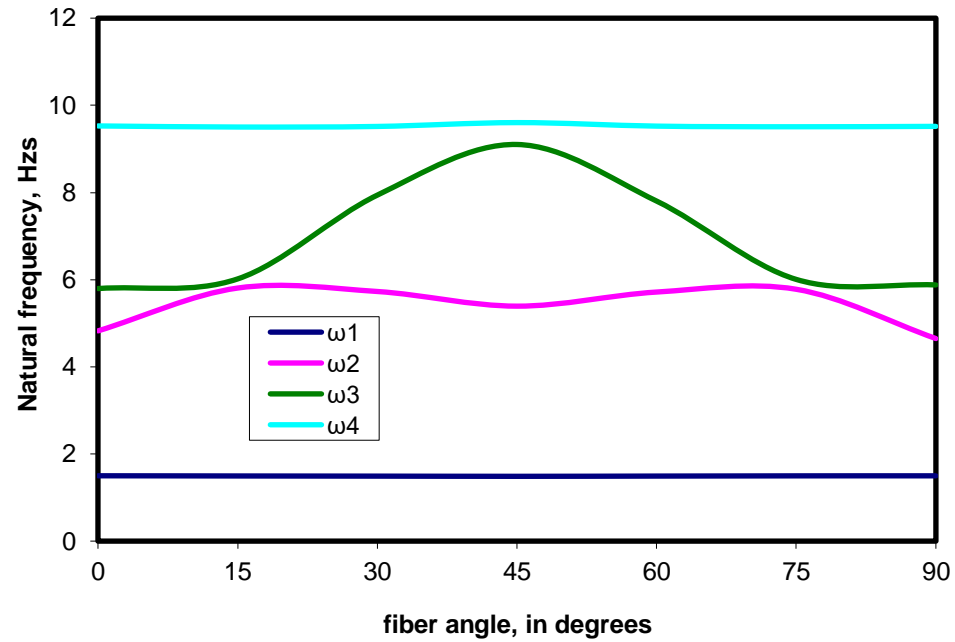


Fig10.11. Variation of the non-dimensional natural frequencies of a Cantilever composite beam with circular holes in web with to fibre angle change in flanges

From fig.10.11, it is observed that natural frequencies of third mode increases with increasing fibre angle from 0 to 45° reaches maximum at 45° and then decreases afterwards. For all other modes, there is no variation in natural frequencies by changing the fibre angle in web.

#### 10.2.1.4. Effect of Elastic modular ratio

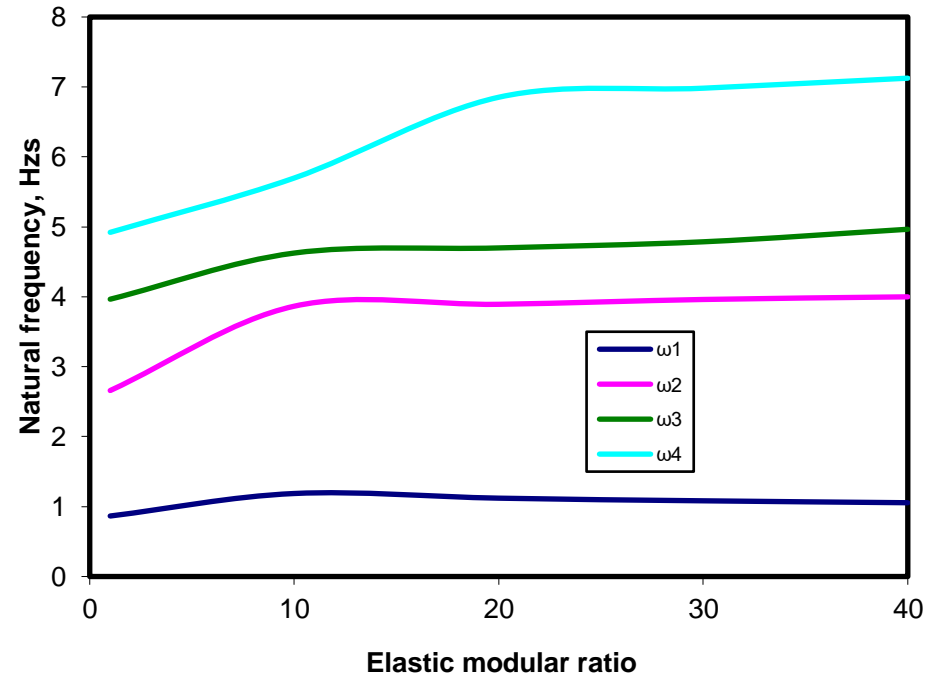


Fig. 10.12. Variation of the non-dimensional natural frequencies of a Cantilever composite beam with circular holes in web with elastic modular ratio

In this, it shows the effects of modulus ratio ( $E_1/E_2$ ) of composite beams on the natural frequencies and mode shapes for uniform Cantilever composite beam with circular holes in web (Fig. 10.12). The stacking sequence of the top and bottom flanges are  $[0/90]_s$ , and web is unidirectional. It is observed that the natural frequencies increase with increasing orthotropy ( $E_1/E_2$ ).



### **10.3. Harmonic Analysis**

The harmonic analysis is carried out for a cantilever composite uniform doubly symmetric I-beam and load of 1 Newton is applied at free end. The study is carried out by varying fibre angle rotation in top and bottom flanges of I- beam and elastic modular ratio and results are obtained and represented in the graphical form as Frequency vs. Displacement.

#### **10.3.1. Effect of fibre angle rotation in top and bottom Flanges**

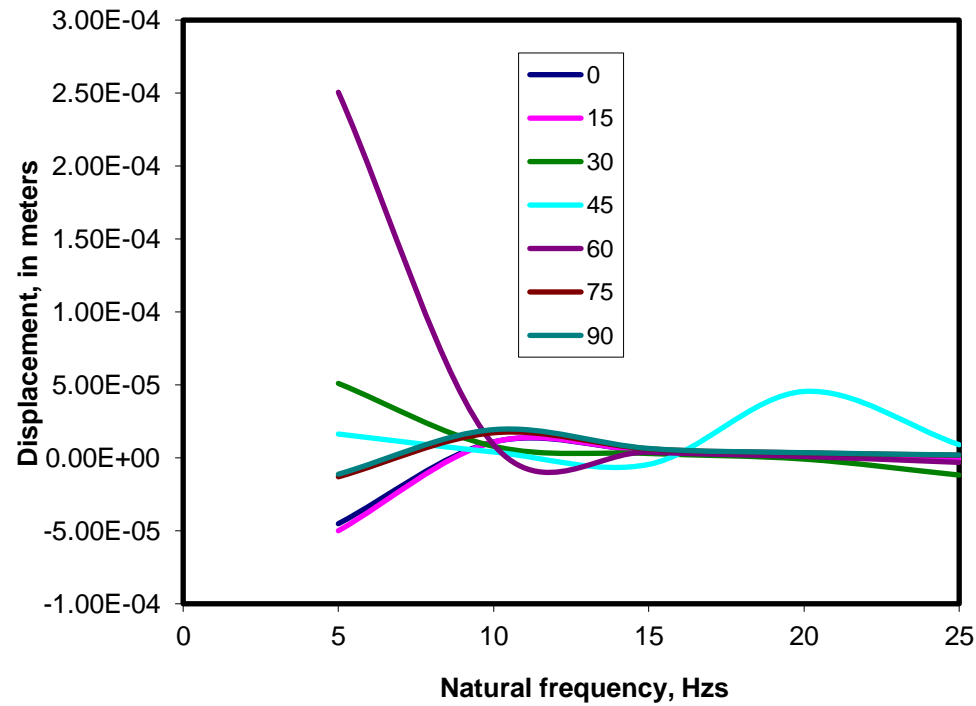


Fig.10.13. Frequency vs. Displacement for fibre angle rotation in two flanges

From fig.10.13, the maximum displacement is observed at natural frequency of 20 Hz. for fibre angle  $45^{\circ}$  and displacement is maximum for fibre angle  $60^{\circ}$  at frequency 5Hz.

### 10.3.2. Effect of fibre angle rotation in web

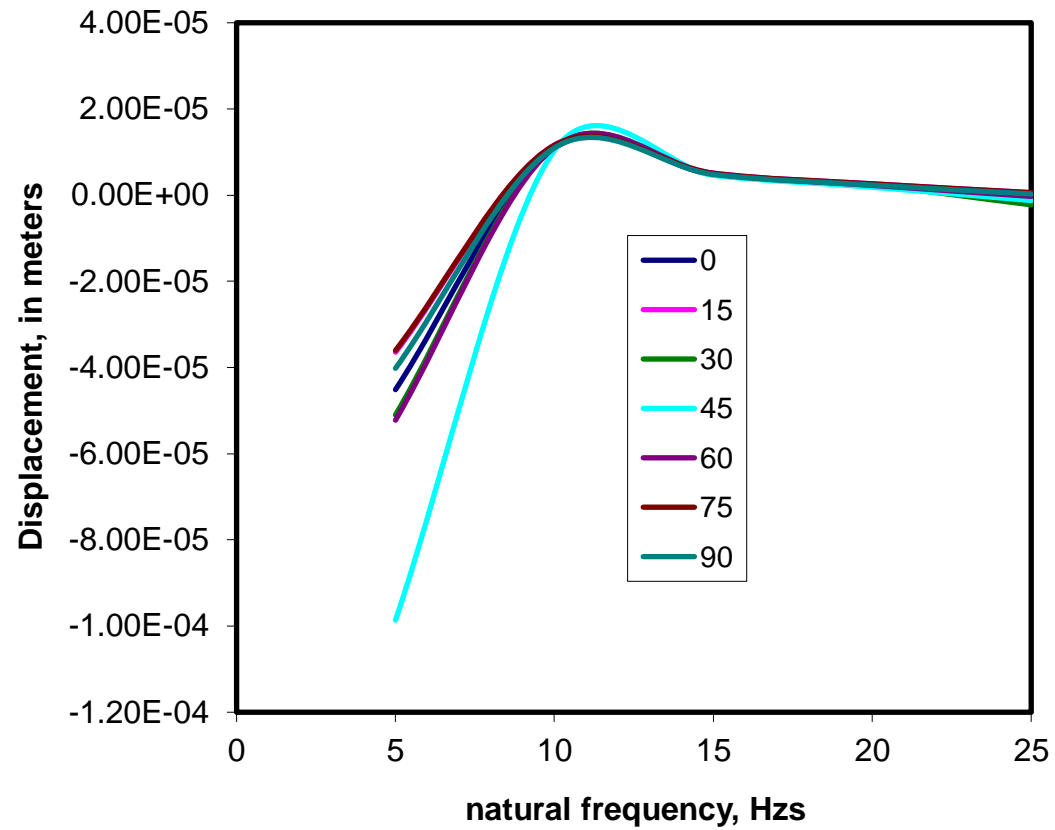


Fig.10.14. Frequency vs. Displacement for fibre angle rotation in web.

From fig.10.14, it is observed that, for fibre angle  $45^0$ , the maximum displacement is at natural frequency of 10 Hz.



### 10.3.3. Effect of modular ratio

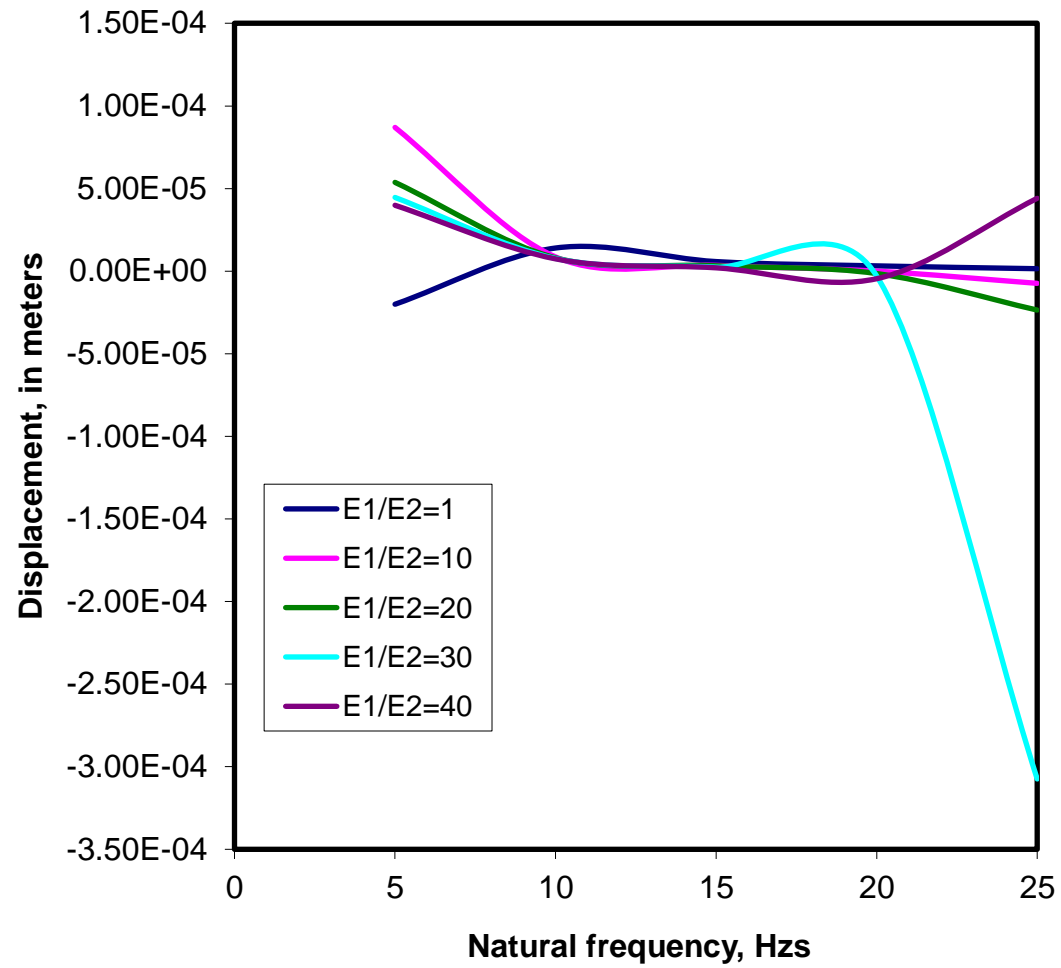


Fig.10.15. Frequency vs. Displacement for various modular ratios.

From fig.10.15. it is observed that, for modulus ratio of 30, the maximum displacement is at natural frequency of 5 Hz.

## **DISCUSSION ON RESULTS**

## DISCUSSION ON RESULTS

1. It was found that the frequencies of standard beams are higher than that of tapered beams, the frequencies of individual beams gradually increases over different sets and also numerical results obtained are almost nearer to the theoretical values obtained by using Wittrick.W.H. & Williams,E.W. Algorithm ,
2. The torsional frequencies of first three modes of vibration are increasing significantly for increasing values of taper ratio  $\beta$  and marginally for increasing values of taper ratios  $\alpha$  and  $\lambda$ .
3. The torsional frequencies of first three modes of vibration are significantly increasing for increasing values of taper ratios  $\beta$  and  $\lambda$  and are decreasing drastically for increasing values of taper ratio  $\alpha$  in second mode and third modes of vibration only.
4. The torsional frequency increases significantly for increasing values of combined influence of negative taper ratios  $\alpha$  and  $\beta$  in first mode. In second and third modes of vibrations the torsional natural frequency gradually decreases to certain value and then starts increasing.

5. An analytical model was developed to study the flexural – torsional vibrations of a laminated composite beam with an I-section. The model is capable of predicting accurate natural frequencies as well as vibration mode shapes for various configurations including boundary conditions, laminate orientation, ratio of Elastic moduli and height to thickness ratio of the composite beams.

## **CONCLUSIONS**

## CONCLUSIONS

The following conclusions are drawn from the results obtained.

1. The theoretical results from Finite Element Analysis showed good agreement with experimental results. Therefore, the model presented is found to be appropriate and efficient in analyzing free vibration problem of a thin walled laminated composite beam. The first four natural frequencies of the rectangular glass epoxy composite beam are found by ANSYS to verify with experimental results and the variation is found to be up to 11%.
2. From the results, it is very clear that changes in laminate sequences yield to different dynamic behaviour of the doubly symmetric thin-walled composite I-beams. From this it is concluded that different natural frequencies can be obtained for the same geometry, mass and boundary conditions.
3. The possibility to change fibre orientations, height to thickness ratio and elastic modulus ratio enables to manufacture thin-walled composite I-beams to get the desired natural frequencies without increasing its mass and geometry of the beam.
4. The experimental results and simulation results are found to be good with a variation up to a maximum of 11% .This is due to the improper fixing of beam at one end and also may be due to improper use of rubber hammer.
5. Modal analysis indicated that  $[0^0]_s$  and  $[0/90]_s$  laminate had higher natural frequencies for vibration and flexural modes when compared with the  $[+/- 45]_s$  laminate, this is due to the higher longitudinal elastic modulus of the laminates.

6. The  $[\pm 45]_s$  laminate had higher torsional modal frequencies due to its higher shear modulus. Harmonic analysis confirmed that large increases in normal displacement, rotational displacement, normal stresses and shear stress can occur at the resonance frequencies under dynamic loading conditions and these effects must be considered carefully in the design mechanical structures that use composite materials.
7. Harmonic analysis confirmed that large increases in normal displacement, rotational displacement, normal stresses and shear stress can occur at the resonance frequencies under dynamic loading conditions and these effects must be considered carefully in the design mechanical structures that use composite materials.
8. It is concluded from the results that  $[+ 45]$  laminate is more stable under loading than  $[0/90]$  laminate, due to the arrangement of the layers.





## **SCOPE OF FUTURE WORK**

## **SCOPE OF FUTURE WORK**

- The thickness of web for composite I-beam is considered as constant in the thesis. In future, the mode shapes and its behaviour can be studied for a tapered beam when the web thickness tapers uniformly from one end to other end so that weight of the beam can be further reduced.
- the work can be extended for the case of non linear torsional vibration of thin walled composite cantilever I-beam, for both symmetric and unsymmetric beams
- The work can be extended to study the effect of beams resting on continuous elastic foundation or Pasternak foundation or generalized foundation on natural frequencies of composite I beams can be studied.
- The effect of elastic end restraints on the frequency of symmetric and unsymmetric composite I beams can be studied.



## **AUTHOR'S INDEX**

## AUTHOR'S INDEX

	Serial no.		Serial no
<b>A</b>		Lin	110
Agarwal	17	Librescu L	10
Anand	87	LeeGC	40
Aucielo N.M	19	Lee J	11
Appala Satyam.A	32	Law	113
Anderson D.L	36	Laura P.A.A	51
Abbas	98	Lee SY	128
Arpci	103	Li	126
<b>B</b>		Lucic	111
Batoz	16	<b>M</b>	
Bauld N R	8	Mahabali Raja	119
Blandford G.E	15 ,23	McGee	6
Bozdag S.E	103	Mei	115
Benerjee J.R	24,25,42,75, 85,95,101	McConnell	64
Brown , T.G.	72,46	Magadi	116
Barsoum,R S	54,62	Mirza	52
<b>C</b>		Momoshine	67

Chan	86	<b>N</b>	
Cranch E.T	17	Nole G	21
Cywinski	73	Nowinski	78
Culver	55	Nole	21
Christiano.P	31	Naidu	23
Claeyssen	79	<b>O</b>	
Chen H	23	Ohga	7
Chen B	22	Owings Mi	6
Chang	82	<b>P</b>	
Cmassey	70	Pratyooosh Gupta	15
Chui	97	Prasad	119
Chi	94	Prokic	111,103
ChuchMei	93	Preg	71
<b>D</b>		Panovko	79
Dragon Marinkovi C.L	18	<b>R</b>	
Dayton.Umekawa, S	51	RobinVitch	124
Dennis	94	Raymond	121
<b>E</b>		Roberts	3
Eslimy-Isfahay,S.H.R.	42	<b>S</b>	

Ewins, D. J	43	Soder	105
<b>F</b>		Song O	10
Farhood	89	Sun C.T.,	13
<b>G</b>		Stanford	117
Gutierrez	37	Shakourzadeh H	16
Gurgose	81	Salmela.L	34
Gere J.M	14,27, 56,57,	Sunbuloglu	103
Gunavardane	85	Szabe B.A	40, 88
Guo Y.Q	15	Sarma P K	48
Goodier	58	Szymczak C	49,86,98
Goodies	59	Shiomi H	47
Gupta.B.V.R	30	Smith	126
Gallagher,R.H	62	Selvakumarr	114
Goel	80	<b>T</b>	
<b>H</b>		Takao H	7
Harris JW	6	Tzeng LS	8
Hetenyi	39	Tang, D	60
Heinz.Koppel	18	Timoshenko	1,29,68,77,104
Hu Y	22	Tin	120
Hanh	49	Tsai	65,66



He	44	<b>U</b>	
Hamachi F	66	Ulrich Glabbert	20
Hutton S.G	36	<b>V</b>	
Hamed	96	Vlasov VZ	9, 83
Hasiq	83	Vossoughi	122
Huebner	45	Venkateswar Rao	23
<b>J</b>		Vla Sov	9
Johnston P R	2	<b>W</b>	
Jones RM	12	Wekezer JW	4,5
Joga Rao.C.V	29	Weaver W	1,2
<b>K</b>		Wu	13,113
Koo	46	Wittrick	36
Kanakargi	21	Williams F.W	26 ,27, 36,130,123
Krishnamurthy	91,29	Wang S.T	15
Kerr	28	Wang I	60
Kara T	7	Wagner,H.,	69
Kameswara Rao.C	30 ,32,34, 35,38,75,104- 112	Wilde P	41,89
Kim	11	Wiedemann	102
Ke,HY	99	<b>X</b>	
Kwok- Tungchan	92	Xi-Xian	13

Kandaswamy	85	Xie W.C	22
Krajcinovic	82	Xiao	120
<b>L</b>		<b>Y</b>	
Lee LHN	63	Young D H	1
Lirani	47	Yecheng Shi	121
Lee, I	46		

## **REFERENCES**

## REFERENCES

1. Timoshenko S.P, Young D H, Weaver W., “Vibration Problems in Engineering”, 4th Ed. New York. Wiley; 1974.
2. Weaver W, Johnston P.R. “Structural Dynamics By Finite Elements.” Englewood Cliffs, NJ. Prentice-Hall; 1987.
3. Roberts TM., “Natural Frequencies of Thin-Walled Bars of Open Cross-Section”, Journal of Structural Engineering, 1987, 113(10), 1584-93.
4. Wekezer JW. “Vibrational Analysis of Thin-Walled Bars With Open Cross Sections”, Journal of Structural Engineering, 1989; 115(12), 2965-78.
5. Wekezer JW. , “Free Vibration Of Thin-Walled Bars With Open Cross Sections. J. Struct., Engg. 1987; 113(10): 1441-53.

6. Mcgee OG, Owings Mi, Harris JW. Torsional Vibration of Pretwisted Thin-Walled Cantilevered I-Beams. J.Comput. Struct., 1993; 47(L): 47-56.
7. Ohga M, Takao H, Kara T., "Natural Frequencies and Mode Shapes Of Thin-Walled Members", Journal of Structural Engineering, 1995; 55(6), 971-978.
8. Bauld NR, Tzeng LS., "A Vlasov Theory For Fibre-Reinforced Beams With Thin-Walled Open Cross Section", Intl. J. Solids and Structures, 1984, 20(3), 277-97.
9. Vlasov VZ., "Thin-Walled Elastic Beams", 2nd Edition, Jerusalem, Israel, Israel Program for Scientific Translation, 1961.
10. Song O, Librescu L., "Free Vibration of Anisotropic Composite Thin-Walled Beams Of Closed Cross-Section Contour", Journal of Sound &Vibration, 1993, 167(1), 129-147.
11. Lee, J, Kim SE. "Flexural-Torsional Buckling of Thin-Walled I- Section Composites", Journal of Composites and Structures, 2001, 79(10), 987-95.
12. Jones RM., "Mechanics of Composite Materials", Washington DC Hemisphere, 1975.
13. Xi-Xian, Wu and Sun C.T., "Simplified Theory for Composite Thin-Walled Beams", AIAA Journal, 10(12), 1992.
14. Gere J.M, "Torsional Vibrations of Thin- Walled Open Sections, "Journal of Applied Mechanics", 29(9), 1987, 381-387.
15. Pratyooosh Gupta, Wang S.T, Blandford, G.E, "Lateral- Torsional Buckling of Non-Prismatic I-Beam", Journal of Structural Engg, July, 1996, 748-755.
16. Shakourzadeh H, Guo Y.Q and Batoz, J.L, "A Torsion Bending Element For Thin-Walled Beams with Open and Closed Cross Sections", Journal of Composites and Structures, 55(6), 1995, 1045-1054.
17. Agarwal, H.R , Cranch E.T., "A Theory of Torsional and Coupled Bending Torsional Waves in Thin-Walled Open Section Beams", Journal of Applied Mechanics, 1967, 337-343.

18. Dragon Marinkovi C.L, Heinz.Koppel, Ulrich Glabbert, “Non Linear Finite Element Analysis of Active Composite Laminates”, Journal of Applied Mechanics, 5, 2005, 111-112.
19. Auciolo N.M.,Nole G, “Vibrations of A Cantilever Tapered Beam With Varying Section Properties and Carrying a Mass at The Free End”, Journal of Sound and Vibration,214(1),1998,105-119.
20. Xie W.C., Lee H.P., Lim S.P, “Normal Modes of A Non-Linear Clamped-Clamped Beam”, Journal of Sound and Vibration, 250(2), 2002, 339-349.
21. Naidu N.R., Venkateswar Rao, G, Kanaka Raju K, “Free Vibration Behaviour of Tapered Beams with Non-Linear Elastic End Rotational Constraints”, Journal of Sound and Vibration, 240(1), 2001, 195-202.
22. Chen B.,Hu Y, “The Torsional Stiffness Matrix Of A Thin Walled Beam and Its Application to Beams Under Combined Loading”, Journal of Composites & Structures,28,1998, 421-431.
23. Chen H., Blandford.A G.E, “C<sub>0</sub> Finite Element Formulation for Thin-Walled Beams”, Intl .Journal of Num. Mech. Engg., 28,1989,2239-2255.
24. Benerjee J.R, And Williams F.W., “Clamped-Clamped Natural Frequencies of A Bending Torsion Coupled Beam, Journal of Sound and Vibration , 176,1994, 301-306.
25. Benerjee J.R and Williams F.W., “Coupled Bending –Torsional Dynamic Stiffness Matrix Of An Axially Loaded Timoshenko Beam Element” Intl. Journal of Solids and Structures, 31, 1994, 209-222.
26. ANSYS<sup>R</sup> Inc. Theory Reference, Release 10.0 Manual,2007.
27. Timoshenko.S.P. and Gere.J.M. “Theory Of Elasticity”, McGraw-Hill, New York, 1961.
28. Kerr.A.D., “Elastic And Viscoelastic Foundation Models”, Journal of Applied Mechanics,31,221-228.
29. Krishnamurthy A.V and Joga Rao C.V., “General Theory of Vibrations Of Cylindrical Tubes”, Journal of Structures, 97, 1971, 1835-1840.

30. Kameswara Rao.C, Gupta.B.V.R.and D.L.N., “Torsional Vibrations of Thin Walled Beams on Continuous Elastic Foundation Using Finite Element Methods In Engineering”, Coimbatore, 1974, 231-48.
31. Christiano.P and Salmela.L. “Frequencies of Beams With Elastic Warping Restraint”, Journal of Aeronautical Society Of India, 20, 1968, 235-58.
32. Kameswara Rao.C & Appala Satyam.A., “Torsional Vibration And Stability of Thin-Walled Beams on Continuous Elastic Foundation”, AIAA Journal, 13, 1975, 232-234.
33. Wittrick.W.H. & Williams,E.W., “A General Algorithm For Computing Natural Frequencies of Elastic Structures”, Quarterly Journal of Mechanics and Applied Mathematics,24,1971,263-84.
34. Kameswara Rao, C., Ph.D Thesis, Andhra University, Waltair, “Torsional Vibrations and Stability of Thin-Walled Beams of Open Sections Resting on Continuous Elastic Foundation”, 1975.
35. Kameswara Rao,C., Sarma P.K, “The Fundamental Flexural Frequency Of Simply-Supported I-Beams With Uniform Taper”, Journal of The Aeronautical Society Of India ,27, , 1975,169-171.
36. Hutton S.G and Anderson D.L, “Finite Element Method, A Galerkin Approach”, Journal of The Engineering Mechanics Division, Proceedings of The American Society of Civil Engineers 97, Em5, 1503-1520, 1971.
37. Gutierrez R.H and Laura P.A.A., “Approximate Analysis of Coupled Flexural-Torsional Vibrations of a Beam of Non-Uniform Cross Section Using the Optimized Rayleigh’s Method”, Journal of Sound and Vibration 114, 1987, 393-397.
38. Kameswara Rao, C. and Mirza, S. “Free Torsional Vibrations Of Tapered Cantilever I-Beams”, Journal Of Sound And Vibration, 124 (3), 1988,489-496.
39. Hetenyi.M., “Beams On Elastic Foundation”, University Of Michigan Press, Ann Arbor,1946.
40. Christiano, P and Salmela, L, “Frequencies of Beams With Elastic Warping Restraint”, Journal of Aeronautical Society of India, 20, 1968, 235-258.

41. Kameswara Rao, C and Appala Satyam. A., "Torsional Vibration and Stability of Thin-Walled Beams on Continuous Elastic Foundation", AIAA Journal, 13(1975),232-234.
42. Eslimy-Isfahay, S.H.R. and Banerjee, J.R., "Dynamic Response of Composite Beams with Application To Aircraft Wings", Journal of Aircraft, 34(6), 1997,785-791.
43. Ewins, D. J., 1984, "Modal Testing: Theory and Practice", Research Studies Press Ltd, London.
44. He, L., Wang, I. and Tang, D , "Dynamic Responses of Aircraft Wing Made of Composite Materials", Proceedings of The 11th IMAC (International Modal Analysis Conference), Kissimme, 2, 1993,1342-1346.
45. Huebner, K.H., "The Finite Element Method for Engineers", J.Wiley, New York. 1994.
46. Koo, K.N. and Lee, I., "Dynamic Behavior of Thick Composite Beams", Journal of Reinforced Plastics and Composites, 14, 1995, 196-210.
47. Lirani, J.,"Sub structuring Techniques in the Analysis of Partially Coated Strucutres", Ph.D. Thesis, Department of Mechanical Engineering, The University of Manchester Institute of Science and Technology, UK., 1978.
48. Mcconnell, K. G., "Vibration Testing (Theory And Practice)", J.Wiley, New York, 1995
49. Tsai, S. W. and Hanh, H. T., "Introduction to Composite Materials", Technomic, Lancaster, 1980.
50. Tsai, S. W., "Composites Design, Think Composite", 1986.
51. Dayton.Umekawa, S. and Momoshima, S., "Composites in Japan", Composite Engineering, 2(8), 1992, 677-690.
52. Timoshenko, S.P., "Theory Of Bending, Torsion, And Buckling of Thin-Walled Members of Open Cross Section", Journal of Franklin Institute, 239, 1945, 201-219.
53. Wagner, H., "Torsion And Buckling of Open Sections", Danzing, Germany, 25<sup>th</sup> Anniversary Publications, 1929.
54. Barsoum,R S., " A Finite Element Formulation For The General Stability of Thin-Walled Members",Ph.D.Thesis, Department of Civil Engineering, Cornell University,Ithaca,1970.



55. Culver,G.C., And Preg,S.M., “ Elastic Stability of Tapered Beam Columns”, Journal of Structural Division , Proceedings Of ASCE,1968,Vol.94,Pp 455-470.
56. Gere,J M., Lin,Y.K., “ Coupled Vibrations of Thin-Walled Beams of Open Cross Section”, Journal of Applied Mechanics,1958, Vol.25,Pp373-374.
57. Gere,J M., and Carter, W.O., “Critical Buckling Loads For Tapered Columns, Journal of Structural Division,ASCE,88, 1962,3045-3049.
58. Goodier, J.N., “Flexural Torsional Buckling Of Bars Of Open Section, Under Bending, Eccentric Thrust Or Torsional Loads”, Cornell University, Engineering Experiment Station, , Bulletin 41, Itheca, 1942.
59. Goodier ,J.N., “ The Buckling Of Compressed Bars By Torsion and Flexure”, Cornell University, Engineering Experiment Station, Bulletin 42, Itheca, 1941.
60. Nowinski,J., “Theory of Thin Walled Bars”, Applied Mechanics Reviews, Vol.12,1959,Pp219-227.
61. Panovko,Y.G., “Thin-Walled Members”, Structural Mechanics Proceedings,1970,Pp142-159.
62. Barsoum ,R.S.,And Gallangher,R.H., “ Finite Element Analysis Of Torsional – Flexural Stability Problems”, International Journal of Numerical Methods In Engg.,Vol.2.,1970.
63. Lee,L.H.N., “ Non-Uniform Torsion of Tapered I-Beams”, Journal Of Franklin Institute,Vol.262, ,Pp.37, 1956.
64. Krajcinovic, D., “A Constant Discrete Elements Techniques for Thin-Walled Assemblages”, Intl Journal of Solids and Structures, 5, 1969,639-662.
65. Szymczak C ,Rozprawy ,“Torsional Vibrations of Thin-Walled Bars With Bisymmetric Cross Section.”, 1978,26,267-274
66. Hamachi F., “On Torsion of I-Beams with Web of Variable Height” Memories of The Faculty of Engg, Hokkaido University, 11, 209, 1961.

67. .Lee G.C and Szabe B.A. "Torsional Response of Tapered I-Girders", Proceedings of The American Society Of Civil Engineers 93, Journal of The Structural Division ST5, 1997, 233-252.
68. Wilde P. "On Torsion of Thin-Walled Bars with Variable Cross-Section", 1968, 20, 431-443.
69. Lee, L H N, "Non Uniform Torsion of Tapered I Beams", Journal of the Franklin Institute 262, 1956, 37-44.
70. Cmassey And Mcguire P.J., "Lateral Stability of Non Uniform Cantilevers", Proceedings of The American Society of Civil Engineers 97, Journal of The Engineering Mechanics Division, 1971, EM3, 673-686. .
71. Kitipornchai S and Trahair N.S., "Elastic Stability of Tapered I Beams", Proceedings of the American Society of Civil Engineers, Journal of the Structural Division. ST3, 98, 1972, 713-728.
72. . Brown T.G, "Lateral-Torsional Buckling of Tapered I-Beams", Proceedings of The American Society of Civil Engineers 94, Journal of The Structural Division St4, 1981, 689-697.
73. Cywinski, Z. "Statistics and Dynamics in Torsion of I-Beams with Variable Bisymmetric Cross-Section ", 1969(17), 185-217.
74. Szymczak,C. "Optimal Design Of Thin Walled I-Beams For Extreme Natural Frequency of Torsional Vibrations", Journal of Sound and Vibration,86, 1983, 235-241.
75. Banerjee, J.R., "Dynamic Stiffness Formulation and Its Application for a combined Beam and a Two Degree of Freedom System", Journal of Vibration and Acoustics, 125, 2003, 351-358.
76. Wiedemann,S.M., "Natural Frequencies And Mode Shapes of Arbitrary Beam Structures with Arbitrary Boundary Conditions", Journal of Sound and Vibration, 300, 2007, 280-291.
77. Prokic,A., " On Triply Coupled Vibrations of Thin Walled Beams With Arbitrary Cross Section", Journal of Sound and Vibration.,279,2005,723-737.
78. Timoshenko,S.P., Young, D.H., Weaver,W. "Vibration Problems In Engineering",Wiley,Newyork,1974.

79. Claeysen,J.R.,Soder,R.A., “ A Dynamical Basis For Computing The Modes of Euler-Bernoulli and Timoshenko Beams” , Journal of Sound And Vibration.,259,Vol.4,2003,986-990.
80. Goel,R.P., “Free Vibrations of A Beam Mass System with Elastically Restrained Ends”, Journal of Sound And Vibration.,47,1976,9-14.
81. Gurgose,M., “A Note on The Vibrations Restrained Beams and Rods with Point Masses”, Journal of Sound And Vibration.,96,,1984,461-468.
82. Chang,T.P., “ Forced Vibrations of a Mass Loaded Beam with a Heavy Tip Body”, Journal of Sound And Vibration.,164,1993,471-484.
83. Lin,S.C., Hsiaq,K.M., “Vibration Analysis of a Rotating Timoshenko Beam”, Journal of Sound and Vibration.,240,Vol.2,2001,303-322.
84. Prokic,A.,Lucic ,D., “Dynamic Analysis of Thin Walled Close Section Beams” ,Journal of Sound and Vibration, 302,2007,962-980
85. Banarjee,J.R., Gunavardana,W.D, “Dynamic Stiffness Matrix Development And Free Vibration Analysis Of A Moving Beam”, Journal of Sound and Vibration, 303, 2007, 135-143.
86. Law,S.S. Wu, Z.M., and Chan, S.L., “Transverse Natural Vibration of a Beam With An Internal Joint Carrying In-Plane Flexibilities”, Journal of Engineering Mechanics, 2005, 80-87.
87. Selva Kumar, Kandasamy, Anand V. Singh, “Transient Vibration Analysis of Open Circular Cylindrical Shells”, Transactions of the ASME, 128, 2006, 366-374.
88. Mei, C., “Free And Forced Wave Vibration Analysis of Axially Loaded Materially Coupled Composite Timoshenko Beam Structures”, Journal of Vibration and Accoustics, 127, 2005, 519-529.

89. Magadi Mohareb, ASCE, M. And Farhood Nowzartash, "Exact Finite Element for Nonuniform Torsion of Open Sections", Journal of Structural Engineering, 2003, 215-223.
90. Gere, J.M., Stanford. Calif, "Torsional Vibrations of Beams of Thin – Walled Open Section", Journal of Applied Mechanics, 1954, 381-387.
91. Prasad, K.S.R.K., Krishna Murty A.V.,and Mahabaliraja , "Iterative Type                      Raleigh Ritz Method For Natural Vibration Problems", AIAA                      Journal,8(10),1970,1884-1886.
92. Kwok-Tung Chan, Xiao-Quan Wang and Tin-Pui Leung," Free Vibration of                      Beams with Two Sections of Distributed Mass", Transactions of The ASME,120,1998,944-948.
93. Yecheng Shi, Raymond Y.Y., Lee, And Chuch Mei, "Finite Element Method for Nonlinear Free Vibrations of Composite Plates", AIAA Journal, 35(1), 1997,                      159-166.
94. Chi, M. ., Dennis B.G and Vossoughi, J., "Transverse and Torsional Vibrations of an Axially Loaded Beam With Elastically Constrained Ends", Journal of Sound and Vibration, 96(2), 1984, Pp.235-241.
95. Banerjee, J.R. and Williams ,F.W., "Exact Dynamic Stiffness Matrix For                      Composite Timoshenko Beams with Applications", Journal of Sound and                      Vibration, 194(4), 1995, 573-585.
96. Hamed,E., And Robinvitch,O.,"Dynamic Behavior of Reinforced Concrete                      Beams Strengthened With Composite Materials", Journal of Composites For                      Construction,2005,429-440.
97. Li, D.B. And Chui, Y.H. And Smith, I. "Effect of Warping On Torsional                      Vibration of Members with Open Cross – Sections", Journal of Sound and                      Vibration, 103, 1992, 135-143.
98. Abbas, B.A.H "Vibrations of Timoshenko Beams with Elastically Restrained Ends", Journal of Sound and Vibration, 94(4), 1984, 541-548.

99. Lee,S.Y., Ke,H.Y., “Free Vibrations of a Non-Uniform Beam With General Elastically Restrained Boundary Conditions”, *Journal of Sound and Vibration*, 136(3), 1990, 425-437.
100. Bishop,R.E.D., Price,W.G., “ Coupled Bending and Twisting of A Timoshenko Beam”, *Journal of Sound And Vibration*, 50(4), 1997, 469-477.
101. Banerjee,J.R.,Williams,F.W., “Coupled Bending-Torsional Dynamic Stiffness Matrix for Timoshenko Beam Elements”, *Journal of Sound and Vibration*, 42(3), 1992, 301-310.
102. Bercin,A.N.,Tanaka,M., Coupled Flexural Torsional Vibrations of Timoshenko Beams”, *Journal of Sound and Vibration*, 207(1), 1997, 47-59.
103. Arpci, A., Bozdag, S.E, Sunbuloglu ,E. “Triply Coupled Vibrations of Thin-Walled Open Cross- Section Beams Including Rotary Inertia Effects”, *Journal of Sound And Vibration*, 260, 2003, 889-900.
104. Kameswara Rao, C., and Ramesh, M., “Free Torsional Vibrations of Generally Restrained Thin-walled Beams of Open Section”, *Proceedings of ICASDA 2005*, 210 – 217.
105. Kameswara Rao, C., "Frequency Analysis of Two-Span Uniform Euler-Bernoulli Beams," *Journal of Sound and Vibration*, 137, 1990.144-150.
106. Kameswara Rao, C., "Frequency Analysis of Clamped-Clamped Uniform Beams with Immediate Elastic Support," *Journal of Sound and Vibration*, 133, 1989, 502-509.
107. Kameswara Rao, C., and Mirza, S., "A Note on Vibrations of Generally Restrained Beams," *Journal of Sound and Vibration*, Vol. 130, pp. 453-465, 1989.

108. Kameswara Rao, C., and Mirza, S., "Vibration Frequencies and Mode Shapes for Generally Restrained Bernoulli-Euler Beams," *Proc. of ASME Pressure Vessels and Piping Conference*, San Diego, Recent Advances in Structural Dynamics, PVP-Vol. 124, 1987, 17-121.
109. Kameswara Rao, C., "Non-linear Torsional Vibrations and Stability of Thin-Walled Beams on Elastic Foundation," *Symposium on Large Deformations*, IIT, New Delhi, December 1979.
110. Rao, N. L. N., and Kameswara Rao, C., "Vibration Frequencies for Uniform Timoshenko Beams with Central Masses," *Machine Building Industry*, , 1978, 5-8.
111. Kameswara Rao, C., "Forced Torsional Vibrations of Thin-Walled Beams of Open Section with Longitudinal Inertia, Shear Deformation and Viscous Damping," *Journal of the Aeronautical Society of India*, Vol. 28, No. 4, pp. 405-412, November 1976.
112. Kameswara Rao, C., "Nonlinear Torsional Vibrations of Thin-Walled Beams of Open Section," *J. of Appl. Mech.*, Trans. ASME, pp. 241-243, March 1975.
113. Jack R. Vinson, "The Behavior of Structures Composed of Composite Materials", Second Edition, Kluwer Academic Publishers, 2004.
114. Sahu S. K. and Asha A.V., "Stability of Laminated Composite Pretwisted Cantilever Panels ", *Journal of Reinforced Plastics and Composites*, Vol.24 (12), PP. 1327-1334, 2005.
115. Tita, V. "Theoretical and Experimental Dynamic Analysis of Fibre Reinforced Composite Beams", *J. of Braz. Soc. Of Mech. Sci. and Eng.* Vol. XXV, No.3, pp. 306-310, 2003.
116. Colakoglu, M. "Damping and vibration analysis of polyethylene fibre under varied temperatures", *Turkish J. Eng. Env. Sci.*, 30, 351-357, 2006.

117. Teng, T.L. and Hu, N.K., "Analysis of damping characteristics for viscoelastic laminated beams", Comput. Methods Appl. Mech. Engrg., Vol.190, pp.3881-3892, 2001.
118. Akira K., Stephen W. and Julie W., "Material Characterization of Glass, Carbon, and Hybrid-Fiber SCRIMP Panels", MSc Thesis Stanford University, Department of Aeronautics and Astronautics, 2002.
119. Hayder M., Al-Shukri, "Experimental and Theoretical Investigation into Some Mechanical Properties of Glass Polyester Composite under Static and Dynamic Loads", MSc Thesis, Engineering Electro mechanics Department, University of Technology, 2007.